RISK BASED APPROACH TO PML ESTIMATION FOR SINGLE-STOREY REINFORCED CONCRETE INDUSTRIAL BUILDINGS AND ITS IMPACT ON EARTHQUAKE INSURANCE RATES

by

Ceyhun Eren

B.S., Civil Engineering, Boğaziçi University, 2001

M.S., Civil Engineering, Boğaziçi University, 2005

Submitted to the Institute for Graduate Studies in
Science and Engineering in partial fulfillment of
the requirements for the degree of
Doctor of Philosophy

Graduate Program in Civil Engineering
Boğaziçi University

2014

ACKNOWLEDGEMENTS

I owe special thanks to Assist. Prof. Hilmi Luş for his helpful guidance throughout this thesis.

I would like to thank Assist. Prof. Kutay Orakçal from Boğaziçi University, Prof. Alper İlki from İstanbul Technical University, and Cüneyt Tüzün from Boğaziçi University Kandilli Observatory and Earthquake Research Center for their valuable contribution throughout this study. I would also like to thank Boğaziçi University PhD Candidate, Tarık Tufan who has supported the study with his valuable knowledge in computer programming.

Supports from Şahin Yılmaz and Allianz Turkey Risk Engineering Team Members have been greatly appreciated and will never be forgotten.

I am grateful to my beloved wife Gökçe Eren for her help, suggestions, endless patience, her positive attitude and encouragement, and most of all, for her love and caring.

I would also like to thank to my beloved son Alp Eren who has never complained when I had to study for writing this PhD Thesis instead of playing with him.

Finally, I would like to thank to my mother and father who have believed in me and supported me during every stage of my life without ever asking for anything.

ABSTRACT

RISK BASED APPROACH TO PML ESTIMATION FOR SINGLE-STOREY REINFORCED CONCRETE INDUSTRIAL BUILDINGS AND ITS IMPACT ON EARTHQUAKE INSURANCE RATES

Estimating earthquake losses is an important issue for many private and public bodies. As a major stakeholder, insurers need realistic Probable Maximum Loss (PML) values to foresee the possible losses they would face after a major earthquake and also to calculate optimal insurance premiums. Insurers generally use fragility curves to manage their portfolio by calculating overall PML values. There are, however, serious impacts of risk based PML estimation on earthquake insurance rates, and in this respect fragility curves, which represent regional losses rather than individual losses, could lead to suboptimal decisions. In this study, a rapid earthquake loss estimation methodology is proposed for single-storey reinforced concrete industrial buildings based on parameters determined after investigating more than 80 industrial building projects in Turkey. 384 analytical structural loss estimation curves were obtained via the non-linear structural performance analysis method proposed in the 2007 Turkish Seismic Design Code. To provide a detailed evaluation of the proposed methodology's performance, fragility curves representative of the structural types and the design levels of the buildings investigated were also developed. Finally, total insurance premiums corresponding to PML values of the inventory buildings were calculated, using the two aforementioned estimation methods and others previously published, by addressing issues such as reinsurance cost, capital cost and profit. Results reveal considerable differences in PML values and eventually earthquake insurance rates for the buildings investigated between the risk based structural loss estimation method and the existing methods, indicating possibilities for improved portfolio analysis and management tools.

ÖZET

TEK KATLI BETONARME SANAYİ YAPILARI İÇİN TEKİL HASAR (PML) TAHMİN YÖNTEMİ GELİŞTİRİLMESİ VE DEPREM SİGORTA PRİMİ ÜZERİNDEKİ ETKİSİNİN ÖLÇÜLMESİ

Deprem hasarlarının önceden tahmin edilmesi, birçok kamu kurumu ve özel şirket açısından büyük önem taşımaktadır. Özellikle sigorta şirketleri, büyük bir deprem sonrasında karşı karşıya kalabilecekleri olası hasarları önceden tahmin edebilmek ve uygun sigorta primi hesaplayabilmek için gerçekçi Olası En Yüksek Hasar (PML) değerlerine ihtiyaç duymaktadır. Sigorta şirketleri portföylerini yönetmek için genellikle hasar görebilirlik eğrilerini kullanarak toplam PML değerlerini hesaplarlar. Ancak risk bazlı PML tahmininin deprem sigorta fiyatlandırması üzerinde ciddi etkileri bulunduğundan tekil bina hasarı yerine bölgesel hasarları yansıtan hasar görebilirlik eğrilerinin kullanılması yanlış kararlar verilmesine neden olabilir. Bu çalışmada, tek katlı betonarme sanayi yapıları için 80'den fazla endüstriyel bina projesi incelenerek belirlenen değişkenlere bağlı hızlı bir deprem hasar tahmin yöntemi önerilmiştir. 2007 tarihli Türkiye Deprem Yönetmeliği'nde önerilen doğrusal elastik olmayan yapı performans analiz yöntemi kullanılarak 384 adet analitik yapısal hasar tahmin eğrisi elde edilmiştir. Yöntemin performansının daha detaylı incelenebilmesi amacıyla kullanılan yapı tipleri ile farklı tasarım seviyelerini yansıtan hasar görebilirlik eğrileri de çizilmiştir. Son olarak, envanterdeki binalar için gerek yeni geliştirilen iki farklı yöntem gerekse mevcut hasar hesaplama yöntemleri kullanılarak bulunan PML değerlerine karşılık gelen toplam sigorta primleri, reasürans gideri, kapital harcama ve kar oranı da dikkate alınarak hesaplanmıştır. Sonuçlar, risk bazlı hasar tahmin yöntemi ya da mevcut yöntemlere göre hesaplanan bina PML değerleri ve dolayısıyla deprem sigorta fiyatlarındaki önemli farklılıkların yanında portföy analizi ve yönetim araçlarının geliştirilebilme olanağını da göstermektedir.

TABLE OF CONTENTS

ACKNOWLEDGEMENTS iii
ABSTRACT iv
ÖZET v
LIST OF FIGURES viii
LIST OF TABLES xi
LIST OF SYMBOLS xvi
LIST OF ACRONYMS/ABBREVIATIONS xix
1. INTRODUCTION 1
2. BUILDING INVENTORY ANALYSIS 7
2.1. Classification of the Reinforced Concrete Industrial Buildings in Turkey . . 7
2.2. Building Models Used in the Existing Loss Estimation Methods 11
2.2.1. John Freeman's Method 12
2.2.2. Karl Steinbrugge's Method 14
2.2.3. ATC-13 Method 15
2.2.4. FEMA 154 v:2 Method 17
2.2.5. HAZUS Method 18
3. STRUCTURAL LOSS ESTIMATION 21
3.1. Structural Models 21
3.1.1. Structural Weight Calculation 22
3.1.2. Moment-Curvature Relationship 24
3.2. Structural Damage States 26
3.3. Capacity (Pushover) Analysis 29
3.4. Structural Performance Analysis 31
3.5. Structural Parameters Investigated 33
3.6. Structural Loss Estimation Curves 35
3.6.1. Critical Mass Calculation 36
3.6.2. Drawing Structural Loss Estimation Curves 39
3.6.3. Investigating Weaknesses at Column-Beam Connections of Precast Concrete Structures (Heavy Roof Structures) 41
3.7. Fragility Curves 44
3.7.1. Drawing Fragility Curves 44

3.8. Comparison of Results Obtained Using Structural Loss Estimation Curves and Fragility Curves . . . 46
3.9. Comparing Results with Existing Loss Estimation Methods . . . 50
3.9.1. John Freeman's Method . . . 50
3.9.2. Karl Steinbrugge's Method . . . 51
3.9.3. ATC-13 Method . . . 53
3.9.4. FEMA 154 v:2 Method . . . 55
3.9.5. HAZUS Method . . . 56
3.10. Comparing the Proposed Loss Estimation Method with Damaged Industrial Buildings . . . 59
4. EARTHQUAKE INSURANCE RATE CALCULATION . . . 62
4.1. Estimating Earthquake Insurance Rate of a Real Portfolio Comprising Single-Storey Reinforced Concrete Industrial Buildings . . . 62
4.2. Comparing the Earthquake Insurance Rates Calculated by Using Different PML Estimation Methods . . . 66
5. CONCLUSIONS AND REMARKS . . . 70
APPENDIX A: DATA CHARTS SHOWING THE APPROXIMATED WEIGHTS OF THE BASIC STRUCTURAL MEMBERS . . . 73
APPENDIX B: STRUCTURAL LOSS ESTIMATION CURVES DEVELOPED FOR THE BUILDING TYPES USED IN THE STUDY . . . 77
APPENDIX C: STRUCTURAL INFORMATION DATA CHARTS FOR THE BUILDING INVENTORY . . . 205
APPENDIX D: COMPARING THE PML VALUES AND CORRESPONDING EARTHQUAKE INSURANCE RATES BY USING DIFFERENT LOSS ESTIMATION METHODS . . . 216
REFERENCES . . . 222

LIST OF FIGURES

Figure 2.1. Typical single-storey reinforced concrete industrial building in Turkey. . 9

Figure 3.1. Effective area calculation for the structures having single span and two or more spans. 22

Figure 3.2. The structural properties of the sample building. 23

Figure 3.3. Demonstration of plastic deformation effect under earthquake loading. . 24

Figure 3.4. Idealized moment-curvature relationship of a 9-m-long, reinforced concrete column which has Type 6a cross-sectional properties under the axial load of 335 kN. 26

Figure 3.5. Typical earthquake damage (plastic deformation) in a precast column during 1999 Kocaeli Earthquake. 27

Figure 3.6. Calculating plastic deformation using a SDOF model subject to P-Δ effects. 29

Figure 3.7. Capacity Curves of 10-m-long reinforced concrete columns which have 60×60 cm cross-section and 1 % reinforcement ratio under the axial load of 465 kN with or without P-Δ effects. 31

Figure 3.8. Graphical representation of the structural performance estimation method used in the study. 31

Figure 3.9. Pushover analyses (a) and comparison of the seismic performances (b) of 9-m-long reinforced concrete columns (Type 6a cross-section), which have different concrete classes under the axial load of 335 kN. 33

Figure 3.10. Column interaction curve of Type 6a cross-section. 34

Figure 3.11. The graphical representation of drawing structural loss estimation curve for a reinforced concrete column: 60×60 cm cross-section, 1% reinforcement ratio, 1st Earthquake Zone and Z3 Soil Class. 39

Figure 3.12. Graphical demonstration of shear failure of a precast concrete structure. . 41

Figure 3.13. Structural fragility curves for single-storey reinforced concrete industrial buildings designed to various seismic design levels. 45

Figure 3.14. Fragility curves for the single-storey precast concrete (Heavy roof structures) industrial buildings. 46

Figure 3.15. Fragility curves for the single-storey reinforced concrete (Light roof structures) industrial buildings. 46

Figure 3.16. Demonstration of PML estimation for the sample buildings selected by using analytical structural loss estimation curves developed. 47

Figure 3.17. Fragility curves for the single-storey reinforced concrete industrial buildings (at minimum design level) located in the 1st Earthquake Zone and are subject to Z3 Soil Class conditions 49

Figure 3.18. Fragility curves for the single-storey precast concrete (Heavy roof structures (at minimum design level) located in the 1st Earthquake Zone and are subject to Z2 Soil Class conditions. 49

Figure 3.19. Probability distribution of damage for low-rise precast concrete buildings (Facility Class 81) at MMI IX. 54

Figure 3.20. Fragility curves for precast concrete industrial buildings designed to ‘’Minimum Code’’ level (subject to 1st Earthquake Zone). 58

Figure 3.21. Loss estimation according to the proposed method by using the structural loss estimation curves for the damaged building. 61

Figure 4.1. Comparing earthquake insurance rates of the entire portfolio calculated by using different PML estimation methods. 68

LIST OF TABLES

Table 2.1. General Types of Reinforced Concrete Industrial Buildings in Turkey. . 8

Table 2.2. The column types for the building inventory used within the study. . . . 10

Table 2.3. Building classification according to the existing loss estimation methods corresponding to the building type investigated in this study. 12

Table 2.4. John Freeman's building classification. 12

Table 2.5. Karl Steinbrugge's building classification. 14

Table 2.6. ATC-13 Earthquake engineering facility classification for buildings. . . 16

Table 2.7. FEMA 154 Building classifications. 18

Table 2.8. Model building types of the FEMA/NIBS methodology. 19

Table 3.1. Effective flexural stiffness coefficient estimation chart for different axial load ratios. 25

Table 3.2. Strain limit values for steel and concrete corresponding to different damage thresholds. 28

Table 3.3. Damage ratios comparison chart. 29

Table 3.4. Seismic performance comparison of the reinforced concrete columns which have different concrete class. 34

Table 3.5. Structural data collection table for the proposed loss estimation method. . 35

Table 3.6. The differences caused by P-Δ effects for 10-m-long reinforced concrete columns (Type 6a cross-section) under the axial load of 465 kN (which is subject to 1. Earthquake Zone and Z3 Soil Class conditions). 37

Table 3.7. The example of critical mass determination for 9-m-long reinforced concrete column, which has Type 6a cross-sectional properties and is subject to 1st Earthquake Zone and Z3 Soil Class conditions. 38

Table 3.8. The maximum axial loads calculated according to the different cross-sections. 40

Table 3.9. Structural fragility curve parameters of single-storey reinforced concrete industrial buildings for two different seismic design levels (Minimum and High-Code). 45

Table 3.10. Architectural and structural properties of the selected industrial buildings. 47

Table 3.11. Natural vibration periods of the inventory buildings according to the type of the structure and seismic design level. 48

Table 3.12. Probable maximum loss (PML) for building classes according to John Freeman's Method. 50

Table 3.13. Probable maximum loss (PML) for building classes according to Steinbrugge's Method. 52

Table 3.14. Beta distribution parameters for standard precast concrete construction low-rise (ATC-13 Facility Class 81). 53

Table 3.15. Standard precast concrete construction, low-rise (ATC-13 Facility Class 81). 55

Table 3.16. FEMA 154 v:2 loss estimation chart 56

Table 3.17. Structural fragility curve parameters of low-rise precast concrete structures (PC2L) for two different seismic design levels (High-Code and Moderate-Code) 57

Table 3.18. Comparison of the results of the analyses conducted by using different loss estimation methods for the sample buildings. 59

Table 3.19. Architectural and structural properties of the damaged industrial building. 60

Table 4.1. Earthquake insurance rate calculations for the building inventory via risk based PML estimation method building. 65

Table 4.2. Premium rates of the compulsory earthquake insurance scheme categorized based on earthquake zones and construction type in Turkey. . 66

Table 4.3. Comparison of the earthquake insurance rates for selected buildings obtained via different PML estimation methods. 67

Table 4.4. Comparison of the parameters used to calculate earthquake insurance rates and the premium for the buildings within the inventory according to different loss estimation methods. 69

Table A.1. Approximated weight calculation chart for different structural members.. 73

Table B.1. Structural loss estimation curves for the single-storey reinforced concrete industrial buildings which are located at 1st Earthquake Zone and Z1 Soil Class. 77

Table B.2. Structural loss estimation curves for the single-storey reinforced concrete industrial buildings which are located at 1st Earthquake Zone and Z2 Soil Class. 85

Table B.3. Structural loss estimation curves for the single-storey reinforced concrete industrial buildings which are located at 1st Earthquake Zone and Z3 Soil Class. 93

Table B.4. Structural loss estimation curves for the single-storey reinforced concrete industrial buildings which are located at 1st Earthquake Zone and Z4 Soil Class. 101

Table B.5. Structural loss estimation curves for the single-storey reinforced concrete industrial buildings which are located at 2nd Earthquake Zone and Z1 Soil Class. 109

Table B.6. Structural loss estimation curves for the single-storey reinforced concrete industrial buildings which are located at 2nd Earthquake Zone and Z2 Soil Class. 117

Table B.7. Structural loss estimation curves for the single-storey reinforced concrete industrial buildings which are located at 2nd Earthquake Zone and Z3 Soil Class. 125

Table B.8. Structural loss estimation curves for the single-storey reinforced concrete industrial buildings which are located at 2nd Earthquake Zone and Z4 Soil Class. 133

Table B.9. Structural loss estimation curves for the single-storey reinforced concrete industrial buildings which are located at 3rd Earthquake Zone and Z1 Soil Class. 141

Table B.10. Structural loss estimation curves for the single-storey reinforced concrete industrial buildings which are located at 3rd Earthquake Zone and Z2 Soil Class. 149

Table B.11. Structural loss estimation curves for the single-storey reinforced concrete industrial buildings which are located at 3rd Earthquake Zone and Z3 Soil Class. 157

Table B.12. Structural loss estimation curves for the single-storey reinforced concrete industrial buildings which are located at 3rd Earthquake Zone and Z4 Soil Class. 165

Table B.13. Structural loss estimation curves for the single-storey reinforced concrete industrial buildings which are located at 4th Earthquake Zone and Z1 Soil Class. 173

Table B.14. Structural loss estimation curves for the single-storey reinforced concrete industrial buildings which are located at 4th Earthquake Zone and Z2 Soil Class. 181

Table B.15. Structural loss estimation curves for the single-storey reinforced concrete industrial buildings which are located at 4th Earthquake Zone and Z3 Soil Class. 189

Table B.16. Structural loss estimation curves for the single-storey reinforced concrete industrial buildings which are located at 4th Earthquake Zone and Z4 Soil Class. 197

Table C.1. Axial load calculation data chart for different reinforced concrete industrial buildings of which the structural properties were estimated during the site surveys. 205

Table D.1. Comparison of the PML values calculated by using different PML estimation methods for each building within the portfolio. 216

Table D.2. Comparison of the earthquake insurance rates calculated by using different PML estimation methods for each building within the portfolio. 219

LIST OF SYMBOLS

A_c	Cross-sectional area of concrete
A_e	Effective area
A_o	Effective ground acceleration coefficient
A_s	Cross-sectional area of steel
$A(T)$	Spectral acceleration coefficient
a, S_{ae}	Elastic spectral acceleration
a_p	Spectral acceleration corresponding to the performance point
a_y	Spectral acceleration corresponding to the yielding point
β_{ds}	The standard deviation of the natural logarithm of spectral displacement for damage state, ds
b_w	Longitudinal bay width
C_R	Spectral displacement coefficient
d, S_{de}	Elastic spectral displacement
d_p	Spectral displacement corresponding to the performance point
d_y	Spectral displacement corresponding to the yielding point
ε_{ds}	A lognormal random variable with a unit median value and a logarithmic standard deviation, β_{ds}
EI_{eff}	Effective flexural stiffness
F_h	The horizontal force exerting to the column-beam connection during an earthquake
f_{yk}	Characteristic strength of the longitudinal reinforcement
f_{ywk}	Characteristic strength of the transverse reinforcement
f_{ck},f_{cm}	Characteristic strength of the concrete
f_s	Equivalent static load
g	Acceleration of gravity
I	Building importance factor
K	Bending stiffness
L	Height of the column
L_p	Plastic hinge length
m	Mass

m_{roof}	Mass of the roof excluding column weight
M_L	Span length – Transverse bay width
M_u	Ultimate moment
M_y	Yielding moment
N_{dm}	Axial load
P_A	Annual probability of an earthquake occurring at the site (SH)
P_y	Lateral load resistance
R_y	Seismic load reduction factor
S_{di}	Inelastic spectral displacement
$\overline{S}_{d,ds}$	The median value of spectral displacement of damage state, ds
$S(T)$	Spectrum coefficient
W	Axial load acting on the column
T	Natural vibration period
T_S	Limit vibration period
u	Top displacement
u_{max}	Maximum top displacement
u_y	Top displacement corresponding to the yielding point
V	Base shear
V_d	Shear capacity of the steel rod
V_y	Lateral load capacity corresponding to the yielding point
V_u	Lateral load capacity corresponding to the ultimate displacement
ω	Natural angular frequency
ω_s	Angular frequency corresponding to the limit vibration period
Δ_{CL}	Displacement corresponding to the Collapse Damage Limit
Δ_{Damage}	Displacement corresponding to any damage limit
Δ_{MN}	Displacement corresponding to the Minimum Damage Limit
Δ_p	Plastic displacement
Δ_{SF}	Displacement corresponding to the Safety Region Limit
Δ_y	Yielding displacement
θ_p	Plastic rotation demand in the column cross-section
ρ_s	The volumetric ratio of the confinement reinforcement present at the critical section

ρ_{sm}	The minimum confinement ratio according to Turkish Seismic Design Code 2007
Φ	Standard normal cumulative distribution function
ϕ_{Damage}	Curvature corresponding to any damage limit
ϕ_p	Plastic curvature demand
ϕ_u	Ultimate curvature
ϕ_y	Yielding curvature

LIST OF ACRONYMS/ABBREVIATIONS

AIR	AIR Worldwide
AL	Annual loss
ASTM	American Society for Testing and Materials
ATC	Applied Technology Council
BR	Base rate
CC	Capital cost
CCE	Capital cost effect
CL	Collapse limit
CS	Collapse state
D	The amount of deductible
EDS	Extensive damage state
EIR	Earthquake insurance rate
FEMA	Federal Emergency Management Agency
HAZUS	Hazards-United States
IV	Insured value
MDS	Moderate damage state
MMI	Modified Mercalli Intensity
MN	Minimum damage limit
P	Profit
PC	Precast reinforced concrete
PGA	Peak ground acceleration
PML	Probable Maximum Loss
PRC	Pure reinsurance cost
PRP	Pure risk premium
RC	Reinsurance cost
RMS	Risk Management Solutions
SDOF	Single Degree of Freedom
SDS	Slight damage state
SF	Safety limit
SH	Annual probability of an earthquake occurring at the site

TSDC07	Turkish Seismic Design Code 2007
TP	Total premium
TRC	Total reinsurance cost
TCIP	Turkish Catastrophe Insurance Pool
USGS	United States Geological Survey

1. INTRODUCTION

Recent destructive earthquakes of the last two decades have resulted in considerably high economical losses for industrial buildings designed for the "Life Safety" performance similar to ordinary residential buildings. The insured losses of the 1999 Kocaeli Earthquake and the 2011 Tohoku Earthquake were estimated as 1.5-3.5 billion USD (RMS, 2000) and 20-30 billion USD (AIR, 2011), respectively. Recent earthquakes have demonstrated that industrial buildings are additionally subject to collateral losses such as fire following earthquakes, sprinkler leakage, hazardous materials release and business interruption. On the other hand, for low-rise industrial facilities, structural damage is still the primary cause for direct and indirect losses in earthquakes.

Site investigations performed after Adana-Ceyhan (1998), Kocaeli (1999) and Düzce (1999) earthquakes have already revealed that seismic performances of precast buildings, which are the predominant structural type for the industrial buildings, are inadequate (Kayhan and Senel, 2010a). The issue is even more pressing for the Marmara Region, a highly industrialized area with a very high seismic risk measured at 2 % annual probability of occurrence of a magnitude 7+ earthquake on the main Marmara Fault (Durukal, *et al.,* 2008).

There is a significant concern for insurers about their potential insolvency due to catastrophic risks (Goda and Yoshikawa, 2012). Earthquake risk is placed at the top of these catastrophic, so called Nat Cat (Natural Catastrophes) risks. The first study of earthquake insurance in Turkey dates back to 1978 (Deniz and Yücemen, 2009) with the consideration of obligatory earthquake insurance feasibility. But only after the 1999 earthquakes could the obligatory insurance system be put into regulation. In 2000, with the formation of the Turkish Catastrophe Insurance Pool (TCIP) earthquake insurance was made compulsory. Although it was a major breakthrough for the Turkish Insurance Sector, the coverage was, and still is, limited to residential buildings and industrial buildings were left out.

In this respect, insurance companies have to use well calibrated loss estimation models to be able to foresee possible losses they could face after a major earthquake and also to calculate the optimal premium. This brings about the need for more realistic earthquake Probable Maximum Loss (PML) values, especially for industrial buildings which constitute a very high portion of the overall portfolio in terms of total values insured. PML can be simply defined as the expected maximum earthquake loss to the building systems in terms of monetary loss, generally expressed in currency or as a percentage of the insured value (Yao, 1981). Although the American Society for Testing and Materials (ASTM, 2007) has published a Standard Guide for the Estimation of Probable Loss to Buildings from Earthquakes (1999, revised in 2007), currently there is no unequivocally accepted standard for the definition of terms and analysis steps in PML estimation.

PML estimates were initially used by the insurance companies to quantify their risks, especially after the 1925 Santa Barbara Earthquake, at a time insurance coverage against earthquakes was rare and only with considerably high premiums. Historically, the PML is based on a deterministic analysis, using an event on the controlling fault for a site having a magnitude that is not expected to occur more than about once in every 475 years (i.e., 475-year return period). On the way to becoming more systematic, PML estimation studies have received considerable help from structural engineers.

One of the first seismic building codes was the by-product of John Freeman's well known book, *Earthquake Damage and Earthquake Insurance* (Freeman, 1932) in which earthquake loss estimation was mentioned possibly for the first time. Within the content of the book, structural lessons and loss ratios for the past destructive earthquakes were reported. Buildings were investigated one by one after these destructive earthquakes and damages were reported for each. The earthquakes investigated were Charleston (1886), San Francisco (1906), Inglewood (Los Angeles) (1920), Santa Barbara (1925), Calexico-Mexicali (1927), Whittier (L.A.) (1929), Japanese (1923), Italian (1930), and New Zealand (1931) Earthquakes.

In the 1980s, two landmark documents were published. Earthquake, Volcanoes, and Tsunamis: An anatomy of Hazards, in which an earthquake PML calculation method was

introduced for the first time by Karl Steinbrugge, was published in 1982 (Steinbrugge, 1982; Kircher, *et al.,*1997a).

The second study, Earthquake Damage Evaluation Data for California by the Applied Technology Council, appeared in 1985. This influential study, commonly called ATC-13 (1985), was developed for estimating earthquake losses using Modified Mercalli Intensity (MMI) based (qualitative) damage probability matrices determined via expert opinions for various building and occupational classes (78 existing facility classes in California including 36 building structure classes; Kircher, *et al.,* 1997a).

Following ATC-13, FEMA published the first edition of Rapid Visual Screening of Buildings for Potential Seismic Hazards: A Handbook (FEMA, 2002) also known as FEMA-154 or ATC-21; the methodology followed therein employed a scoring system based on the damage probability matrices of ATC-13. In 1989, FEMA published the National Academy of Sciences report Estimating Losses from Future Earthquakes, a valuable contribution listing guidelines for conducting loss estimation studies (Whitman, *et al.,* 1997).

The last major effort to improve vulnerability assessment was undertaken by the National Institute of Building Sciences. The result was HAZUS, a comprehensive loss assessment software program first released in 1997. It was aimed to reduce the uncertainty, especially in the vulnerability assessment, by replacing MMI with objective measures of ground motion such as spectral displacement and spectral acceleration. For this purpose, fragility curves were constructed for each building type by using the capacity spectrum method similar to NEHRP Guidelines for the Seismic Rehabilitation of Buildings and Seismic Evaluation and Retrofit of Concrete Buildings, known as ATC 40 (1996). This approach classifies buildings in terms of their use (occupancy class) and their structural system (building type). Twenty-eight occupancy classes and 36 model building types are defined (FEMA, 2001; Kircher, *et al.,* 1997b).

In 2002, the second edition of FEMA 154 Report, Rapid Visual Screening of Buildings for Potential Seismic Hazards: A Handbook, was published with a new scoring

system based on the HAZUS Methodology and fragility curves, replacing the expert-opinion Damage Probability Matrices of ATC-13 (FEMA, 2002).

Within the last decade, several earthquake loss estimation methodologies and computer programs based on deterministic or probabilistic approaches have also been developed by third party companies. Such efforts are generally tailored to the insurance sector and governmental programs, aiming to bridge the gap between technical engineering evaluations and non-technical decision-makers. Most of these existing models, however, are focused on regional earthquake loss estimation instead of individual structural analysis, and the structural parameter on which the fragility curves are based is generally the load bearing system, without much significant attention being given to other structural parameters that may adversely affect structural performance. Even if the two buildings, which are at the same region, have the same type of load bearing structure, the seismic performances could be totally different against the same seismic demand since the real earthquake behavior is hidden in the details. Therefore, during the loss estimation methods, the analysis criteria should comprise of at least, story height, architectural details, and cross-sectional properties including mainly the reinforcement ratio for reinforced concrete buildings.

Another important reason to show interest in individual seismic performance analysis is that design criteria of industrial buildings in Turkey, most of which are precast reinforced concrete, has changed considerably in parallel with modifications in earthquake design codes. As an example, the earthquake load reduction factor was decreased from 5 of the 1998 code to 3 of the existing Turkish Seismic Design Code (2007) (TSDC07).

The aim of this study is to discuss a new analytical methodology which provides fast, easy and reliable earthquake loss estimation for single-storey reinforced concrete industrial buildings, and to assess its impact on earthquake insurance rates derived from such risk based PML assessments. The risk based PML estimation refers to individual seismic performance analysis conducted for each building within the inventory instead of conducting portfolio loss estimation. The structural assessment method used is the non-linear static pushover analysis as per described in TSDC07. The main steps followed in the study can be summarized as the following:

- Site surveys of more than 80 single-storey reinforced concrete industrial buildings constructed at different regions of Turkey were completed. In addition, data was collected from various producers of precast structural members. Thus the main descriptive parameters of the load bearing system, including architectural dimensions, column heights, cross-sectional properties including reinforcement ratios, roof details, and material properties were identified, and their variations were estimated.
- Analysis parameters were determined by investigating the sensitivity of seismic performance to these descriptive parameters.
- The contributions of the structural elements and the roof types to the mass of the structure were estimated in detail.
- Representative single degree of freedom models of the inventory buildings were developed and analyzed via the static pushover analysis described in TSDC07. During these analyses, the critical mass values or weights (axial load) corresponding to individual damage states were calculated by keeping the parameters of column heights and the cross-sectional properties constant. Then the same procedure was applied for the other column heights. Since the moment curvature relationships and eventually unit deformation values change when the mass value changes, an iterative analysis procedure was applied to determine the critical mass values. P-Δ effects were also taken into consideration to account for second-order effects
- The procedure described above was repeated for each earthquake zone and soil type defined in TSDC07. As a result, 384 structural loss estimation curves, in which the main parameters are column height and axial load, were obtained.
- To discuss an alternative loss estimation approach for comparison purposes, fragility curves were also drawn by considering the structural types and the design levels of the buildings investigated.
- Insurance premiums corresponding to PML values of the inventory buildings were calculated using different loss estimation methods and by paying attention to the reinsurance cost, the capital cost and the profit that will be charged by the insurance companies.
- To conclude, PML estimates and earthquake insurance rate calculations obtained for the inventory buildings via the proposed loss estimation methodology were

compared with those that would be obtained via existing loss estimation methods for the inventory buildings.

The results indicate that the proposed methodology is quite sensitive to structural properties and can be used for determining optimal insurance premium rates in order to overcome a potential insolvency.

2. BUILDING INVENTORY ANALYSIS

The building inventory used in this study comprises pin-connected precast and cast-in-place reinforced concrete industrial buildings which have reinforced concrete columns with square cross-sections. This inventory was constructed after evaluating the structural projects of more than 80 reinforced concrete industrial buildings in Turkey and interviews with producers of precast structural members to decide on representative structural properties. In Appendix C, Table C.1 summarizes both structural properties and the axial loads calculated for the each industrial building within the inventory.

2.1. Classification of the Reinforced Concrete Industrial Buildings in Turkey

Most of the industrial buildings in Turkey are single-storey precast concrete frame structures or reinforced concrete structures with single columns (precast or cast-in-place) carrying lightweight roof structures because of the short duration of construction period and respectively low investment prices (Karaesmen, 2001). There exist comprehensive studies performed after the Adana-Ceyhan (1998), Kocaeli (1999) and Düzce (1999) earthquakes, in which structural properties and seismic performances of such precast buildings were documented (Kayhan and Senel, 2010a). On the other hand, structural properties of such buildings built after TSDC07 was published would show significant differences; it is worth mentioning, for example, that the cross-sections of the columns have increased with the new regulations.

These buildings generally have symmetrical plans and have a few spans in one direction whereas several more in the other. The lateral and vertical loads acting on the frame are carried by the cantilever columns which have rigid joints at the bottom (foundation) and pin connections at the top. Since the roofs (precast roof beams, gutter beams or the steel truss) are connected to the columns with hinge joints, the use of independent frames in structural analyses is generally considered acceptable (Kayhan and Senel, 2010a). Some examples showing general structural properties of single-storey reinforced concrete industrial buildings in Turkey can be seen in Table 2.1.

Table 2.1. General Types of Reinforced Concrete Industrial Buildings in Turkey.

Building Type	Load Bearing System	Roof Type			
		Bearing System			Cover
	Precast Columns	Precast Beam	Precast Gutter Beam	Precast Purlin	Aluminum Sandwich Panel (Poly-urethane Isolation)
	Precast Columns	Steel Truss	Precast Gutter Beam	Steel Purlin	Aluminum Sandwich Panel (Poly-urethane Isolation)
	RC Columns (Cast-in-place)	Steel Girder		Steel Purlin	Aluminum Sandwich Panel (Rockwool Isolation)
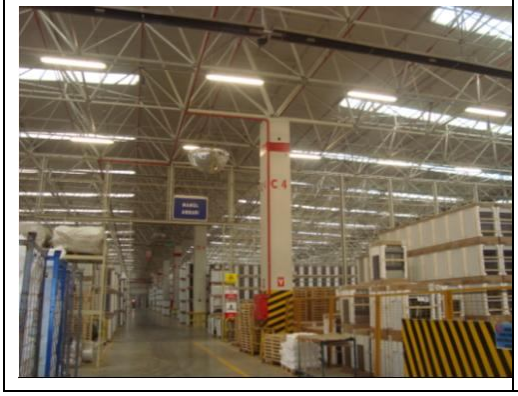	RC Columns (Cast-in-place)	Steel Space Truss System			Aluminum Sandwich Panel (Poly-urethane Isolation)

Both architectural and structural details of a typical single-storey reinforced concrete industrial building in Turkey are shown in Figure 2.1.

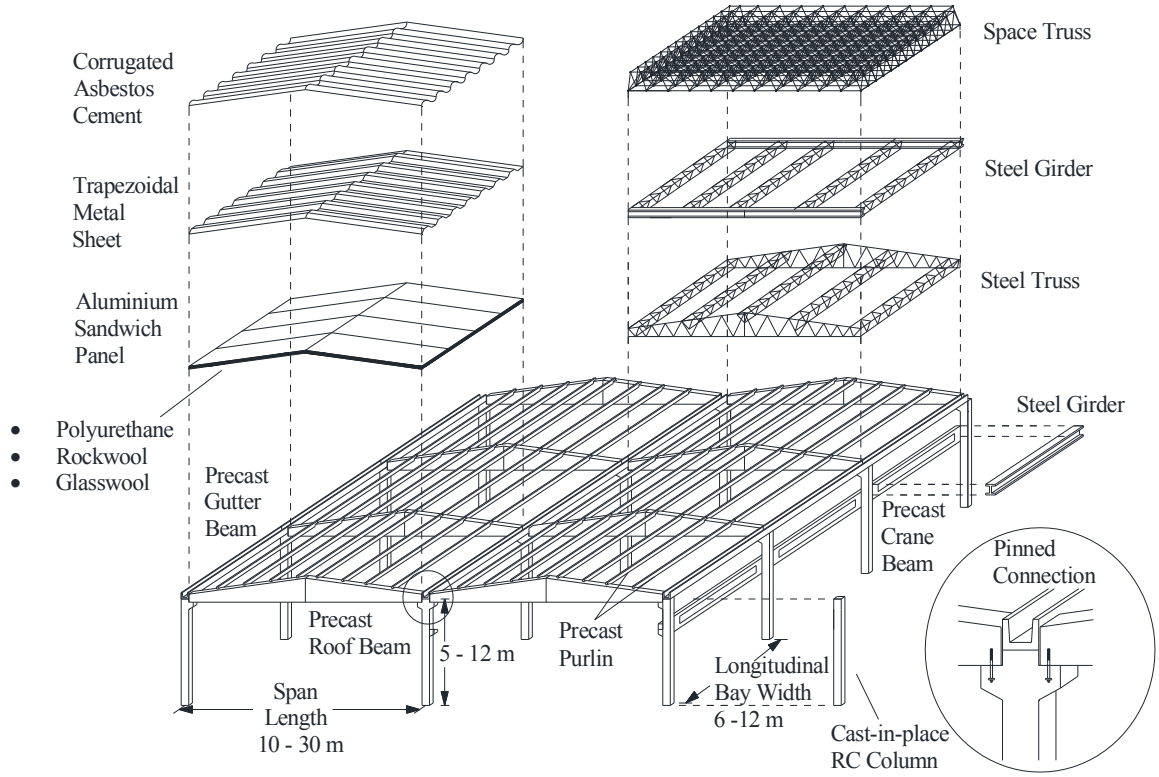

Figure 2.1. Typical single-storey reinforced concrete industrial building in Turkey.

Based on site investigations, interviews and questionnaires, minimum and maximum values of the architectural and structural parameters were determined. According to the data gathered, almost all columns have square cross-sections varying between 35×35 and 70×70 cm for the precast structures, whereas the dimensions vary between 50×50 and 80×80 cm for the cast-in-place reinforced concrete structures; column heights vary between 6 m and 12 m for both types of buildings. Span lengths (transverse bay widths) vary between 10 m and 30 m for the precast structures whereas they vary between 10 m and 24 m for the cast-in-place ones. While the longitudinal bay widths of the precast structures vary between 6 m and 12 m, they may increase up to 24 m for the cast-in-place buildings. S 420 steel bars (hot rolled ribbed reinforcement with yield strength $f_{yk}= f_{ywk}$ = 420 MPa) are used for both longitudinal and transverse reinforcement. The reinforcement ratio generally varies between 1.6 % and 2 % and rarely equals to 3 % for the precast buildings (heavy roof structures) whereas this ratio is generally equal to 1 % , the minimum reinforcement ratio according to the TSDC07, for the cast-in-place, light roof

structures. Almost in every column, stirrups have diameters of 8 mm and their spacing is generally 10 cm within the critical regions. Concrete class of C 30 (characteristic compressive strength f_{ck}= 30 MPa), with relatively high levels of quality control, is most frequently encountered in the columns. Precast beams and purlins are preferred at the roof in precast structures, whereas steel space truss systems are employed in cast-in-place structures. It was observed that sandwich panels isolated with polyurethane or rockwool are often preferred as roof cover. Based on available data, 24 different column types, with square cross-sections changing between 35×35 cm and 80×80 and three different reinforcement ratios (minimum, moderate, high) have been defined for the analyses (See Table 2.2).

Table 2.2. The column types for the building inventory used within the study.

Type	Column Section (cm)	Reinforcement Ratio		
		a) Minimum	b) Moderate	c) High
1	35×35	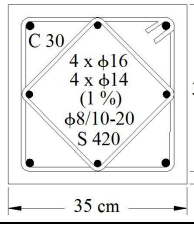	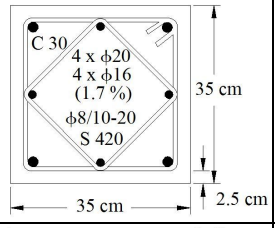	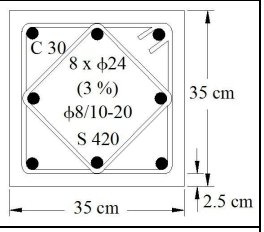
2	40×40	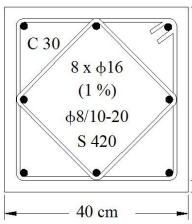	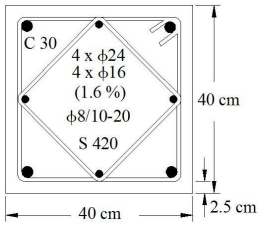	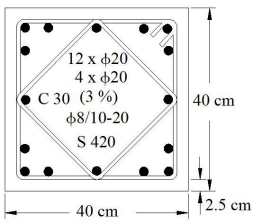
3	45×45	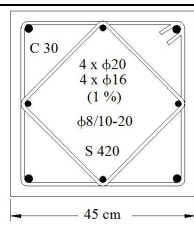	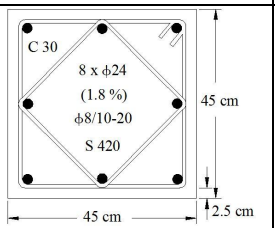	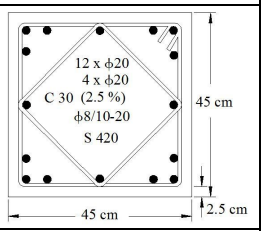
4	50×50	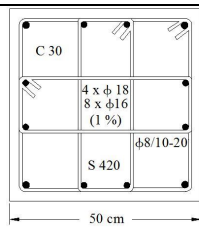	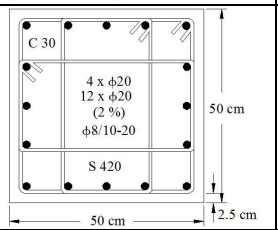	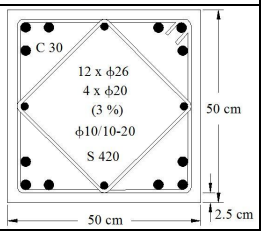

Table 2.2. The column types for the building inventory used within the study (cont.).

Type	Column Section (cm)	Reinforcement Ratio		
		a) Minimum	b) Moderate	c) High
5	55×55	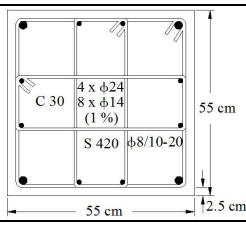	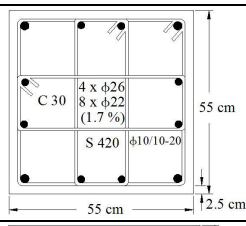	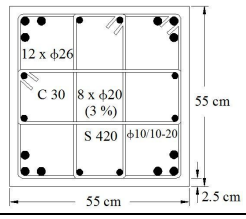
6	60×60	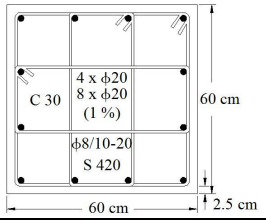	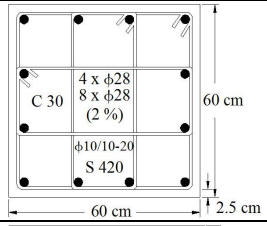	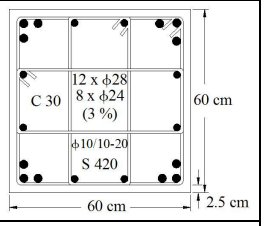
7	70×70	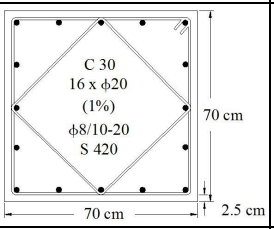	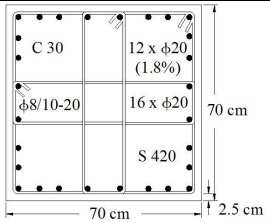	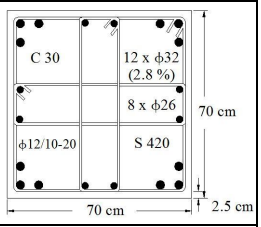
8	80×80	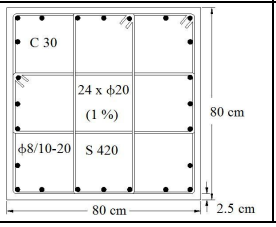	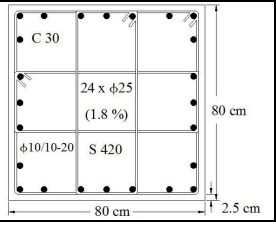	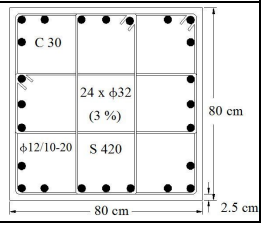

2.2. Building Models Used in the Existing Loss Estimation Methods

Within the building inventories of the existing loss estimation methods since the classification spectrum is considerably wide from wooden structures to reinforced concrete structures with or without shear walls, for single-storey precast concrete structures there is only one alternative except HAZUS Method (1997). In HAZUS Methodology, there are two different classes based on design code level. Although, there is no alternative for the industrial buildings which have single cast-in-place reinforced concrete columns carrying steel roof systems, the closest building type has been selected to use these loss estimation methods. Table 2.3 summarizes the building type classes defined in various methodologies to address single-storey reinforced concrete industrial buildings.

Table 2.3. Building classification according to the existing loss estimation methods corresponding to the building type investigated in this study (Freeman, 1932; Steinbrugge, 1982; ATC, 1985; FEMA, 2001; FEMA, 2002).

Method	Building Class	Description
John Freeman	9	Commercial buildings with reinforced concrete frames and columns
Karl V. Steinbrugge	4C	Lift-slab, precast
ATC-13	81	Precast concrete (Low rise) (other than tilt-up)
FEMA 154	PC2	Precast concrete frame
HAZUS	PC2L	Precast concrete frames (Low rise) (Minimum or High-Code)

2.2.1. John Freeman's Method

In John Freeman's Method, there are 11 different building classes which are changing according to the load bearing systems and also to the occupancy type. Most of them are reflecting the general building types constructed at that time. Table 2.4 summarizes these building classes.

Table 2.4. John Freeman's building classification (Freeman, 1932).

Class of Construction	Description
1	Steel-frame buildings on reinforced concrete mat foundation, having rigid cross-bracing, with strong gusset plates uniting columns to strong horizontal girders between windows, with curtain walls of reinforced concrete poured around the steel frame, and with ordinary interior finish. Not more than 100 feet tall. (Expected damage, chiefly cracked plaster.)
2	Tall steel-frame buildings with less-rigid cross-bracing than Class 1, with ordinary brick curtain walls and rock –concrete floors and uncertain foundations. Not more than 100 feet tall.

Table 2.4. John Freeman's building classification (Freeman, 1932) (cont.).

Class of Construction	Description
3	Tall reinforced concrete buildings without riveted or welded structural steel-frame and with ample strength at column connections and having ample horizontal cross-bracing by walls around windows, particularly in first story. Not over than 100 feet tall.
4	Wood –frame dwellings, set on good foundation walls (not on posts or slender piers), not above 2½ stories high, excluding stucco exteriors. (Expected damage chiefly cracked plastering and chimneys.) If on tall posts or slender piers the loss ratio will probably be 5 to 10 times as great.
5	Factory buildings of good design having bearing walls of brick in cement mortar, or of reinforced concrete. Strong wood floors, with little expensive interior finish. No plastered walls or ceilings. Not more than 4 stories tall.
6	Ordinary brick residence, mercantile and office buildings, of excellent design with brick bearing walls and wood floors. General average of unrated risks not exceeding 2½ stories.
7	Same as Class 6, but for general average of unrated risks, not exceeding 4 stories.
8	Brick veneered wood-frame or concrete-frame residence, mercantile and office buildings, or stucco exterior on wood lath, or with hollow-tile partitions.
9	General average of commercial buildings with reinforced concrete frames and columns, (no steel frame) with curtain walls and partitions of hollow-tile, and large window openings in lower story.
10	Buildings of doubtful quality of design and construction, uncertain wall ties, unanchored parapets, uncertain quality of mortar.
11	Concrete-block and hollow-tile buildings.

Although there is no building class corresponding to precast or reinforced concrete columns carrying light roof structures, Class 9 which is defined as ''Commercial buildings with reinforced concrete frames and columns'' was selected as the reinforced concrete industrial building for comparison purposes.

2.2.2. Karl Steinbrugge's Method

In Karl Steinbrugge's Method, the buildings were classified according to the load bearing systems only. Table 2.5 shows the building classification used in this method.

Table 2.5. Karl Steinbrugge's building classification (Steinbrugge, 1982).

1983 ISO Manual Classes	Description	Figure
1A, 1B	Wood frame	No Figure
2A, 2B	All-metal buildings	No Figure
3A, 3B, 3C	Steel-frame buildings	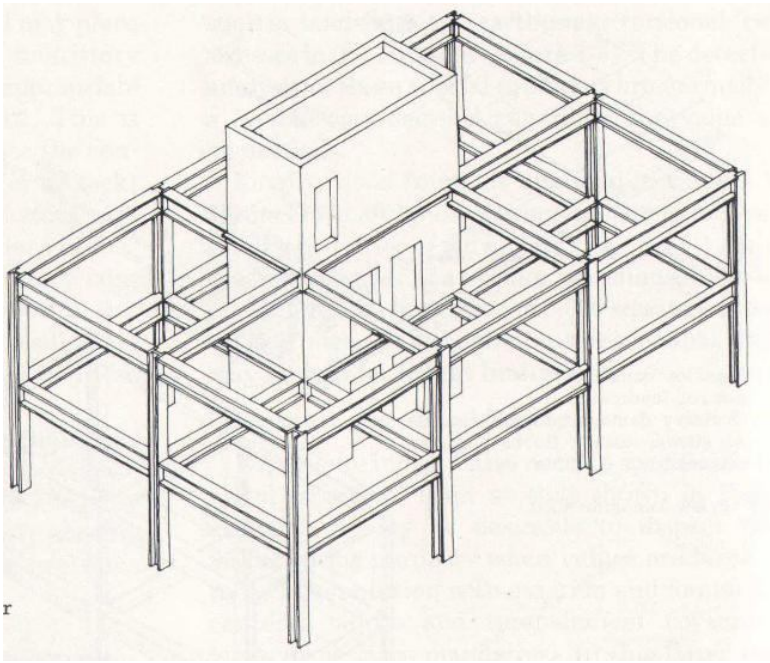
4A, 4B, 4D	Reinforced Concrete Frame	No Figure

Table 2.5. Karl Steinbrugge's building classification (Steinbrugge, 1982) (cont.).

1983 ISO Manual Classes	Description	Figure
4C	Lift-slab, precast	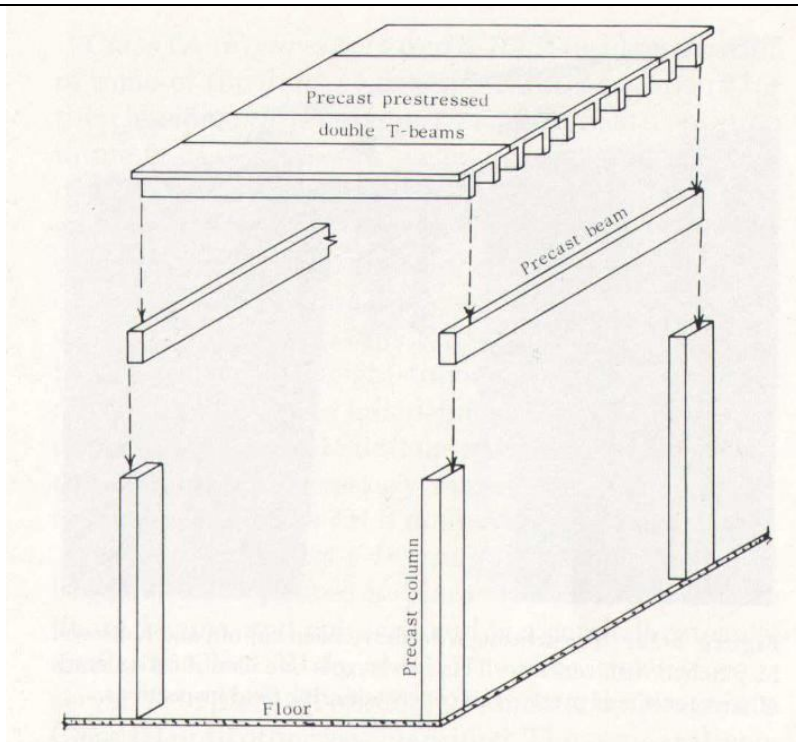
5A, 5B, 5C	Mixed construction buildings	No Figure
6	Special design for damage control	No Figure

Although there is no building class corresponding to precast or reinforced concrete columns carrying light roof structures, Class 4C which is defined as ''Lift-slab, precast'' was selected as the reinforced concrete industrial building for comparison purposes.

2.2.3. ATC-13 Method

In ATC-13 report, there are 78 different building classes, 40 of which were the buildings and 38 of which are the other structure types, such as bridges, pipelines, dams,

tunnels, storage tanks, high industrial chimneys, cranes, conveyor systems, on-shore and off-shore towers, and equipment. The 40 building facility classes, also known as the building types are described in Table 2.6. Each building class can be additionally classified as having Standard, Nonstandard, or Special construction (ATC, 1985).

Since the date of publication of ATC-13 goes back to 1985s, these 40 building classes have been determined among the ones which are widely constructed in most regions of USA. In addition, ATC-13 does not contain a detailed description of the building classes in terms of their construction characteristic and their lateral-load-carrying systems. There is no description about the meanings of S*tandard*, *Nonstandard*, and *Special* construction for each class (ATC, 2002).

Table 2.6. ATC-13 Earthquake engineering facility classification for buildings (ATC, 2002).

Building Description	Class Number
Wood Frame (Low Rise)	1
Light Metal (Low Rise)	2
Unreinforced Masonry (Bearing Wall) – Low Rise (1-3 Stories)	75
Unreinforced Masonry (Bearing Wall) – Medium Rise (4-7 Stories)	76
Unreinforced Masonry (with Load-Bearing Frame) – Low Rise	78
Unreinforced Masonry (with Load-Bearing Frame) – Medium Rise	79
Unreinforced Masonry (with Load-Bearing Frame) – High Rise (8 or more Stories)	80
Reinforced Concrete Shear Wall (with Moment-Resisting Frame) - Low Rise	3
Reinforced Concrete Shear Wall (with Moment-Resisting Frame) – Medium Rise	4
Reinforced Concrete Shear Wall (with Moment-Resisting Frame) - High Rise	5
Reinforced Concrete Shear Wall (without Moment-Resisting Frame) - Low Rise	6
Reinforced Concrete Shear Wall (without Moment-Resisting Frame) – Medium Rise	7
Reinforced Concrete Shear Wall (without Moment-Resisting Frame) - High Rise	8
Reinforced Masonry Shear Wall (with Moment-Resisting Frame) – Low Rise	84
Reinforced Masonry Shear Wall (with Moment-Resisting Frame) – Medium Rise	85
Reinforced Masonry Shear Wall (with Moment-Resisting Frame) – High Rise	86
Reinforced Masonry Shear Wall (without Moment-Resisting Frame) – Low Rise	9

Table 2.6. ATC-13 Earthquake engineering facility classification for buildings (ATC, 2002) (cont.).

Building Description	Class Number
Reinforced Masonry Shear Wall (without Moment-Resisting Frame) – Medium Rise	10
Reinforced Masonry Shear Wall (without Moment-Resisting Frame) – High Rise	11
Braced Steel Frame – Low Rise	12
Braced Steel Frame – Medium Rise	13
Braced Steel Frame – High Rise	14
Moment Resisting Steel Frame (Perimeter Frame) – Low Rise	15
Moment Resisting Steel Frame (Perimeter Frame) – Medium Rise	16
Moment Resisting Steel Frame (Perimeter Frame) – High Rise	17
Moment Resisting Steel Frame (Distributed Frame) – Low Rise	72
Moment Resisting Steel Frame (Distributed Frame) – Medium Rise	73
Moment Resisting Steel Frame (Distributed Frame) – High Rise	74
Moment Resisting Ductile Concrete Frame (Distributed Frame) – Low Rise	87
Moment Resisting Ductile Concrete Frame (Distributed Frame) – Medium Rise	88
Moment Resisting Ductile Concrete Frame (Distributed Frame) – High Rise	89
Precast Concrete (other than Tilt-up) – Low Rise	81
Precast Concrete (other than Tilt-up) – Medium Rise	82
Precast Concrete (other than Tilt-up) – High Rise	83
Long Span Construction (Shear walls of reinforced masonry or concrete having also frames of steel)	91
Tilt-up Construction	21
Mobile Homes	23

According to ATC-13, Class 81 which is defined as ‘’ Precast Concrete (other than Tilt-up) – Low Rise’’ was selected for representing the single-storey reinforced concrete industrial building for comparison purposes.

2.2.4. FEMA 154 v:2 Method

In FEMA 154 Methodology, buildings are classified according to their load bearing system which is defined in detail within the manuals. Some minor changes have been made

after publishing the second edition and the number of building types has increased to 15 from 12 (See Table 2.7).

Table 2.7. FEMA 154 Building classifications (FEMA, 2002).

FEMA 154 v:1		FEMA 154 v:2	
Symbol	Identifier	Symbol	Identifier
W	Wood Frame	W1	Light wood-frame residential and commercial buildings smaller than or equal to 5,000 square feet
		W2	Light wood-frame buildings larger than 5,000 square feet
S1	Steel moment resisting frame	S1	Steel moment resisting frame
S2	Braced Steel Frame	S2	Braced steel frame
S3	Light Metal	S3	Light metal buildings
S4	Steel frame with concrete shear walls	S4	Steel frame with cast-in-place concrete shear walls
		S5	Steel frame with unreinforced masonry infill walls
C1	Reinforced concrete moment resisting frame	C1	Concrete moment-resisting frame
C2	Reinforced concrete shear walls, no MRF	C2	Concrete shear-wall buildings
C3/S5	Concrete or steel frame buildings with URM infill walls	C3	Concrete frame buildings with URM infill walls
PC1	Tilt-Up concrete buildings	PC1	Tilt-Up concrete buildings
PC2	Precast concrete frame	PC2	Precast concrete frame
RM	Reinforced masonry	RM1	Reinforced masonry buildings with flexible floor and roof diaphragms
		RM2	Reinforced masonry buildings with rigid floor and roof diaphragms
URM	Unreinforced masonry	URM	Unreinforced masonry bearing-wall buildings

2.2.5. HAZUS Method

In HAZUS Methodology, buildings are classified both in terms of their use or occupancy (residential, commercial, etc.) and in terms of their structural system, or model building type (construction material, height) (See Table 2.8). There are twenty-eight occupancy classes, such as residential, commercial, and industrial or other buildings and

36 model building types, which are used to classify buildings within the overall categories of wood, steel, concrete, masonry or mobile homes (HAZUS 1997).

Table 2.8. Model building types of the FEMA/NIBS methodology (Kircher, *et al.,* 1997b).

No	Label	Description	Height			
			Range		Typical	
			Name	Stories	Stories	Feet
1 2	W1 W2	Wood, Light Frame ($\leq$ 5.000 m^2) Wood, Light Frame (> 5.000 m^2)		All	1 2	14 24
3 4 5	S1L S1M S1H	Steel Moment Frame	Low Rise Mid-Rise High-Rise	1-3 4 -7 8+	2 5 13	24 60 156
6 7 8	S2L S2M S2H	Steel Braced Frame	Low Rise Mid-Rise High-Rise	1-3 4 -7 8+	2 5 13	24 60 156
9	S3	Steel Light Frame		All	1	15
10 11 12	S4L S4M S4H	Steel Frame with Cast-in-Place Concrete Shear Walls	Low Rise Mid-Rise High-Rise	1-3 4 -7 8+	2 5 13	24 60 156
13 14 15	S5L S5M S5H	Steel Frame with Unreinforced Masonry Infill Walls	Low Rise Mid-Rise High-Rise	1-3 4 -7 8+	2 5 13	24 60 156
16 17 18	C1L C1M C1H	Concrete Moment Frame	Low Rise Mid-Rise High-Rise	1-3 4 -7 8+	2 5 12	20 50 120
19 20 21	C2L C2M C2H	Concrete Shear Walls	Low Rise Mid-Rise High-Rise	1-3 4 -7 8+	2 5 12	20 50 120
22 23 24	C3L C3M C3H	Concrete Frame with Unreinforced Masonry Infill Walls	Low Rise Mid-Rise High-Rise	1-3 4 -7 8+	2 5 12	20 50 120
25	PC1	Precast Concrete Tilt-Up Walls		All	1	15
26 27 28	PC2L PC2M PC2H	Precast Concrete Frames with Concrete Shear Walls	Low Rise Mid-Rise High-Rise	1-3 4 -7 8+	2 5 12	20 50 120
29 30	RM1L RM1M	Reinforced Masonry Bearing Walls with Wood or Metal Deck	Low Rise Mid-Rise	1-3 4+	2 5	20 50

Table 2.8. Model building types of the FEMA/NIBS methodology (Kircher, *et al.,* 1997b) (cont.).

No	Label	Description	Height			
			Range		Typical	
			Name	Stories	Stories	Feet
31 32 33	RM2L RM2M RM2H	Reinforced Masonry Bearing Walls with Precast Concrete Diaphragms	Low Rise Mid-Rise High-Rise	1-3 4 -7 8+	2 5 12	20 50 120
34 35	URML URMM	Unreinforced Masonry Bearing Walls	Low Rise Mid-Rise	1-2 3+	1 3	15 39
36	MH	Mobile Homes		All	1	12

Since, the lateral forces are resisted by reinforced concrete columns with hinge joints for the buildings within the inventory of this study, it would be more appropriate to take PC2L other than PC1 according to the definition given in the method (HAZUS, 1997).

3. STRUCTURAL LOSS ESTIMATION

As the main objective of this study is to evaluate the impact of risk based PML calculation on earthquake insurance rates, a rapid analytical method for individual building loss estimation under a specific seismic risk was developed. In order to achieve this, analytical structural loss estimation curves were drawn via the non-linear structural performance analysis method proposed in TSDC07, for all earthquake zones and soil classes defined by using two main variables, namely the height of the column and axial load for each cross-section within the building inventory. As the lateral column stiffness depends on the height, axial load and the column height were taken as the main parameters to base the loss estimation curves on. The probability of the seismic risk was taken as equal to a severe earthquake with a 475 years return period (10 % probability of exceedance in 50 years), which is the commonly accepted risk level for earthquake PML in the insurance sector (Durukal*, et al.,* 2006). As an alternative, fragility curves, which have been employed as a tool for loss estimation in various studies (Kircher, *et al.,* 1997b, Kayhan and Senel, 2010b), were developed, in which structural types and design levels of the buildings were taken explicitly into account.

3.1. Structural Models

Making use of the expected behavior due to the pin connections between beams and columns at the roof level, analytical studies were carried out by reducing three-dimensional building models into Single Degree of Freedom (SDOF) systems; this simplification has previously been used by various researches (Kayhan and Senel, 2010a). Since the columns within the building inventory have square cross-sections, the loading direction has no effect. Similar SDOF models may be used for both cast-in-place and precast concrete structures since their load bearing systems are similar, with hinge joints at the top and rigid joints at the bottom.

3.1.1. Structural Weight Calculation

In the idealized models, the mass of the structure is lumped at the roof level. The axial load *W,* on the critical column of the structure includes the weight of the main frame members, such as the roof beam/truss and its covers along with the insulation, and it is determined according to the number of spans and both longitudinal and transverse bay widths. Thus it will be possible to calculate the axial force exerted to each column by using these information.

It is also important to know how many spans exist in the building in addition to roof weights during the calculation of the axial load. It was assumed that the critical frame placed at the middle of the building in order to account for the worst case scenario. For this reason, the effective area A_e, can be calculated as simply span length-transverse bay width M_L times longitudinal bay width b_w for the multi-span buildings whereas the effective area is taken as the half of this value for the single span buildings. The half-length of the column (*L/2)* and the full length of the gutter beam are also taken into account for both cases. Besides, the weights of the beams, roof structure, and purlins are estimated according to the number of spans (See Equation 3.1). Figure 3.1 shows impact of the number of spans on effective area calculation. The critical column was named as B2 in both cases.

$$W = \underbrace{W_{Roof} + W_{Purlin}}_{Area\ afffected} + W_{Beam} + W_{Gutter\ Beam} + \frac{W_{Column}}{2} \tag{3.1}$$

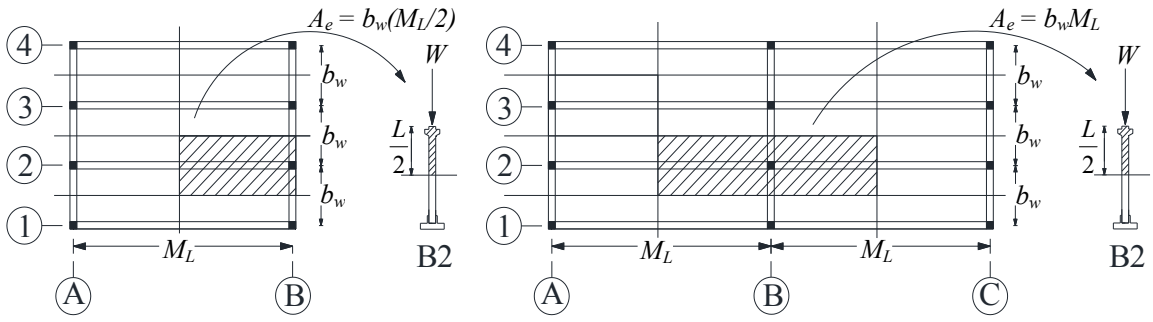

Figure 3.1. Effective area calculation for the structures having single span and two or more spans.

As one of the most important contributions to the mass calculation, the approximated weights of different structural members for load bearing members, such as roof beams, purlins and roof coverings, insulation materials were determined after the site surveys, discussions with the producers of precast reinforced concrete members and also investigating existing studies (Odabaşı, 2000). The approximated weights of the basic structural members generally used for the single-storey reinforced concrete industrial buildings can be found in Appendix A (See Table A.1).

Here is a computational example for finding the axial load value exerted on the critical column of a sample single-storey precast concrete industrial building. Figure 3.2 summarizes the structural properties of the building.

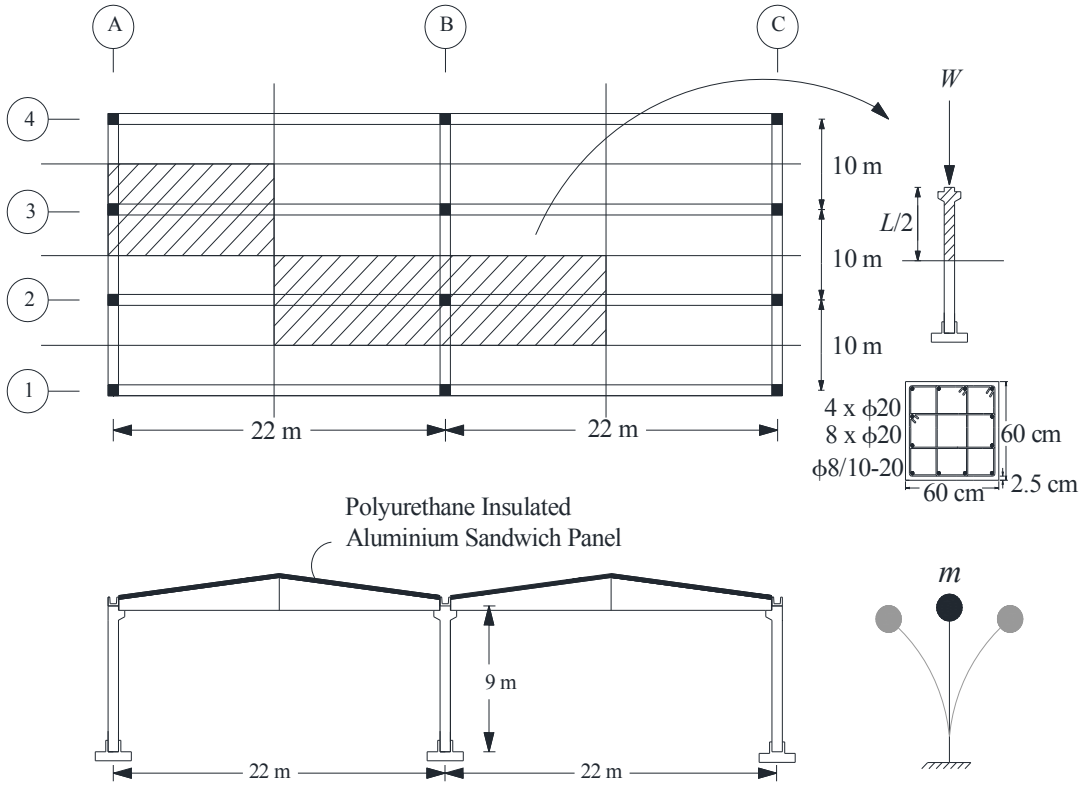

Figure 3.2. The structural properties of the sample building.

$$A_e = aL = 10 \times 22 = 220\ m^2 \tag{3.2}$$

$$W_R = (0.12) \times 220 = 26.4\ kN \qquad \text{(Roof Cover)} \tag{3.3}$$

$$W_P = (0.5) \times 220 = 110\ kN \qquad \text{(Precast Purlin)} \tag{3.4}$$

$$W_G = (3.25)\times 10 = 32.5\ kN \qquad \text{(Precast Gutter Beam)} \qquad (3.5)$$

$$W_B = (5.6)\times 22 = 123.2\ kN \qquad \text{(Precast Beam)} \qquad (3.6)$$

$$W_C = (26)\times(0.6\times 0.6)(9) \cong 84\ kN \qquad \text{(Precast Column)} \qquad (3.7)$$

$$W = 26.4 + 110 + 32.5 + 123.2 + 42$$
$$\cong 335\ kN$$

3.1.2. Moment-Curvature Relationship

One of the most important relationships during the damage state estimation procedure is the determination of moment-curvature relationships for each cross-section belonging to the critical columns of the frame systems for each building type. In order to draw loss estimation curves according to two important parameters, namely column height and axial load, moment curvature analyses have been repeated for every axial load change in each nonlinear static analysis.

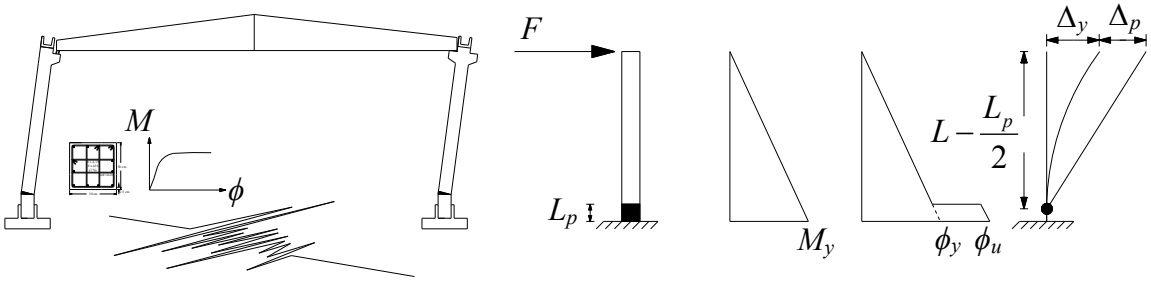

Figure 3.3. Demonstration of plastic deformation effect under earthquake loading (Kayhan and Senel, 2010b).

The moment-curvature relationships were determined by using the plastic hinge hypothesis. Representation of building model, location of plastic hinges and typical moment curvature response at these hinge regions are shown schematically on Figure 3.3. Moment-curvature analyses of the column sections were performed by using a special computer program. The material models for confined and unconfined concrete and also for reinforcement steel were represented by the models proposed in TSDC07.

Column capacity is modeled by a bilinear moment-curvature relationship that takes into account hardening effects for the reinforcement steel. The yield curvature ϕ_y of the cross-section was calculated by using yield moment M_y and effective flexural stiffness EI_{eff} with the following equation:

$$\phi_y = \frac{M_y}{EI_{eff}} \tag{3.8}$$

Effective flexural stiffness for the cracked section of reinforced concrete columns exposed to flexural stress was calculated by multiplying the flexural stiffness $(EI)_o$ by a coefficient (C) as per described in TSDC07 (See Table 3.1). These coefficients, which vary according to different axial load ratios, can be found in Table 4. Although the axial load values of the columns of the single-storey industrial buildings are at low levels (generally lower than 10 %), required controls were handled during the analyses in order to find out if the axial load ratio exceed the limit value of 0.1 or not. For the situations when the axial load ratio is in between (0.1 - 0.4) linear interpolation procedure was applied (TSDC07). A_c is the area of the column cross-section whereas f_{cm} is the concrete characteristic compressive strength.

Table 3.1. Effective flexural stiffness coefficient estimation chart for different axial load ratios (TSDC07).

Axial Load Ratio ($W/A_c f_{cm}$)	Effective Flexural Stiffness Coefficient (C) [$(EI_{eff}) = C\ (EI)_o$]
≤ 0.1	0.40
≥ 0.4	0.80

During the idealization process of the moment-curvature relationship, the first slope of the curve was assumed to be equal to the slope when reinforcement steel has yielded. The areas between the actual and the idealized curves were balanced while finding the yield and the ultimate moments (M_u). Ultimate curvature (ϕ_u) has been defined as the value

of curvature when the concrete reached to the ultimate deformation (ε_{cu}) or the deformation in steel reached to the critical ratio of 8 %, which is also complaint with the experiment results (Fischinger, *et al.,* 2008). Ultimate curvature was accepted as the curvature of Collapse Damage State if this value is smaller than the curvature of Collapse Damage State, which is calculated by unit deformation limits (See Figure 3.4).

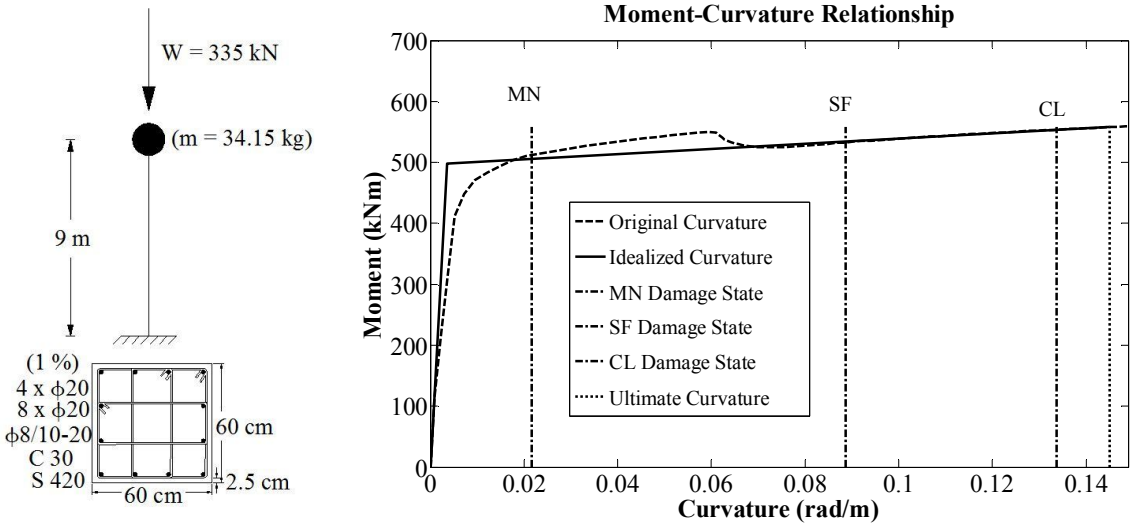

Figure 3.4. Idealized moment-curvature relationship of a 9-m-long, reinforced concrete column which has Type 6a cross-sectional properties under the axial load of 335 kN

Inelastic behavior of the column is modeled via a plastic hinge, which has a length L_p equal to half of the width of the cross-section in the loading direction; although there exist certain number of studies (Zhao, *et al.,* 2011) about the length of plastic hinge region for reinforced concrete columns, the choice employed here is that proposed by TSDC07. Moreover, it has been concluded that the displacement values are very close to the real values during the comparison of the analytical studies and the results of the experiments conducted for the estimation of seismic behavior of the precast concrete columns (Fischinger, *et al.,* 2008). Shear deformations were neglected by considering the slenderness of these structures (Kayhan and Senel, 2010b).

3.2. Structural Damage States

In recent seismic events such as the Ceyhan (1998) and the Kocaeli (1999) earthquakes, severe damage was observed in industrial buildings in Turkey, and the big

displacements caused by insufficient stiffness of the columns were cited as the main reason for the poor performance (Posada and Wood, 2002; Kayhan and Senel, 2010a). Based on such observations, the scope of this study has been limited to damage caused by the lateral displacements of columns; this choice, which was previously employed in other studies (Kayhan and Senel, 2010a), stems in part from the key performance issues identified based on analytical studies and field observations, and in part from the lack of data on acceleration sensitive data. The methodology discussed below may easily be extended to include other sources of failure once sufficient data is available.

Figure 3.5 shows a real seismic performance during 1999 Kocaeli Earthquake of a precast building of which the column placed at the middle has considerable moved laterally while the columns at the side moved slightly since the highest amount of vertical load affects the columns located at the middle.

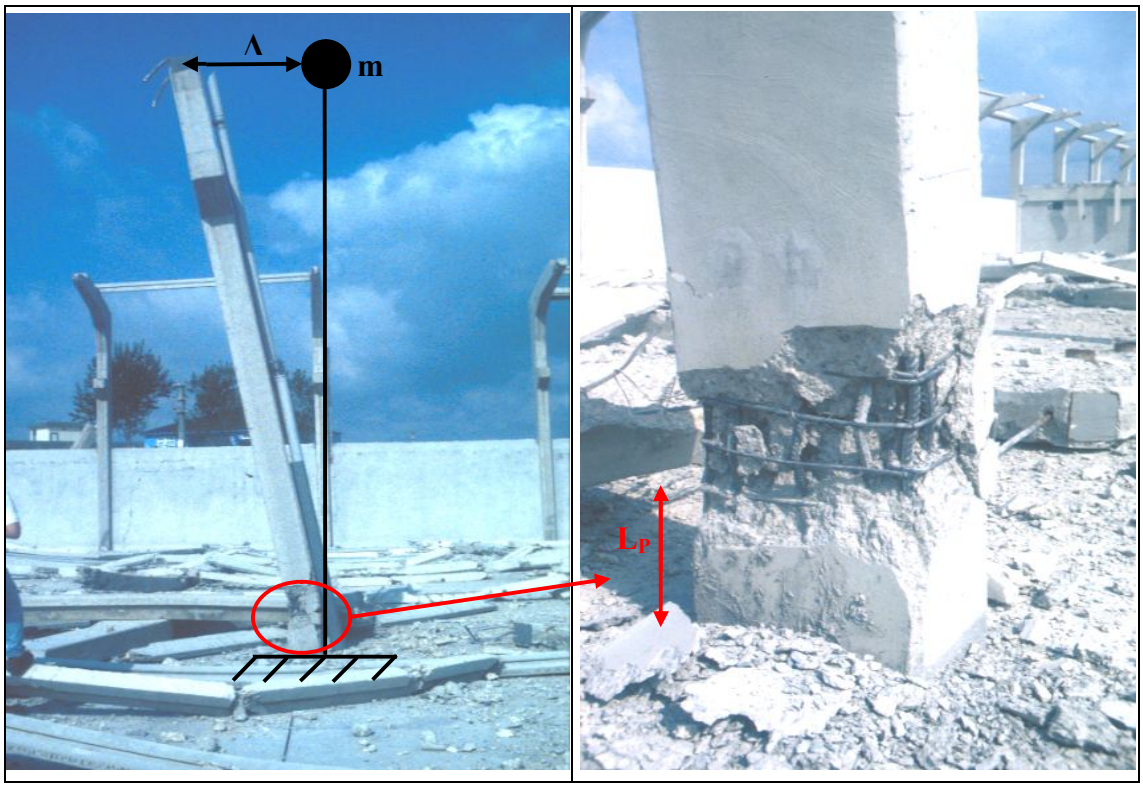

Figure 3.5. Typical earthquake damage (plastic deformation) in a precast column during 1999 Kocaeli Earthquake (Aschheim, 2001).

The damage thresholds are classified as *Minimum Damage Limit* (MN), *Safety Limit* (SF), and *Collapse Limit* (CL), based on limit deformations provided in TSDC07 for concrete and steel. Strain limits for concrete depend on the volumetric ratio of the confinement reinforcement present at the critical section (ρ_{sm}) and the minimum code requirement of this ratio (ρ_s). The strain limits given in Table 3.2 were used in the pushover analyses to find the limit displacement values corresponding to different damage threshold for each column cross-section analyzed. These damage thresholds are used to determine the damage states if the structural performance exceeds these limits or not. The damage states are designated as Slight (SDS), Moderate (MDS), Extensive (EDS) and Collapse (CS), similar to the classification in HAZUS (1997).

Table 3.2. Strain limit values for steel and concrete corresponding to different damage thresholds (TSDC07).

Material Type	Strain Limit Values		
	Minimum Damage Limit	Safety Limit	Collapse Limit
Concrete	0.0035	$0.0035+0.01(\rho_s/\rho_{sm}) \leq 0.0135$	$0.004+0.014(\rho_s/\rho_{sm}) \leq 0.018$
Steel	0.01	0.04	0.06

One other important issue related with structural loss estimation is the problem of relating a damage state to monetary loss. A measure used in this context is the replacement cost, often defined as the ratio of the cost of repair to the cost of reconstruction (Durukal, *et al.,* 2006). The replacement costs used in this study are taken from the damage probability matrix for reinforced concrete buildings based on empirical observations conducted by Gürpınar (1978) since the central damage ratios are compatible with the real structural earthquake damage ratios observed after 1999 Kocaeli and Düzce Earthquakes (Deniz, 2006). Table 3.3 summarizes the central damage ratios used in various studies.

Table 3.3. Damage ratios comparison chart (Durukal, *et al.,* 2006; Deniz, 2006).

Damage State	Central Damage Ratios (%)				
	Gürpınar (1978)	HAZUS (1997)	Bommer (2002)	DEE-KOERI (2003)	Yücemen (2005)
None	0	0	0	5	0
Slight	5	2	2	20	5
Moderate	30	10	10	50	30
Extensive	70	50	75	80	85
Complete	100	100	75	100	85

3.3. Capacity (Pushover) Analysis

A building capacity curve, also called a pushover curve, is a plot of a building's lateral load resistance F as a function of a characteristic lateral displacement Δ. Pushover curves may generally be idealized as bilinear based on observations of rectangular reinforced concrete cantilever columns subjected to cyclic lateral load tests (Fischinger, *et al.,* 2008).

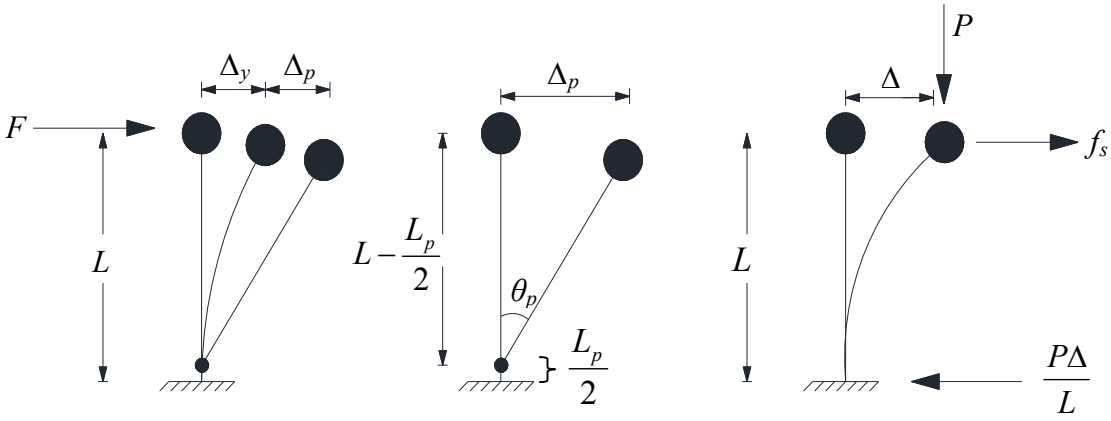

Figure 3.6. Calculating plastic deformation using a SDOF model subject to P-Δ effects

The elastic (yield) displacement Δ_y and the plastic displacement Δ_p can be calculated as follows (See Figure 3.6):

$$\Delta_y = \frac{FL^3}{3EI} \qquad \Rightarrow \qquad \Delta_y = \frac{M_y L^2}{3EI} = \phi_y \frac{L^2}{3} \tag{3.9}$$

$$\Delta_p = L_p \phi_p \left(L - \frac{L_p}{2} \right) \tag{3.10}$$

The relationship between the plastic curvature capacity ϕ_p and the plastic rotation capacity θ_p is given by

$$\phi_p = \frac{\theta_p}{L_p} = \phi - \phi_y \tag{3.11}$$

where, ϕ is a curvature value beyond the elastic limit.

After finding elastic and plastic displacements, total top displacement, yield lateral load capacity V_y and ultimate lateral load capacity V_u are evaluated using the following equations:

$$\Delta = \Delta_y + \Delta_p \tag{3.12}$$

$$V_y = \frac{M_y}{L};\ V_u = \frac{M_u}{L} \tag{3.13}$$

Reinforced concrete columns with high ductility are subject to second-order moments under high axial loads. To take into account these so-called P-Δ effects, both the initial bending stiffness k and the strength must be appropriately reduced. New values of bending stiffness k', yield lateral load capacity V_y' and ultimate lateral load capacity V_u' may be evaluated as:

$$f_s = k\Delta - \frac{P\Delta}{L} = k'\Delta \quad \left(k' = k - \frac{P}{L} \right) \tag{3.14}$$

$$V_y^{'} = V_y - \frac{P\Delta_y}{L};\ V_u^{'} = V_u - \frac{P\Delta_u}{L} \tag{3.15}$$

where, f_s is the equivalent static load (Kwak and Kim, 2007).

In order to take into account the strength degradation caused by P-Δ effects, the ultimate displacement is taken to be the value of the top displacement corresponding to a strength degradation of 20 % (See Figure 3.7), a value that complies with results of experiments conducted on precast concrete columns (Fischinger, *et al.,* 2008)

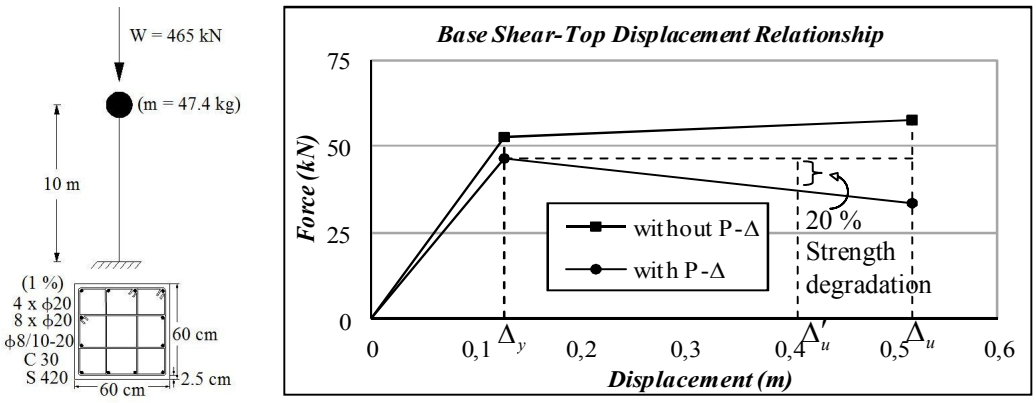

Figure 3.7. Capacity Curves of 10-m-long reinforced concrete columns which have 60×60 cm cross-section and 1 % reinforcement ratio under the axial load of 465 kN with or without P-Δ effects.

3.4. Structural Performance Analysis

The performance point is determined by simply intersecting the line, which has the same slope as the initial tangent of the building capacity curve, with the elastic response spectrum of an earthquake which has 10 % probability of exceedance in 50 years (return period of 475 years) as defined in TSDC07 (See Figure 3.8).

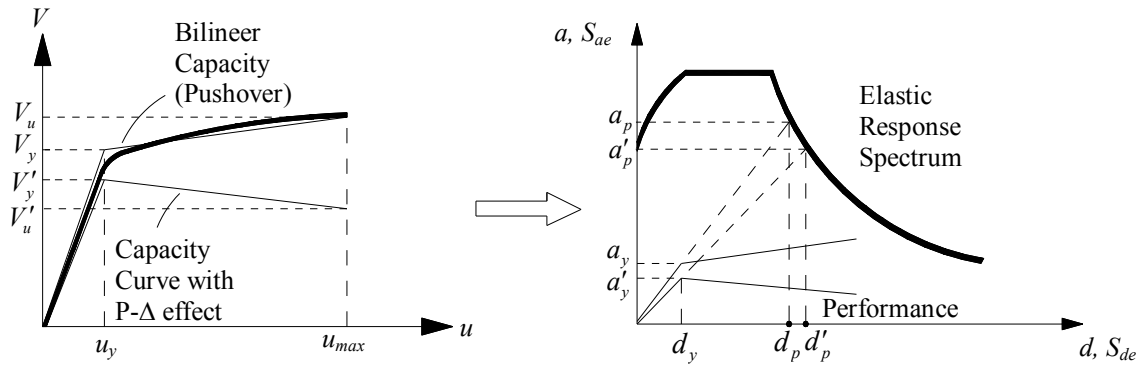

Figure 3.8. Graphical representation of the structural performance estimation method used in the study.

In order to find the structural performances of the buildings within the inventory of this study, firstly the new stiffness values were calculated by taking into consideration of P-Δ effects. Then, the line drawn by using this value as the slope was intersected with elastic response spectrum. While calculating the performance point, Equal Displacement Rule was applied for the systems of which the natural vibration period (T) is longer ($T > T_S$) than the limit vibration period (T_S). Thus, it was accepted that elastic spectral displacement (S_{de}) is equal to inelastic spectral displacement (S_{di}). For the systems of which the natural vibration period is shorter ($T < T_S$) than the limit vibration period, it was accepted that the inelastic spectral displacement is bigger than elastic spectral displacement at certain amount (See Equation 3.10). The Spectral Displacement Coefficient (C_R), which depends on Load Reduction Factor (R_y), is calculated by using Equation 3.17 as proposed in TSDC07.

$$S_{di} = C_R S_{de} \tag{3.16}$$

$$C_R = \frac{1 + \left(R_y - 1\right) T_S / T}{R_y} \tag{3.17}$$

Elastic Spectral Acceleration, $S_{ae}(T)$, which is used to estimate seismic forces, is equal to Spectral Acceleration Coefficient, $A(T)$ multiplied by ground acceleration, g. Spectral Acceleration Coefficient is calculated by multiplying Effective Ground Acceleration (A_o), building Importance Factor (I), which are taken from TSDC07 and also with Spectrum coefficient $S(T)$, which depends on soil conditions and natural vibration period.

$$S_{ae}(T) = A(T) g \tag{3.18}$$

$$A(T) = A_o \left(I\right) S(T) \tag{3.19}$$

3.5. Structural Parameters Investigated

A sensitivity analysis was conducted to determine those parameters which have high impact on seismic performance; these parameters were identified as column cross-section dimensions, longitudinal reinforcement ratio, height of the column, mass (or axial load), earthquake zone, and soil type. Although the diameter and the spacing of the stirrups have considerable impact on the seismic performance, it was observed that the spacing of the stirrups was almost the same in all instances and the diameter changed in correlation with the cross-sectional dimensions for the inventory buildings used in this study. The concrete class, which is generally a very important parameter for seismic performance, also played no significant part for the inventory buildings (Eren, 2014). This important result has been determined by conducting capacity analyses in which different concrete classes (C20, C30, C40) were used for the models which have the same structural properties. In these analyses, it was determined that the performance points of the models, which have different concrete classes, were corresponded to the same damage states for every different earthquake zone and also soil type (See Figure 3.9).

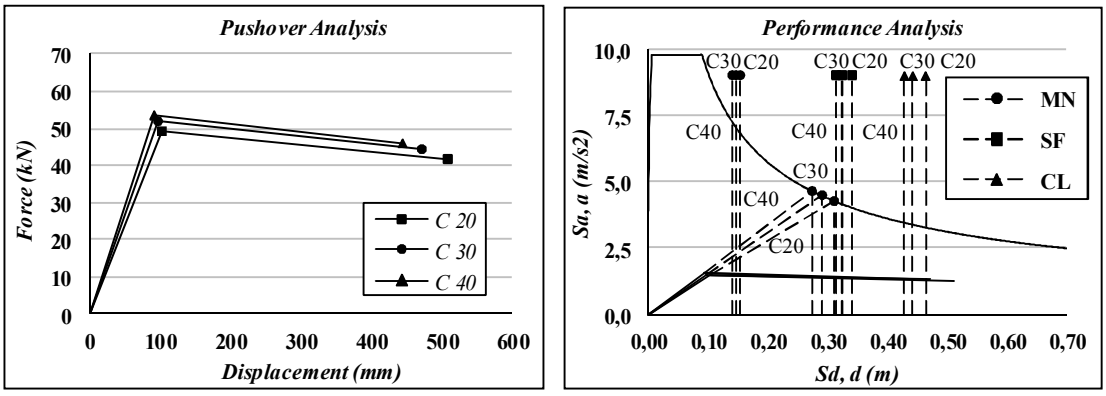

(a) (b)

Figure 3.9. Pushover analyses (a) and comparison of the seismic performances (b) of 9-m-long reinforced concrete columns (Type 6a cross-section), which have different concrete classes under the axial load of 335 kN.

Although there are some minor differences in the capacity curves of the columns which have different concrete classes, it can be seen that the performance points are corresponding to the same damage state for all three columns (See Table 3.4). The main

reason is having similar moment-curvature relationships for all three columns since the axial load ratio is relatively small (Ersoy, 1985).

Table 3.4. Seismic performance comparison of the reinforced concrete columns which have different concrete class.

Concrete Class	T (sn)	M_y (kNm)	M_u (kNm)	Δ_{MN} (mm)	Δ_{SF} (mm)	Δ_{CL} (mm)	S_{di} (mm)	Damage State
C20	1.69	478.4	544.7	154.4	341.1	464.6	310.7	Moderate
C30	1.60	498.5	557.8	145.9	323.9	443.4	289.8	Moderate
C40	1.53	512.3	565.9	139.8	312.8	429.3	274.7	Moderate

In addition, when the column interaction curves are investigated, it can also be stated that these types of columns are acting like beams since the ultimate moment capacities are under the balanced point even against an axial load bigger than the load under which the seismic performance of the column corresponds to the Collapse Limit (See Figure 3.10).

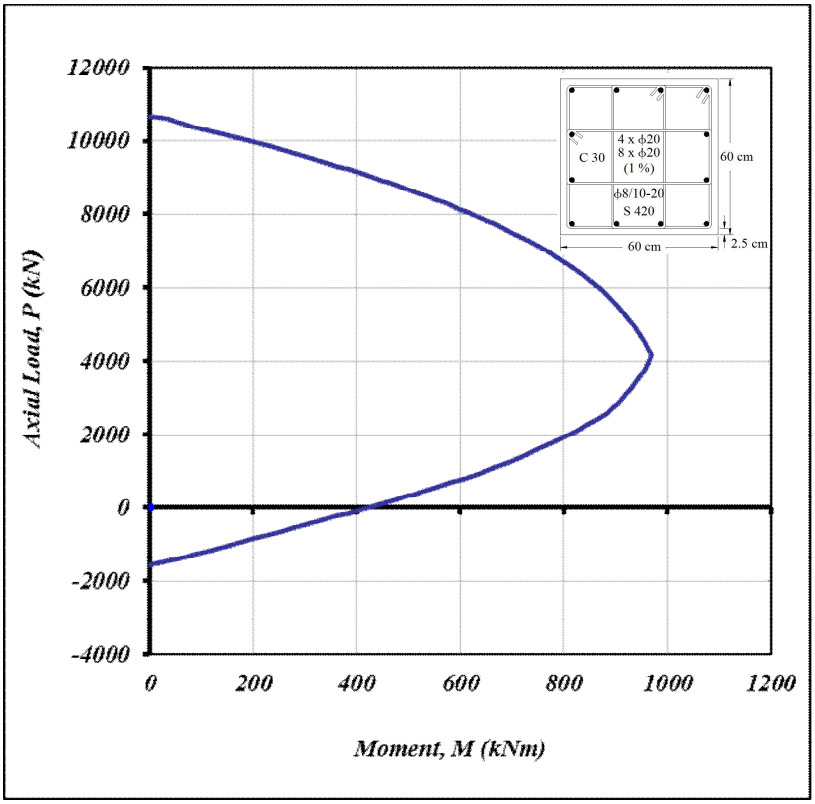

Figure 3.10. Column interaction curve of Type 6a cross-section.

In conclusion the structural parameters of the rapid earthquake loss estimation tool recently developed, were determined as earthquake zone, soil class, height of the column, cross-sectional properties, and also axial load which is related to longitudinal reinforcement ratio, transverse and longitudinal bay widths, roof structure, and roof covering. Table 3.5 shows the structural parameters used to calculate PML values in this study.

Table 3.5. Structural data collection table for the proposed loss estimation method.

<table>
<tr><td>Column Cross-section (cm)</td><td>Reinforcement Ratio</td><td>No of Span</td><td>Transverse Bay Width (m)</td><td>Longitudinal Bay Width (m)</td><td>Column Height (m)</td></tr>
<tr><td>☐ 35×35
☐ 40×40
☐ 45×45
☐ 50×50
☐ 55×55
☐ 60×60
☐ 70×70
☐ 80×80</td><td>☐ Min.
☐ Moderate
☐ High</td><td>☐ =1
☐ ≥2</td><td>……
(10-30)</td><td>……
(6-24)</td><td>……
(5-12)</td></tr>
<tr><td colspan="3">Roof Bearing System</td><td colspan="3">Roof Cover</td></tr>
<tr><td rowspan="2">☐ Precast Beam
☐ Steel Beam
☐ Space Truss
☐ Steel Truss</td><td>Gutter Beam</td><td>Purlin</td><td>☐ Sandwich Panel</td><td colspan="2">Insulation</td></tr>
<tr><td>☐ Precast
☐ Steel
☐ None</td><td>☐ Precast
☐ Steel
☐ None</td><td>☐ Corrugated Cement
☐ Trapezoidal Metal Sheet
☐ Metal Sheet</td><td colspan="2">☐ Polyurethane
☐ Rockwool
☐ Glasswool</td></tr>
</table>

3.6. Structural Loss Estimation Curves

The initial step in drawing the proposed structural loss estimation curves is to identify the critical mass values which will lead to the top displacements (Δ_{Damage}) corresponding to all three damage thresholds; these values are obtained from the non-linear structural performance analysis method as described in Section 3.4. Once the critical value of natural vibration period is found, the corresponding axial load is recorded as the critical weight.

3.6.1. Critical Mass Calculation

Critical mass calculation can be defined as finding the mass which will create the top displacement corresponding to all three damage limits by using non-linear structural performance analysis method proposed in TSDC07 by keeping constant the parameters, such as column cross-section properties, longitudinal reinforcement ratio, and height of the column. Since the natural vibration period of the building changes when the mass of the structure changes, the inelastic displacement demanded by the same seismic risk will also change. In this situation, the problem can be simplified as finding the axial load which will create the same lateral displacement with the limit displacements corresponding to the damages levels which were determined by using moment-curvature analyses. An iterative process has been followed in order to find the best natural vibration period couples since for every change in the mass, the limit displacements corresponding to different damage thresholds are also changing according to the moment-curvature relationships. After the critical value of natural vibration period had been found, the corresponding axial load was recorded as the critical weight.

For a system of which the natural vibration period T is longer than the spectrum characteristic period T_S, the critical vibration period is calculated as follows:

$$\Delta_{Damage} = S_{di} = S_{de} = \frac{S_{ae}}{\omega^2} \qquad (T > T_S) \quad \omega_S^2 = \left(\frac{2\pi}{T_S}\right)^2 \tag{3.20a}$$

$$\frac{\phi_y L^2}{3} + L_p\left(\phi - \phi_y\right)\left(L - \frac{L_p}{2}\right) = \frac{S_{ae}}{\left(\frac{2\pi}{T}\right)^2} \qquad \left(T > T_S\right) \tag{3.20b}$$

where, S_{ae} is the elastic spectral acceleration calculated according to TSDC07, and ω is the natural frequency.

Since P-Δ effects have also been considered during the calculations, the new stiffness value was used according to the changes in the axial load and also corresponding top displacement. In addition, when the new ultimate displacement value, which was

calculated by considering the decrease in the strength, is smaller than the one corresponding to Collapse Limit, then it was accepted as the collapse displacement (Δ_{CL}). The differences caused by P-Δ effects are summarized in Table 3.6. The most important one among these differences is having different damage states according to P-Δ effects. The damage state in the column cross-section could be ‘’Complete’’ if P-Δ effects are also considered while the damage state is ‘’Extensive’’ if P-Δ effects are neglected.

Table 3.6. The differences caused by P-Δ effects for 10-m-long reinforced concrete columns (Type 6a cross-section) under the axial load of 465 kN (which is subject to 1. Earthquake Zone and Z3 Soil Class conditions).

P-Δ Effect	T (sn)	V_y (kN)	V_u (kN)	Δ_{MN} (mm)	Δ_{SF} (mm)	Δ_{CL} (mm)	Δ_u (mm)	S_{di} (mm)	a_y (m/s^2)
No	2.13	52.51	57.78	181.0	382.4	517.8	519.9	409.3	1.11
Yes	2.26	46,59	33.60	181.0	382.4	409.1	409.1	439.8	0.98

During the calculations for finding critical mass values, a special computer program has been developed to achieve the iteration steps since moment-curvature relationship and effective flexural stiffness is changed according to the changes in axial load and also the natural vibration period and ultimate displacement are changed when P-Δ effects are also taken into considerations. The mass values were assumed as in between 1 kg and 300 kg and this interval was decreased when the inelastic displacement values demanded by the scenario earthquake has approached to the displacement values corresponding different damage states. The iteration process has been ended when the difference between the lateral displacement under a specific axil load and the displacement corresponding to the damage states is equal to % 0.1 or smaller. Table 3.7 shows sample outputs of the program developed for calculating the critical weight corresponding to the height of 9 m for the reinforced concrete column, which has Type 6a cross-sectional properties. The elastic spectrum curve used for the earthquake demand was corresponding to 1. Earthquake Zone and Z3 Soil Class.

Table 3.7. The example of critical mass determination for 9-m-long reinforced concrete column, which has Type 6a cross-sectional properties and is subject to 1st Earthquake Zone and Z3 Soil Class conditions.

No	T (sn)	Axial Load (kN)	Axial Load Ratio (%)	M_y (kNm)	M_u (kNm)	ϕ_y (rad/m)	ϕ_{Damage} (rad/m)	Δ_{Damage} (mm)	S_{di} (mm)
1	0.265	9.810	0.09	429.72	503.65	0.00313	0.02105	132.1	17.39
2	0.910	113.7	1.05	451.74	521.54	0.00329	0.02126	136.5	147.4
3	0.667	61.73	0.57	440.49	512.88	0.00321	0.02115	134.2	101.6
4	0.797	87.69	0.81	446.00	517.30	0.00325	0.02121	135.3	125.8
5	0.855	100.7	0.93	448.78	519.50	0.00327	0.02123	135.9	136.8
6	0.826	94.18	0.87	447.54	518.25	0.00326	0.02122	135.6	131.4
7	0.841	97.43	0.90	448.19	518.81	0.00326	0.02122	135.8	134.1
8	0.848	99.05	0.92	448.63	519.10	0.00327	0.02123	135.9	135.5
9	0.852	99.86	0.92	448.89	519,19	0.00327	0.02123	135.9	136.2
10	**0.850**	**99.46**	**0.92**	**448.48**	**519.35**	**0.00326**	**0.02123**	**135.8**	**135.8**
11	1.512	302.1	2.80	491.59	552.57	0.00358	0.08838	321.8	271.2
12	1.766	403.5	3.74	512.50	568.43	0.00373	0.08943	328.3	326.8
13	1.884	454.1	4.20	522.94	576.17	0.00381	0.08998	331.6	353.1
14	1.826	428.8	3.97	517.53	572.46	0.00377	0.08970	329.9	340.1
15	1.796	416.1	3.85	515.15	570.32	0.00375	0.08956	329.1	333.4
16	1.781	409.8	3.79	513.60	569.53	0.00374	0.08950	328.6	330.1
17	**1.774**	**406.6**	**3.77**	**513.15**	**568.93**	**0.00374**	**0.08946**	**328.5**	**328.5**
18	2.023	516.5	4.78	535.75	585.61	0.00390	0.13352	364.4	384.6
19	1.901	461.5	4.27	524.40	577.34	0.00382	0.13588	409.1	356.9
20	1.962	489.0	4.53	529.87	581.64	0.00386	0.13510	385.5	370.8
21	1.993	502.7	4.65	532.81	583.64	0.00388	0.13430	374.5	377.7
22	1.978	495.9	4,59	531.35	582.62	0.00387	0.13471	379.8	374.3
23	1.985	499.3	4.62	53221	583.02	0.00387	0.13455	376.7	376.0
24	1.989	501.0	4.64	532.34	583.43	0.00387	0.13438	376.1	376.9
25	**1.987**	**500.2**	**4.63**	**532.36**	**583.16**	**0.00388**	**0.13449**	**376.1**	**376.4**

3.6.2. Drawing Structural Loss Estimation Curves

The other critical mass values were calculated with the same methodology by increasing the height of the columns for every 25 cm between 5 and 7 m and for every 1 m in between 7 and 12 m. All these critical mass values were used to draw structural loss estimation curves together with the corresponding column heights after converting these values to the critical weight values (See Figure 3.11).

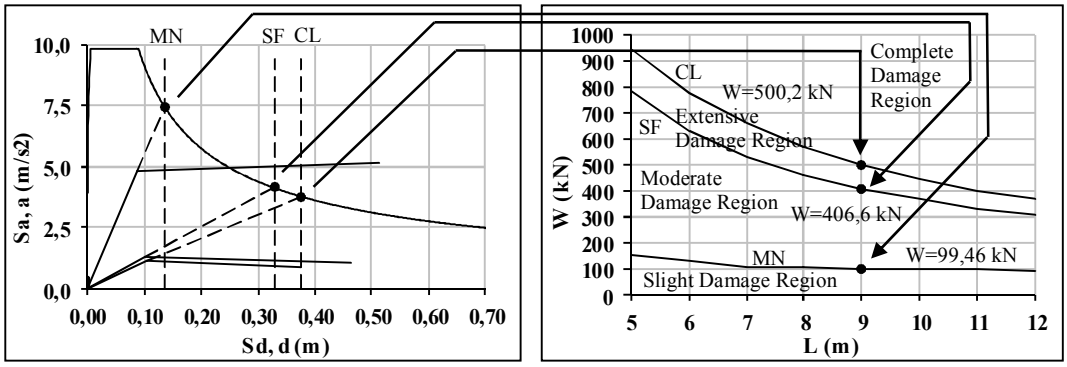

Figure 3.11. The graphical representation of drawing structural loss estimation curve for a reinforced concrete column: 60×60 cm cross-section, 1 % reinforcement ratio, 1st Earthquake Zone and Z3 Soil Class.

Using the same procedure, column height-axial load couples were calculated separately for all 24 types of column cross-sections, for 4 different earthquake zones and 4 soil classes. As the result, 384 different structural loss estimation cures were obtained. All these curves can be found in Appendix B.

It should also be noted that the structural loss estimation curves were developed only for assessing the structural performance of an existing structure. Thus it is not suitable to use these curves during the structural design phase. Moreover, the minimum requirements for the reinforced concrete structures defined in TSDC07 should also be checked together with these curves. As one of the most important requirements, the maximum axial load could be lower than the defined weight values especially for the big-sized cross-sections exposed to considerably low earthquake demand (corresponding to 4th Earthquake Zone in Turkish Earthquake Zoning Map). The maximum axial loads changing according to the column cross-sections can be calculated by using the following formula (TSDC07):

$$N_{dm} \leq (0.5) A_c f_{ck} \tag{3.21}$$

where, N_{dm} is the axial load; A_c is the area of the cross-section; f_{ck} is the characteristic compressive strength.

The maximum axial load values calculated according to the different cross-sections within the inventory of this study are given by Table 3.8. It is also worth mentioning that the values of structural weight exerted on the critical column of the single-storey reinforced concrete industrial buildings are generally changing between 50 kN and 600 kN which are considerably low when we compare with the maximum allowable axial loads according to TSDC07. This also means that, the damage states of these industrial building are at ‘’Slight’’ damage state especially for the 4th Earthquake Zone without using structural loss estimation curves in detail. Still, the structural loss estimation curves belonging to all different cross-sections were drawn although the seismic demand is at the low levels (See Tables B.9, B.10, B.13, B.14, B.15, and B.16 in Appendix B).

Table 3.8. The maximum axial loads calculated according to the different cross-sections.

Cross-section (cm)	Maximum axial load allowed by TSDC07 (kN)
35 × 35	1837.5
40 × 40	2400
45 × 45	3037.5
50 × 50	3750
55 × 55	4537.5
60 × 60	5400
70 × 70	7350
80 × 80	9600

3.6.3. Investigating Weaknesses at Column-Beam Connections of Precast Concrete Structures (Heavy Roof Structures)

Although the scope of this study has been limited to damage caused by the lateral displacements of columns during the structural loss estimation, damages caused by weak column-beam connections in the precast concrete structures have also been observed during the site investigations (Zorbozan, *et al.,* 1998). Therefore, it is suggested to conduct safety analysis at the column-beam connections by taking additional information for the connection details before using the structural loss estimation curves to estimate PML values for the precast concrete structures **(**Heavy roof structures) according to the proposed method. In this section, a method, which shows how to take into consideration of the shear failure risk at the column-beam connections for this type of structures, is also proposed.

One of the main reasons for damages at the column-beam connections is exceeding the shear capacity of the steel rods under the seismic forces (Şenel, *et al.,* 2013). Figure 3.12 shows a typical shear failure of a precast concrete structure.

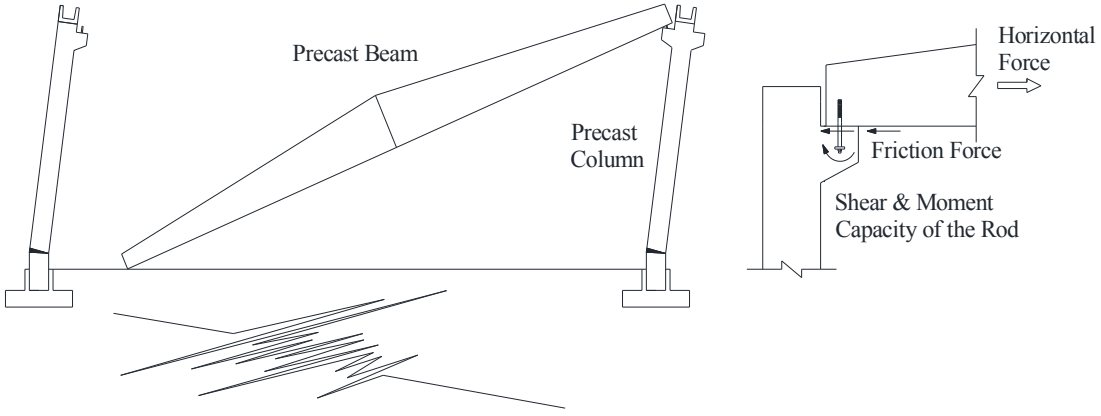

Figure 3.12. Graphical demonstration of shear failure of a precast concrete structure (Şenel, *et al.,* 2013).

According to the previous studies (Şenel, *et al.,* 2013), it has been stated that shear failure mechanism is close to the real behavior of the connections and bending failure mechanism is not expected. Therefore, the proposed method comprises controlling the shear capacity at the column-beam connections against horizontal force demanded by the earthquake. The shear capacity of the steel rods can be found by using Equation 3.22 as proposed by Park and Pauley (1975).

$$V_d = \frac{A_s f_y}{\sqrt{3}} \tag{3.22}$$

where, V_d is the shear capacity of the steel rod; A_s is the area of the cross-section of steel; f_y is the yield strength of steel.

The horizontal force, F_h exerting to the column-beam connection during an earthquake can be calculated as the following;

$$F_h = m_{roof} S_{ae} \tag{3.23}$$

where, m_{roof} is the mass of the roof excluding column weight; S_{ae} is the elastic spectral acceleration calculated according to TSDC07.

In order to estimate if there would be a shear failure or not, the horizontal force can be simply compared with the shear capacity of the steel rods by neglecting the friction force. If the force is higher than the capacity, it can be assumed that the beam would collapse and eventually the damage state can be assessed as ‘’Complete’’.

According to the site investigations, it was observed that the number of rods used for column-beam connections in general is two. In addition steel rods with diameters of 20 mm are widely used (Şenel, *et al.,* 2013). The shear capacity of a 20 mm diameter steel road can be calculated as the following;

$$V_d = \frac{\left[\pi (10)^2\right] \times (420)}{\sqrt{3}}$$
$$= 76.2 \text{ kN}$$

If we assume that there exists two rods at the connection, then the total shear capacity at the column-beam connection will be equal to 152.4 kN.

In order to find the horizontal force exerting to the column-beam connection during a major earthquake, the same sample building which was shown in Figure 3.4 is selected by

assuming it was constructed on 1st Earthquake Zone and Z3 Soil Type conditions. The mass of the roof can be calculated by simply subtracting the weights of gutter beam and half length of the column from the total weight exerting to the column as follows:

$$m_{roof} = \frac{(26.4+110+123.2)}{g} = \frac{159.6}{g} \text{ kg}$$

Spectral acceleration can be calculated by using Equations 3.18 and 3.19:

$$S_{ae}(T) = (0.4)\times\left[(0.4)\times\left(\frac{0.6}{1.60}\right)^{0.8}\right]g$$
$$= (0.46)\,g$$

Finally, the horizontal force can be calculated as the following:

$$F_h = \left(\frac{159.6}{g}\right)\times(0.46)\,g$$
$$= 73.4\ kN$$

When we compare the horizontal force with the shear capacity of the steel rod, it can be stated that even one rod is sufficient to prevent shear failure at the column-beam connection (73.4 kN < 76.3 kN). Since two rods are used for this type of connections in general, then the connections would be even safer (The shear capacity will be 152.4 kN).

Moreover, the analytical studies conducted to investigate structural safety at the connections of single-storey precast industrial buildings have shown that the horizontal forces demanded by the earthquake decreases when the building period increases and even one rod prevents the shear failure for such structures. It was also added that there was not any problem at the connections provided by using two steel rods (Şenel, *et al.,* 2013).

Thus, shear failure control can be conducted by using the proposed method after gathering the required data (the number of steel rods and also the diameter) during the site surveys before using the structural loss estimation curves developed. If it is detected that there is no rod at the column-beam connections, then the structural damage state could be taken as equal to ‘’Complete’’ without using any loss estimation techniques.

3.7. Fragility Curves

Fragility curves are lognormal functions that describe the probability of reaching or exceeding a damage state for a given ground motion indicator as, for example, peak ground acceleration, spectral acceleration S_a or spectral displacement S_d here, the spectral displacement is used as the input parameter. These curves take into account the variability and uncertainty associated with the capacity curve properties, damage states and ground shaking (Kircher, *et al.,* 1997b).

The fragility curves generally distribute structural damage among Slight, Moderate, Extensive and Complete damage states. For any given spectral displacement, the exceeding probability of a specific damage state can be calculated as the difference of the cumulative probabilities of the successive damage states. The sum of the probabilities corresponding to the various damage states for a given spectral displacement will be 100 % (FEMA, 2001).

FEMA (2001) defines the conditional probability of being in, or exceeding, a particular damage state, *ds*, given the spectral displacement S_d as:

$$P\left[ds \middle| S_d\right] = \Phi\left[\frac{1}{\beta_{ds}} \ln\left(\frac{S_d}{S_{dm,ds}}\right)\right] \tag{3.23}$$

where $S_{dm,ds}$ is the median value of spectral displacement at which the building reaches the threshold of damage state, d*s*; β_{ds} is the standard deviation of the natural logarithm of spectral displacement for damage state, *ds* and Φ is the standard normal cumulative distribution function.

3.7.1. Drawing Fragility Curves

In this study, the median spectral displacement values and lognormal standard deviation values for the Minimum Damage Limit, Safety Limit, and Collapse Limit were calculated based on the results obtained via the pushover analyses, as per explained in Section 3.3, of all the buildings in the portfolio. Since fragility curves are tailored for the

assessment of the damage potential for a given set of buildings instead of precise individual risk assessment, various fragility curves have been produced according to the type of the structure and also the reinforcement level in order to improve their reliability for individual building risk assessment. Table 3.9 summarizes the structural fragility curve parameters of single-storey reinforced concrete industrial buildings in Turkey for two different design levels as per defined in HAZUS (1997).

Table 3.9. Structural fragility curve parameters of single-storey reinforced concrete industrial buildings for two different seismic design levels (Minimum and High-Code).

Type of the Structure	Seismic Design Level	Spectral Displacements (m)					
		Minimum Damage Limit		Safety Limit		Collapse Limit	
		Median	Beta	Median	Beta	Median	Beta
General	Mixed	0.1223	0.363	0.2656	0.263	0.3378	0.262
Precast Concrete (Heavy Roof)	Minimum	0.1285	0.328	0.2792	0.248	0.3262	0.274
	High-Code	0.1793	0.489	0.3412	0.347	0.4189	0.347
Reinforced Concrete (Light Roof)	Minimum	0.1060	0.292	0.2549	0.228	0.3574	0.213
	High-Code	0.1246	0.217	0.2819	0.147	0.3755	0.151

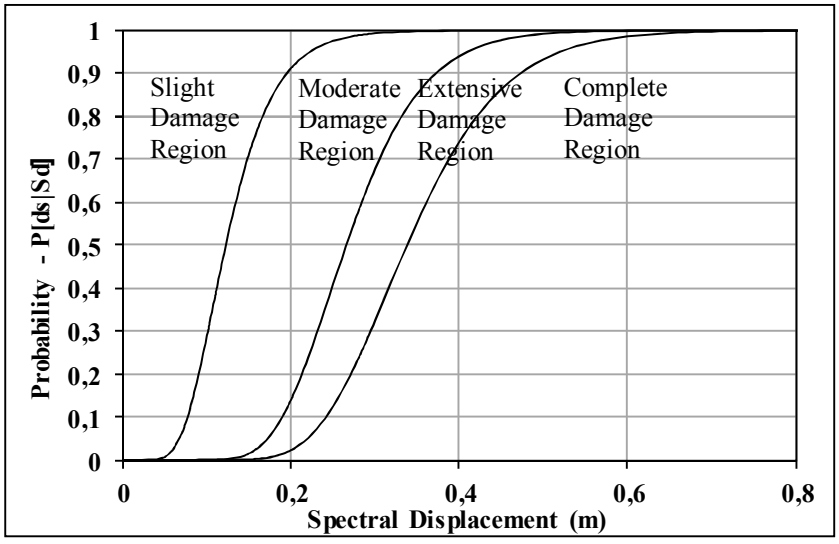

Figure 3.13. Structural fragility curves for single-storey reinforced concrete industrial buildings designed to various seismic design levels.

While Figure 3.13 shows sample fragility curves drawn according to the parameters calculated for the entire portfolio, Figures 3.14 and 3.15 show the diversified fragility curves according to more granular structural information.

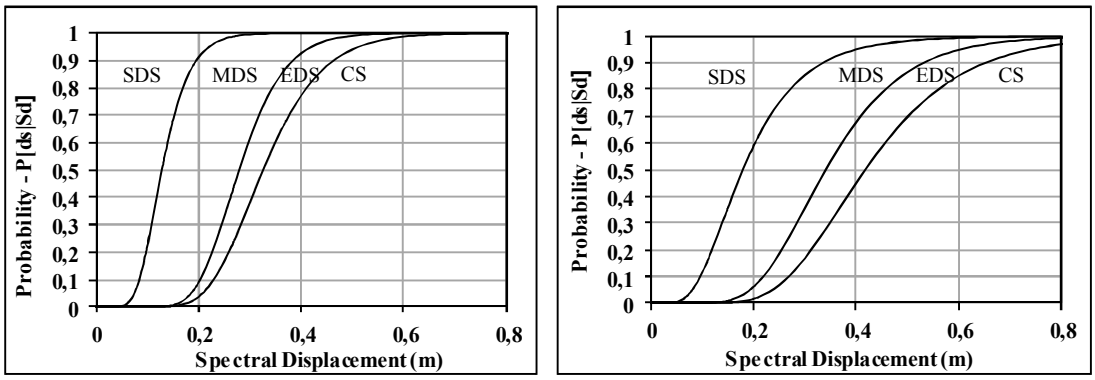

a) Minimum Design Level b) High-Code Design Level

Figure 3.14. Fragility curves for the single-storey precast concrete (Heavy roof structures) industrial buildings.

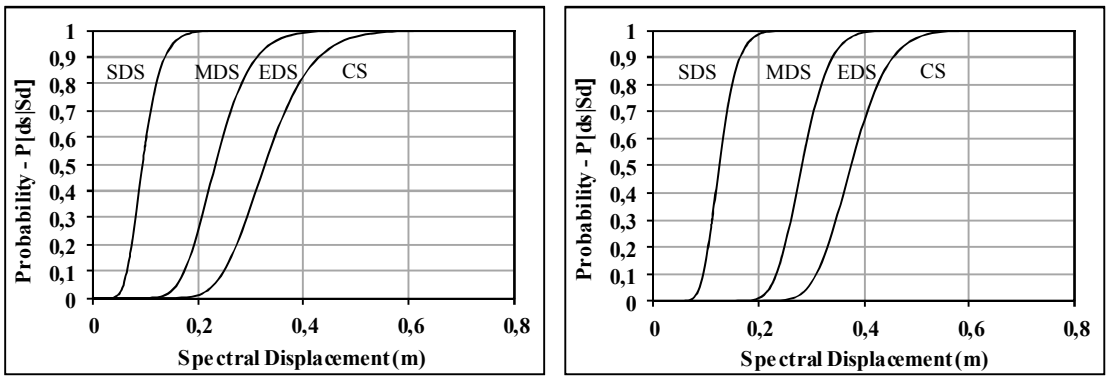

a) Minimum Design Level b) High-Code Design Level

Figure 3.15. Fragility curves for the single-storey reinforced concrete (Light roof structures) industrial buildings.

3.8. Comparison of Results Obtained Using Structural Loss Estimation Curves and Fragility Curves

PML estimation analyses are conducted in order to measure the speed and the reliability of the proposed structural loss estimation curves for 4 different industrial buildings which were selected from the building inventory; the properties of these

structures are summarized in Table 3.10. The selected buildings are all in the 1st Earthquake Zone (PGA = 0.4g), with two of them (1 and 2) built on Z3 type soil whereas the other two (3 and 4) are built on Z2 type soil according to TSDC07.

Table 3.10. Architectural and structural properties of the selected industrial buildings.

No	Column Section (cm)	Span Length (m)	Bay Width (m)	*L* (m)	Roof System			Axial Load (kN)
					Bearing System		Covering	
1	60 x 60 (ρ= %1)	(≥2) 14	11	6	Steel Beam IPE550	Steel Purlin	Sandwich Panel (Rockwool)	89
2	60 x 60 (ρ= %1)	(≥2) 25	8	12	Precast Beam	Precast Purlin	Metal Sheet (Rockwool)	313
3	50 x 50 (ρ= %1)	(≥2) 15	7.5	7.75	Precast Beam	Precast Purlin	Sandwich Panel (Polyurethane)	152
4	50 x 50 (ρ= %1)	(≥2) 28	10	8	Precast Beam	Precast Purlin	Sandwich Panel (Polyurethane)	389

After the axial load on the critical columns are calculated, structural loss estimation curves specific to the type of the column cross-sections, earthquake zone and soil class is used to estimate the structural damage state. This is easily done by finding the intersection point of the curve parameters, height of the column and axial load (See Figure 3.16). The central damage ratios corresponding to the damage states estimated were accepted as the PML values.

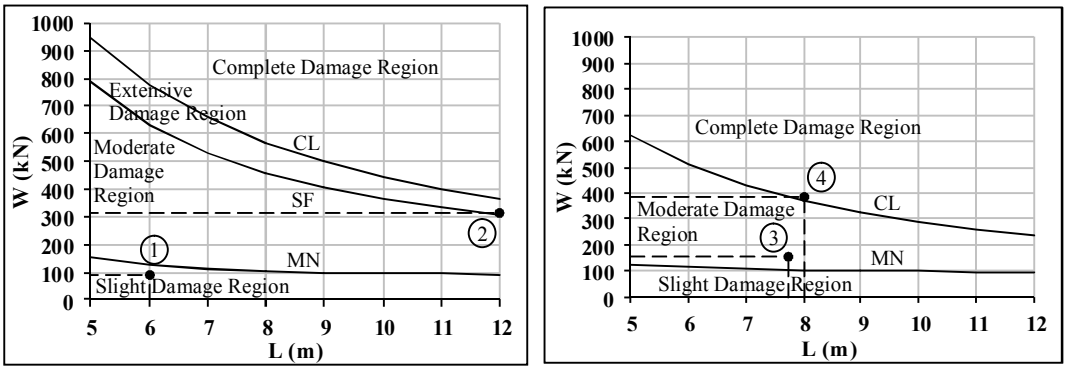

a) Type 6a Loss Estimation Curve (E1 Z3) b) Type 4a Loss Estimation Curve (E1 Z2)

Figure 3.16. Demonstration of PML estimation for the sample buildings selected by using analytical structural loss estimation curves developed.

In order to use the fragility curves as a PML estimation tool, it is essential to know the average natural vibration period of the buildings since the spectral displacement demand is calculated via this information. Therefore such fragility curves can be used for PML estimation only if the corresponding natural vibration periods are provided as well. Table 3.11 shows the average natural vibration periods of the buildings used to draw the aforementioned fragility curves.

Table 3.11. Natural vibration periods of the inventory buildings according to the type of the structure and seismic design level.

Type of the Structure	Seismic Design Level	Average Natural Vibration Period (sn)
General	Mixed	1.187
Precast Concrete *(Heavy roof)* Structures	Minimum	1.508
	High-Code	1.208
Reinforced Concrete *(Light roof)* Structures	Minimum	0.629
	High-Code	0.718

For PML estimation via fragility curves, inelastic spectral displacement demands for each of the selected buildings are calculated using the design spectrum defined in TSDC07 and the periods given in Table 7. Then the exceedence probabilities corresponding to each damage state for each of the given spectral displacements are read from the fragility curves (See Figure 3.17). For the buildings 1 and 2, which were located in the 1st Earthquake Zone and are subject to Z3 Soil Class conditions, the PML values were calculated by using the exceedence probabilities and corresponding damage states as below;

$$PML = 0.01\times(0.05)+0.54\times(0.3)+0.20\times(0.7)+0.24\times(1) = 54.9\ \%\ \text{(heavy roof)} \quad (3.24a)$$

$$PML = 0.49\times(0.05)+0.51\times(0.3)+0.00\times(0.7)+0.00\times(1) = 17.8\ \%\ \text{(light roof)} \quad (3.24b)$$

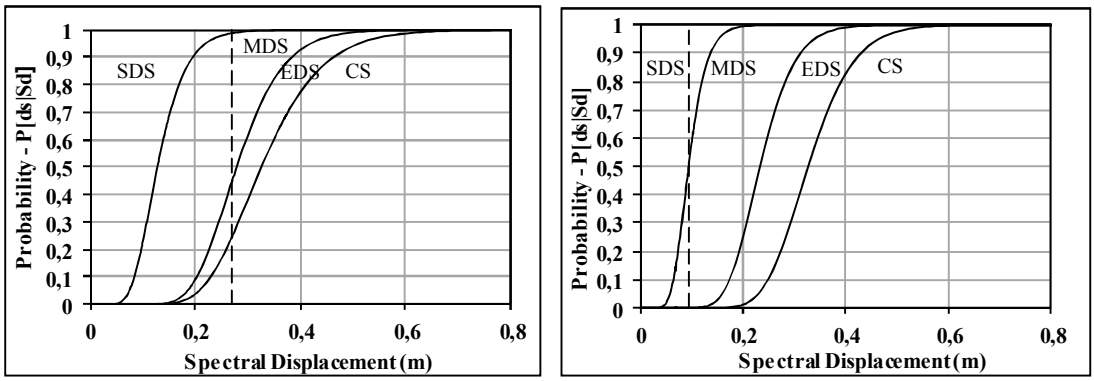

a) Single-storey precast concrete (heavy roof) structures

b) Single-storey reinforced concrete (light roof) structures

Figure 3.17. Fragility curves for the single-storey reinforced concrete industrial buildings (at minimum design level) located in the 1st Earthquake Zone and are subject to Z3 Soil Class conditions.

For the buildings 3 and 4, which were located in the 1st Earthquake Zone and are subject to Z2 Soil Class conditions, the PML values were calculated by using the exceedence probabilities and corresponding damage states similarly (See Figure 3.18) as below;

PML= 0.10×(0.05)+0.82×(0.3)+0.04×(0.7)+0.03×(1) = 31.3 % (Minimum Design) (3.24c)

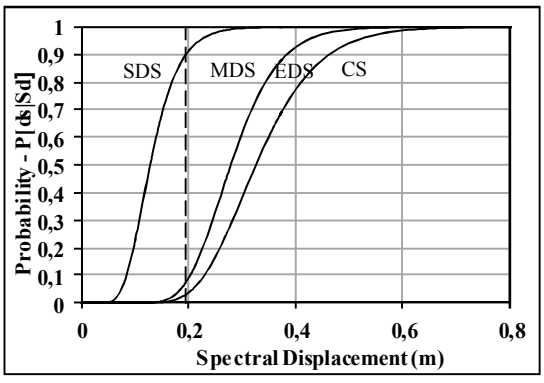

Figure 3.18. Fragility curves for the single-storey precast concrete (Heavy roof structures) (at minimum design level) located in the 1st Earthquake Zone and are subject to Z2 Soil Class conditions.

3.9. Comparing Results with Existing Loss Estimation Methods

For comparison purposes, the following methods, which were previously proposed, are employed to calculate the PML values, first for the four selected buildings and then for the rest of the buildings within the inventory.

3.9.1. John Freeman's Method

Earthquake loss estimation studies or PML estimates began with the classical book, *Earthquake Damage and Earthquake Insurance*, of John Freeman (Freeman, 1932). Within the content of the book, structural lessons and loss ratios for the past destructive earthquakes were reported. Probable average loss ratios for certain type of structures, which were estimated by John Freeman's judgment, were listed in a table in this book (See Table 3.12). The ratios in the mentioned table are the expected average loss ratios for mainly insurance purposes. There are also some proposals for increasing or decreasing this average PML values by applying some modifiers according to soil type and the structural conditions.

Table 3.12. Probable maximum loss (PML) for building classes according to John Freeman's Method (Freeman, 1932).

Class of Construction	Expected Average Loss Ratio
1. Steel-frame buildings on reinforced concrete mat foundation, having rigid cross-bracing, with strong gusset plates uniting columns to strong horizontal girders between windows, with curtain walls of reinforced concrete poured around the steel frame, and with ordinary interior finish. Not more than 100 feet tall. (Expected damage, chiefly cracked plaster.)	3 %
2. Tall steel-frame buildings with less-rigid cross-bracing than Class 1, with ordinary brick curtain walls and rock –concrete floors and uncertain foundations. Not more than 100 feet tall.	5 %
3. Tall reinforced concrete buildings without riveted or welded structural steel-frame and with ample strength at column connections and having ample horizontal cross-bracing by walls around windows, particularly in first story. Not over than 100 feet tall.	8 %
4. Wood –frame dwellings, set on good foundation walls (not on posts or slender piers), not above 2½ stories high, excluding stucco exteriors. (Expected damage chiefly cracked plastering and chimneys.) If on tall posts or slender piers the loss ratio will probably be 5 to 10 times as great.	3 %
5. Factory buildings of good design having bearing walls of brick in cement mortar, or of reinforced concrete. Strong wood floors, with little expensive interior finish. No plastered walls or ceilings. Not more than 4 stories tall.	5 %

Table 3.12. Probable maximum loss (PML) for building classes according to John Freeman's Method (Freeman, 1932) (cont.).

Class of Construction	Expected Average Loss Ratio
6. Ordinary brick residence, mercantile and office buildings, of excellent design with brick bearing walls and wood floors. General average of unrated risks not exceeding 2½ stories.	6 %
7. Same as Class 6, but for general average of unrated risks, not exceeding 4 stories.	10 %
8. Brick veneered wood-frame or concrete-frame residence, mercantile and office buildings, or stucco exterior on wood lath, or with hollow-tile partitions.	25 %
9. General average of commercial buildings with reinforced concrete frames and columns, (no steel frame) with curtain walls and partitions of hollow-tile, and large window openings in lower story.	10 % to 20%
10. Buildings of doubtful quality of design and construction, uncertain wall ties, unanchored parapets, uncertain quality of mortar.	20 % to 40 %
11. Concrete-block and hollow-tile buildings.	50 % +

For the application example, it can be assumed that a single-storey reinforced concrete industrial building can be treated as an average commercial building with reinforced concrete columns (no steel frame) which is in Class 9. Then PML values change between 10 % and 20 % for reinforced concrete industrial buildings, with 20 % being the conservative proposal.

3.9.2. Karl Steinbrugge's Method

The work of the Insurance Services Office (ISO) was especially influential, as discussed in Karl Steinbrugge's (1982) famous book, *Earthquake, Volcanoes, and Tsunamis: An anatomy of Hazards*, which was also a breakthrough that Earthquake PML calculation method was firstly told. (Kircher, *et al.,*1997a).

According to the approach proposed by Karl Steinbrugge (Steinbrugge, 1982), firstly a base PML value corresponding to different building classes is determined from the table given within the book (See Table 3.13). Then these base PML values are modified by the certain parameters changing according to the occupancy type, general structural properties, basic soil conditions, and etc.

Table 3.13. Probable maximum loss (PML) for building classes according to Steinbrugge's Method (Steinbrugge, 1982).

Building Class	Summary Description	Class PML (%)
1A, B, C	Wood frame-small, habitation	7
1D	Wood frame-large	15
2A	All metal-small	7
2B	All metal-large	15
3A	Steel frame-superior earthquake (EQ) resistive	20
3B	Steel frame-ordinary	30
3C	Steel frame-other	35
4A	Reinforced concrete-superior EQ resistive	25
4B	Reinforced concrete-ordinary	40
4C	Reinforced concrete-precast	60
4D	Reinforced concrete-other	55
5A	Mixed construction-superior EQ resistive	30
5AA	Mixed construction-ordinary EQ resistive	45
5B	Mixed construction-ordinary non-EQ resistive	70
5C	Mixed construction-hollow masonry, adobe	85
6	Special design for damage control	-

Since the buildings within the inventory of this study can be classified as Class 4C, the corresponding base PML value for this class of buildings is 60 % which can be seen from Table 3.14. Since the selected four sample buildings are subject to soft soil conditions and the occupancy type is manufacturing (-10 % credit) with everything else is average, the PML values may be calculated using damage factors as:

$$PML = 60\times[1+(-10+5+10)/100] = 63\ \% \quad (3.25)$$

3.9.3. ATC-13 Method

In ATC-13 Method intensity based damage probability matrices, which were developed by taking the opinions of more than 70 senior-level earthquake engineering experts for 78 existing facility classes in California including 36 building structure classes, are used for earthquake loss estimation. For each facility class, the experts were asked to provide a low, best, and high estimate of Damage Factors (DF), which means the monetary loss expressed in percentage, at Modified Mercalli Intensities (MMI) VI through XII (McCornack, 1997). The weighted statistics of the expert responses were used to develop probability distributions of the damage factor at every MMI level between VI and XII. In this method, the loss estimation curves are assumed to follow the beta distribution whose parameters depend on MMI and damage probability matrices.

In order to draw the loss estimation curves for the selected buildings, firstly the beta distribution parameters are determined according to the type of the building and the Earthquake Zone. As an example, for standard and low-rise precast concrete buildings with facility class 81 subject to MM IX (1st Earthquake Zone) seismic demand, the beta distribution parameters are 7.16 and 24.4 (ATC, 1985) (See Table 3.14). When the loss estimation curve is drawn by the beta variables, the median value, which is to be accepted as the PML value, is estimated as 22 % (See Figure 3.19).

Table 3.14. Beta Distribution parameters for standard precast concrete construction, low-rise (ATC-13 Facility Class 81) (ATC, 2002).

MMI	λ	v	Mean damage factor (%)	Standard deviation of damage factor (%)
VI	0.70	66.64	1.04	1.23
VII	1.14	50.88	2.19	2.01
VIII	2.75	36.19	7.05	4.05
IX	7.16	24.44	22.66	7.33
X	6.41	10.31	38.34	11.55
XI	6.61	6.56	50.19	13.28
XII	5.25	3.43	60.50	15.72

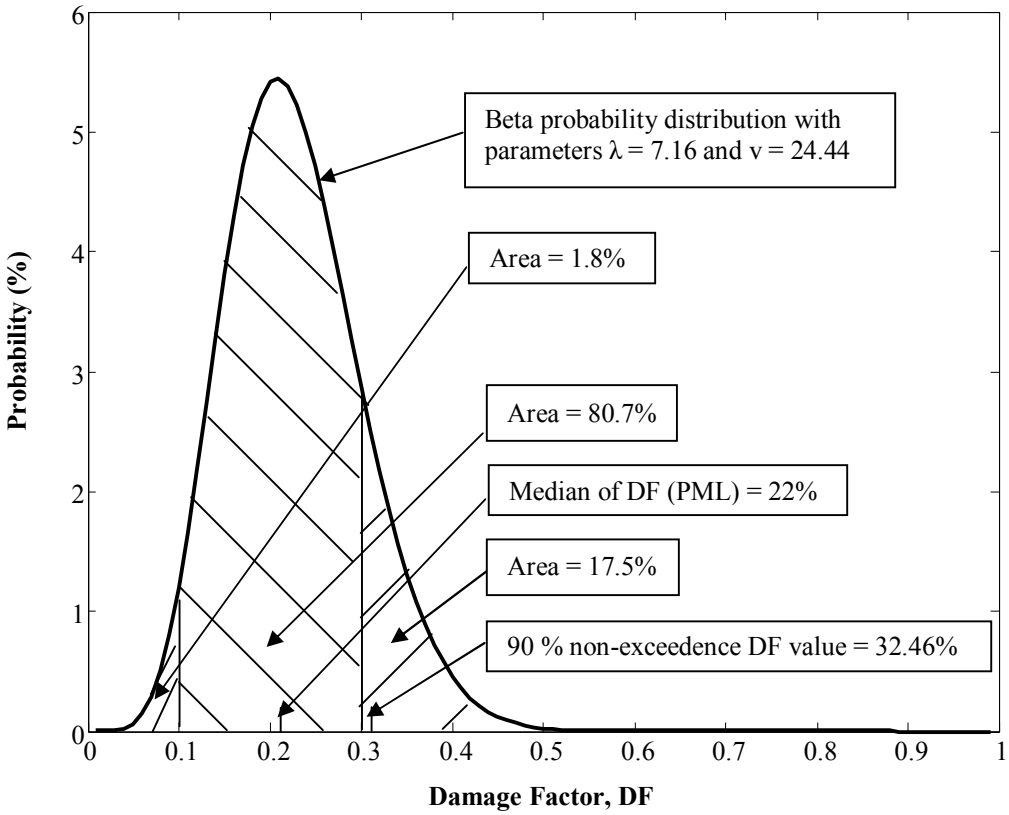

Figure 3.19. Probability distribution of damage for low-rise precast concrete buildings (Facility Class 81) at MMI IX.

The main steps followed during PML calculation according to this method can be summarized as the follows:

- Firstly, the seismic demand has been converted from PGA (in cm/sec^2) to MMI using the relationship of Trifunac and Brady (1975) as follows:

$$\log (PGA) = 0.014 + 0.3 (MMI) \qquad (3.26)$$

$$MMI = (1/0.3) [\log (0.4 \times 980) - 0.014]$$

$$MMI = 8.6 = IX \text{ (by rounding up)}$$

- Then, the building class corresponding to the building inventory of this study was determined as Low-Rise, Standard Precast Concrete Construction, (ATC-13 Facility Class 81)
- Two Beta distribution parameters for this class of buildings subject to shaking of MMI IX are determined as by $\lambda = 7.16$ and $v = 24.44$ from Table 3.14 (ATC, 2002).
- Using these Beta parameters and the Microsoft Excell© statistical function BETAINV, the 90 % non-exceedence damage factor value is found to be 32.46 % and the median damage factor value, which can be used as the PML value, is calculated as 22 % according to the Table 3.15 (Table C-35 given in ATC 13-1).

Table 3.15. Median values of damage factor for standard precast concrete construction, low-rise (ATC-13 Facility Class 81) (ATC, 2002).

MMI	Median value of damage factor (%)	90 % non-exceedence damage factor value (%)
VI	0.61	2.61
VII	1.61	4.86
VIII	6.33	12.55
IX	22.07	32.46
X	37.87	53.72
XI	50.20	67.61
XII	61.34	80.66

3.9.4. FEMA 154 v:2 Method

Following the ATC 13 Report, FEMA published the first edition of the FEMA 154 Report, *Rapid Visual Screening of Buildings for Potential Seismic Hazards: A Handbook*, also known as the ATC-21 report, which describes a rapid visual screening procedure for identifying those buildings which might expose to high structural risk during a severe earthquake. In the first edition of FEMA 154 (ATC-21) Methodology, there is a scoring system (Basic Structural Hazard Scores and Performance Modification Factors) developed by using expert-opinion Damage Probability Matrices from the ATC-13 report and NEHRP ground motion maps (FEMA, 2002).

In 2002, the second edition of FEMA 154 Report (FEMA 154 v:2), *Rapid Visual Screening of Buildings for Potential Seismic Hazards: A Handbook*, was published with the new scoring system which is based on the HAZUS Methodology and fragility curves instead of expert-opinion Damage Probability Matrices from the ATC-13 report. For the ground motion parameters, new seismic design spectral acceleration response values, which were developed by USGS, were used (FEMA, 2002).

The following is a computational example of this method. Assume a single-storey standard precast concrete industrial building which is identified as PC2 in the building classification. Also, assume that there is no vertical or horizontal irregularity and the building was constructed after the code in High Seismicity Region. Then, the Structural Score (S) can be calculated as the follows:

$$S = 2.4 - 0.4 = 2.0 \text{ (for ST C)} \tag{3.27}$$

The final score of the sample buildings selected, all of which have basic score = 2.4 is calculated as 2.0, with the decrease of 0.4 caused by soft soil conditions. This score leads to the PML value of 60 %, which is the limit value for "Complete Damage" State (FEMA, 2002). Table 3.16 summarizes these varying scores and corresponding approximate PML values according to this method.

Table 3.16. FEMA 154 v:2 loss estimation chart.

Soil Type	FEMA 154 Second Edition	
	Scores	PML
SL 2 / C	2.0	60 %
SL 3 / D	1.8	100 %

3.9.5. HAZUS Method

In HAZUS Methodology, the fragility curves drawn by the specific parameters, which were determined after site surveys and individual seismic performance analysis (pushover analyses), are used to perform earthquake loss estimation. Unlike previous

building loss models that are based on Modified Mercalli Intensity, HAZUS Method use quantitative measures of ground shaking and structural analyses (Kircher, *et al.,* 1997b).

HAZUS Method estimates building damage based on threshold values of inter-story drift corresponding different damage states, such as Slight, Moderate, Extensive and Complete. These threshold values of damage states represent generic building types and are not necessarily appropriate for a specific building (FEMA, 2001).

To apply the HAZUS Method, which provides an analytic approach to earthquake loss estimation, the first step is to draw the fragility curves using the median and beta variables defined for precast concrete buildings (PC2L, the building type corresponding to the inventory buildings). These median and lognormal standard deviation (β_{ds}) values were given in *HAZUS Technical Manual* (FEMA, 2001) for Slight, Moderate, Extensive and Complete structural damages states for different kinds of building types designed to different seismic design levels, as well. Table 3.17 summarizes structural curve parameters of Low-Rise Precast Concrete Structures (PC2L).

Table 3.17. Structural fragility curve parameters of low-rise precast concrete structures (PC2L) for two different seismic design levels (High-Code and Moderate-Code) (FEMA, 2001).

Seismic Design Level	Spectral Displacements (inches)							
	Slight		Moderate		Extensive		Complete	
	Median	Beta	Median	Beta	Median	Beta	Median	Beta
High-Code	0.72	0.84	1.44	0.88	4.32	0.98	12.6	0.94
Moderate-Code	0.72	0.96	1.25	1.00	3.37	1.03	9.45	0.88

By using these given parameters, fragility curves of PC2L Building Type were drawn with the help of Microsoft Excell© statistical function NORMSDIST for two different seismic design levels, namely Moderate-Code and High-Code. Then, the inelastic displacement demands for the scenario earthquake (depending on the earthquake zone and soil class) are calculated by using the vibration period values defined in the HAZUS Manual (FEMA, 2001) for this class of buildings and the design spectrum provided in

TSDC07. The exceedence probabilities corresponding to each damage state are read from the fragility curves (See Figure 3.20). PML values for the selected buildings are finally calculated by using the exceedence probabilities and corresponding damage states as follows:

$$PML = 0.17\times(0)+0.18\times(0.05)+0.37\times(0.1)+0.25\times(0.5)+0.03\times(1) = 20\ \% \quad (3.28a)$$

$$PML = 0.26\times(0)+0.21\times(0.05)+0.34\times(0.1)+0.17\times(0.5)+0.01\times(1) = 14.4\ \% \quad (3.28b)$$

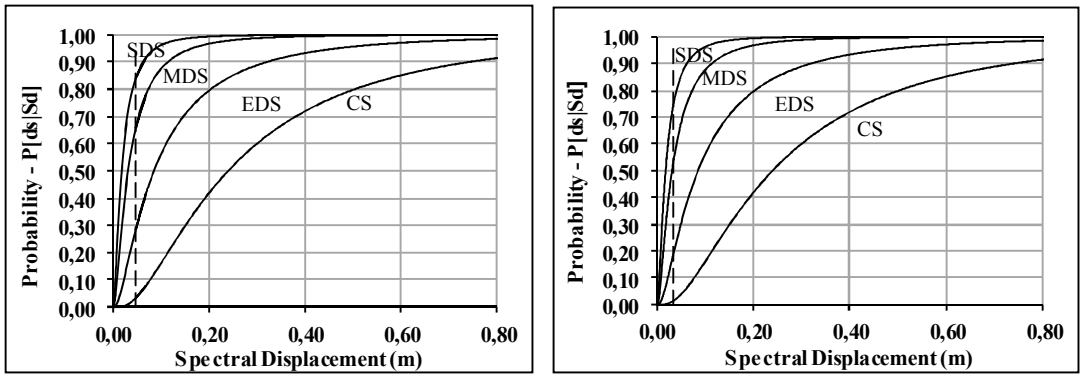

a) For the buildings built on Z3 Soil Type b) For the buildings built on Z2 Soil Type

Figure 3.20. Fragility curves for precast concrete industrial buildings designed to ''Minimum Code'' level (subject to 1st Earthquake Zone).

The results, which are shown in Table 3.18, show considerable differences among the PML values calculated with the proposed method and other existing loss estimation methods. The damage states of the sample buildings selected can change from ''Slight'' to ''Complete (Collapse)'' when the proposed structural loss estimation curves are used. On the other hand, there are no major differences observed in the seismic performances of the selected buildings according to the existing loss estimation methods since their load bearing systems are the same. Another important result of this comparison is that even the PML values calculated via the fragility curves drawn based on data from the inventory buildings, may lead to significantly different results from the ones calculated by using structural loss estimation curves developed.

Table 3.18. Comparison of the results of the analyses conducted by using different loss estimation methods for the sample buildings.

No	Structural Loss Estimation (PML values) (%)						
	John Freeman	Karl V. Steinbrugge	ATC-13	FEMA 154 v:2	HAZUS	Proposed Method	
						Fragility	Risk Based
1	20	63	22	60	20	17.8	5
2	20	63	22	60	20	54.9	70
3	20	63	22	60	14.4	31.3	30
4	20	63	22	60	14.4	31.3	100

The PML values for the other buildings within the inventory were calculated by using the similar calculation methods for each loss estimation technique. In Appendix D, Table D.1 shows the PML values for the entire building inventory comprising 80 single-storey reinforced concrete industrial building. It is also worth mentioning that the average PML values of the John Freeman Method and Proposed method (both fragility and risk based) are nearly the same. This shows that how it is important to investigate real damages by adding also expert opinion before estimating future losses.

It should also be noted that during the calculations, the reinforcement ratios of the buildings of which the exact ratios could not be gathered from the site surveys, were taken as minimum ratio (1 %). In Appendix C, Table C.1 summarizes both structural properties and the axial loads calculated for the each industrial building within the inventory.

3.10. Comparing the Proposed Loss Estimation Method with Damaged Industrial Buildings

It is very important to compare the results of the proposed method recently developed by applying the same methodology on the damaged buildings for determining the sensitivity of the method. In this respect, the PML value has been estimated by using the proposed method on a severely damaged single-storey precast concrete industrial building during 1999 Kocaeli Earthquake after obtaining the detailed structural information

of this building (See Table 3.19). It was stated that the mentioned building had been constructed on 1st Earthquake Zone and subject to Z3 Soil Class (Arslan, *et al.,* 2006).

Table 3.19. Architectural and structural properties of the damaged industrial building (Arslan, *et al.,* 2006).

<table>
<tr><th rowspan="2">Column Cross-section (cm)</th><th rowspan="2">Span Length (m)</th><th rowspan="2">Bay Width (m)</th><th rowspan="2">L (m)</th><th colspan="3">Roof System</th><th rowspan="2">Axial Load (kN)</th></tr>
<tr><th colspan="2">Bearing System</th><th>Covering</th></tr>
<tr><td rowspan="2">35 × 55
(ρ= %1.5)
 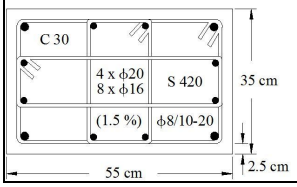
</td><td rowspan="2">(2)
20</td><td rowspan="2">6</td><td rowspan="2">6</td><td>Precast Beam</td><td>Precast Beam</td><td>None</td><td rowspan="2">205</td></tr>
<tr><td colspan="3">(There are 2 different crane beams on the columns located at the middle)</td></tr>
</table>

Before performing structural loss estimation, the weight exerted on the critical column has been calculated by using the following equation:

$$W = \frac{W_{Frame}}{2} + W_{Gutter\ Beam} + \left(2 \times W_{Crane\ Beam}\right) + W_{Purlin} \tag{3.29}$$

The effective area can be calculated by using Equation 3.2:

$$A_e = 6 \times 20 \ = 120\ m^2$$

Then, the weight exerted on the critical column can be calculated as follows:

$$W = \frac{200}{2} + \left(2.6 \times 6\right) + \left[2 \times \left(4.9 \times 6\right)\right] + \left(0.25 \times 120\right)$$

$$W = 204.4 \text{ kN}$$

Since the column cross-section of the mentioned building is not square, there have been two different structural loss estimation curves developed for both longitudinal and transverse bay directions according to the earthquake zone, soil class, and the cross-

sectional properties. The damage state of the building has been determined as ‘’Complete’’, beyond the Collapse Damage Limit by using the axial load and column height parameters on the most vulnerable structural loss estimation curve (See Figure 3.21).

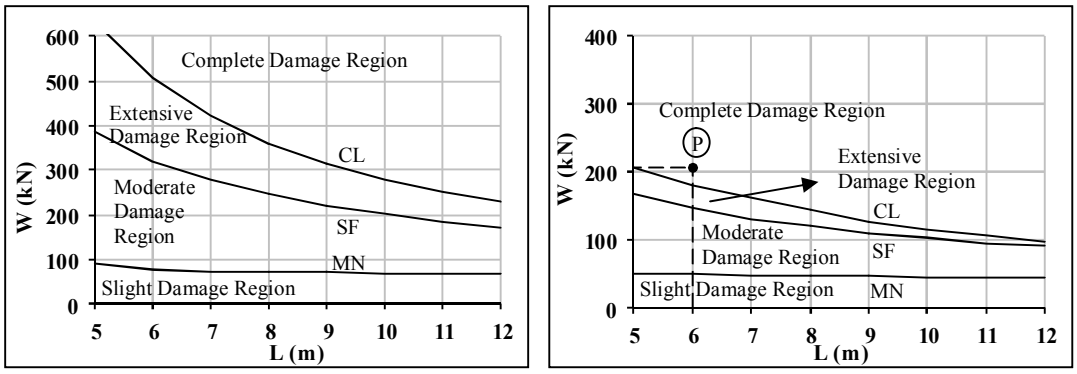

a) Transverse Bay Direction (D1, Z3) b) Longitudinal Bay Direction (D1, Z3)

Figure 3.21. Loss estimation according to the proposed method by using the structural loss estimation curves for the damaged building.

When the damages occurred in single-storey reinforced concrete industrial buildings have been investigated, it was observed that the damages were generally concentrated on the columns located at the middle part of the building if the number of spans is 2 or more. (Arslan, *et al.,* 2006). This information provides that the approach of selecting critical columns during the seismic performance analyses is reasonable. In addition, it was observed that the amount of damages has decreased in the industrial buildings which have bigger size cross-sections (Ozden, *et al.,* 2013). Thus, it can be stated that the properties of the structural loss estimation curves, such as upward movement of the loss estimation curves when the sizes of the cross-sections get bigger and also bigger axial forces are needed for the same damage threshold is in compliance with the data obtained from damaged buildings.

4. EARTHQUAKE INSURANCE RATE CALCULATION

As for the other types of the risks, the insurance rates against earthquake risk could be calculated based on the frequency and the severity of the risk. This corresponds to a conditional probability of damage given a range of earthquake hazard levels. The frequency of earthquakes at a site will be the same for all structures. However the severity of damage will change depending on the structural properties of the building. Hence, severity of damage to different building classes should be considered separately (Deniz and Yücemen, 2009).

4.1. Estimating Earthquake Insurance Rate of a Real Portfolio Comprising Single-Storey Reinforced Concrete Industrial Buildings

In order to calculate the earthquake insurance premium, the possible amount of loss and the probability of occurrence of the scenario event need to be estimated. Multiplying the seismic hazard (*SH*) by the structural loss estimate (PML) gives the base rate (*BR*) (Yücemen, 2005; Yücemen, *et al.,* 2008; Deniz and Yücemen, 2009);

$$BR = SH \times PML \tag{4.1}$$

where, *SH* = annual probability of an earthquake occurring at the site.

In this study, *SH* value is taken as equal to the annual probability of an event with a return period of 475 years, which is the seismic demand considered during the PML estimation studies. It was also assumed that the scenario earthquake follows a homogeneous Poisson process (Faber, 2007);

$$SH = P_A = \frac{1}{475} \tag{4.2}$$

The risk premium (*PRP*) of a property can be calculated by multiplying the base rate (*BR*) with the building insured value (*IV*), calculated as the product of the net floor

area and the pre-defined reconstruction cost per square meter. For simplicity, the insured values of the buildings analyzed in the scope of this study have been considered as equal to 1.000.000 TL.

Since the pure risk premium reflects only the risk of damage, the total insurance premium (*TP*) or the commercial insurance premium that will be charged by an insurance company should be determined to allow for recovery of expenses and profit. For this purpose, in classical studies, the *PRP* is increased by some margin. In the previous studies carried out in Turkey, the corresponding factor was taken as 1.67 (Deniz and Yücemen, 2009). However, the insurance rate charged by a company is a function of its capital and demand from the public and also reinsurance rates which are generally controlled by the foreign reinsurance firms and market conditions (Deniz and Yücemen, 2009). Moreover, the size of the portfolio comprising buildings of a single class is also an important factor in calculating the risk based earthquake insurance premium. Therefore in this study, the reinsurance cost, capital cost and profit are also included in the premium calculations. The formulation used in calculating the earthquake insurance rate can be summarized as follows;

- The amount of annual loss (*AL*) or pure risk premium is calculated for each building by simply multiplying the insured values (*IV*) and the base rates (*BR*):

$$AL = BR \times IV \tag{4.3}$$

- The total annual loss of the portfolio is calculated by adding up annual loss amounts calculated separately for each building.
- Before calculating the reinsurance cost (*RC*), a deductible amount (*D*) was determined. The deductible amount is the limit above which the reinsurance company would be responsible to pay the loss (minus the deductible); it should be kept in mind that there is no need to reinsure if the annual loss is less than the deductible.
- In order to find out the total reinsurance cost, first the pure reinsurance cost (*PRC*) is calculated by subtracting annual loss amounts of each risk which are below the annual deductible amounts from the total annual loss:

$$PRC = \begin{cases} 0 & AL \le D \times P_A \ , \\ \sum_{Portfolio} \left[AL - \left(D \times P_A \right) \right] & AL > D \times P_A \end{cases} \tag{4.4}$$

- Capital cost (*CC*) and some profit (*P*) for the reinsurance company are added to find the total reinsurance cost (*TRC*):

$$TRC = \left[PRC \times \left(1 + CCE \right) \right] \times \left[1 + P \right] \tag{4.5}$$

- The total reinsurance cost is distributed to each building according to the risk based PML values by also paying attention to the loss amount (if it is smaller or higher than the deductible of 10 % of insured value) :

$$RC = \begin{cases} 0 & AL \le D \times P_A, \\ TRC \times \left[\dfrac{AL - \left(D \times P_A \right)}{\sum_{Portfolio} \left[AL - \left(D \times P_A \right) \right]} \right] & AL > D \times P_A \end{cases} \tag{4.6}$$

- The capital cost (*CC*) is calculated by loading certain percentage (*CCE*), namely 10 % in this study, to the annual loss amount of each risk. During these calculations if the annual loss amount is higher than the reinsurance deductible, this time the deductible amount was used as the annual loss amount which will be loaded by the capital cost effect since the loss amount above the deductible would be directly transferred to the reinsurance company:

$$CC = \begin{cases} \left[\left(AL \right) \times \left(CCE \right) \right] & AL \le D \times P_A \ , \\ \left[\left(DxP_A \right) \times \left(CCE \right) \right] & AL > D \times P_A \end{cases} \tag{4.7}$$

- Finally, the total premium (*TP*) is calculated for each building by applying a certain amount of profit (*P*), namely 10 % in this study, after adding both reinsurance cost and capital cost to the base premium:

$$TP = \left[PRP + RC + CC \right] \times \left[1 + P \right] \tag{4.8}$$

- Then, the earthquake insurance rate (*EIR*) for each building is calculated by simply dividing the total premium by the building insured value. Note that if there exists also accumulation risk in a specific region, special loadings determined by the reinsurance agreements could be made by using the same methodology.

$$EIR = \frac{TP}{IV} \tag{4.9}$$

Table 4.1 summarizes sample calculations conducted by using analytical PML estimation tool recently developed to find out the earthquake insurance rates for the portfolio consists of 80 different single-storey reinforced concrete industrial buildings in Turkey.

Table 4.1. Earthquake insurance rate calculations for the building inventory via risk based PML estimation method.

Damage State	PML	Base Rate (‰)	Annual Loss (TL)	Capital Cost (TL)	Reinsurance Cost (TL)	Total Premium (TL)	Net Rate (‰)
Slight	5 %	0.11	105.3	10.5	0.00	127.4	0.13
Moderate	30 %	0.63	631.6	21.1	509.5	1,278.3	1.28
Extensive	70 %	1.47	1473.7	21.1	1,528.4	3,325.5	3.33
Complete	100 %	2.11	2105.3	21.1	2,292.6	4,860.8	4.86
Total Portfolio	15.3 mio TL		32,210	1,178.9	24,709.5	63,908.9	

4.2. Comparing the Earthquake Insurance Rates Calculated by Using Different PML Estimation Methods

Clearly one of the most important inputs for estimating earthquake insurance rate is the structural loss estimates (PML). In order to analyze the impacts of risk based PML estimation versus portfolio based PML estimation on earthquake insurance rates, the calculations summarized in Section 4.1 have been repeated with all other PML estimation methods. The results indicate that the average earthquake insurance rates obtained from the PML estimates by the fragility analyses and the risk based approach are similar but that there is a huge deviation for the individual earthquake insurance premiums of the same buildings. As an example; while the rate of risk based PML estimation is 1.28 ‰ for the risks which are at ''Moderate Damage'' State, the rates of fragility based PML estimation can change from 0.26 ‰ to 2.55 ‰. The rates of the fragility based PML estimation (0.72 ‰ - 2.55 ‰) for the risks which are at ''Collapse'' State are quite low compared to risk based PML estimation rate (4.86 ‰).

The analysis results of the risk based PML estimation were also compared with Turkish Catastrophe Insurance Pool (TCIP), the compulsory insurance system, which has five tariff zones and also charges different premium rates depending on the construction type (steel, reinforced concrete, masonry and others). The rates charged by the insurance companies, as specified by TCIP, range from 5.50 to 0.44 per 1000 units of insured property. The scheme has a deductible of 2 % of the insured value for each property (TCIP, 2014). Table 4.2 shows the premium rates of the compulsory earthquake insurance scheme, categorized based on earthquake zones and construction type.

Table 4.2. Premium rates of the compulsory earthquake insurance scheme, categorized based on earthquake zones and construction type in Turkey (TCIP, 2014).

Construction Type	Earthquake Insurance Rates (‰)				
	I. Zone	II. Zone	III. Zone	IV. Zone	V. Zone
A. Steel and Reinforced Concrete	2.20	1.55	0.83	0.55	0.44
B. Masonry	3.85	2.75	1.43	0.60	0.50
C. Other	5.50	3.53	1.76	0.78	0.58

When the results were compared with the maximum possible insurance rate for the reinforced concrete residential buildings (2.20 per 1000 units of insured property) in TCIP (2014), it was determined that the earthquake insurance rates defined in TCIP is very low for the buildings which have ‘’Extensive’’ and ‘’Complete’’ damage states according to the risk based loss estimation method. It can be stated that TCIP is mainly appropriate for the buildings which have ‘’Moderate’’ or ‘’Slight’’ Damage States, although it was designed for only residential buildings.

Table 4.3 shows the comparison of the earthquake rates calculated by using the PML values of the results of using different PML estimation methods for the four buildings described in Table 3.18. Other important parameters, such as total reinsurance costs, the average and total values of PML and earthquake insurance premium of the same building inventory calculated by using all different PML estimation methods are summarized in Table 4.4.

Table 4.3. Comparison of the earthquake insurance rates for selected buildings obtained via different PML estimation methods.

No	Earthquake Insurance Rates (‰)						
	John Freeman	Karl V. Steinbrugge	ATC-13	FEMA 154 v:2	HAZUS	Proposed Method	
						Fragility	Risk Based
1	0.77	2.97	0.87	2.81	0.77	0.65	0.13
2	0.77	2.97	0.87	2.81	0.77	2.55	3.33
3	0.77	2.97	0.87	2.81	0.48	1.34	1.28
4	0.77	2.97	0.87	2.81	0.48	1.34	4.86

Figure 4.1 shows the comparison of the earthquake insurance rates of the entire portfolio comprising 80 different single-storey reinforced concrete industrial buildings in Turkey calculated by using different PML estimation methods.

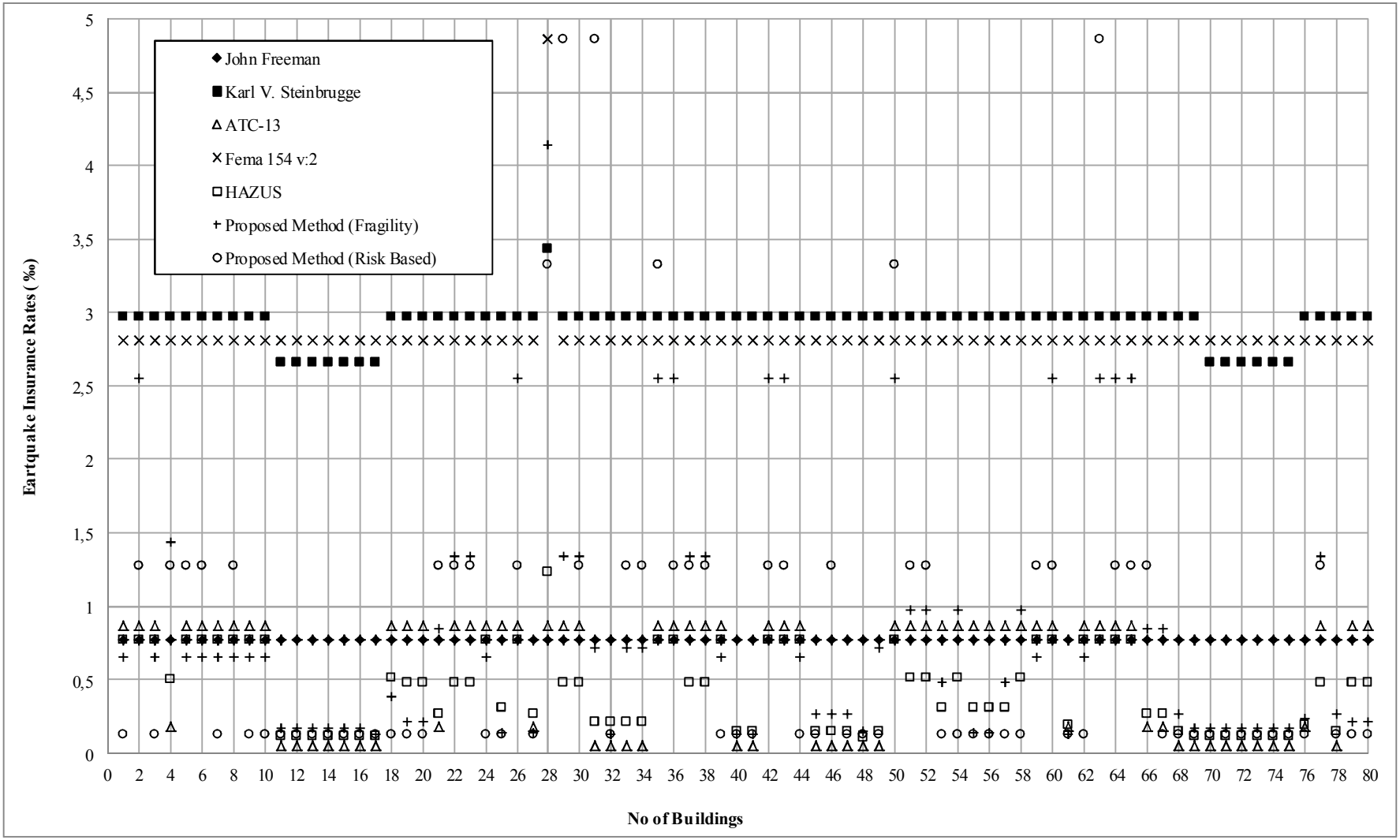

Figure 4.1. Comparing earthquake insurance rates of the entire portfolio calculated by using different PML estimation methods.

Earthquake insurance rates for the other buildings within the inventory were calculated by using the similar calculation methods corresponding to different PML values calculated by using each loss estimation technique. Table D.2 shows earthquake insurance rates for the entire building inventory comprising 80 single-storey reinforced concrete industrial building.

Table 4.4. Comparison of the parameters used to calculate earthquake insurance rates and the premium for the buildings within the inventory according to different loss estimation methods.

Method		PML		Total Reinsurance Cost (TL)	Premium	
		Average (%)	Total (TL)		Average (TL)	Total (TL)
John Freeman		20	16,000,000	20,378.9	766.5	61,322.1
Karl V. Steinbrugge		62.14	49,710,000	106,250.7	2,923.1	233,846
ATC-13		13.94	11,150,000	14,061.4	532.4	42,592.5
FEMA 154 v:2		60.5	48,400,000	102,913.7	2,839.3	227,142
HAZUS		12.65	10,119,000	7,219	432.4	34,591.2
Proposed Method	Fragility	21.05	16,840,000	25,035.5	852	68,160.8
	Risk Based	19.1	15,300,000	24,709.5	798.9	63,908.8

5. CONCLUSION AND REMARKS

Estimating expected major losses due to a large magnitude earthquake has been a major concern for the insurance sector. Over the last two decades considerable efforts have been spent by the insurers to tackle the problem of how to conduct reliable estimates of future earthquake losses and eventually how to overcome a potential insolvency. Recent destructive earthquakes reiterated the need by the insurance companies to obtain reliable estimates of potential seismic losses not only for having sufficient reserves but also for calculating the right premiums to survive in the competitive market.

In this study, a rapid, analytical earthquake loss estimation (PML) methodology, which can be used even by the ones who are not experts in earthquake engineering, has been developed for single-storey reinforced concrete industrial buildings in order to find out the impact of risk based PML estimation on earthquake insurance rates.

Based on detailed analyses the parameters which affect the seismic performance have been identified as column cross-sectional dimensions, longitudinal and transverse reinforcement, stirrup spacing, column height, axial load, earthquake zone, and soil class. For the specific buildings contained in the inventory, the concrete class did not differ significantly to cause any appreciable effect.

Structural loss estimation curves used were drawn based on the structural performance evaluation procedure proposed in TSDC07 and by taking P-Δ effects into consideration. The important results gained from these curves can be summarized as the following;

- If the longitudinal reinforcement is increased when the other parameters are kept constant, the curve which defines the Minimum Damage Limit becomes parallel to the column height axis by moving upwards. At the same time, both the curves which define Safety Limit and Collapse Limit move upwards with the similar ratios, although by the limited ratios for the smaller column heights (Bigger axial load amounts required for the same damage state).

- If only the sizes of the column cross-sections are increased then the curves corresponding to the same damage thresholds move upwards.
- If only the column heights are increased then the column can collapse before reaching to the unit deformations defined in TSDC-07 for the Collapse State and the P-Δ effects become predominant because of the strength degradation.

When the analysis results of the proposed method have been compared with the damaged buildings in order to estimate the reliability of the proposed method, it was observed that the damage states of the heavily damaged buildings were beyond the Collapse Limit also for the results of proposed method, although the information gathered was very limited. Moreover, the changes in the loss estimation curves are consistent with the statement of less damage occurs if the sizes of the column cross-sections are bigger according to the analyses of the damaged industrial buildings.

In addition, detailed fragility curves were also drawn by considering the structural types and the design levels of the buildings investigated as an alternative PML estimation tool.

In order to measure the impact of risk based PML estimation approach on the earthquake insurance rates, the total insurance premiums corresponding to PML values of the inventory buildings for each loss estimation method discussed were calculated by also paying attention to the reinsurance cost, capital cost and the profit that will be charged by the insurance companies.

It was observed that the PML values of the industrial buildings in the inventory varied significantly between the proposed risk based approach and the existing loss estimation methods. This variance had a significant impact on the earthquake insurance rates since these rates are sensitive to structural loss estimates. Similar variances were also obtained between the fragility based and the risk based approaches. Although fragility curves have been employed for different structural classes within the last decade, the use of these curves for individual risk assessment is somewhat controversial since they are tailored to represent the general damageability of a given set of buildings. As such, the earthquake insurance rates calculated by using the PML values obtained via the fragility

based and the risk based loss estimates led to significantly different results for the same buildings within the inventory.

Based on the results obtained, the use of risk based PML estimations rather than regional loss estimations including structural fragility curves may be expected to have a significant impact in determining the optimum insurance premium. Such an approach would decrease the risk of a potential insolvency by identifying the particular buildings susceptible to high seismic risk and increase the ability of the insurer to compete in the market by identifying those buildings susceptible to low seismic risk by allowing the calculation of optimum insurance premiums in all cases.

APPENDIX A: DATA CHARTS SHOWING THE APPROXIMATED WEIGHTS OF THE BASIC STRUCTURAL MEMBERS

In the following Data Charts, the approximated weights of the basic structural members generally used for the single-storey reinforced concrete industrial buildings, were summarized.

Table A.1. Approximated weight calculation chart for different structural members.

Structural System	Member		Weight
Roof Structure	Steel Girder	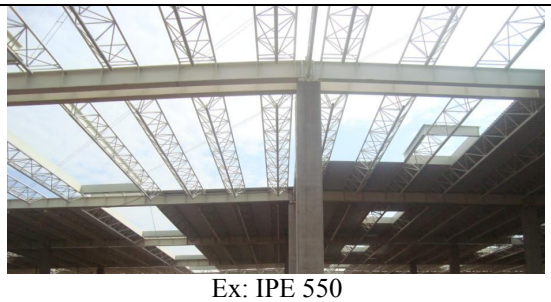 Ex: IPE 550 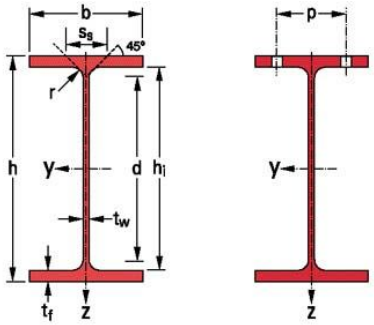	1 kN/m
	Steel Truss		0.17 kN/m^2
	Steel Purlin	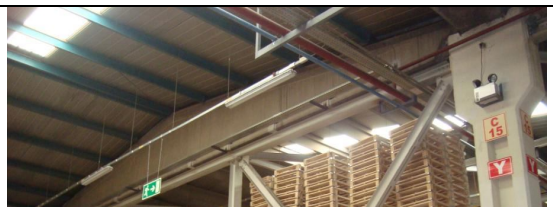	0.1 kN/m^2

Table A.1. Approximated weight calculation chart for different structural members (cont.).

Structural System	Member			Weight
Roof Structure	Space Truss			0.15 kN/m^2
	Precast Beam	12-16 m		4.1 kN/m
		17-20 m		4.7 kN/m
		21-30 m		5.6 kN/m
	Precast Purlin	6 m		0.25 kN/m^2
		8 m		0.3 kN/m^2
		10 m		0.5 kN/m^2
		12 m		0.65 kN/m^2
	Precast Gutter Beam	6 – 8 m		2.6 kN/m
		10 - 12 m		3.25 kN/m

Table A.1. Approximated weight calculation chart for different structural members (cont.).

Roof Cover	Sandwich Panel		0.10 kN/m^2
	Trapezoidal Sheet (Single)		0.05 kN/m^2
	Corrugated Asbestos Cement	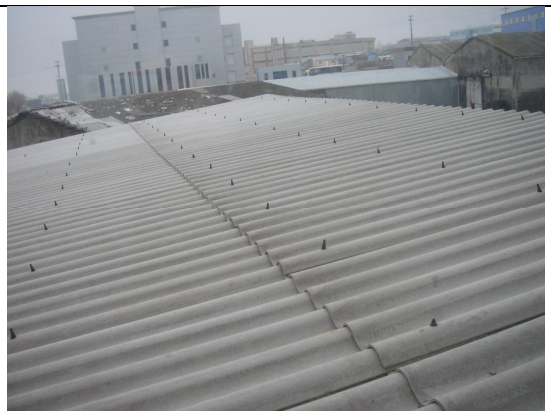	0.20 kN/m^2
Insulation Material	Polyurethane (6 cm thickness as average)		0.02 kN/m^2

Table A.1. Approximated weight calculation chart for different structural members (cont.).

<table>
<tr><td rowspan="2">Insulation Material</td><td>Rock Wool (10 cm thickness as average)</td><td colspan="2"> 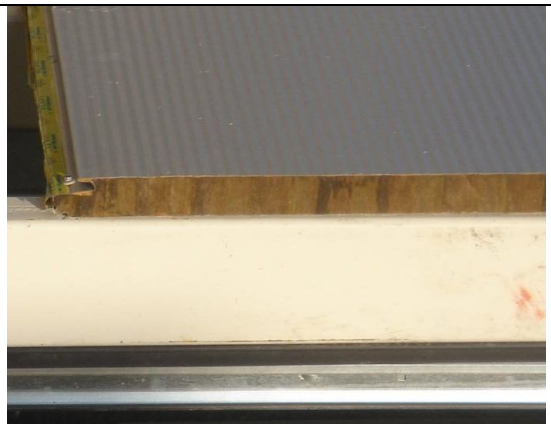 </td><td>0.1 kN/m^2</td></tr>
<tr><td>Glass Wool</td><td colspan="2"> 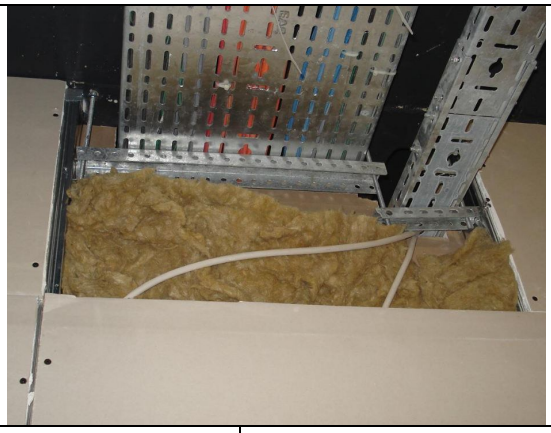 </td><td>0.07 kN/m^2</td></tr>
<tr><td rowspan="5">Crane Structures</td><td rowspan="4">Precast Crane Girder</td><td>5 ton</td><td rowspan="4">  </td><td>4.9 kN/m</td></tr>
<tr><td>10 ton</td><td>5.2 kN/m</td></tr>
<tr><td>15 ton</td><td>5.5 kN/m</td></tr>
<tr><td>20 ton</td><td>6.5 kN/m</td></tr>
<tr><td>Steel Crane Girder</td><td colspan="2">  </td><td>1.5 – 2 kN/m^2</td></tr>
</table>

APPENDIX B: STRUCTURAL LOSS ESTIMATION CURVES DEVELOPED FOR THE BUILDING TYPES USED IN THE STUDY

Table B.1. Structural loss estimation curves for the single-storey reinforced concrete industrial buildings which are located at 1st Earthquake Zone and Z1 Soil Class.

Cross-Section (cm)	Reinforcement Ratio	Structural Loss Estimation Curves
35×35	Minimum	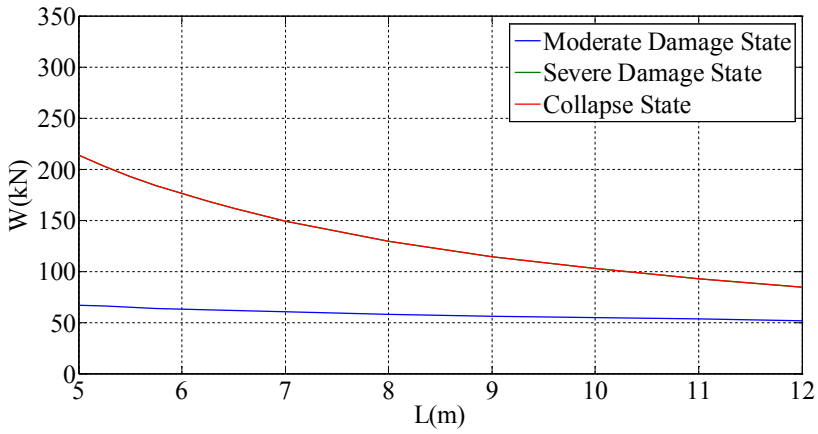
	Moderate	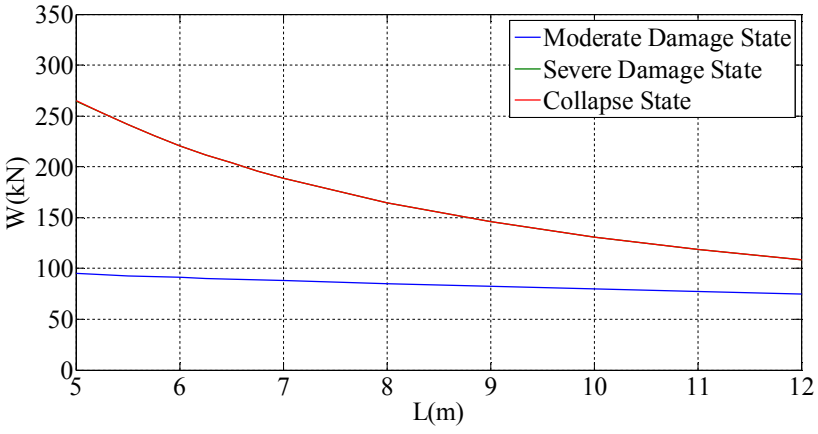
	High	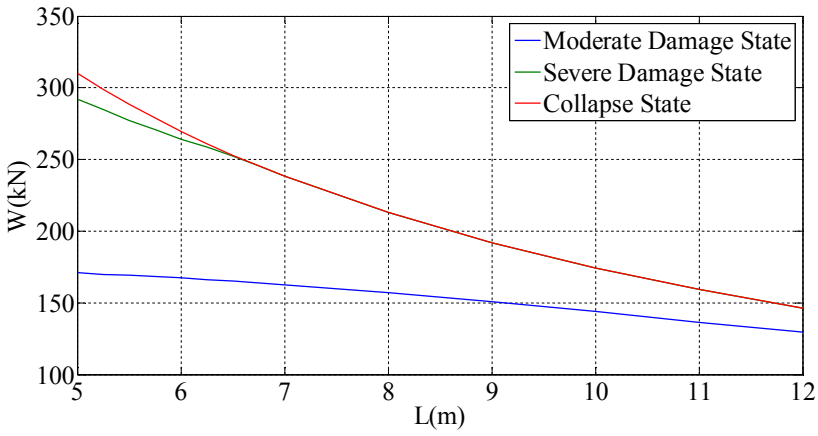

Table B.1. Structural loss estimation curves for the single-storey reinforced concrete industrial buildings which are located at 1st Earthquake Zone and Z1 Soil Class (cont.).

Cross-Section (cm)	Reinforcement Ratio	Structural Loss Estimation Curves
40×40	Minimum	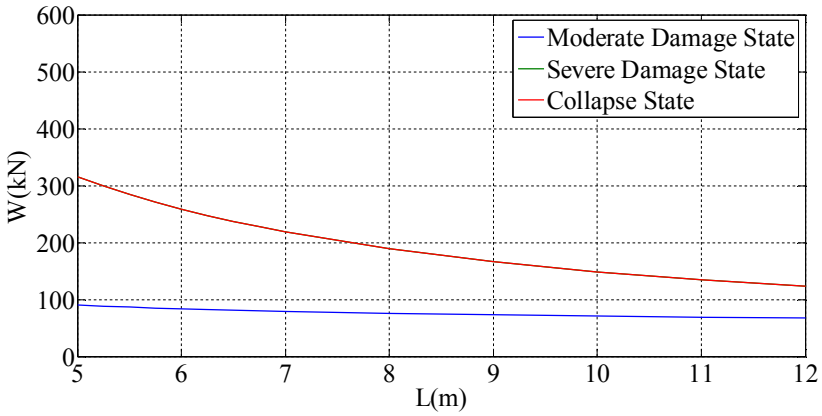
	Moderate	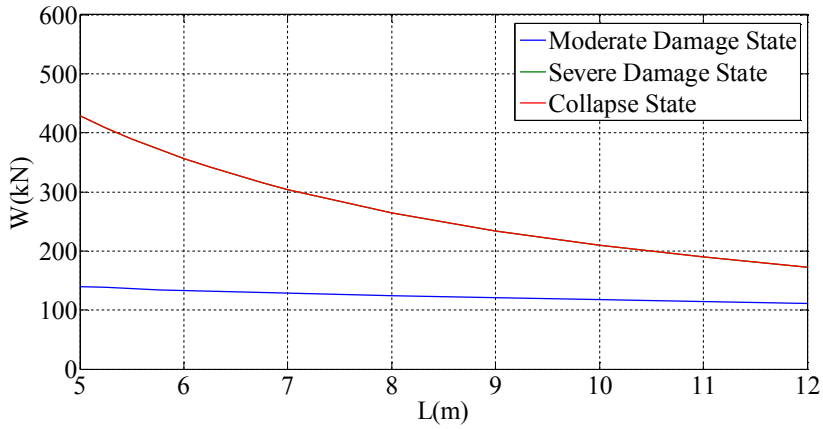
	High	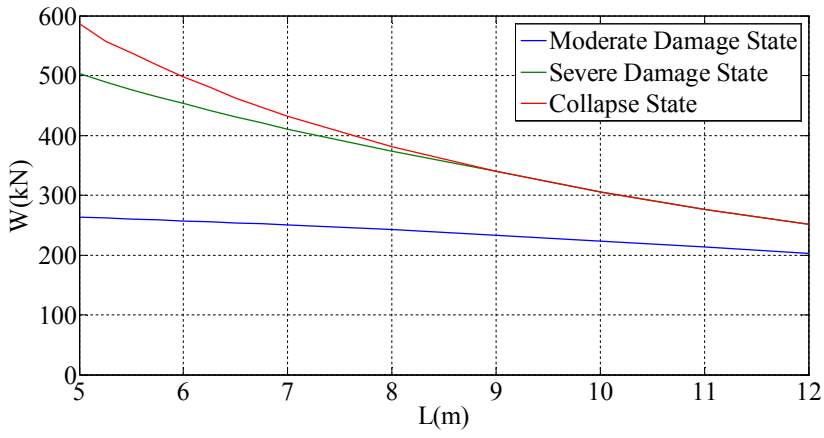

Table B.1. Structural loss estimation curves for the single-storey reinforced concrete industrial buildings which are located at 1st Earthquake Zone and Z1 Soil Class (cont.).

Cross-Section (cm)	Reinforcement Ratio	Structural Loss Estimation Curves
45×45	Minimum	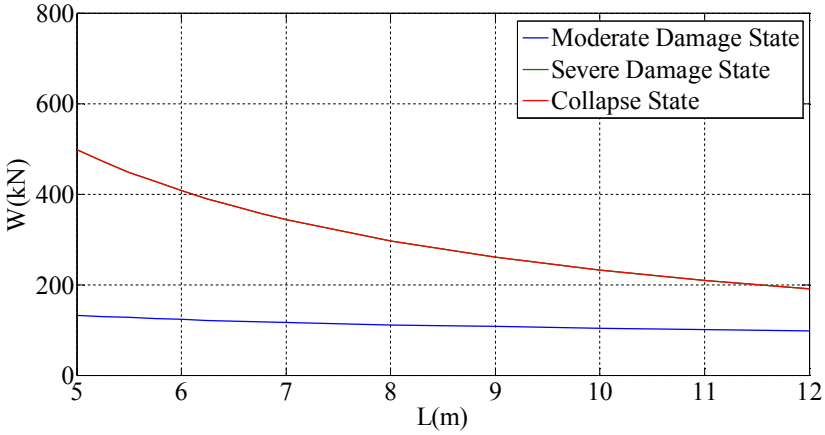
	Moderate	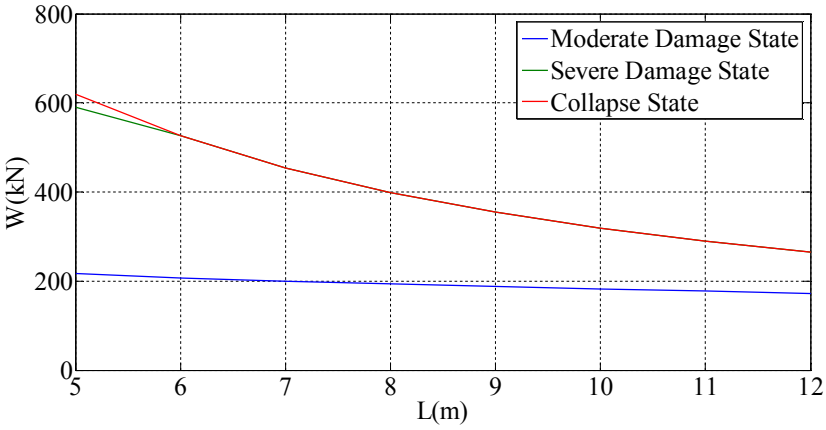
	High	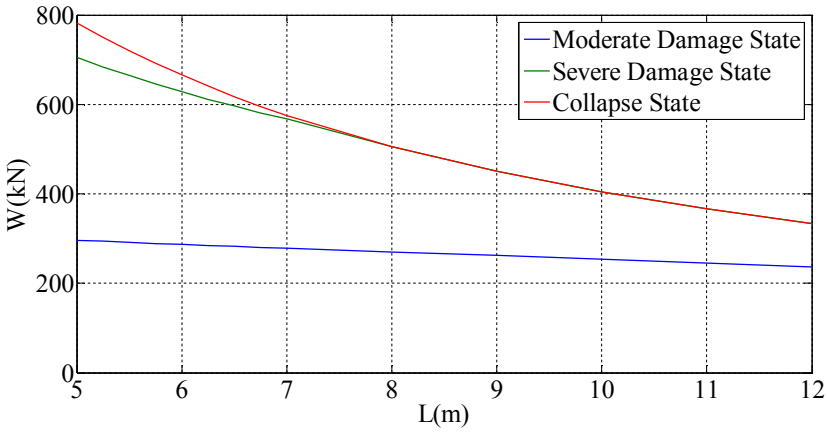

Table B.1. Structural loss estimation curves for the single-storey reinforced concrete industrial buildings which are located at 1st Earthquake Zone and Z1 Soil Class (cont.).

Cross-Section (cm)	Reinforcement Ratio	Structural Loss Estimation Curves
50×50	Minimum	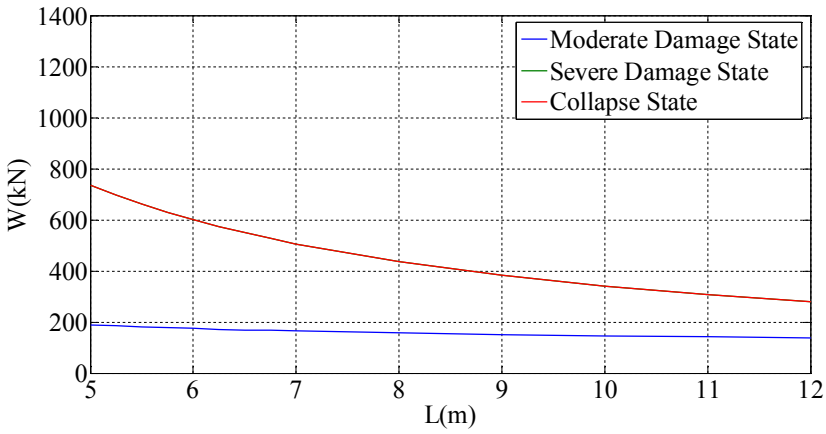
	Moderate	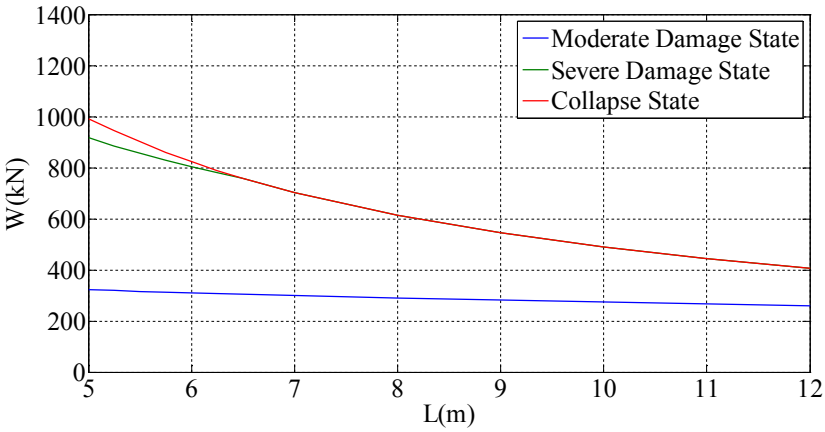
	High	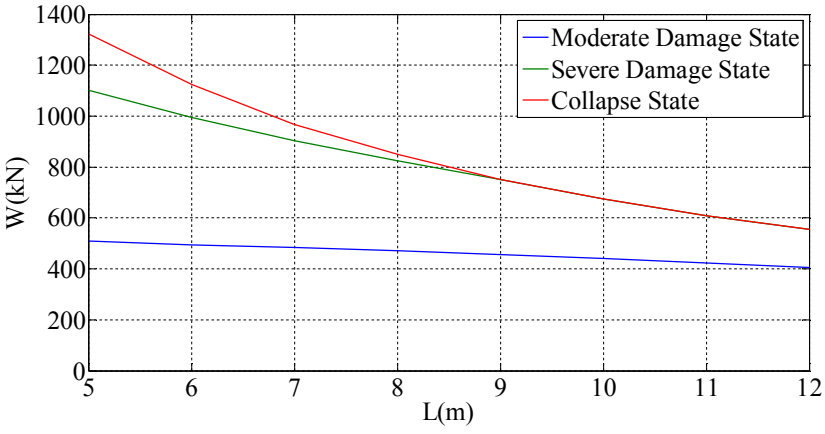

Table B.1. Structural loss estimation curves for the single-storey reinforced concrete industrial buildings which are located at 1st Earthquake Zone and Z1 Soil Class (cont.).

Cross-Section (cm)	Reinforcement Ratio	Structural Loss Estimation Curves
55×55	Minimum	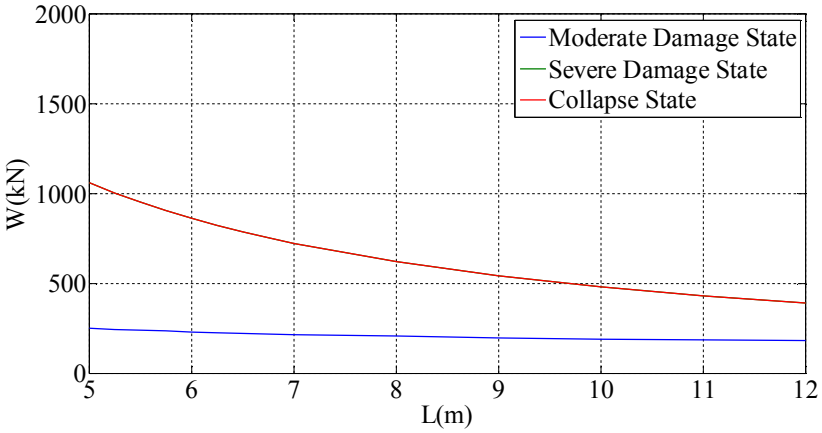
	Moderate	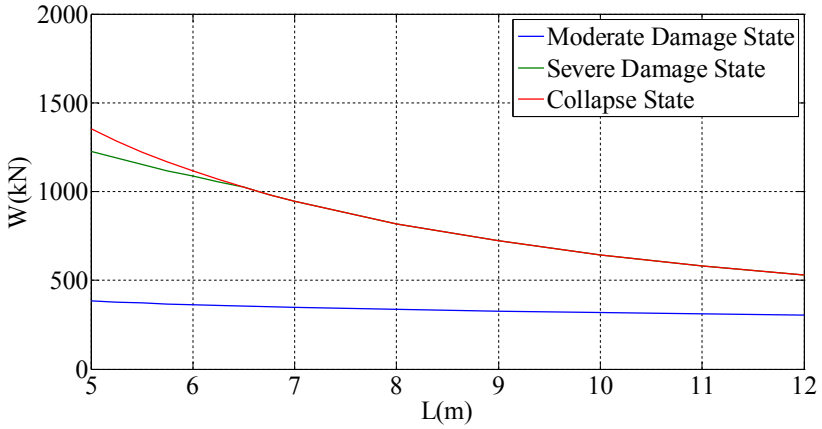
	High	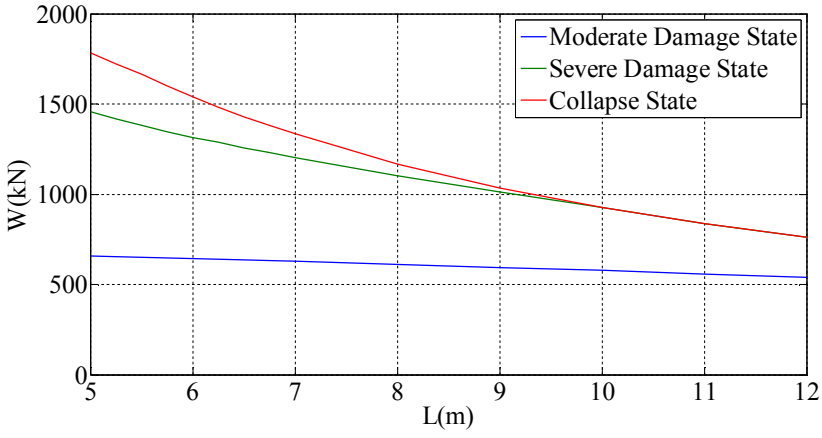

Table B.1. Structural loss estimation curves for the single-storey reinforced concrete industrial buildings which are located at 1st Earthquake Zone and Z1 Soil Class (cont.).

Cross-Section (cm)	Reinforcement Ratio	Structural Loss Estimation Curves
60×60	Minimum	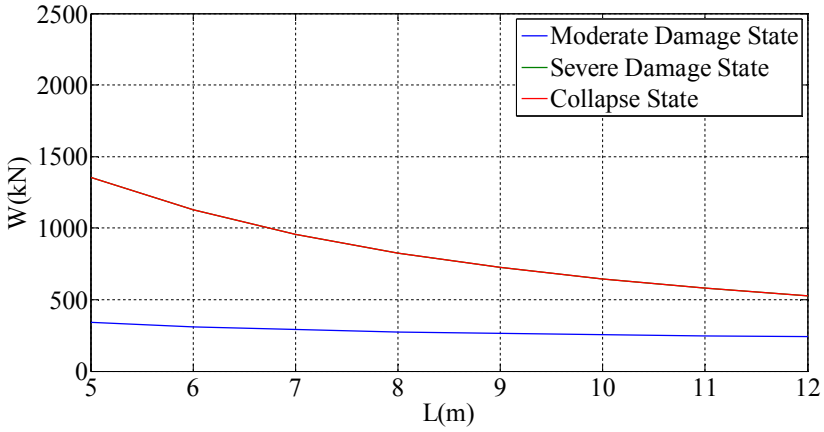
	Moderate	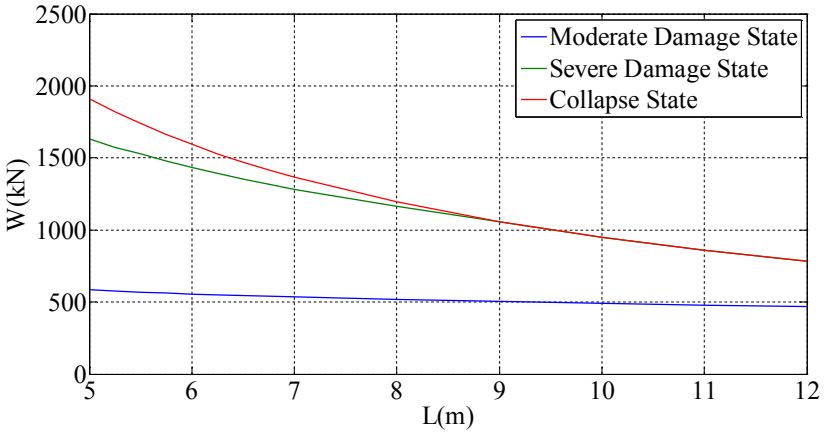
	High	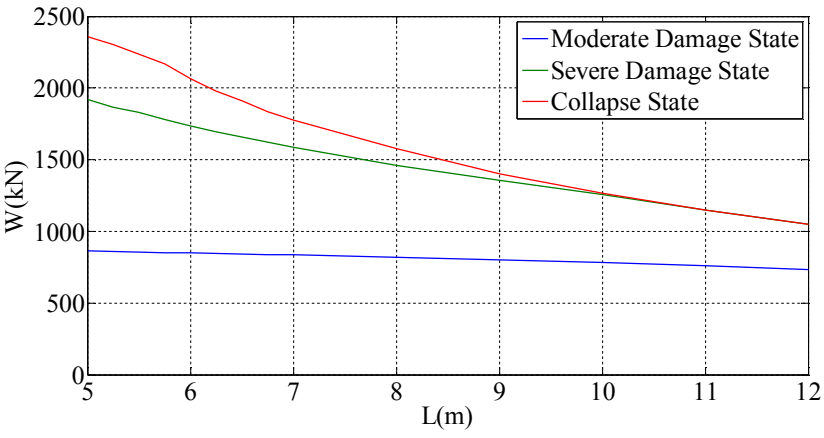

Table B.1. Structural loss estimation curves for the single-storey reinforced concrete industrial buildings which are located at 1st Earthquake Zone and Z1 Soil Class (cont.).

Cross-Section (cm)	Reinforcement Ratio	Structural Loss Estimation Curves
70×70	Minimum	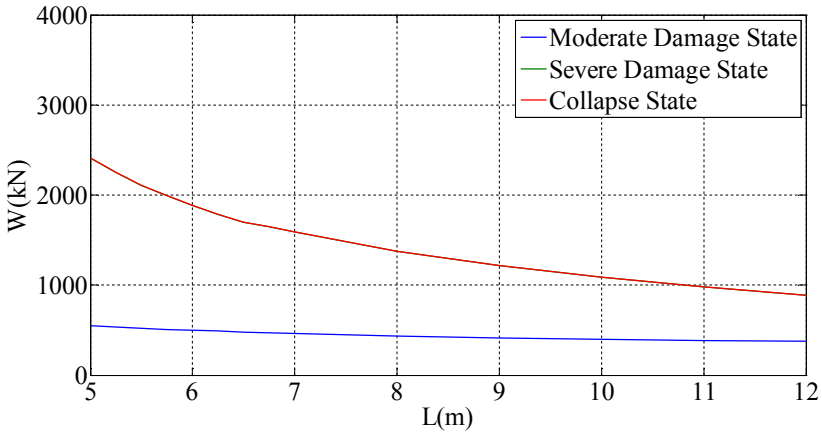
	Moderate	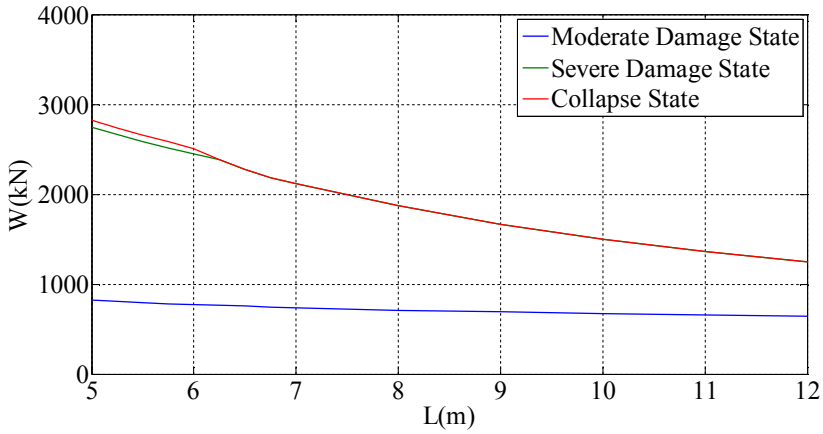
	High	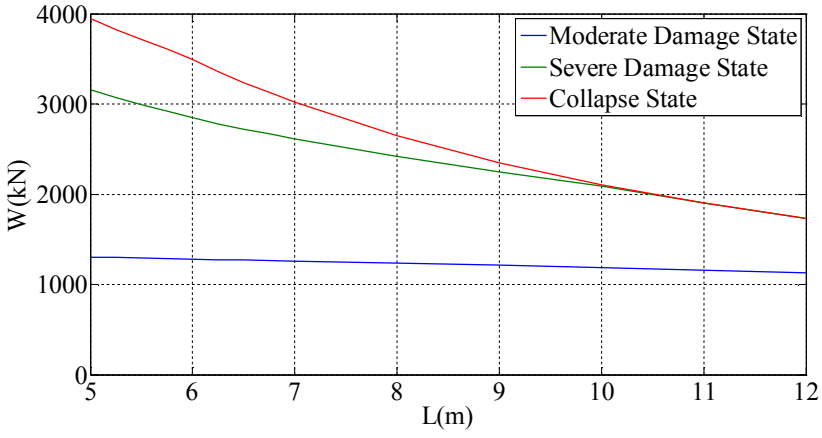

Table B.1. Structural loss estimation curves for the single-storey reinforced concrete industrial buildings which are located at 1st Earthquake Zone and Z1 Soil Class (cont.).

Cross-Section (cm)	Reinforcement Ratio	Structural Loss Estimation Curves
80×80	Minimum	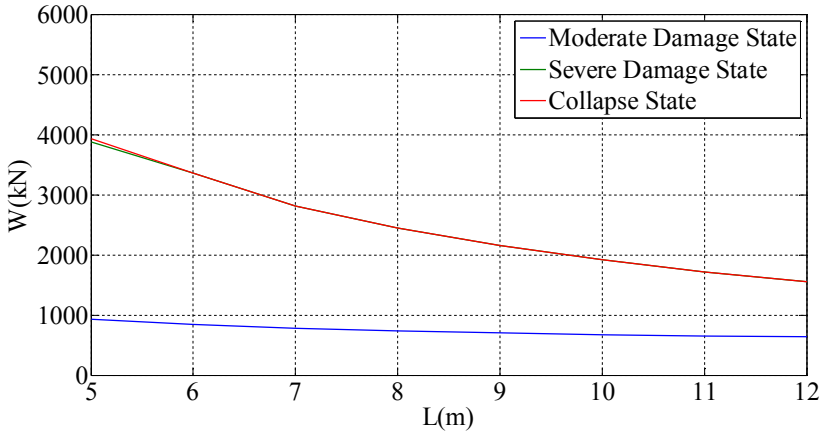
	Moderate	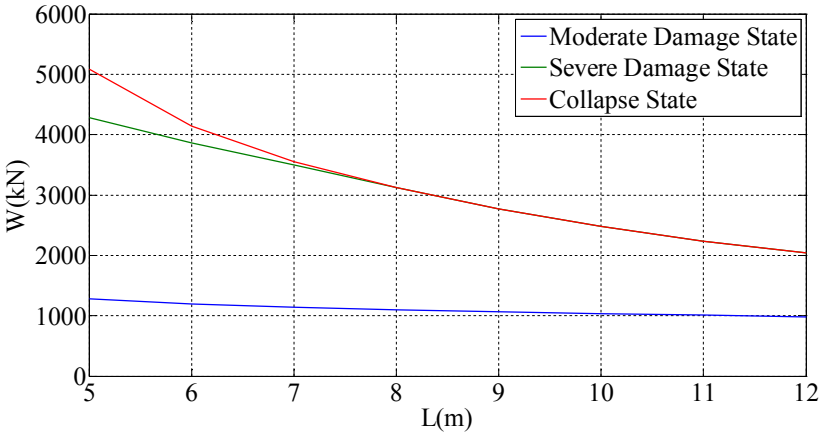
	High	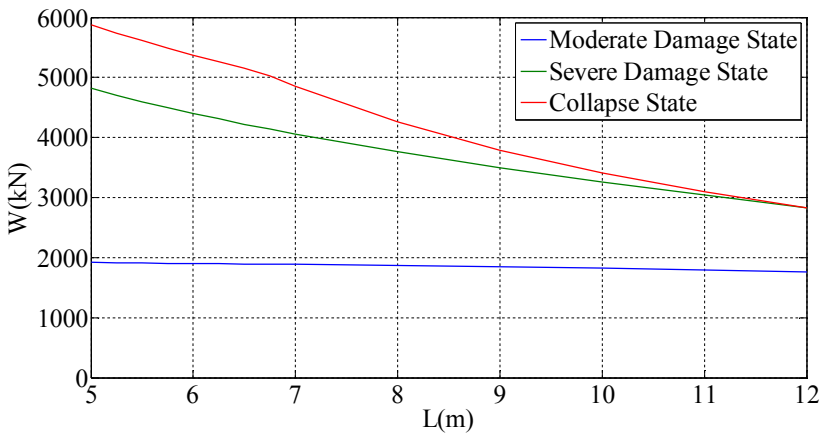

Table B.2. Structural loss estimation curves for the single-storey reinforced concrete industrial buildings which are located at 1st Earthquake Zone and Z2 Soil Class.

Cross-Section (cm)	Reinforcement Ratio	Structural Loss Estimation Curves
35×35	Minimum	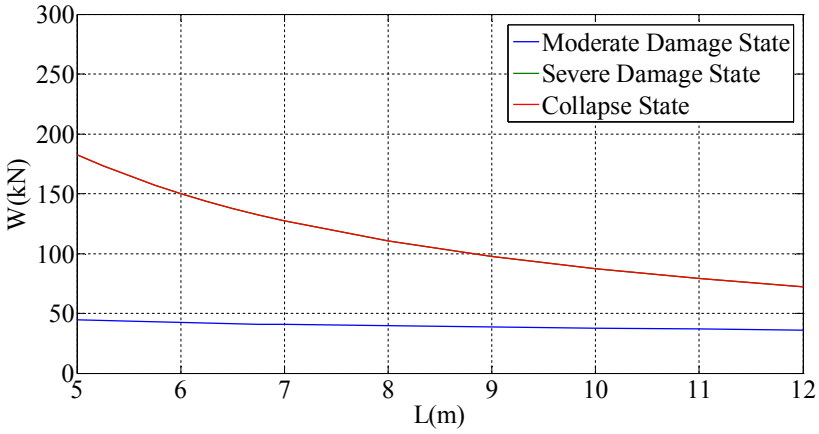
	Moderate	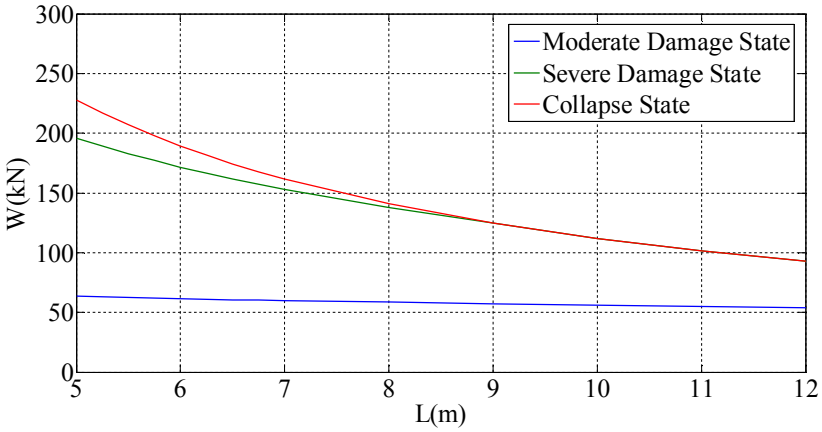
	High	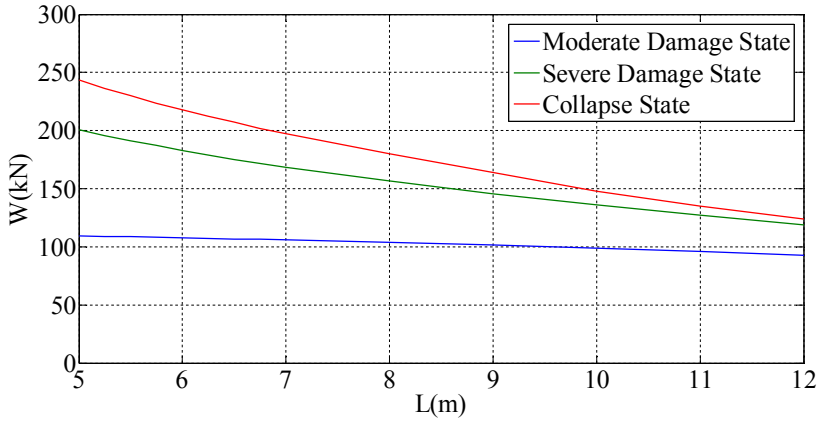

Table B.2. Structural loss estimation curves for the single-storey reinforced concrete industrial buildings which are located at 1st Earthquake Zone and Z2 Soil Class (cont.).

Cross-Section (cm)	Reinforcement Ratio	Structural Loss Estimation Curves
40×40	Minimum	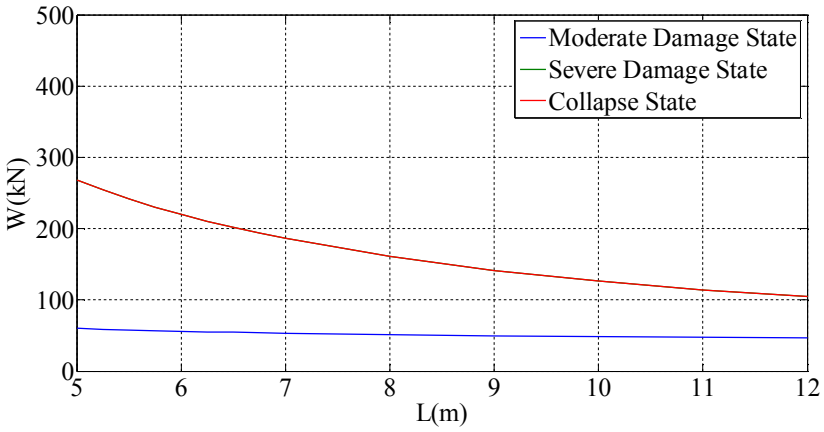
	Moderate	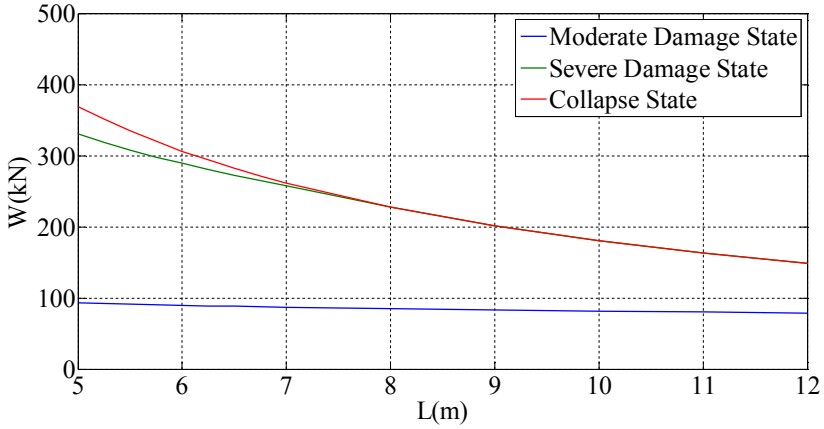
	High	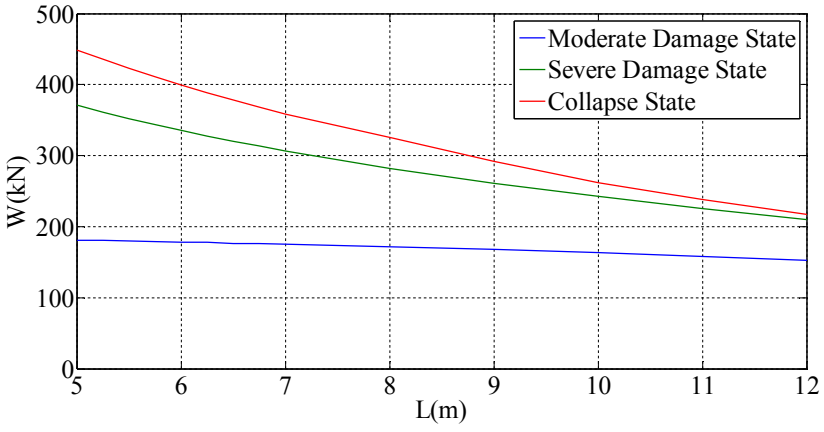

Table B.2. Structural loss estimation curves for the single-storey reinforced concrete industrial buildings which are located at 1st Earthquake Zone and Z2 Soil Class (cont.).

Cross-Section (cm)	Reinforcement Ratio	Structural Loss Estimation Curves
45×45	Minimum	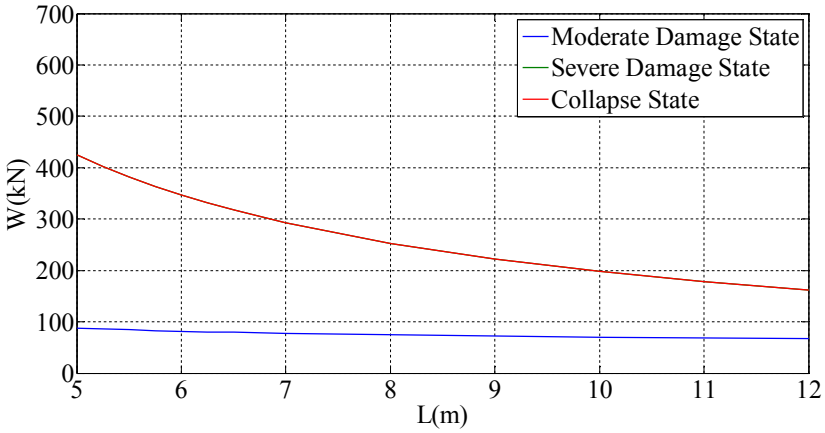
	Moderate	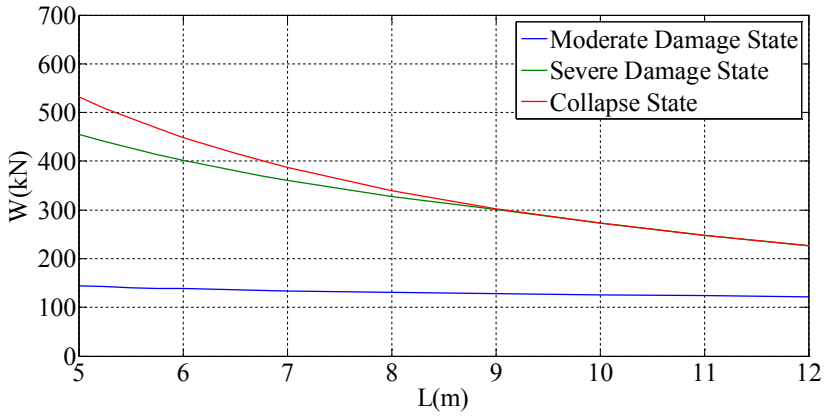
	High	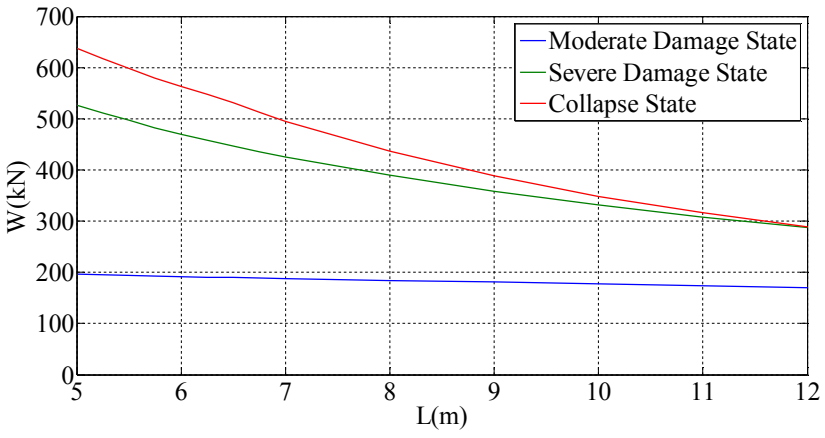

Table B.2. Structural loss estimation curves for the single-storey reinforced concrete industrial buildings which are located at 1st Earthquake Zone and Z2 Soil Class (cont.).

Cross-Section (cm)	Reinforcement Ratio	Structural Loss Estimation Curves
50×50	Minimum	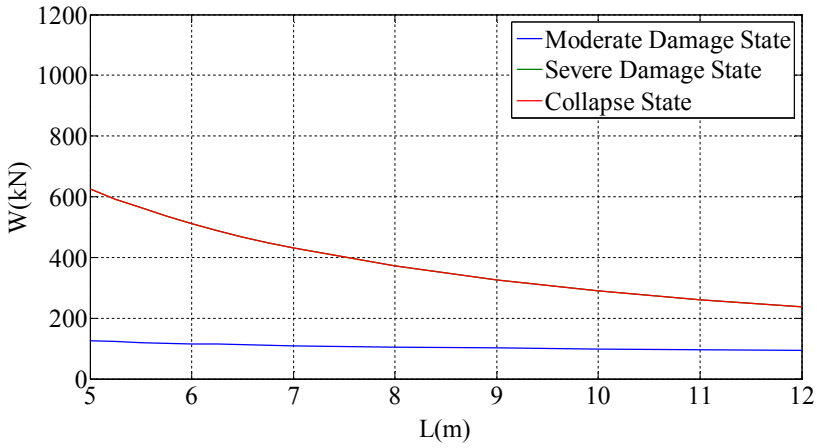
	Moderate	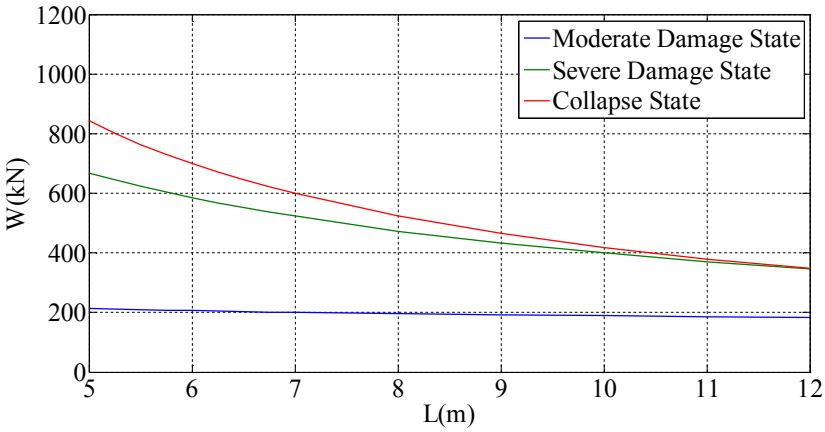
	High	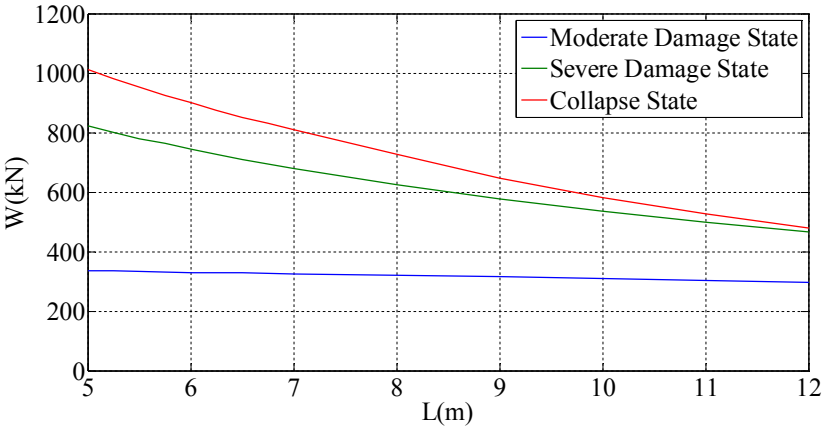

Table B.2. Structural loss estimation curves for the single-storey reinforced concrete industrial buildings which are located at 1st Earthquake Zone and Z2 Soil Class (cont.).

Cross-Section (cm)	Reinforcement Ratio	Structural Loss Estimation Curves
55×55	Minimum	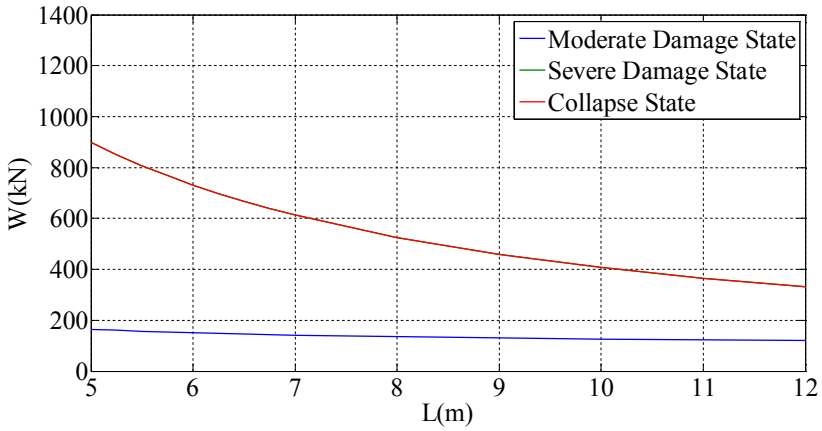
	Moderate	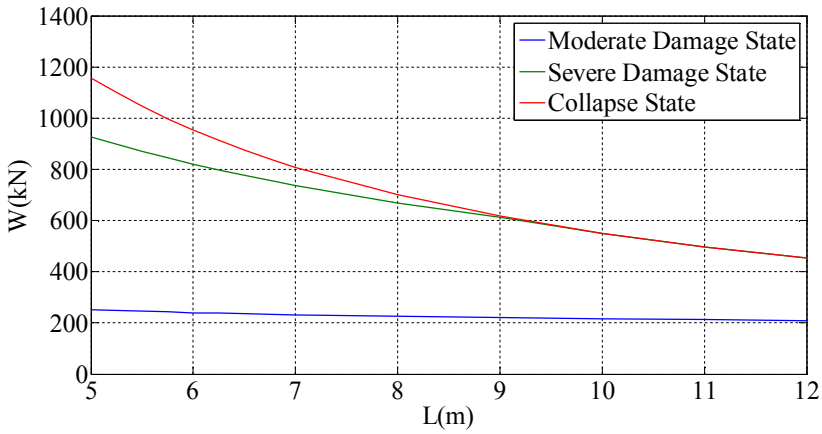
	High	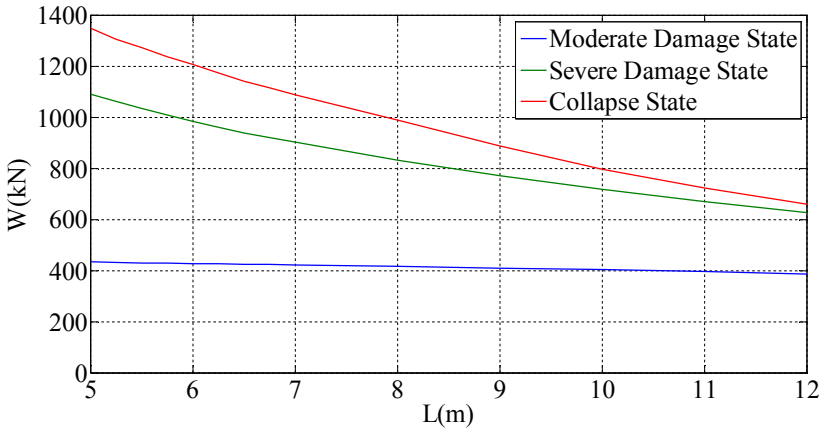

Table B.2. Structural loss estimation curves for the single-storey reinforced concrete industrial buildings which are located at 1st Earthquake Zone and Z2 Soil Class (cont.).

Cross-Section (cm)	Reinforcement Ratio	Structural Loss Estimation Curves
60×60	Minimum	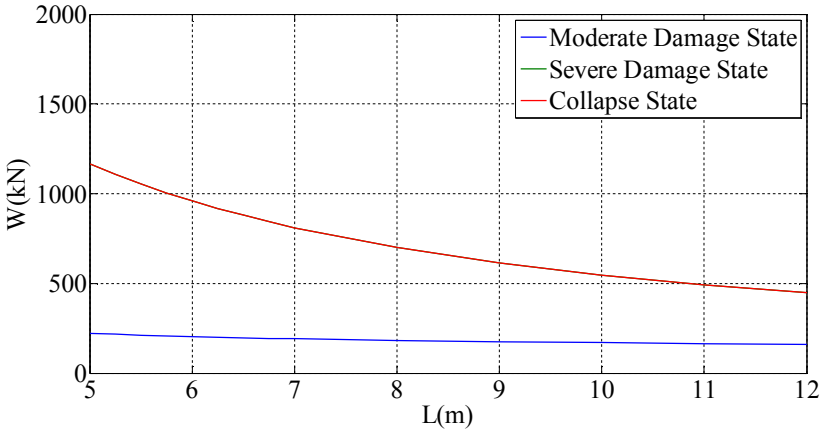
	Moderate	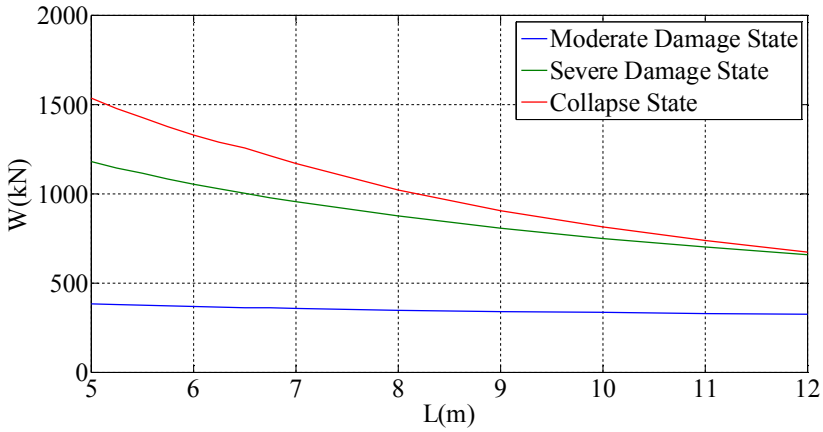
	High	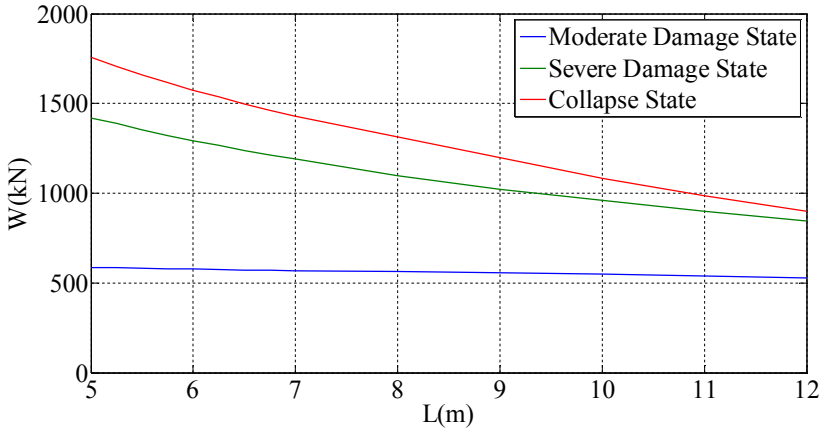

Table B.2. Structural loss estimation curves for the single-storey reinforced concrete industrial buildings which are located at 1st Earthquake Zone and Z2 Soil Class (cont.).

Cross-Section (cm)	Reinforcement Ratio	Structural Loss Estimation Curves
70×70	Minimum	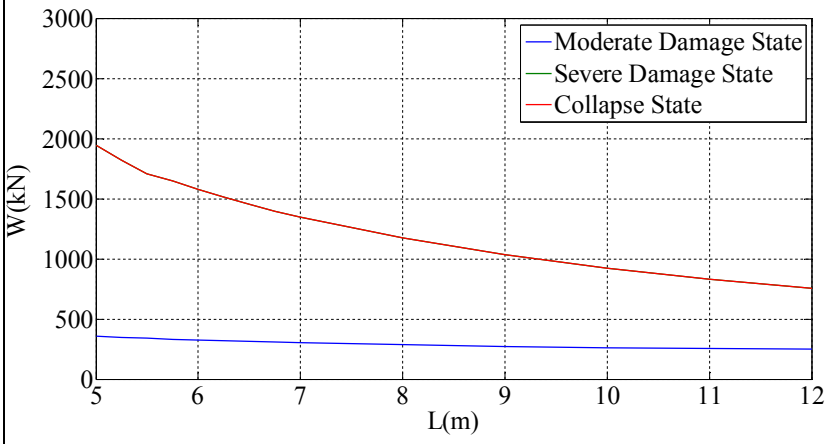
	Moderate	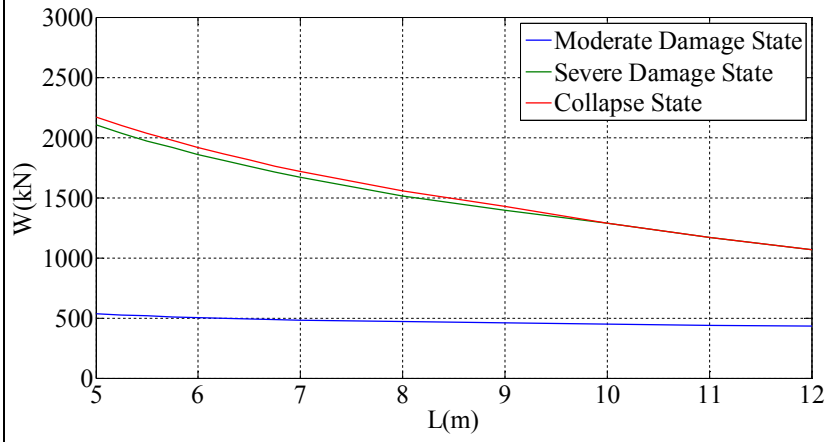
	High	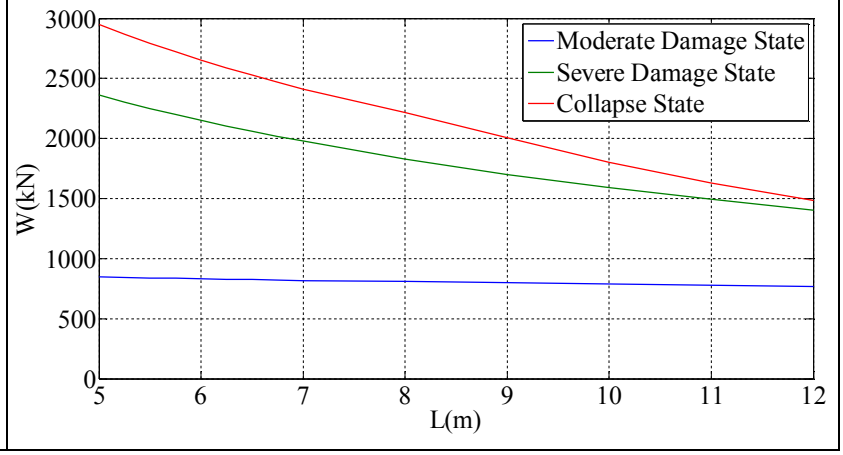

Table B.2. Structural loss estimation curves for the single-storey reinforced concrete industrial buildings which are located at 1st Earthquake Zone and Z2 Soil Class (cont.).

Cross-Section (cm)	Reinforcement Ratio	Structural Loss Estimation Curves
80×80	Minimum	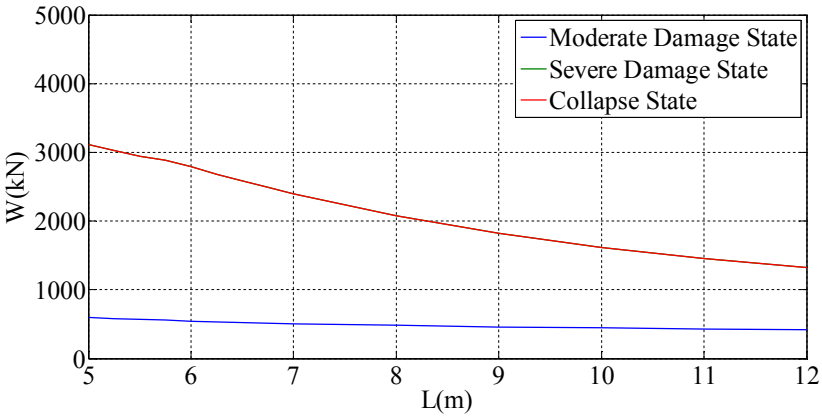
	Moderate	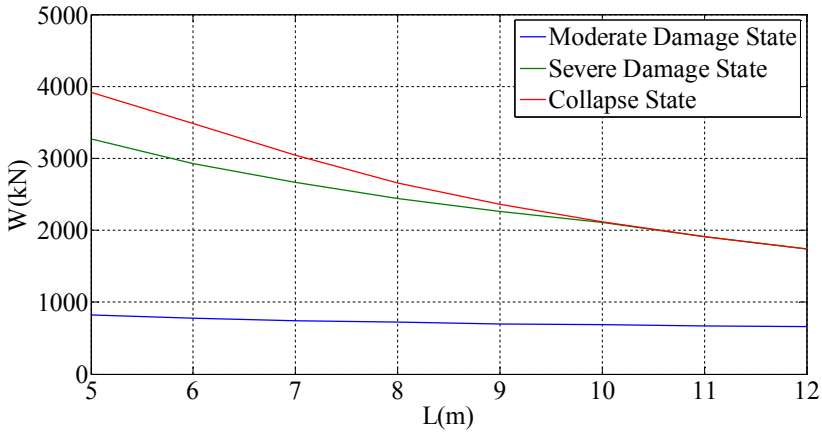
	High	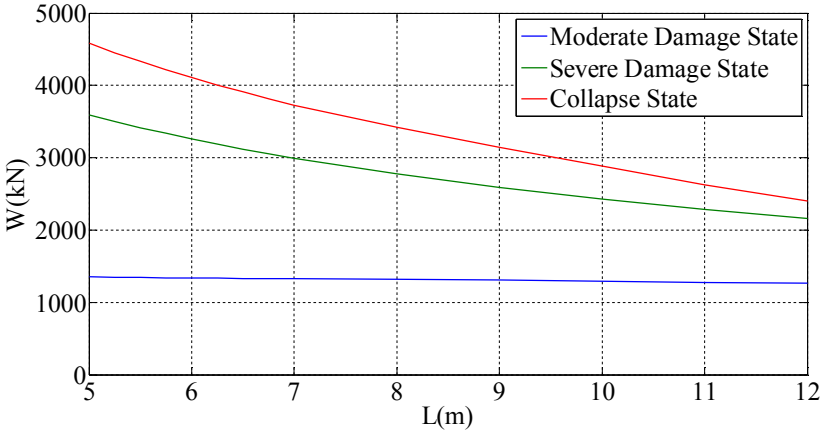

Table B.3. Structural loss estimation curves for the single-storey reinforced concrete industrial buildings which are located at 1st Earthquake Zone and Z3 Soil Class.

Cross-Section (cm)	Reinforcement Ratio	Structural Loss Estimation Curves
35×35	Minimum	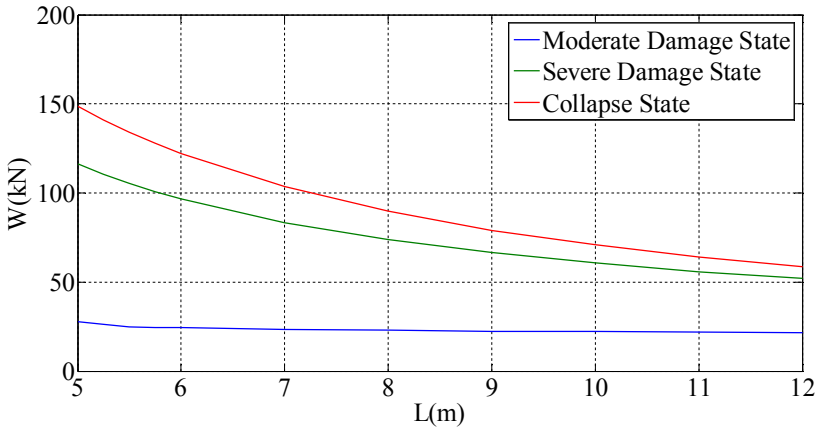
	Moderate	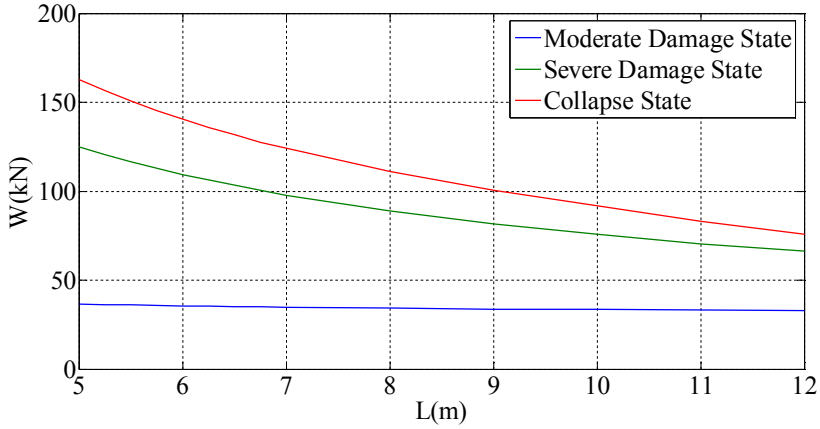
	High	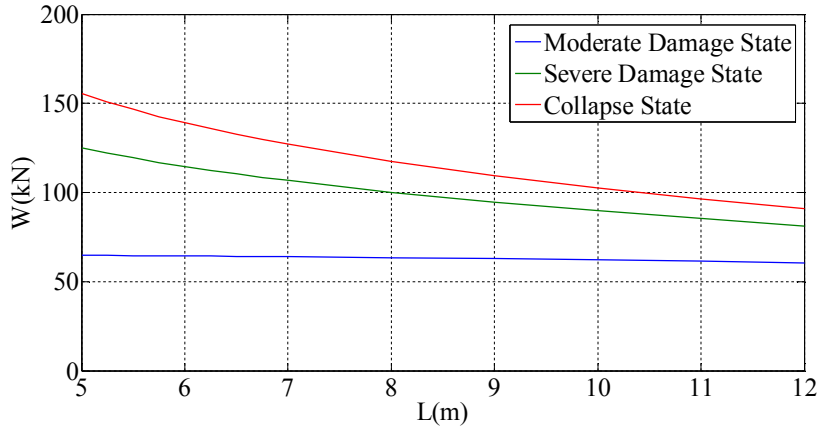

Table B.3. Structural loss estimation curves for the single-storey reinforced concrete industrial buildings which are located at 1st Earthquake Zone and Z3 Soil Class (cont.).

Cross-Section (cm)	Reinforcement Ratio	Structural Loss Estimation Curves
40×40	Minimum	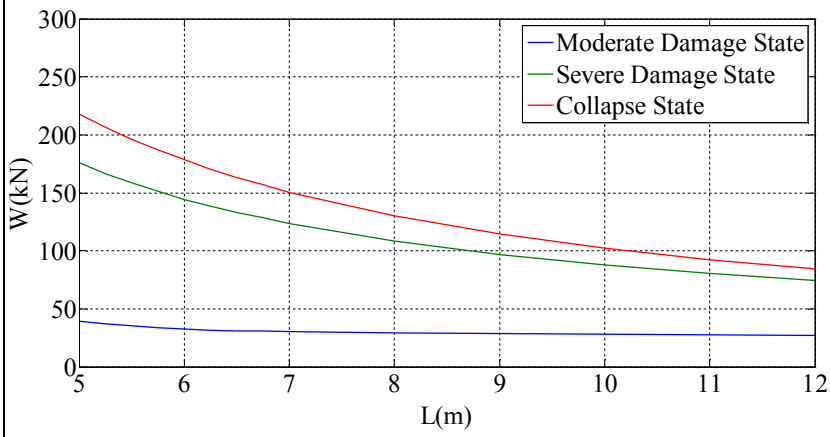
	Moderate	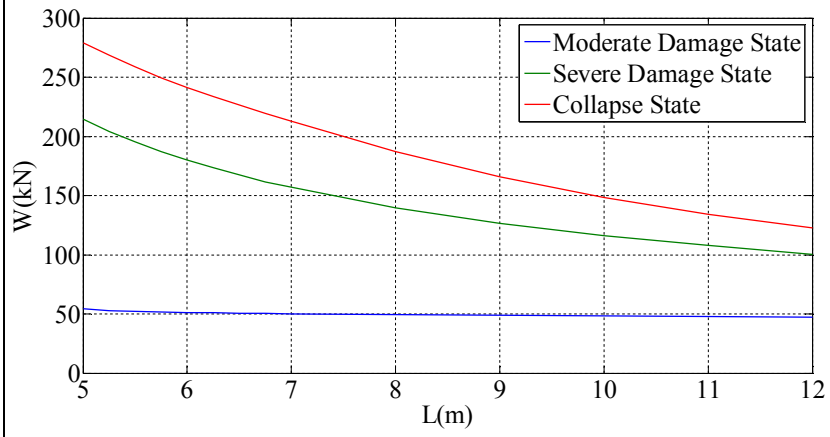
	High	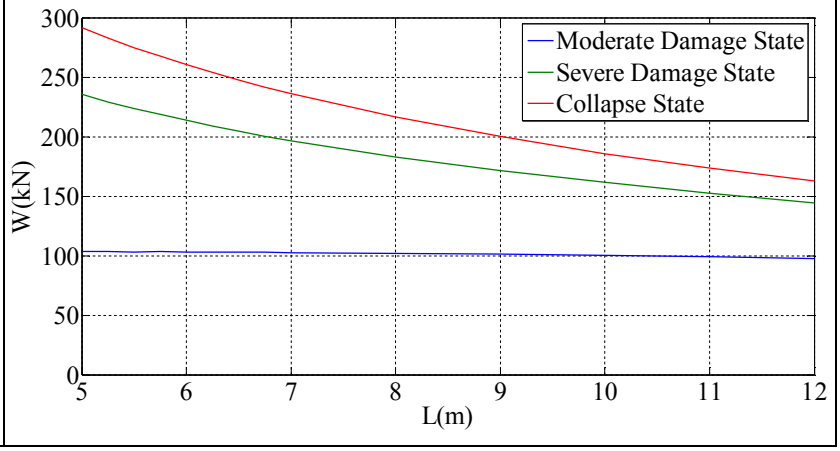

Table B.3. Structural loss estimation curves for the single-storey reinforced concrete industrial buildings which are located at 1st Earthquake Zone and Z3 Soil Class (cont.).

Cross-Section (cm)	Reinforcement Ratio	Structural Loss Estimation Curves
45×45	Minimum	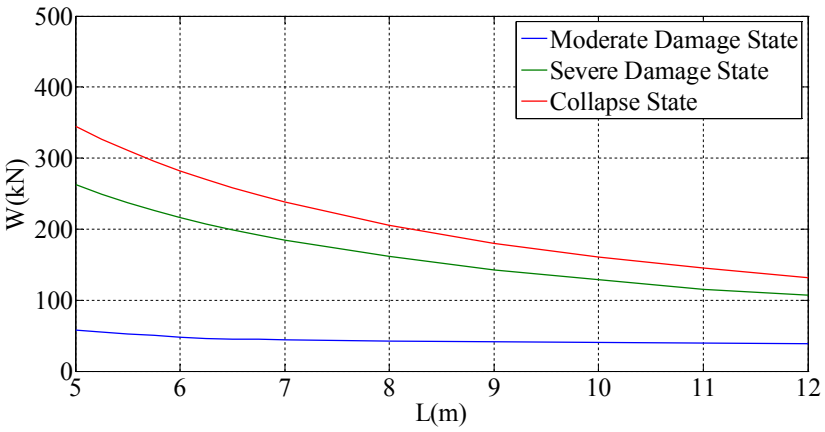
	Moderate	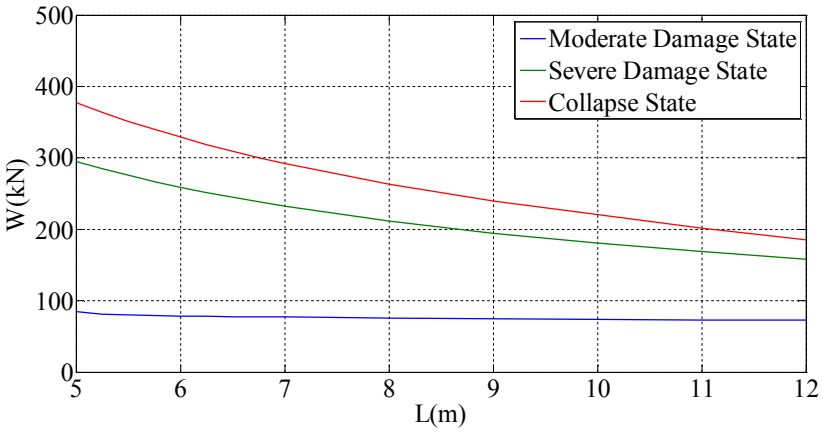
	High	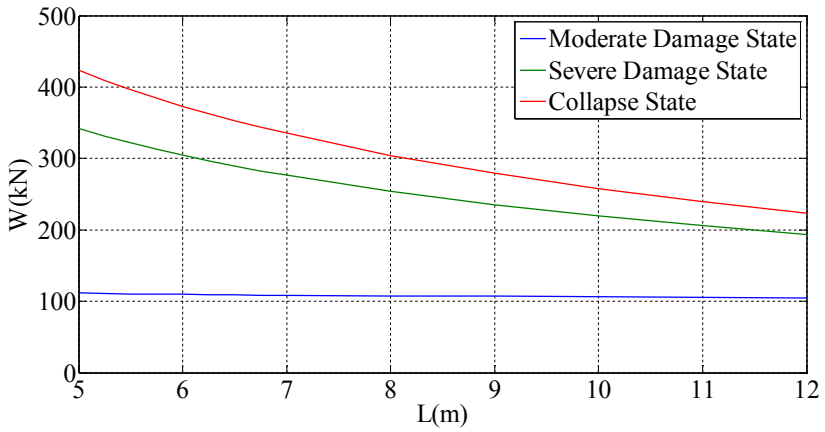

Table B.3. Structural loss estimation curves for the single-storey reinforced concrete industrial buildings which are located at 1st Earthquake Zone and Z3 Soil Class (cont.).

Cross-Section (cm)	Reinforcement Ratio	Structural Loss Estimation Curves
50×50	Minimum	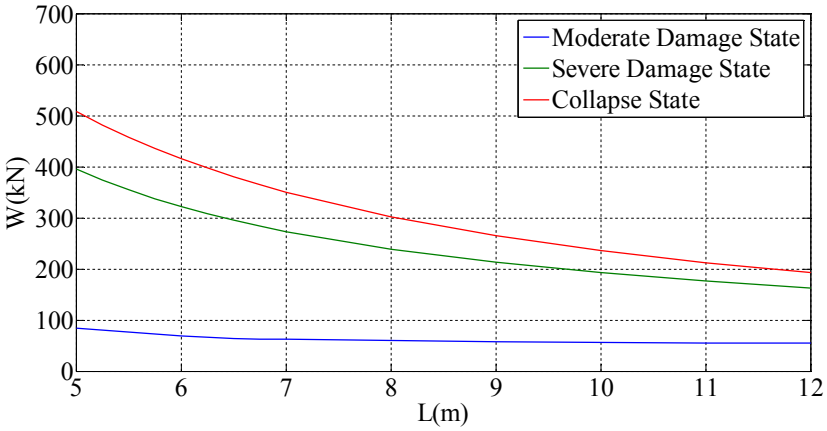
	Moderate	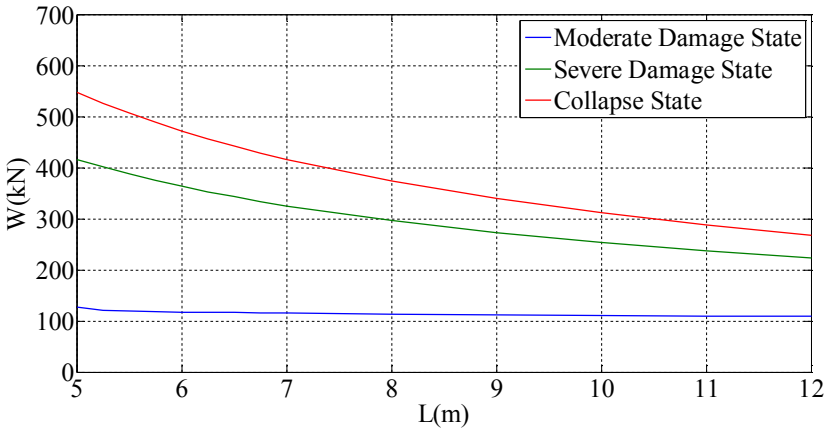
	High	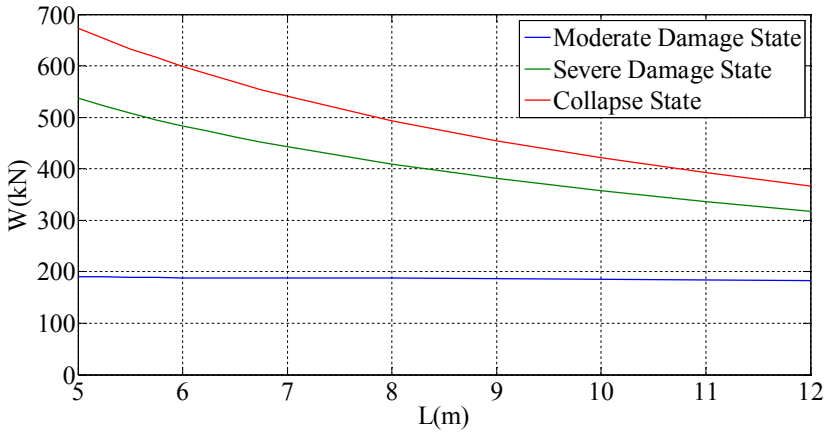

Table B.3. Structural loss estimation curves for the single-storey reinforced concrete industrial buildings which are located at 1st Earthquake Zone and Z3 Soil Class (cont.).

Cross-Section (cm)	Reinforcement Ratio	Structural Loss Estimation Curves
55×55	Minimum	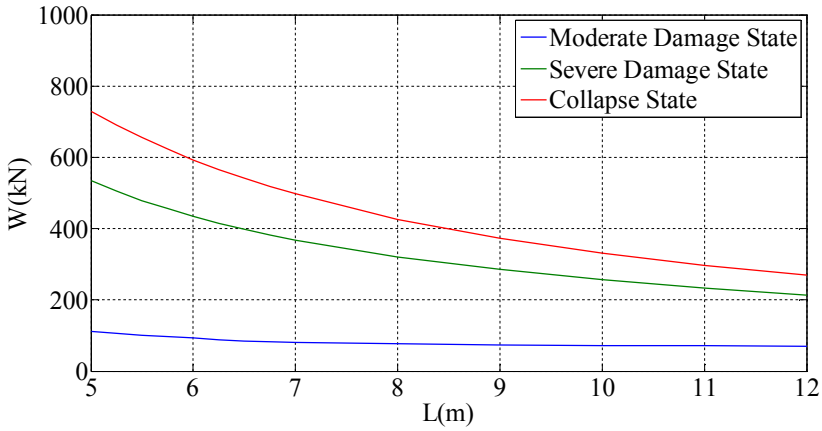
	Moderate	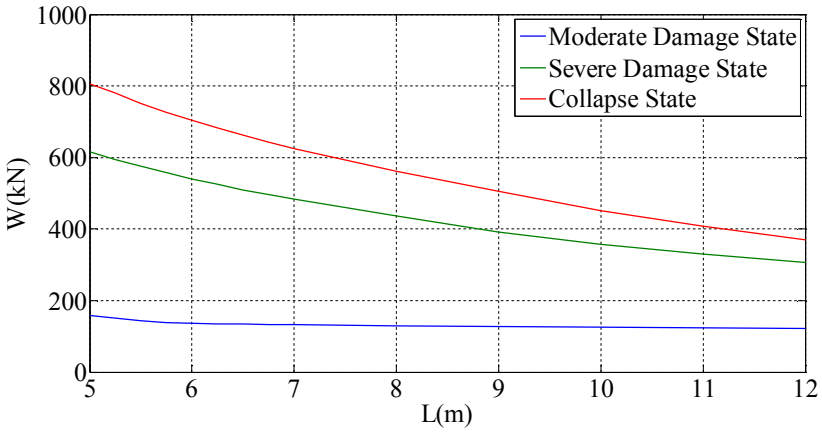
	High	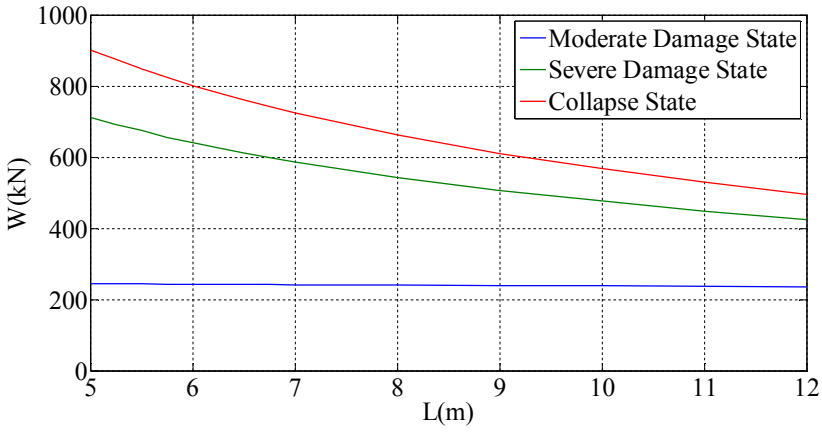

Table B.3. Structural loss estimation curves for the single-storey reinforced concrete industrial buildings which are located at 1st Earthquake Zone and Z3 Soil Class (cont.).

Cross-Section (cm)	Reinforcement Ratio	Structural Loss Estimation Curves
60×60	Minimum	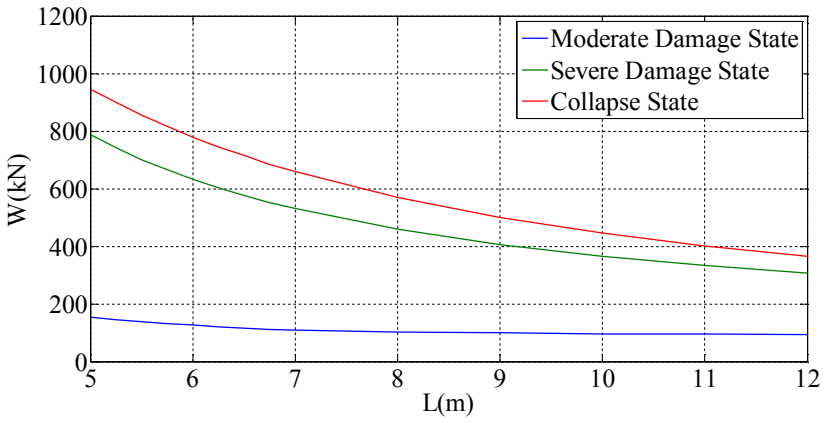
	Moderate	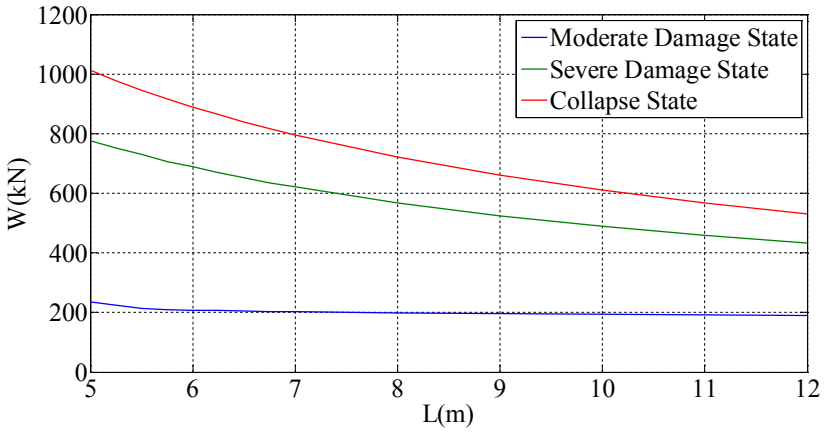
	High	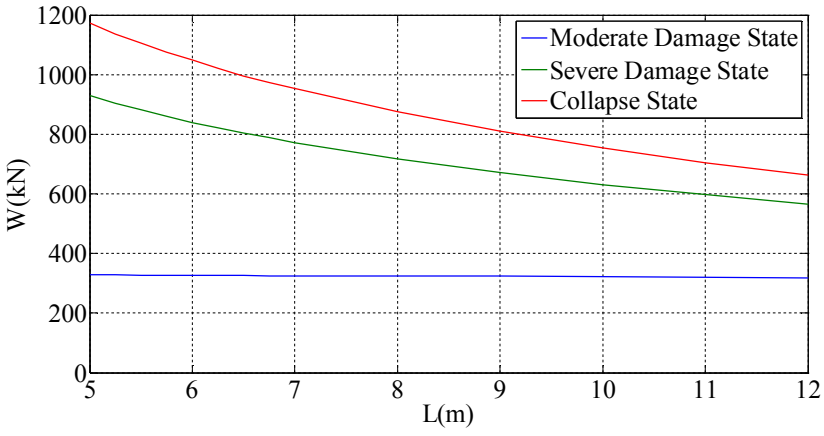

Table B.3. Structural loss estimation curves for the single-storey reinforced concrete industrial buildings which are located at 1st Earthquake Zone and Z3 Soil Class (cont.).

Cross-Section (cm)	Reinforcement Ratio	Structural Loss Estimation Curves
70×70	Minimum	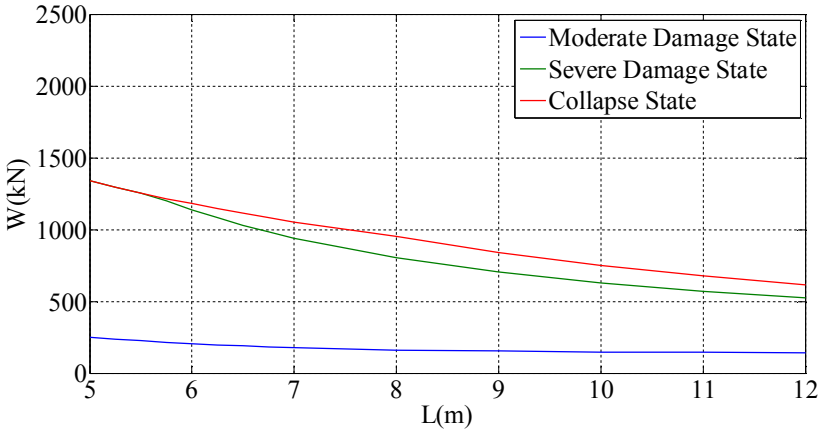
	Moderate	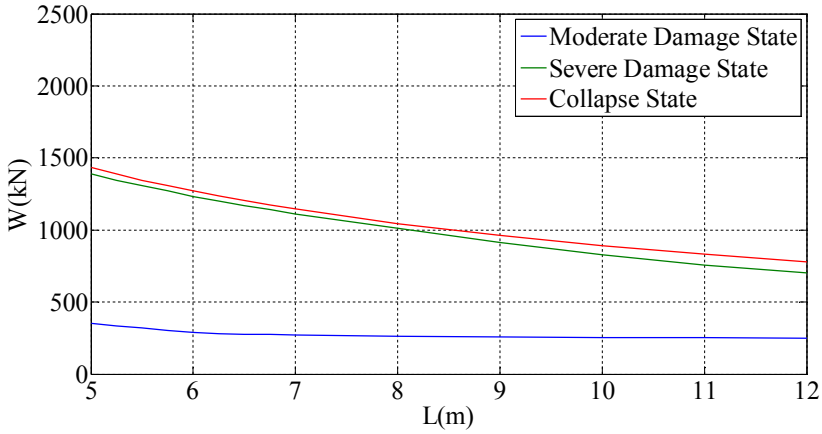
	High	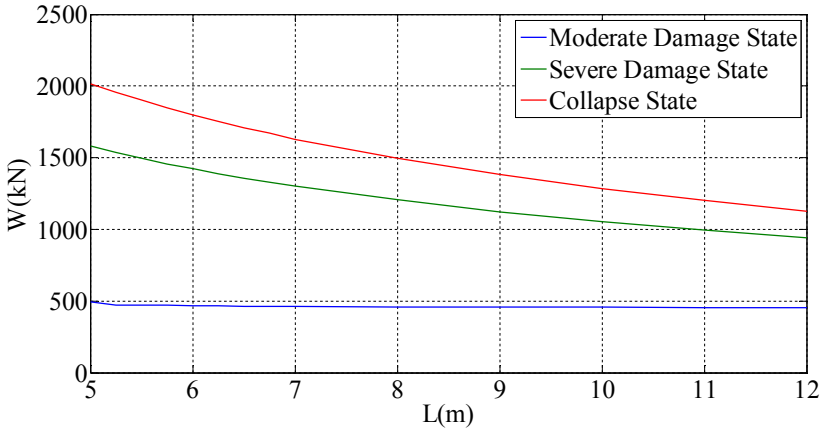

Table B.3. Structural loss estimation curves for the single-storey reinforced concrete industrial buildings which are located at 1st Earthquake Zone and Z3 Soil Class (cont.).

Cross-Section (cm)	Reinforcement Ratio	Structural Loss Estimation Curves
80×80	Minimum	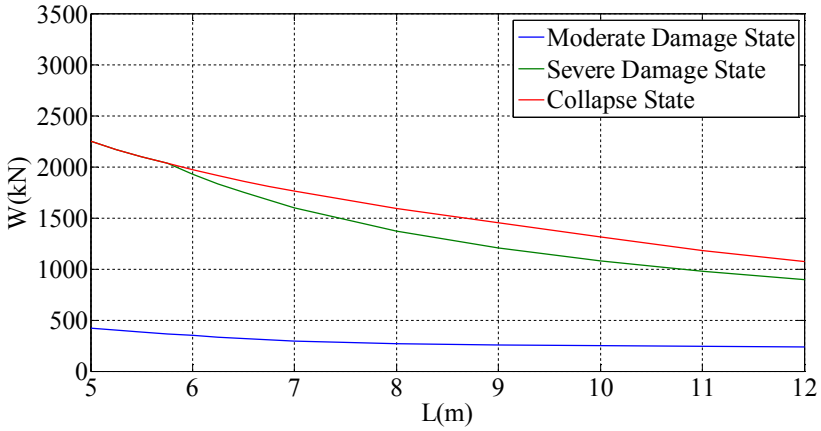
	Moderate	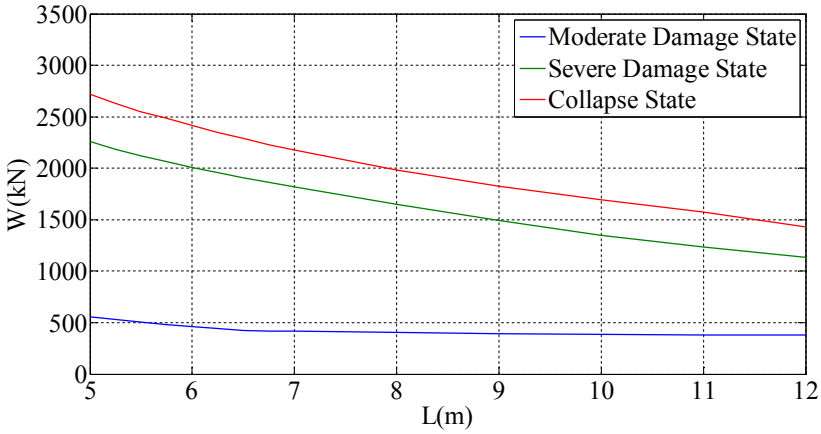
	High	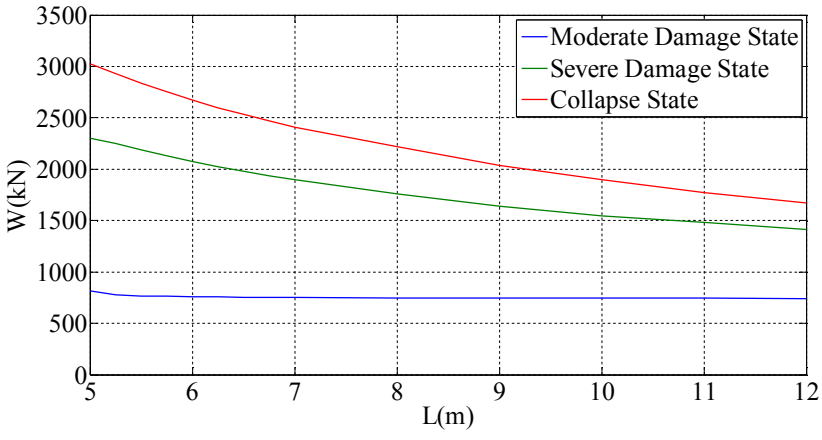

Table B.4. Structural loss estimation curves for the single-storey reinforced concrete industrial buildings which are located at 1st Earthquake Zone and Z4 Soil Class.

Cross-Section (cm)	Reinforcement Ratio	Structural Loss Estimation Curves
35×35	Minimum	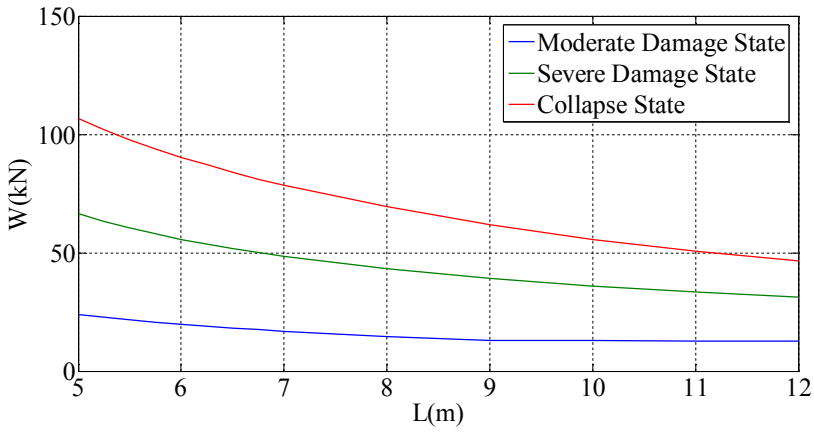
	Moderate	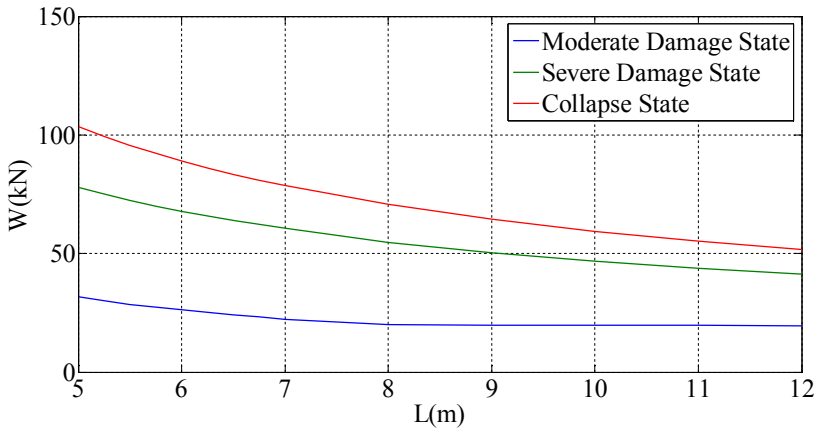
	High	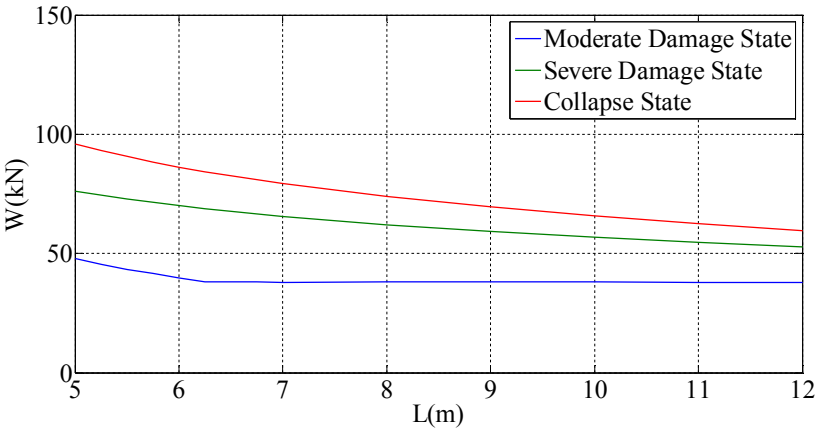

Table B.4. Structural loss estimation curves for the single-storey reinforced concrete industrial buildings which are located at 1st Earthquake Zone and Z4 Soil Class (cont.).

Cross-Section (cm)	Reinforcement Ratio	Structural Loss Estimation Curves
40×40	Minimum	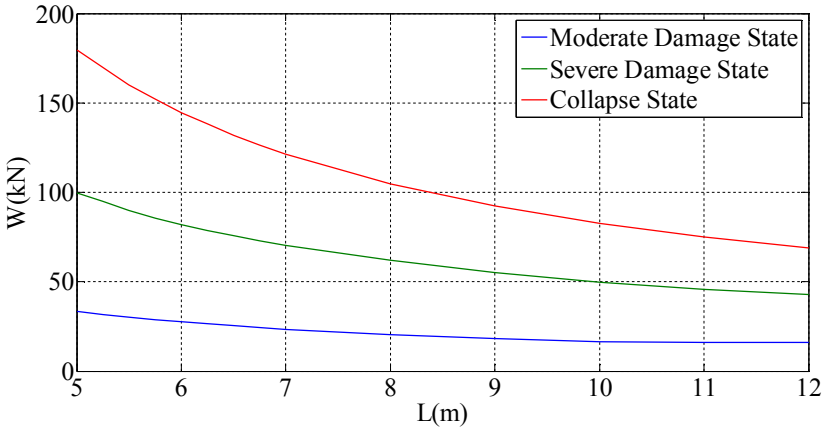
	Moderate	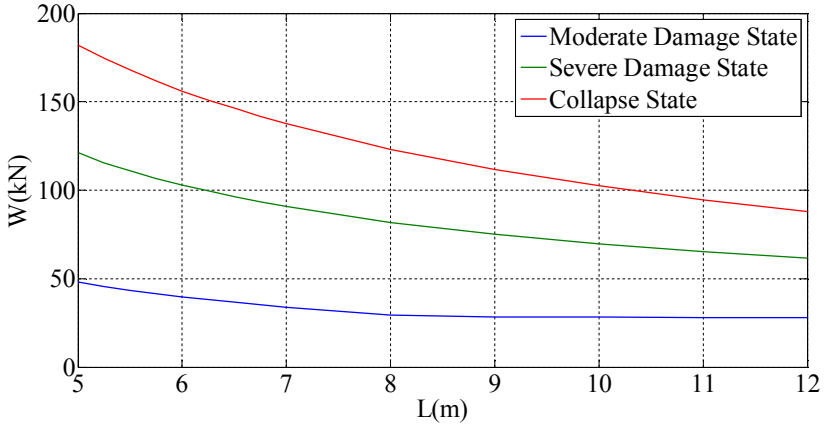
	High	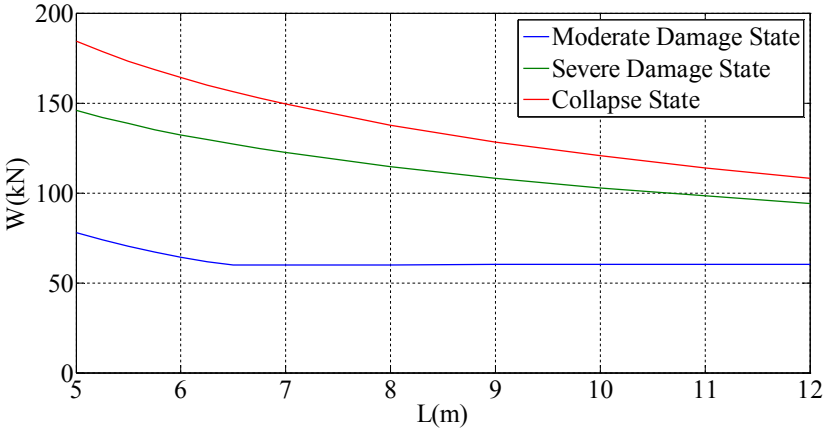

Table B.4. Structural loss estimation curves for the single-storey reinforced concrete industrial buildings which are located at 1st Earthquake Zone and Z4 Soil Class (cont.).

Cross-Section (cm)	Reinforcement Ratio	Structural Loss Estimation Curves
45×45	Minimum	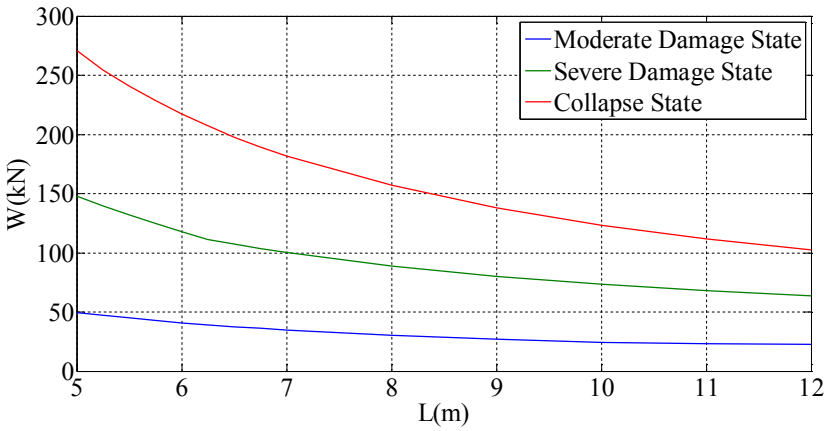
	Moderate	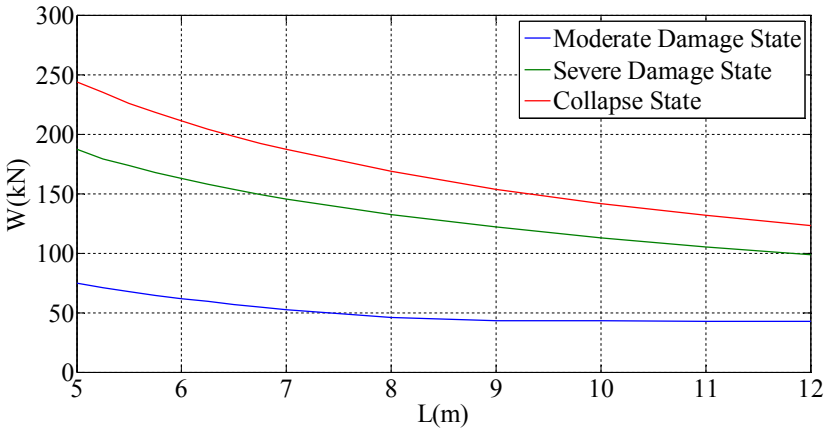
	High	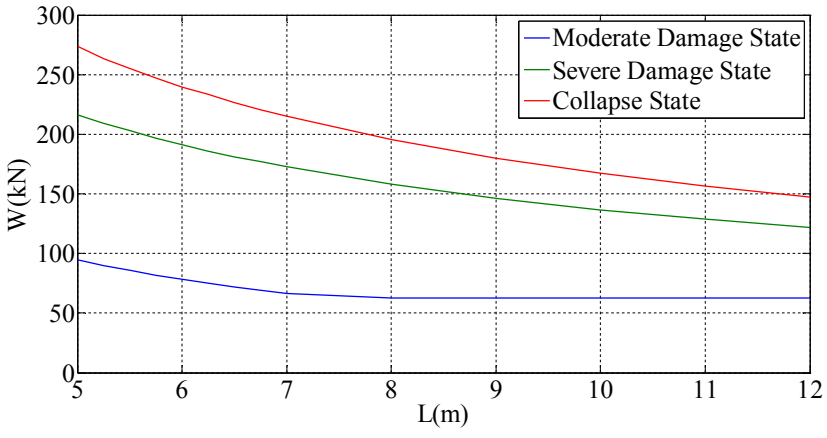

Table B.4. Structural loss estimation curves for the single-storey reinforced concrete industrial buildings which are located at 1st Earthquake Zone and Z4 Soil Class (cont.).

Cross-Section (cm)	Reinforcement Ratio	Structural Loss Estimation Curves
50×50	Minimum	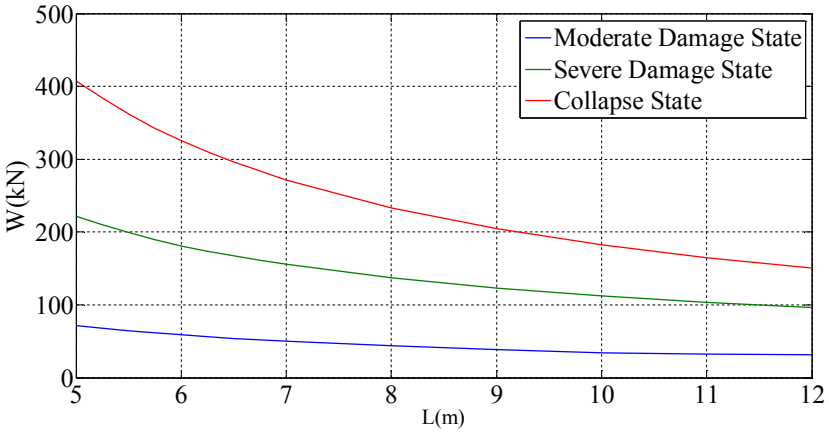
	Moderate	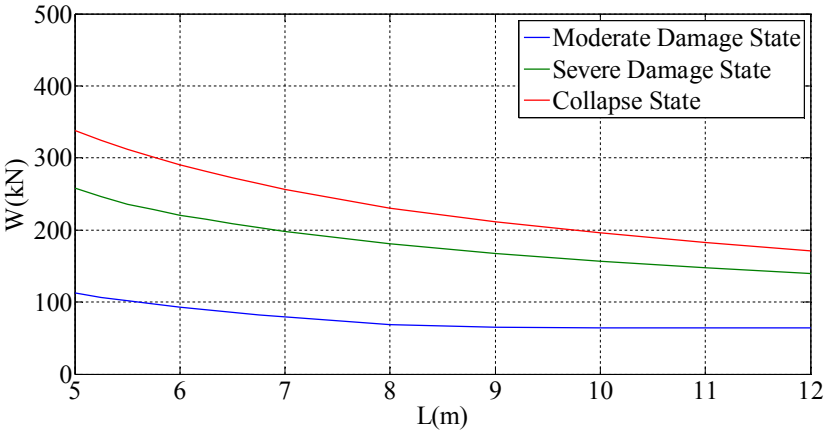
	High	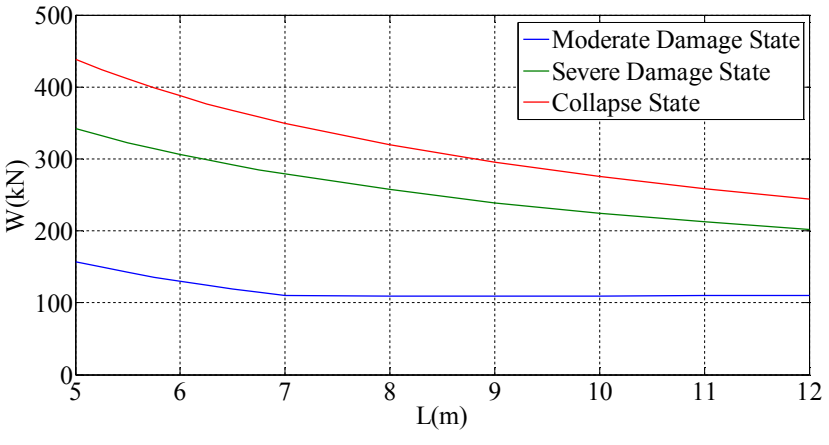

Table B.4. Structural loss estimation curves for the single-storey reinforced concrete industrial buildings which are located at 1st Earthquake Zone and Z4 Soil Class (cont.).

Cross-Section (cm)	Reinforcement Ratio	Structural Loss Estimation Curves
55×55	Minimum	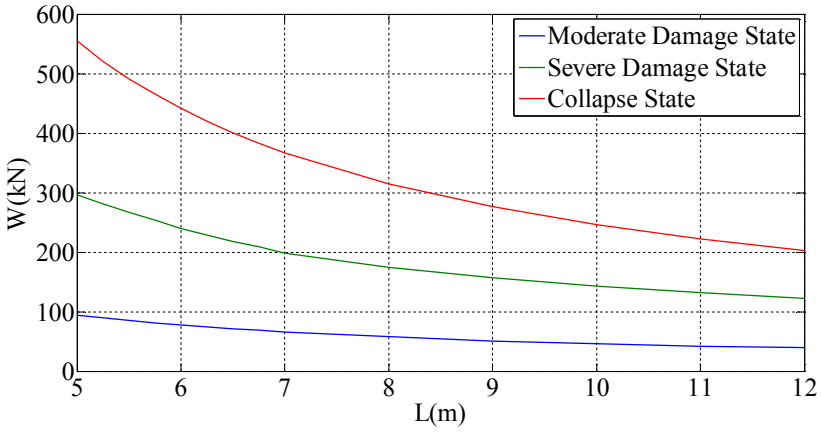
	Moderate	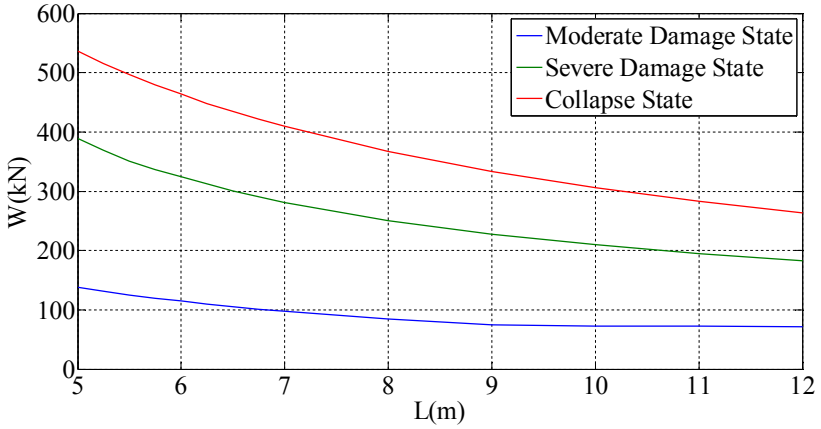
	High	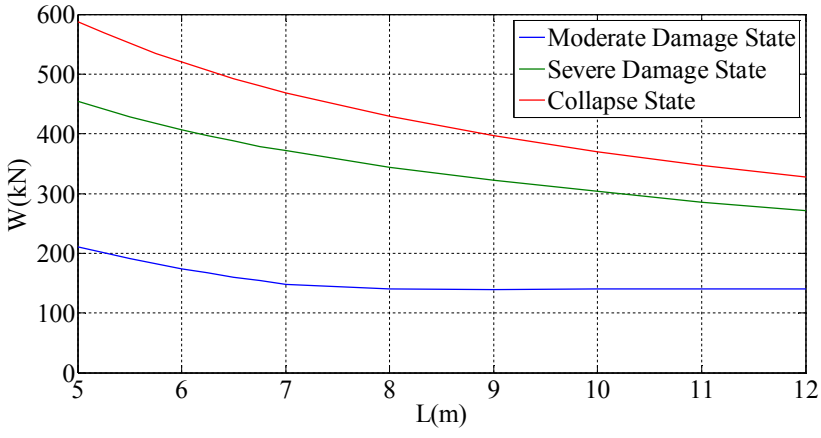

Table B.4. Structural loss estimation curves for the single-storey reinforced concrete industrial buildings which are located at 1st Earthquake Zone and Z4 Soil Class (cont.).

Cross-Section (cm)	Reinforcement Ratio	Structural Loss Estimation Curves
60×60	Minimum	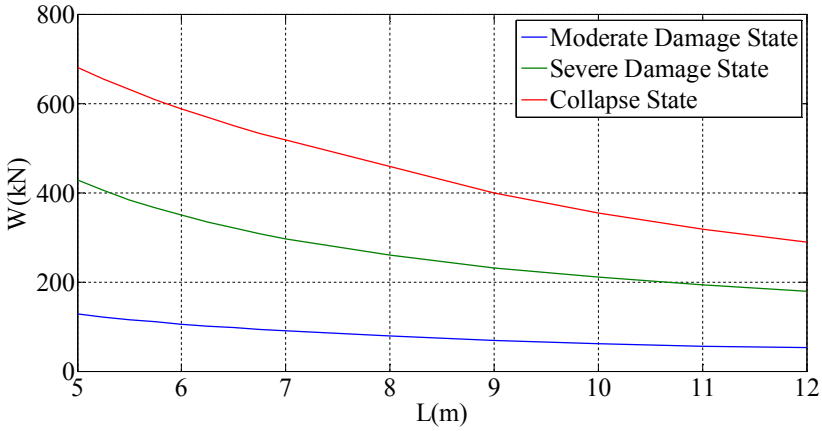
	Moderate	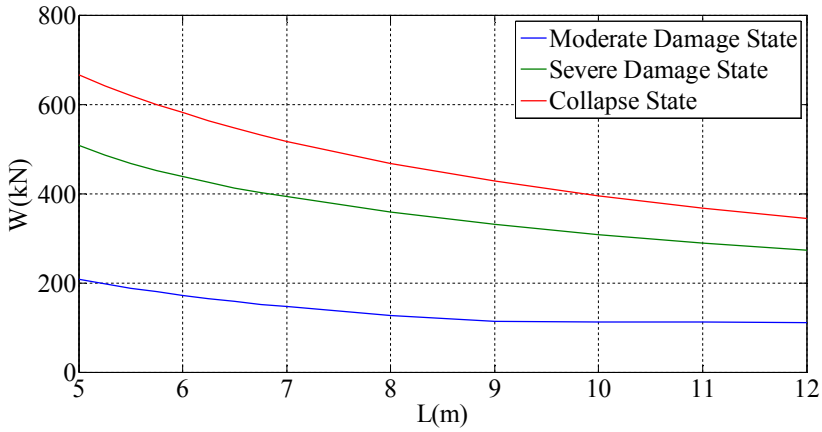
	High	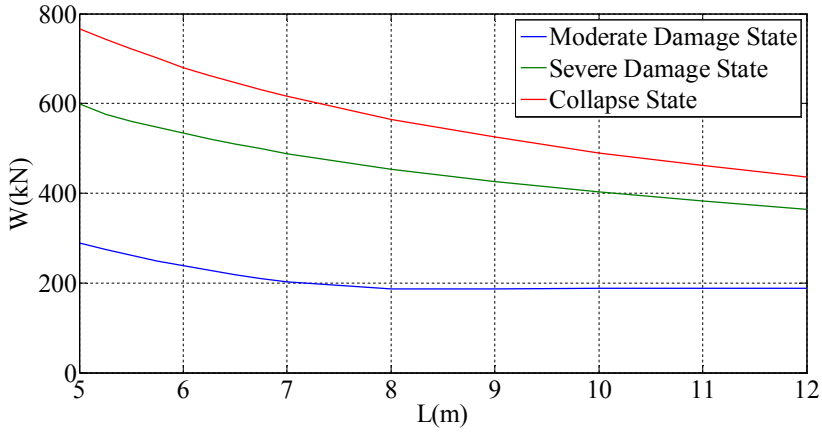

Table B.4. Structural loss estimation curves for the single-storey reinforced concrete industrial buildings which are located at 1st Earthquake Zone and Z4 Soil Class (cont.).

Cross-Section (cm)	Reinforcement Ratio	Structural Loss Estimation Curves
70×70	Minimum	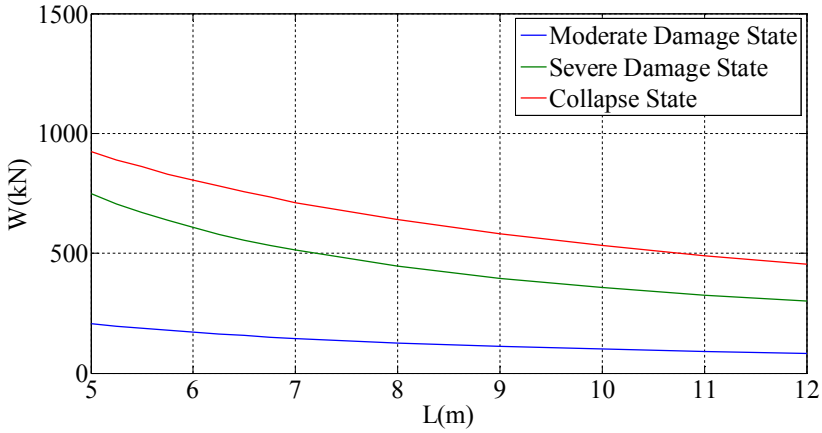
	Moderate	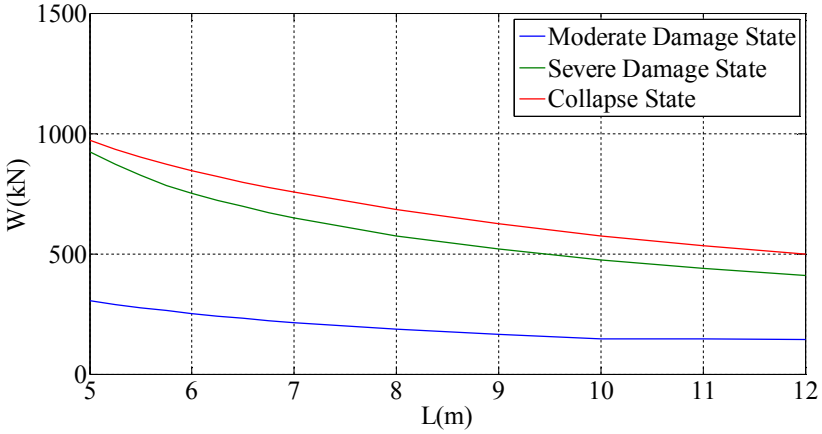
	High	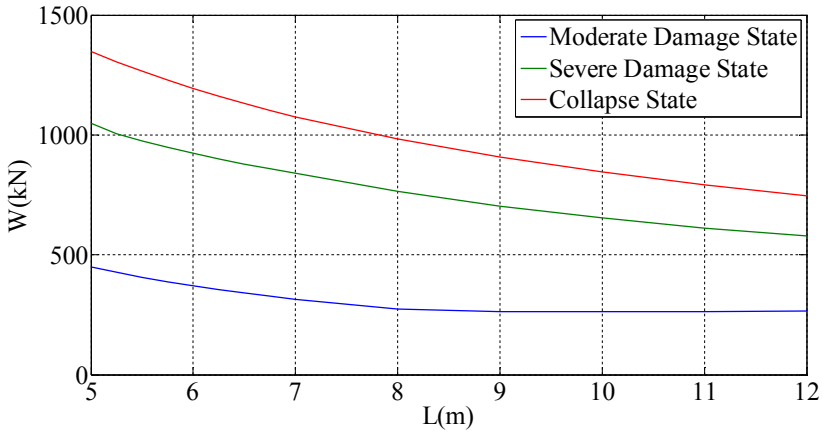

Table B.4. Structural loss estimation curves for the single-storey reinforced concrete industrial buildings which are located at 1st Earthquake Zone and Z4 Soil Class (cont.).

Cross-Section (cm)	Reinforcement Ratio	Structural Loss Estimation Curves
80×80	Minimum	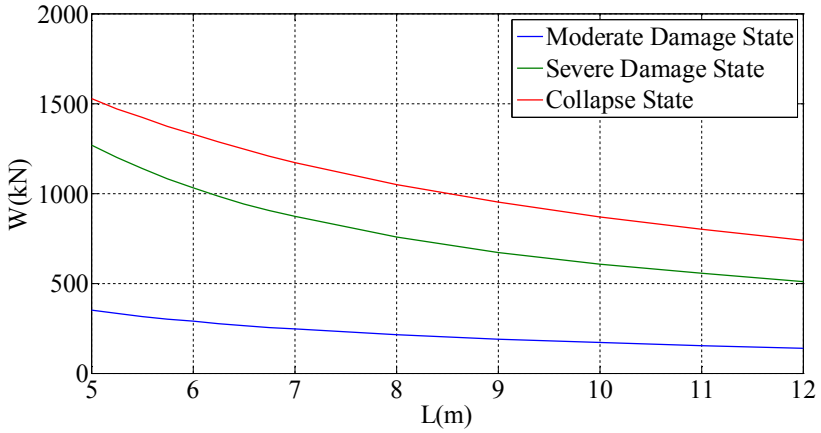
	Moderate	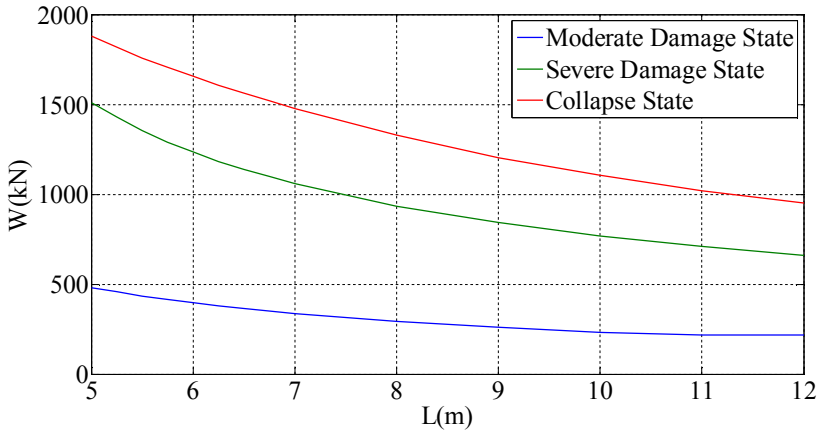
	High	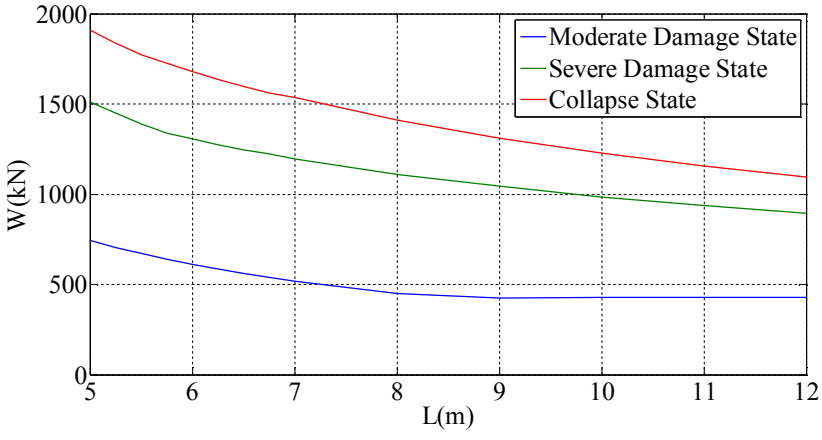

Table B.5. Structural loss estimation curves for the single-storey reinforced concrete industrial buildings which are located at 2nd Earthquake Zone and Z1 Soil Class.

Cross-Section (cm)	Reinforcement Ratio	Structural Loss Estimation Curves
35×35	Minimum	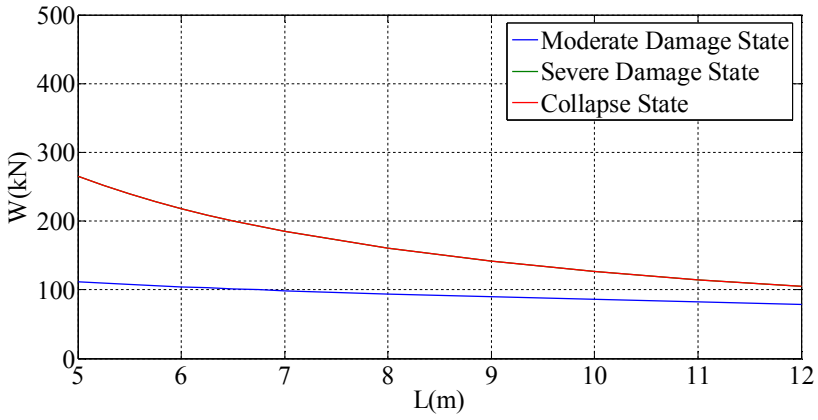
	Moderate	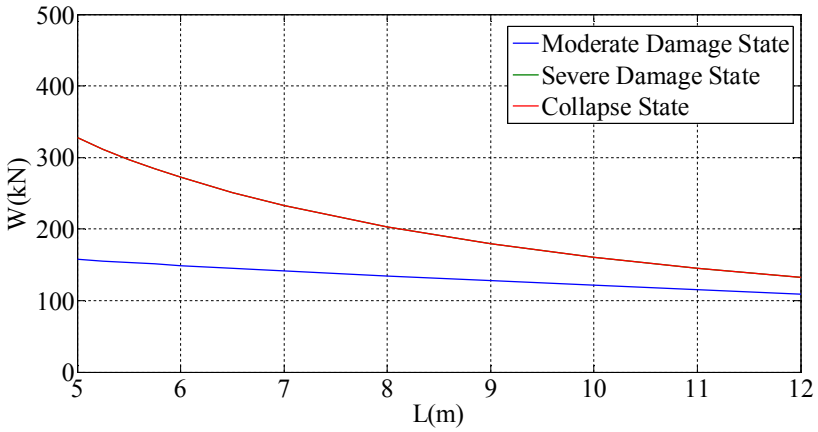
	High	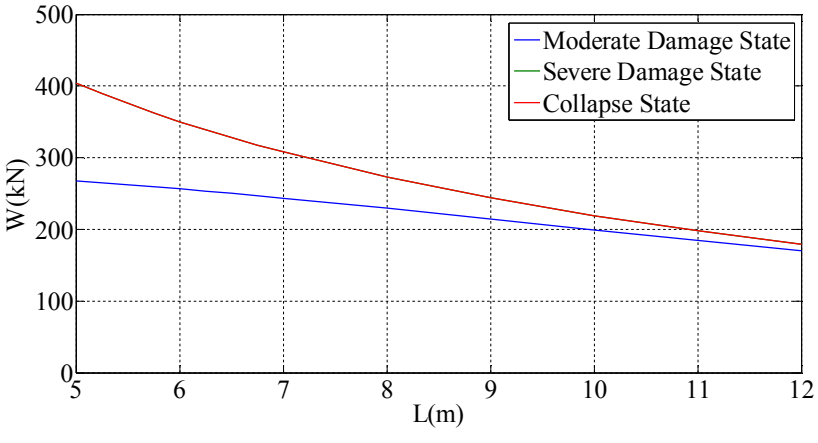

Table B.5. Structural loss estimation curves for the single-storey reinforced concrete industrial buildings which are located at 2nd Earthquake Zone and Z1 Soil Class (cont.).

Cross-Section (cm)	Reinforcement Ratio	Structural Loss Estimation Curves
40×40	Minimum	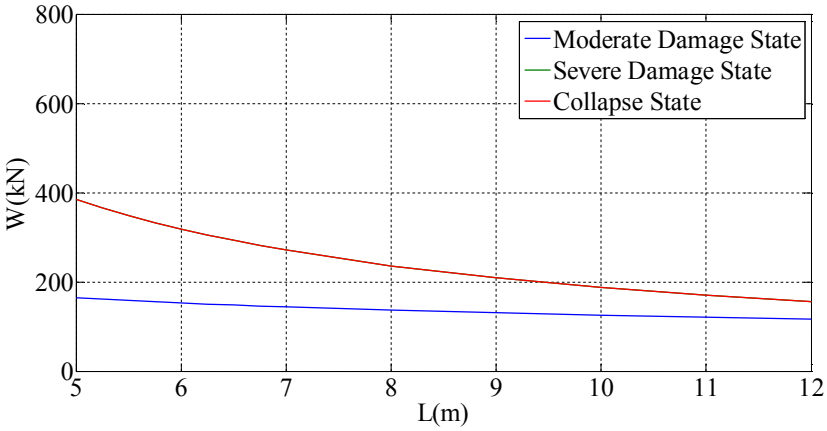
	Moderate	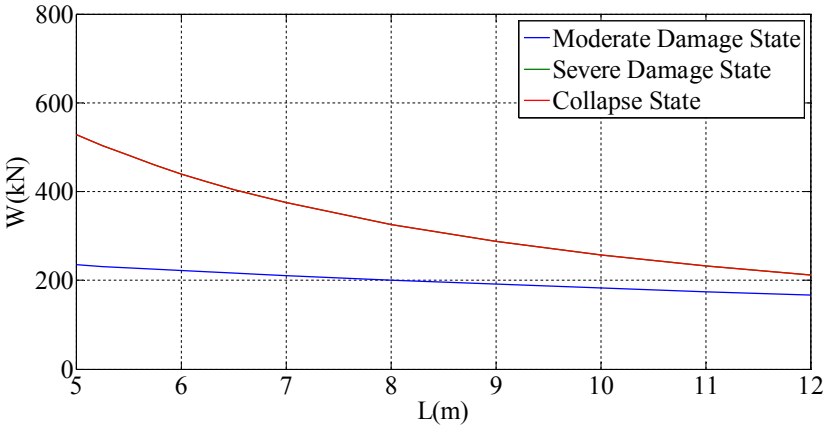
	High	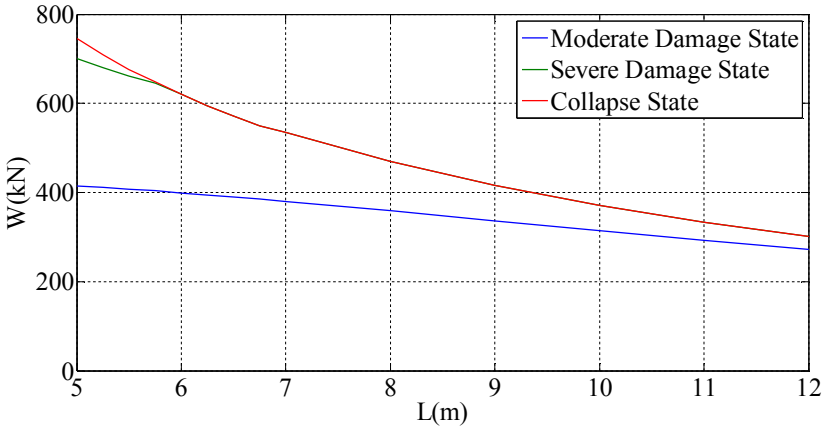

Table B.5. Structural loss estimation curves for the single-storey reinforced concrete industrial buildings which are located at 2nd Earthquake Zone and Z1 Soil Class (cont.).

Cross-Section (cm)	Reinforcement Ratio	Structural Loss Estimation Curves
45×45	Minimum	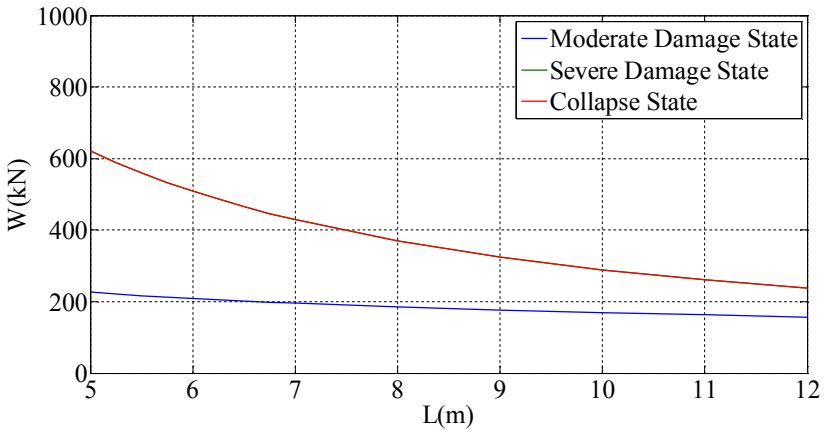
	Moderate	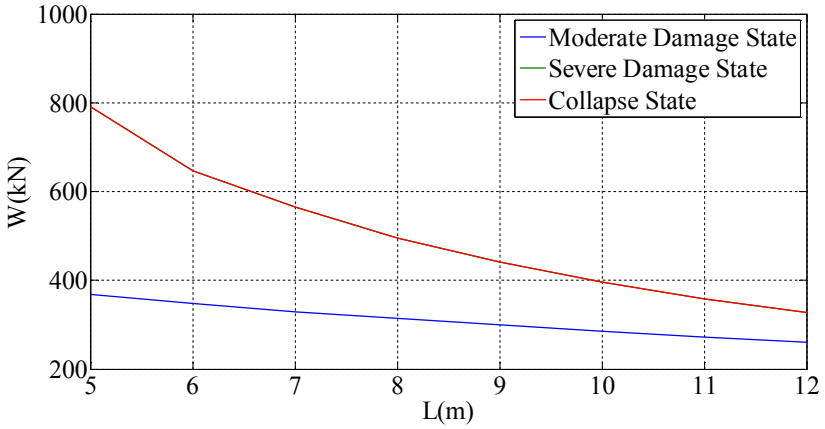
	High	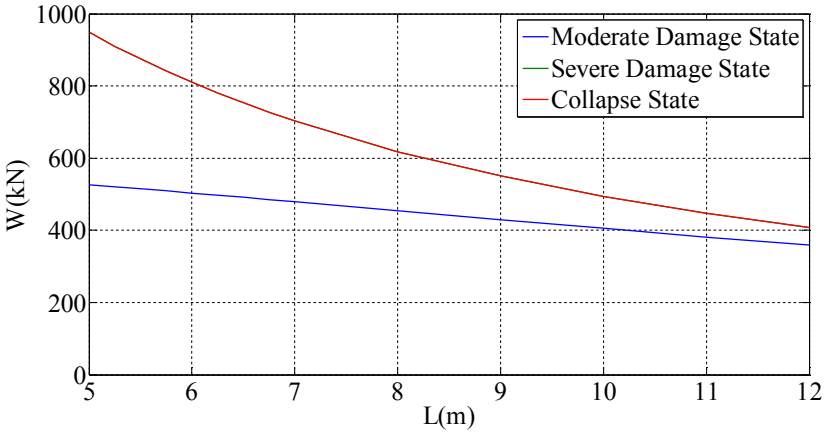

Table B.5. Structural loss estimation curves for the single-storey reinforced concrete industrial buildings which are located at 2nd Earthquake Zone and Z1 Soil Class (cont.).

Cross-Section (cm)	Reinforcement Ratio	Structural Loss Estimation Curves
50×50	Minimum	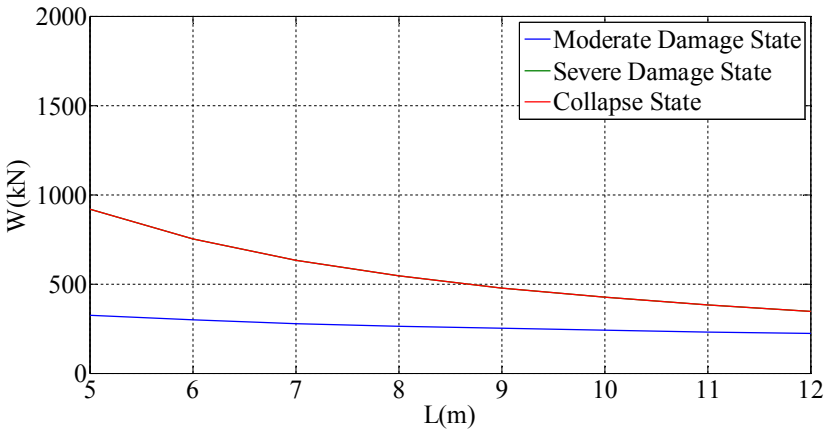
	Moderate	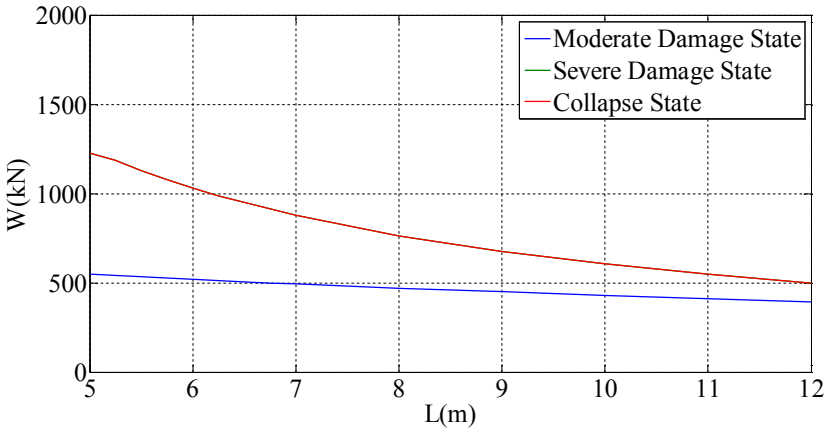
	High	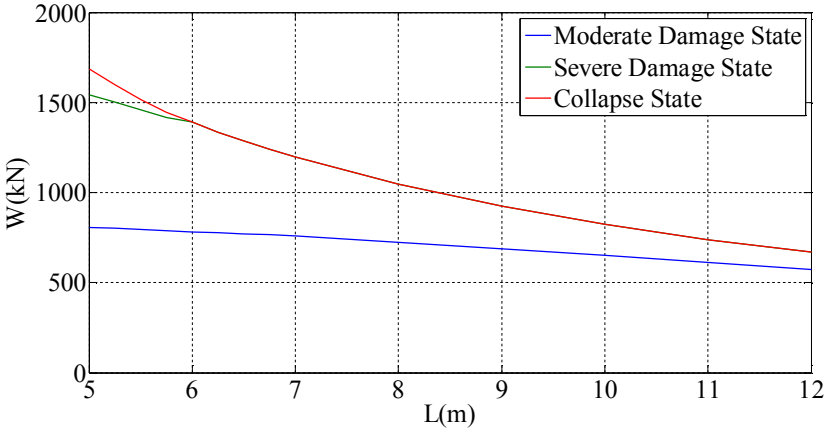

Table B.5. Structural loss estimation curves for the single-storey reinforced concrete industrial buildings which are located at 2nd Earthquake Zone and Z1 Soil Class (cont.).

Cross-Section (cm)	Reinforcement Ratio	Structural Loss Estimation Curves
55×55	Minimum	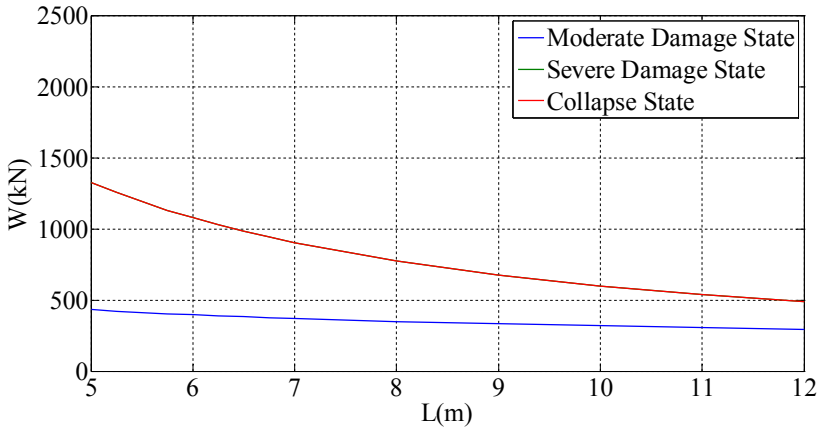
	Moderate	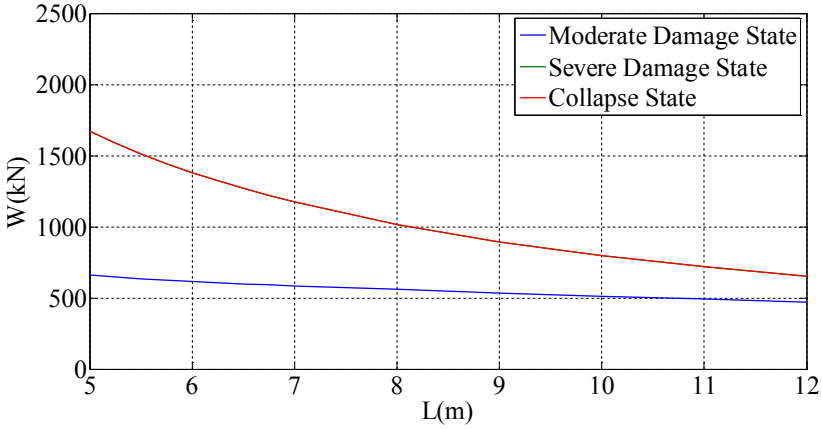
	High	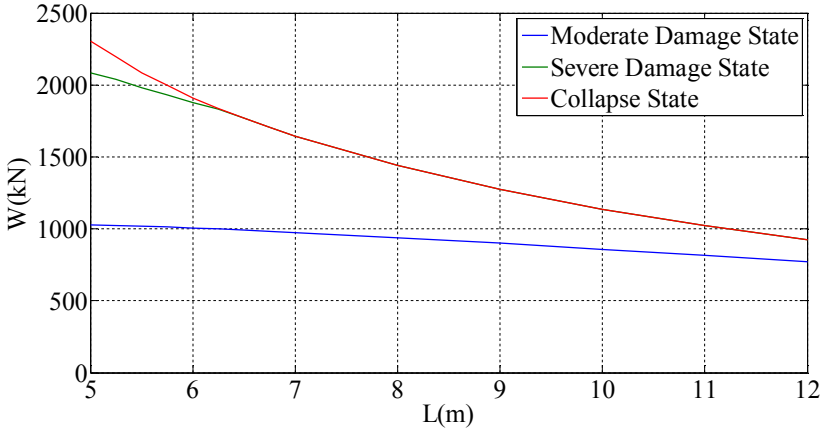

Table B.5. Structural loss estimation curves for the single-storey reinforced concrete industrial buildings which are located at 2nd Earthquake Zone and Z1 Soil Class (cont.).

Cross-Section (cm)	Reinforcement Ratio	Structural Loss Estimation Curves
60×60	Minimum	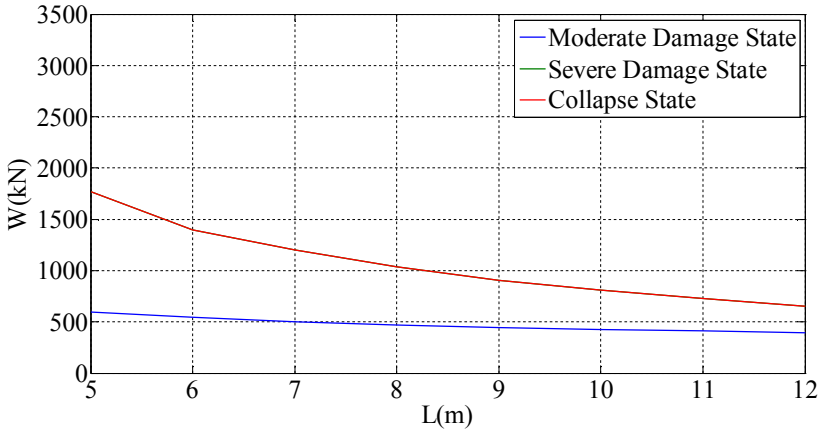
	Moderate	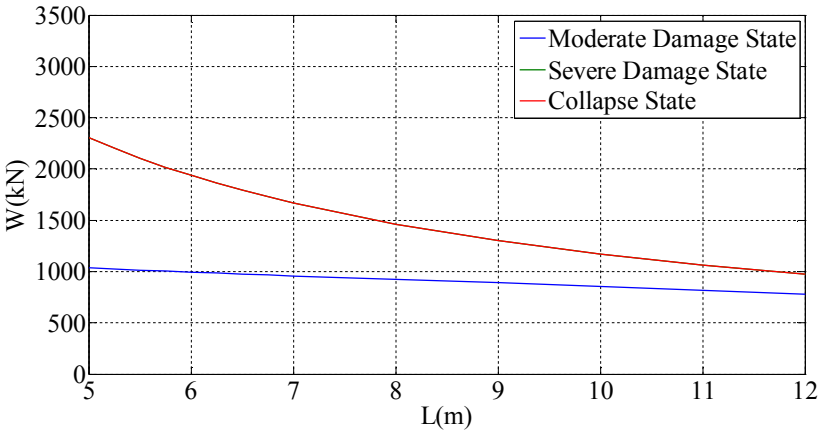
	High	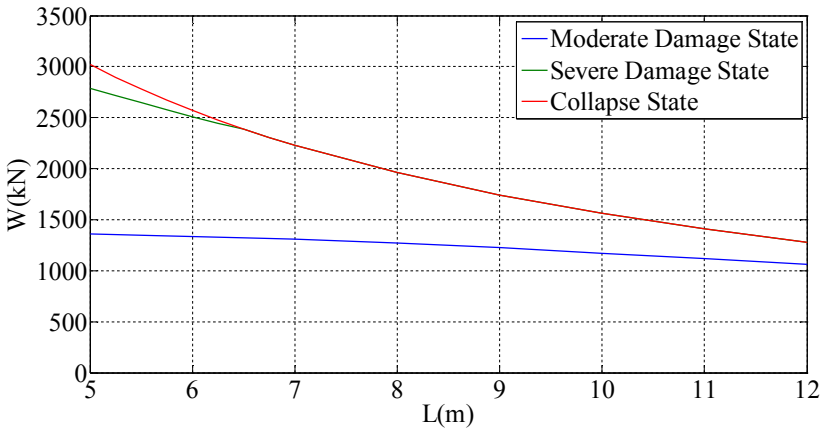

Table B.5. Structural loss estimation curves for the single-storey reinforced concrete industrial buildings which are located at 2nd Earthquake Zone and Z1 Soil Class (cont.).

Cross-Section (cm)	Reinforcement Ratio	Structural Loss Estimation Curves
70×70	Minimum	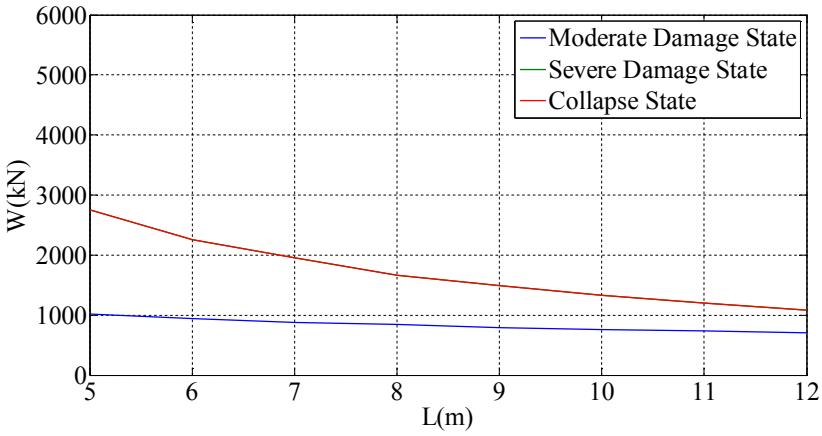
	Moderate	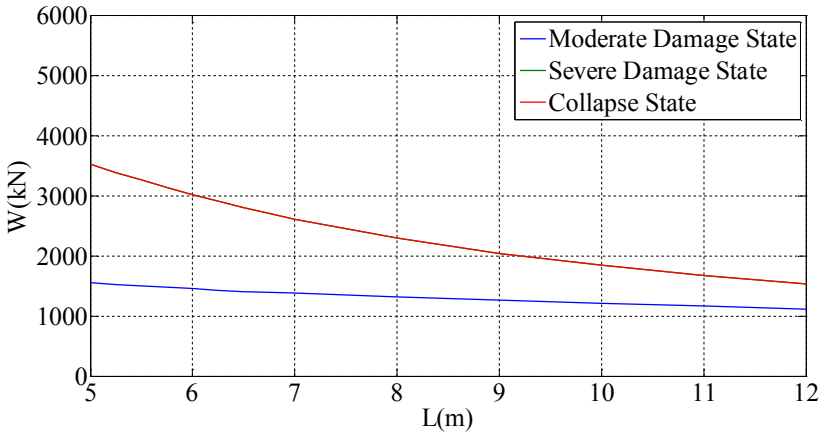
	High	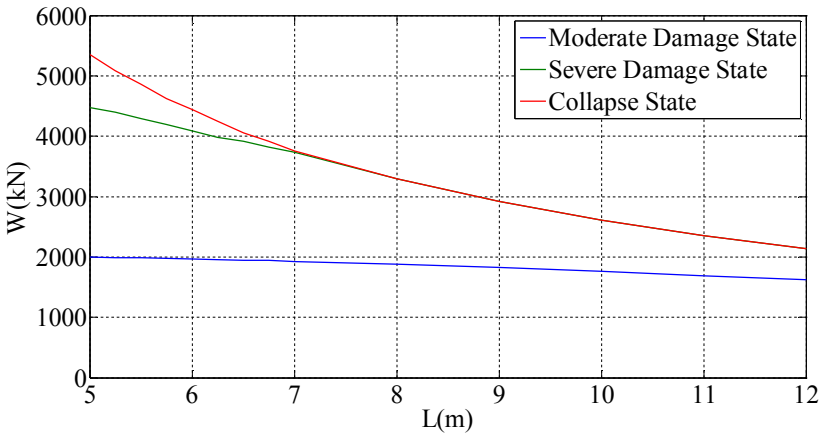

Table B.5. Structural loss estimation curves for the single-storey reinforced concrete industrial buildings which are located at 2nd Earthquake Zone and Z1 Soil Class (cont.).

Cross-Section (cm)	Reinforcement Ratio	Structural Loss Estimation Curves
80×80	Minimum	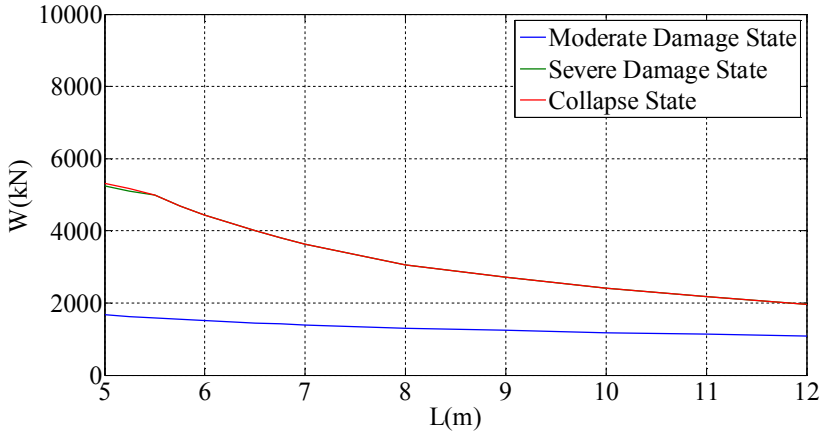
	Moderate	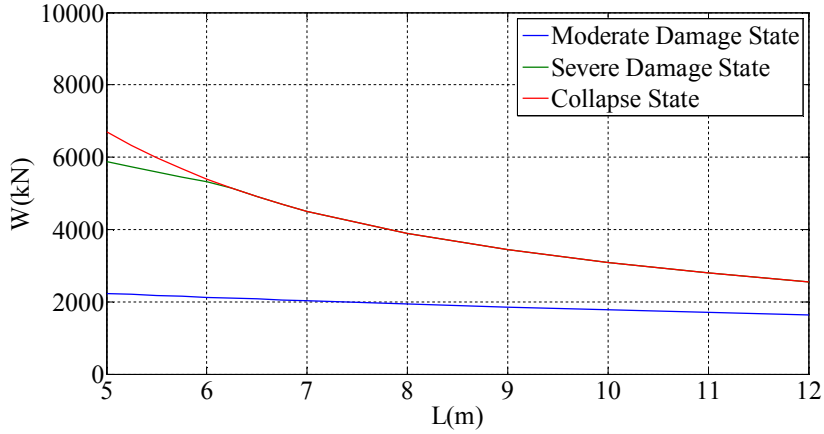
	High	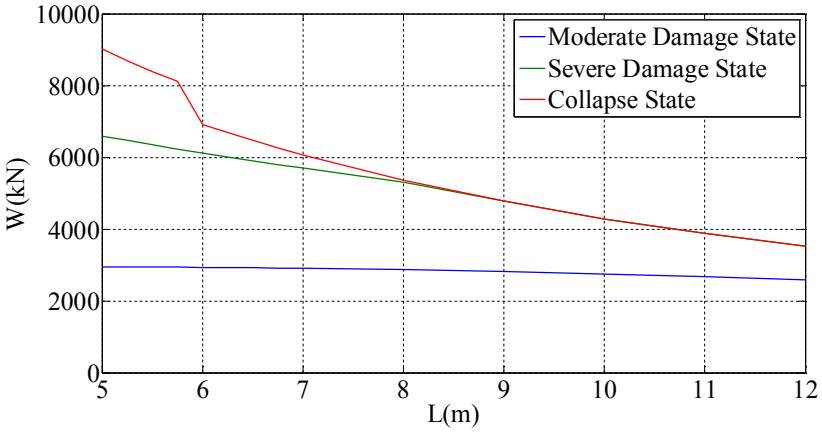

Table B.6. Structural loss estimation curves for the single-storey reinforced concrete industrial buildings which are located at 2nd Earthquake Zone and Z2 Soil Class.

Cross-Section (cm)	Reinforcement Ratio	Structural Loss Estimation Curves
35×35	Minimum	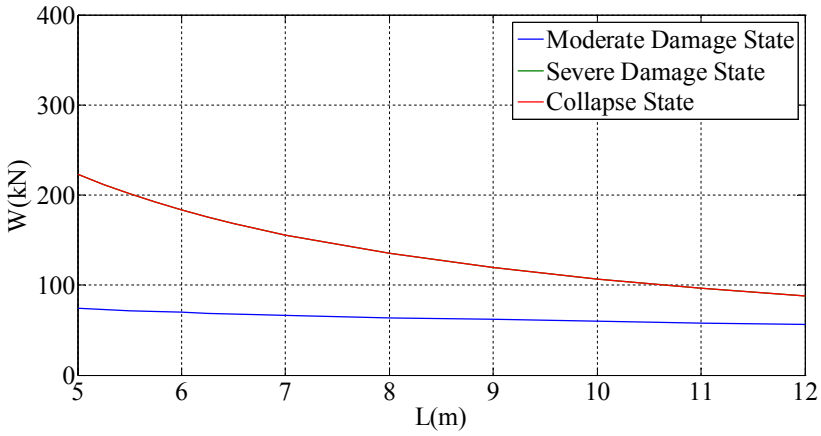
	Moderate	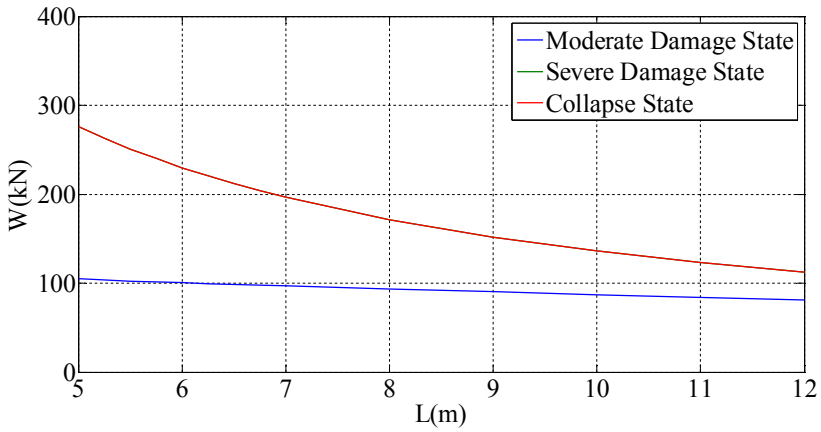
	High	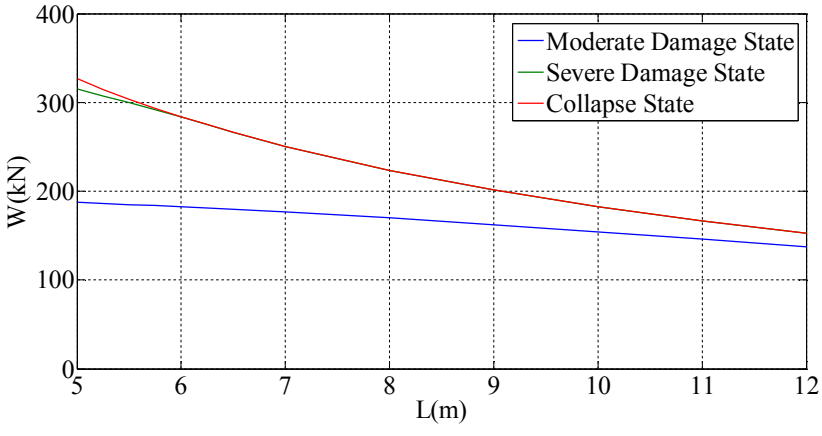

Table B.6. Structural loss estimation curves for the single-storey reinforced concrete industrial buildings which are located at 2nd Earthquake Zone and Z2 Soil Class (cont.).

Cross-Section (cm)	Reinforcement Ratio	Structural Loss Estimation Curves
40×40	Minimum	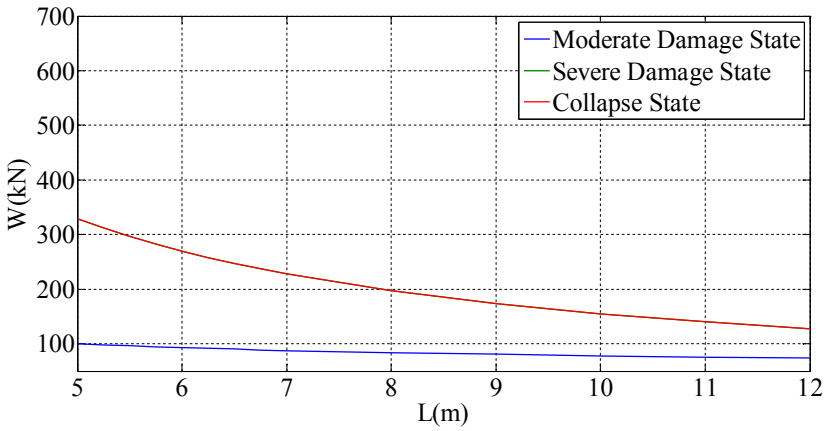
	Moderate	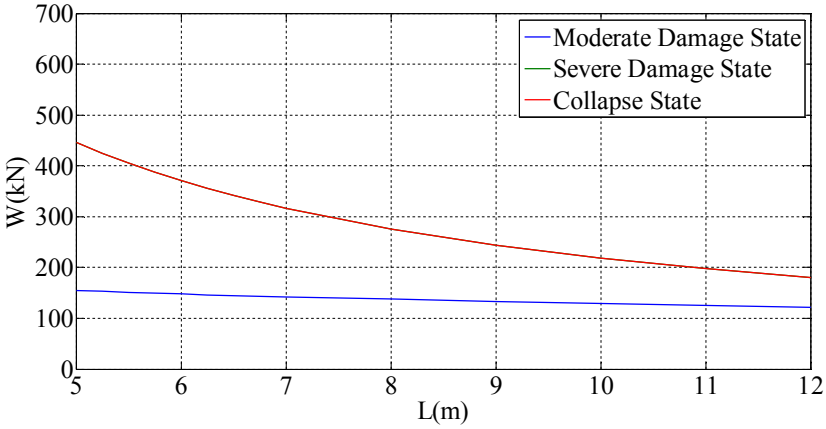
	High	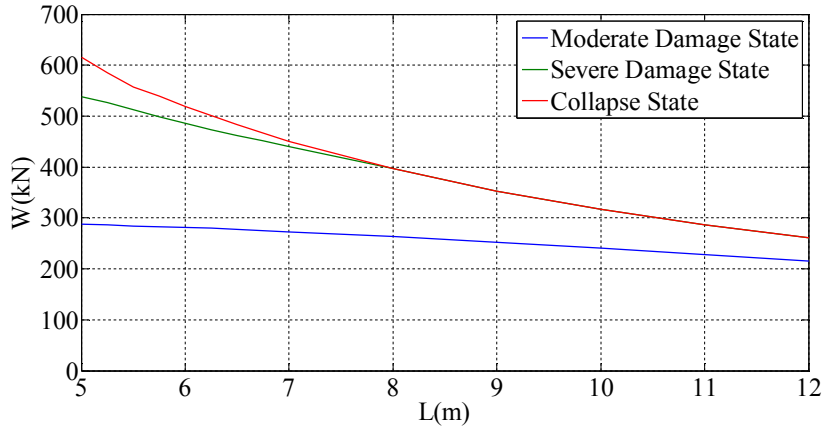

Table B.6. Structural loss estimation curves for the single-storey reinforced concrete industrial buildings which are located at 2nd Earthquake Zone and Z2 Soil Class (cont.).

Cross-Section (cm)	Reinforcement Ratio	Structural Loss Estimation Curves
45×45	Minimum	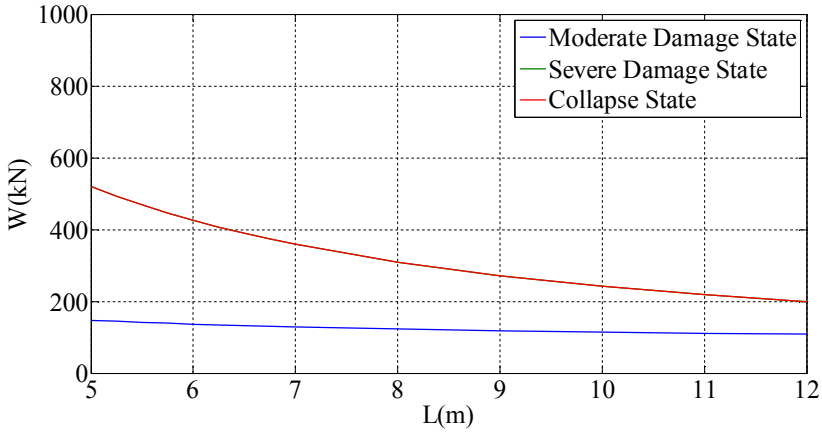
	Moderate	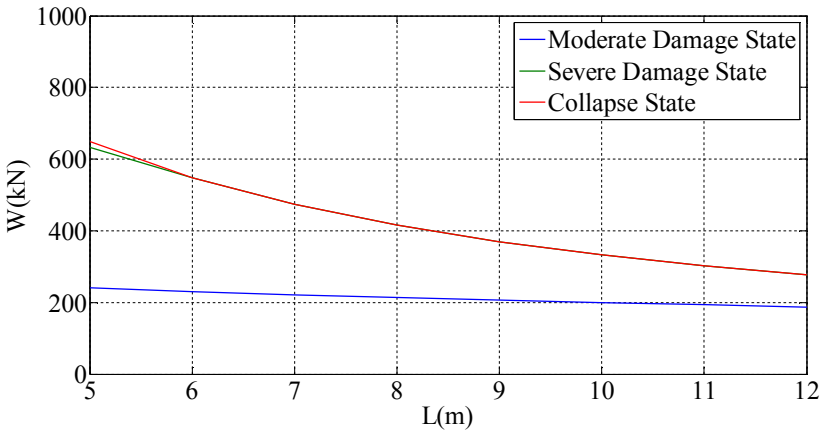
	High	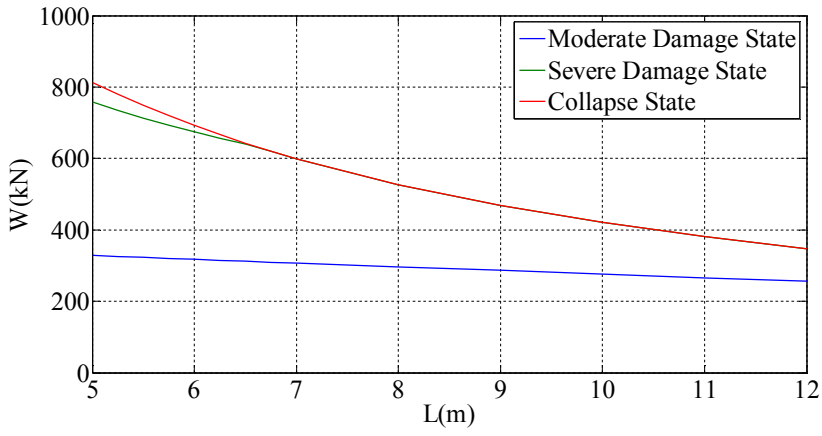

Table B.6. Structural loss estimation curves for the single-storey reinforced concrete industrial buildings which are located at 2nd Earthquake Zone and Z2 Soil Class (cont.).

Cross-Section (cm)	Reinforcement Ratio	Structural Loss Estimation Curves
50×50	Minimum	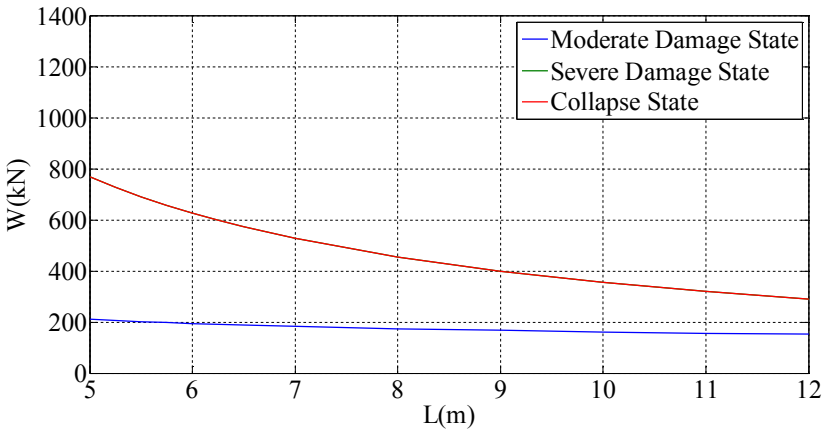
	Moderate	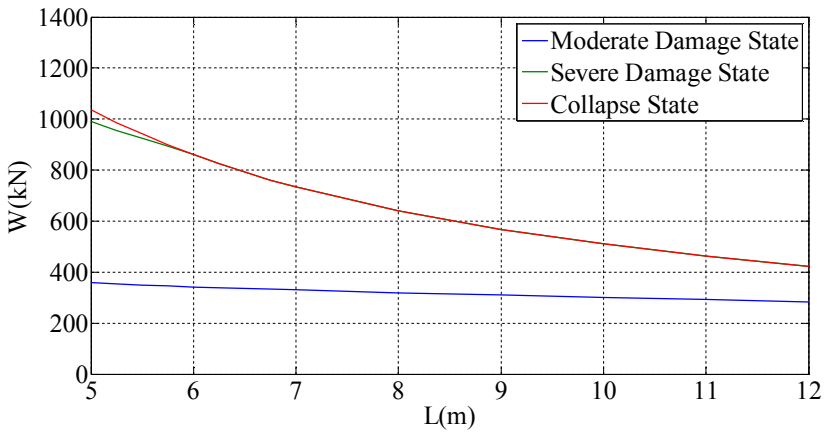
	High	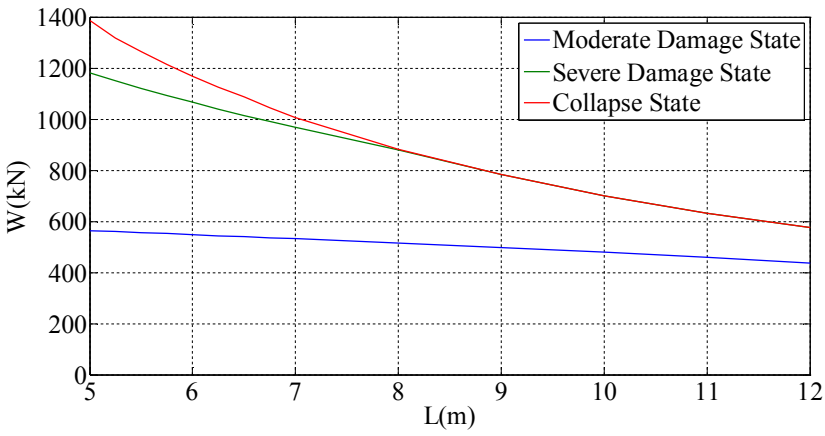

Table B.6. Structural loss estimation curves for the single-storey reinforced concrete industrial buildings which are located at 2nd Earthquake Zone and Z2 Soil Class (cont.).

Cross-Section (cm)	Reinforcement Ratio	Structural Loss Estimation Curves
55×55	Minimum	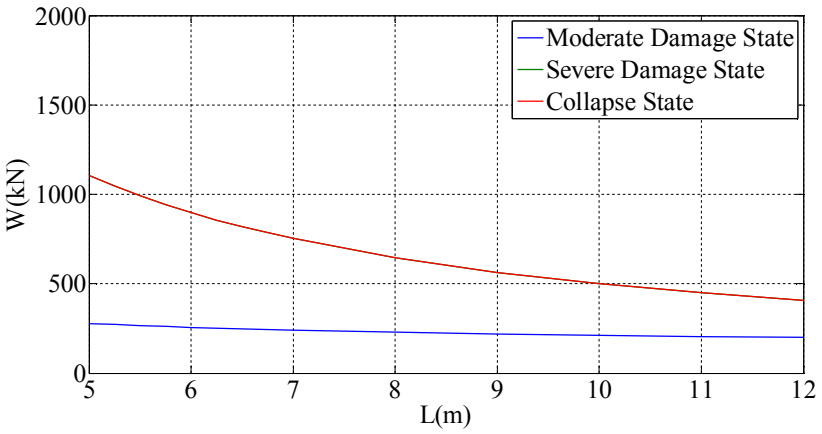
	Moderate	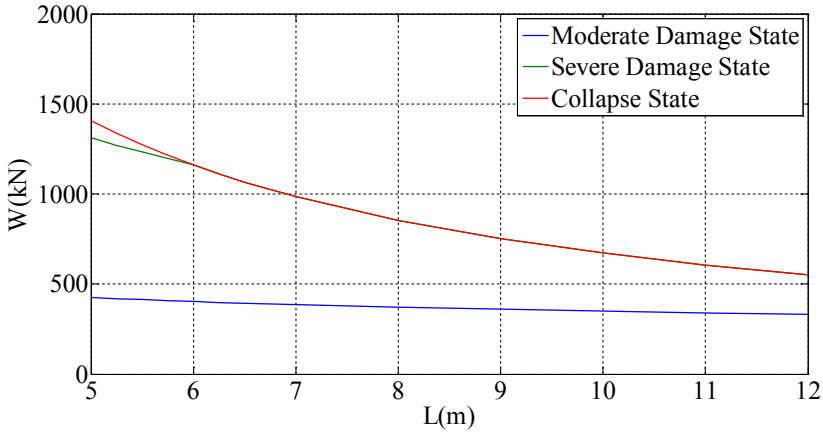
	High	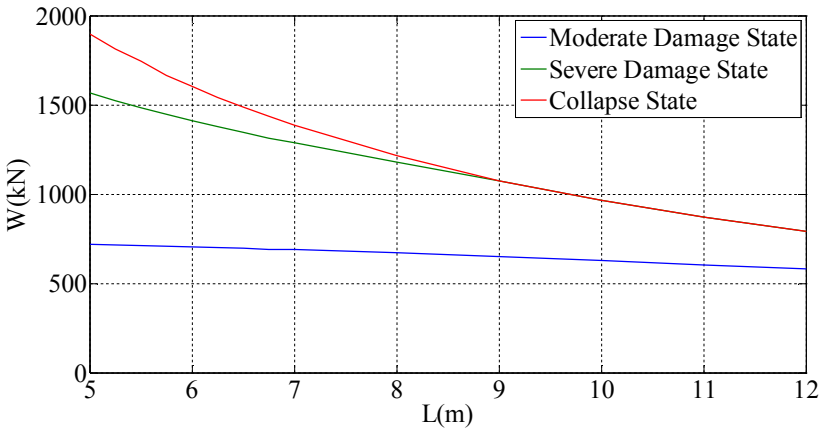

Table B.6. Structural loss estimation curves for the single-storey reinforced concrete industrial buildings which are located at 2nd Earthquake Zone and Z2 Soil Class (cont.).

Cross-Section (cm)	Reinforcement Ratio	Structural Loss Estimation Curves
60×60	Minimum	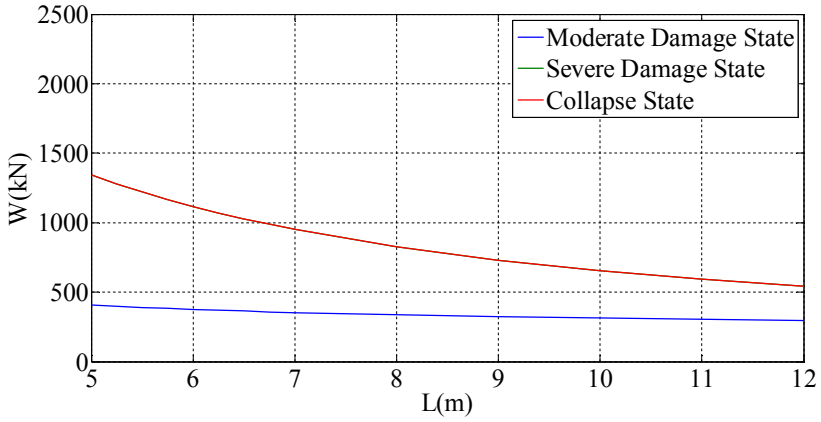
	Moderate	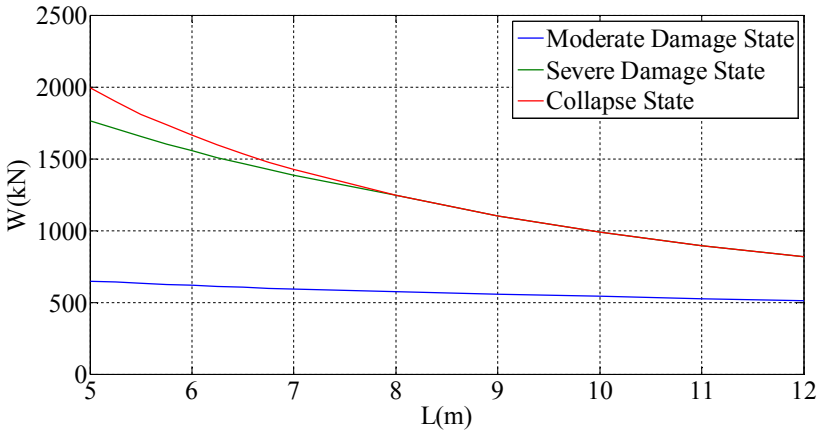
	High	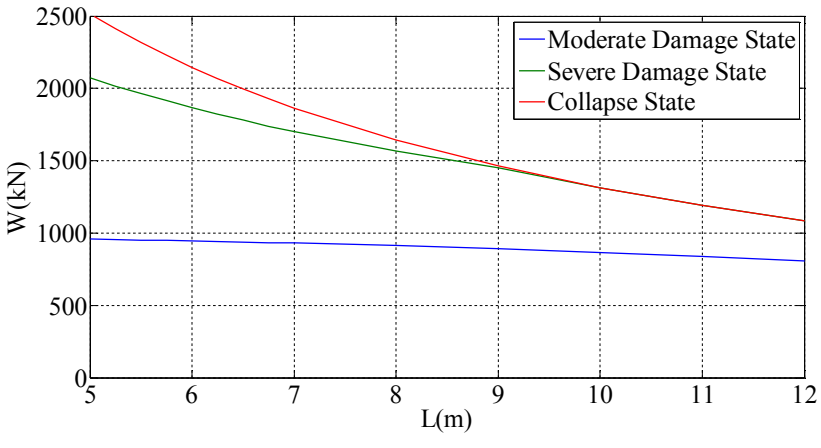

Table B.6. Structural loss estimation curves for the single-storey reinforced concrete industrial buildings which are located at 2nd Earthquake Zone and Z2 Soil Class (cont.).

Cross-Section (cm)	Reinforcement Ratio	Structural Loss Estimation Curves
70×70	Minimum	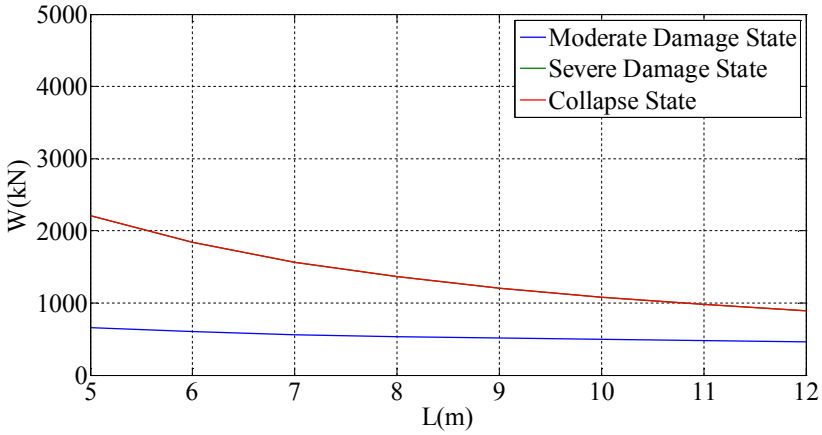
	Moderate	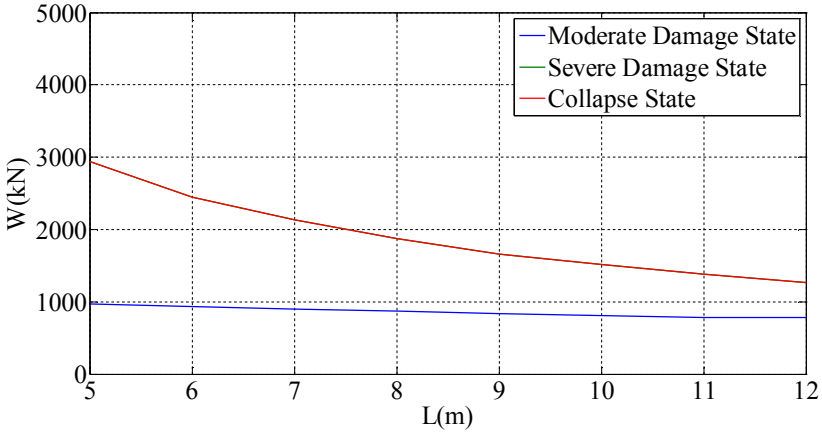
	High	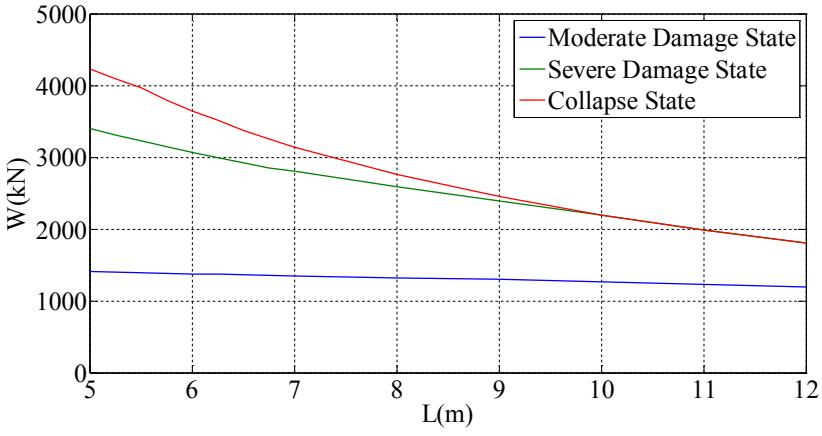

Table B.6. Structural loss estimation curves for the single-storey reinforced concrete industrial buildings which are located at 2nd Earthquake Zone and Z2 Soil Class (cont.).

Cross-Section (cm)	Reinforcement Ratio	Structural Loss Estimation Curves
80×80	Minimum	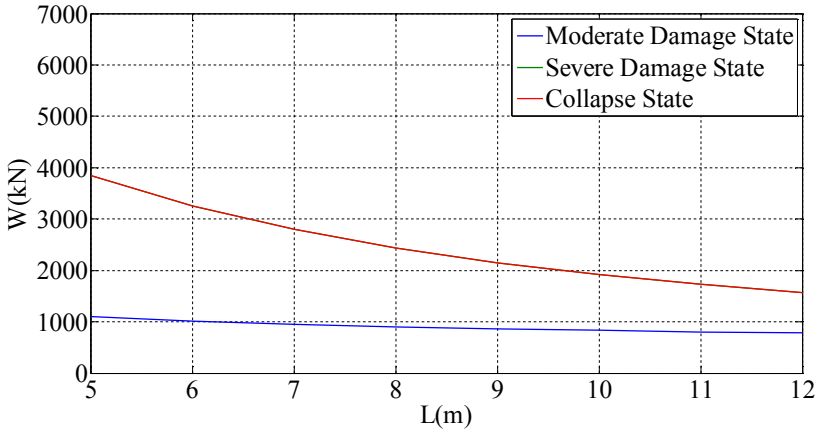
	Moderate	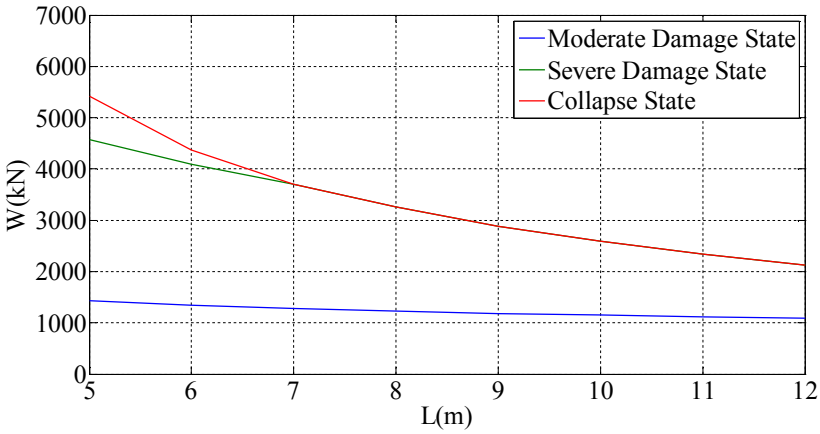
	High	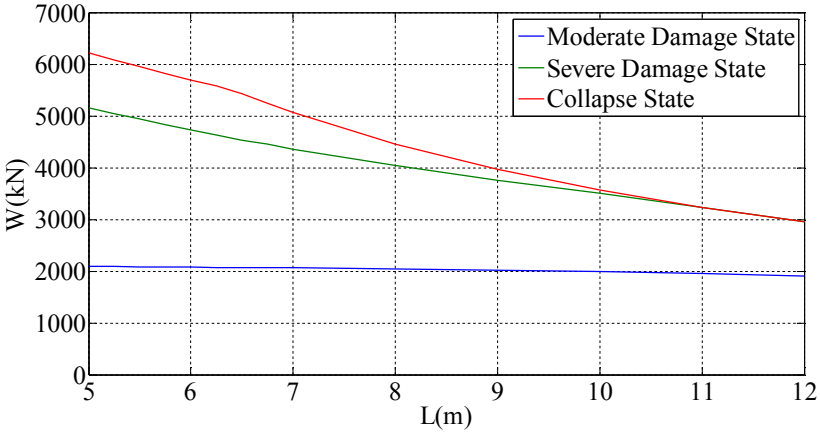

Table B.7. Structural loss estimation curves for the single-storey reinforced concrete industrial buildings which are located at 2nd Earthquake Zone and Z3 Soil Class.

Cross-Section (cm)	Reinforcement Ratio	Structural Loss Estimation Curves
35×35	Minimum	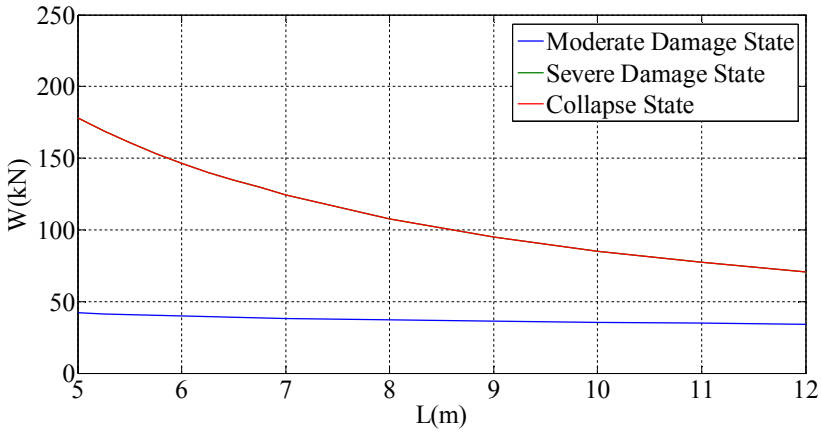
	Moderate	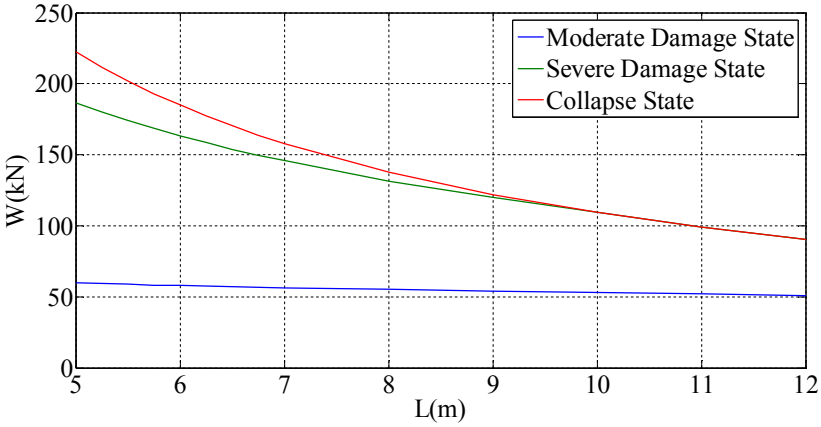
	High	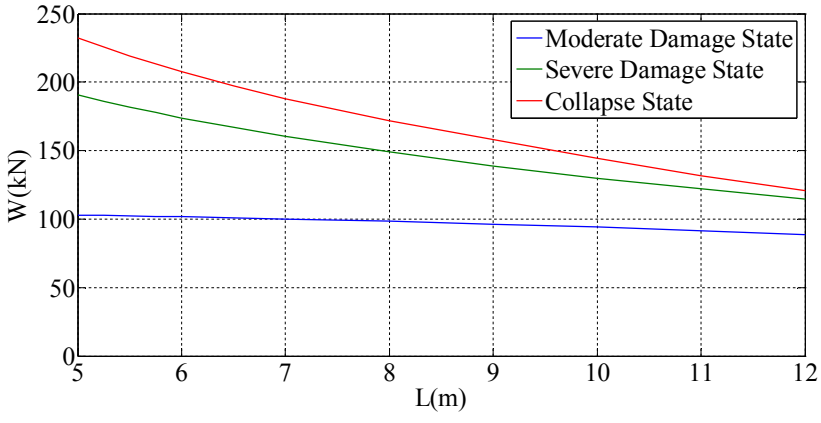

Table B.7. Structural loss estimation curves for the single-storey reinforced concrete industrial buildings which are located at 2nd Earthquake Zone and Z3 Soil Class (cont.).

Cross-Section (cm)	Reinforcement Ratio	Structural Loss Estimation Curves
40×40	Minimum	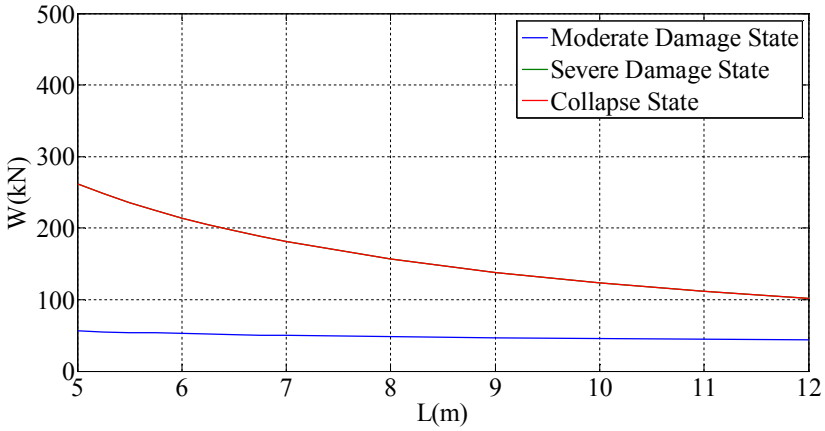
	Moderate	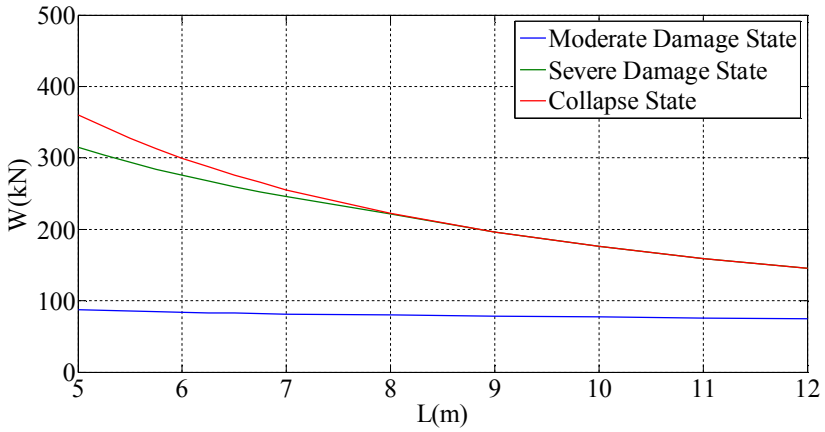
	High	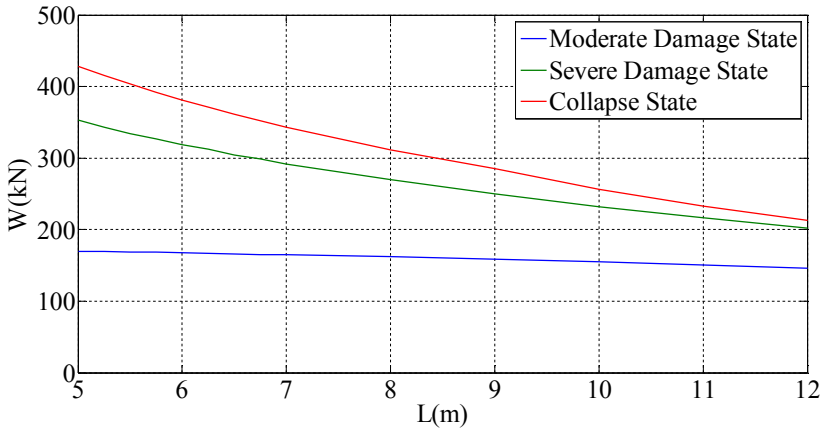

Table B.7. Structural loss estimation curves for the single-storey reinforced concrete industrial buildings which are located at 2nd Earthquake Zone and Z3 Soil Class (cont.).

Cross-Section (cm)	Reinforcement Ratio	Structural Loss Estimation Curves
45×45	Minimum	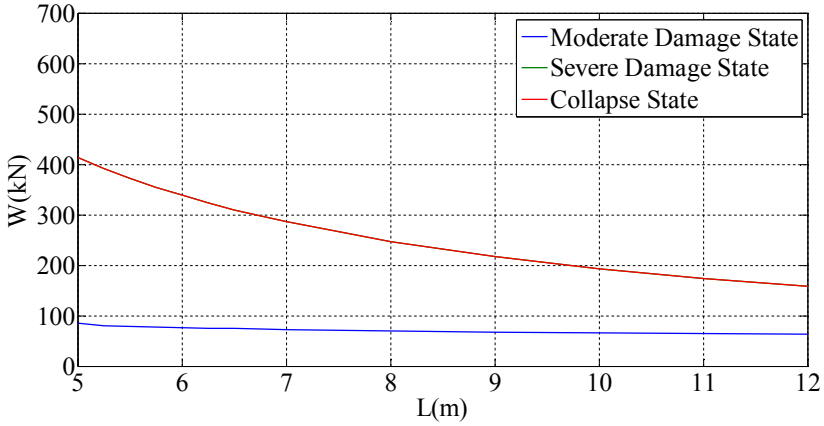
	Moderate	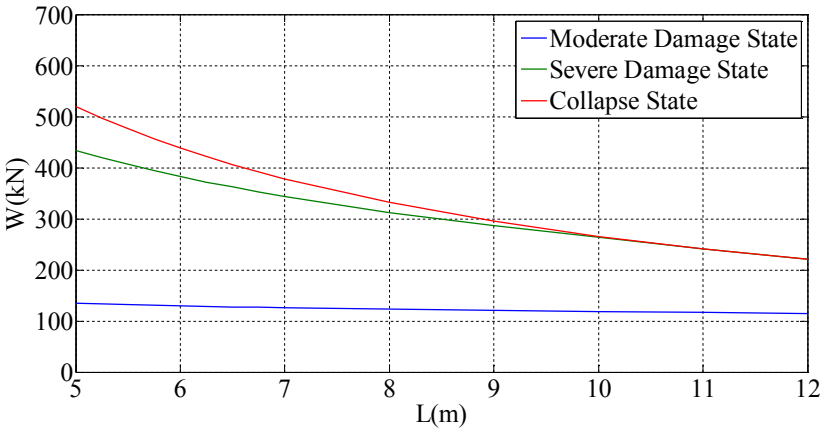
	High	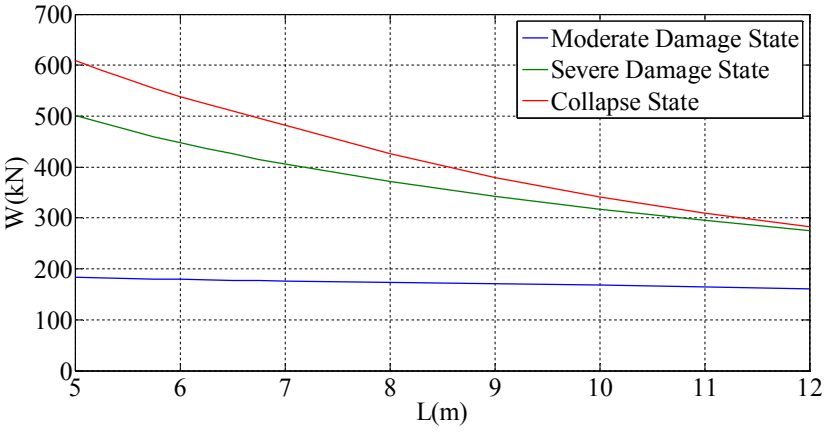

Table B.7. Structural loss estimation curves for the single-storey reinforced concrete industrial buildings which are located at 2nd Earthquake Zone and Z3 Soil Class (cont.).

Cross-Section (cm)	Reinforcement Ratio	Structural Loss Estimation Curves
50×50	Minimum	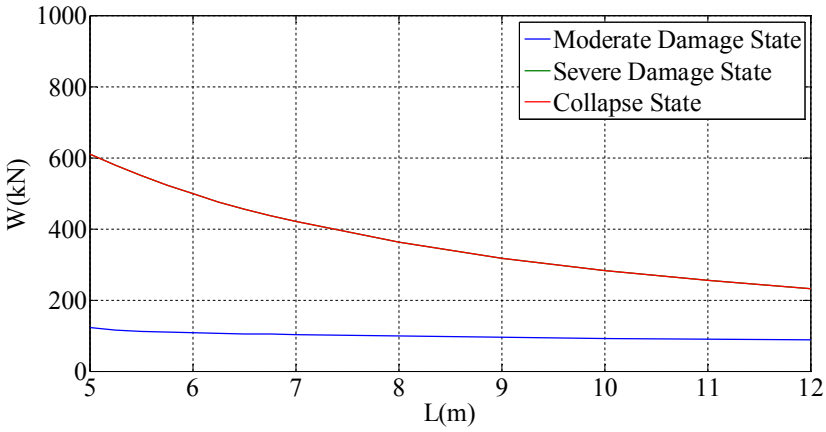
	Moderate	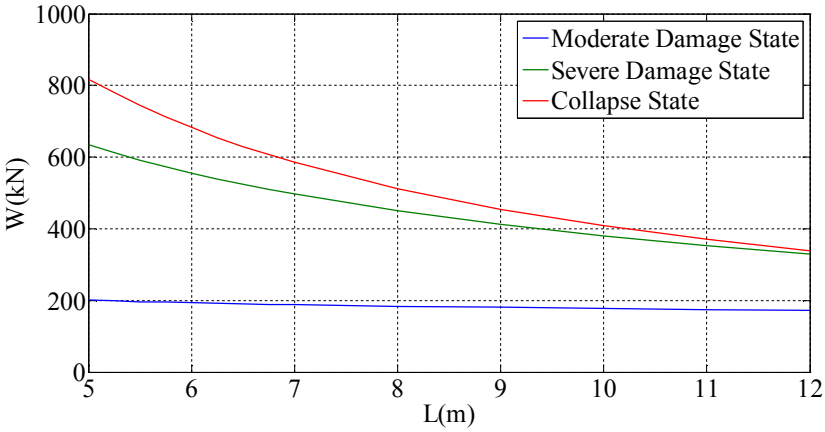
	High	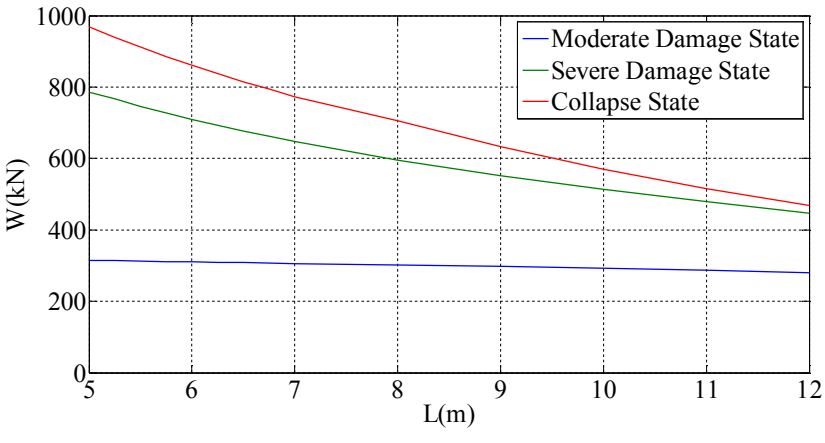

Table B.7. Structural loss estimation curves for the single-storey reinforced concrete industrial buildings which are located at 2nd Earthquake Zone and Z3 Soil Class (cont.).

Cross-Section (cm)	Reinforcement Ratio	Structural Loss Estimation Curves
55×55	Minimum	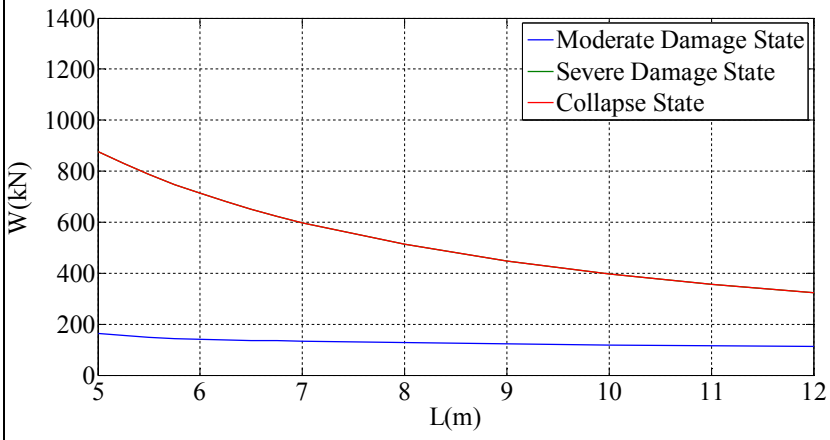
	Moderate	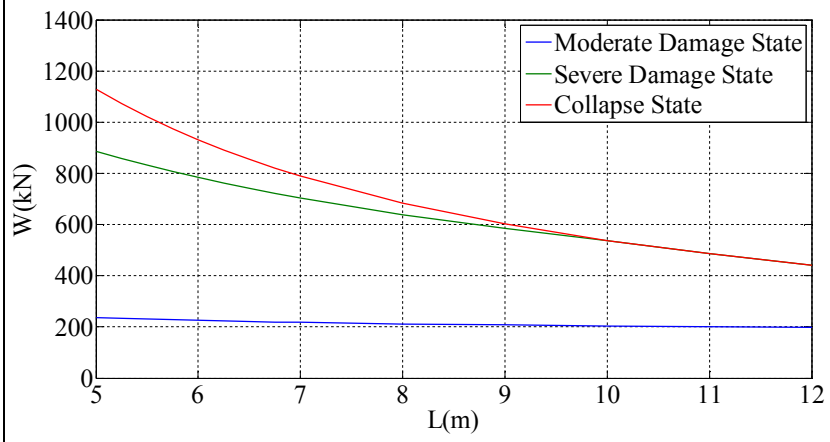
	High	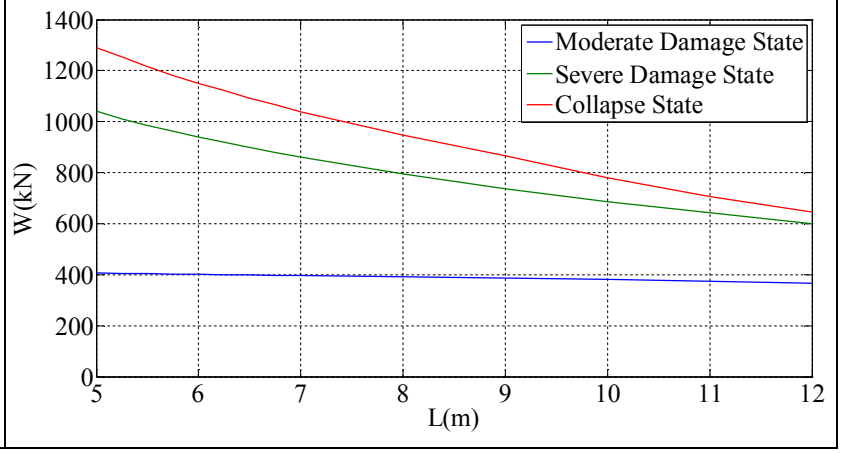

Table B.7. Structural loss estimation curves for the single-storey reinforced concrete industrial buildings which are located at 2nd Earthquake Zone and Z3 Soil Class (cont.).

Cross-Section (cm)	Reinforcement Ratio	Structural Loss Estimation Curves
60×60	Minimum	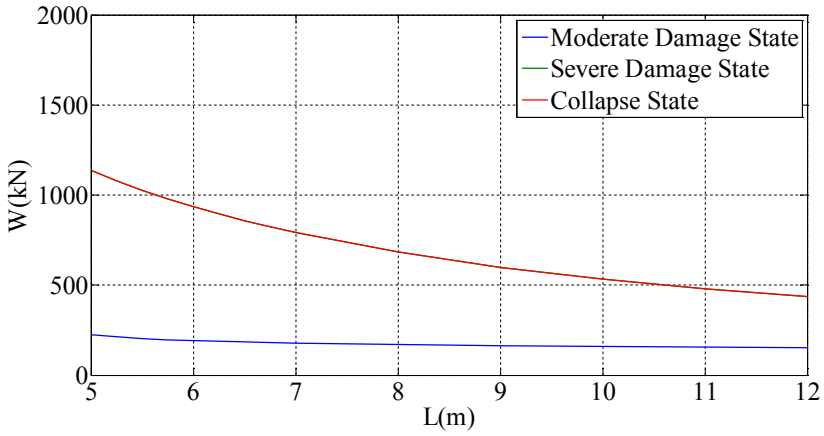
	Moderate	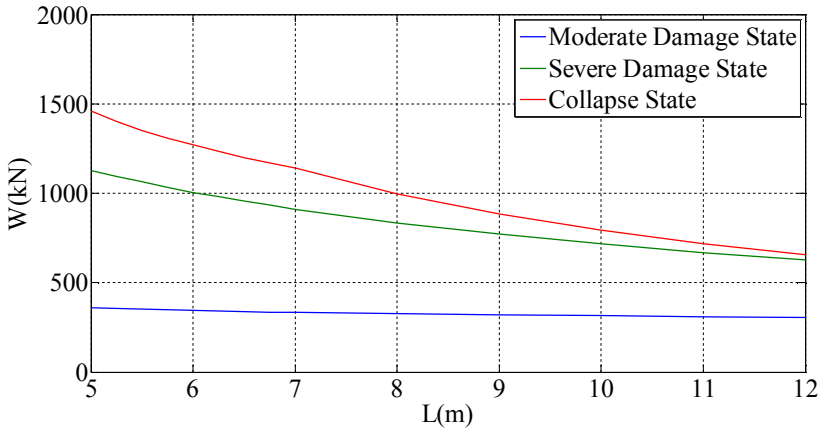
	High	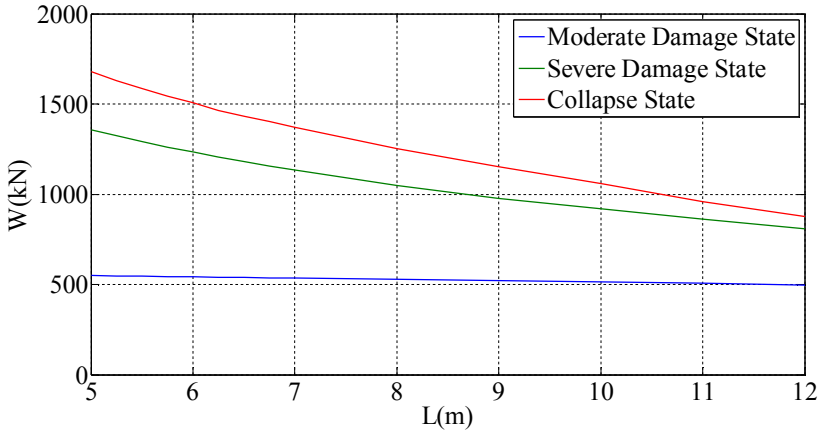

Table B.7. Structural loss estimation curves for the single-storey reinforced concrete industrial buildings which are located at 2nd Earthquake Zone and Z3 Soil Class (cont.).

Cross-Section (cm)	Reinforcement Ratio	Structural Loss Estimation Curves
70×70	Minimum	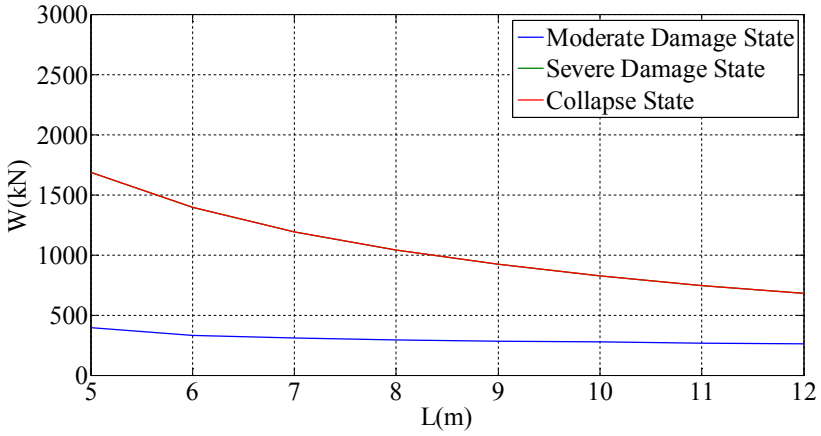
	Moderate	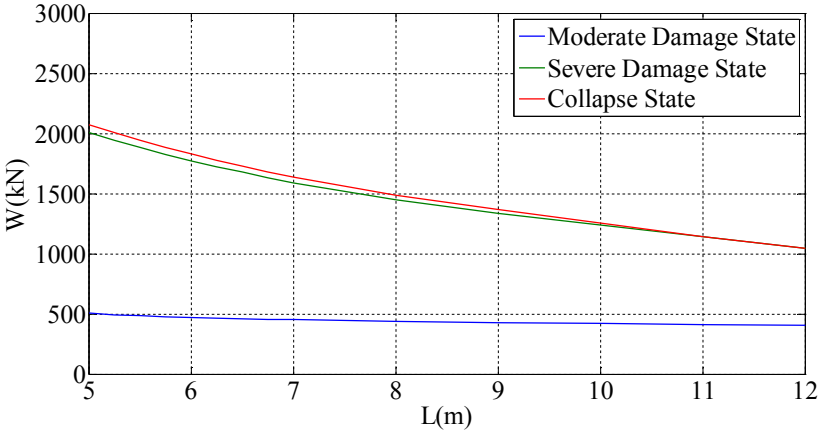
	High	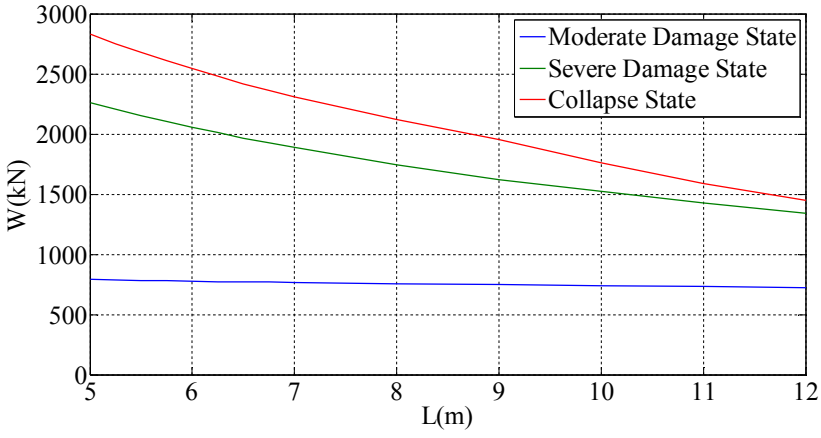

Table B.7. Structural loss estimation curves for the single-storey reinforced concrete industrial buildings which are located at 2nd Earthquake Zone and Z3 Soil Class (cont.).

Cross-Section (cm)	Reinforcement Ratio	Structural Loss Estimation Curves
80×80	Minimum	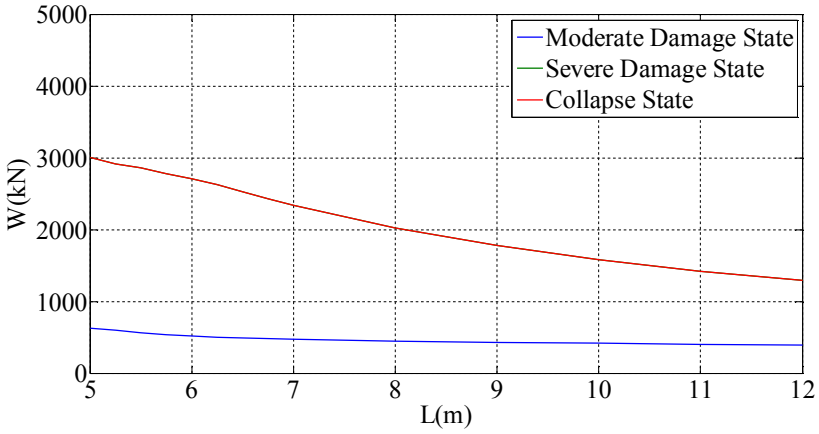
	Moderate	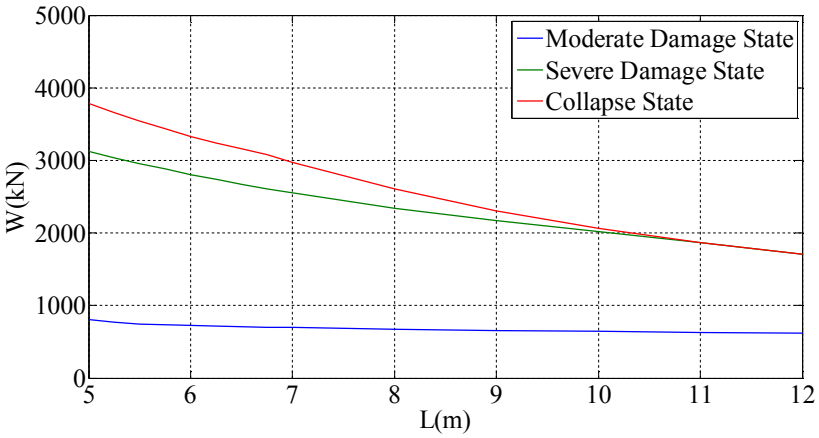
	High	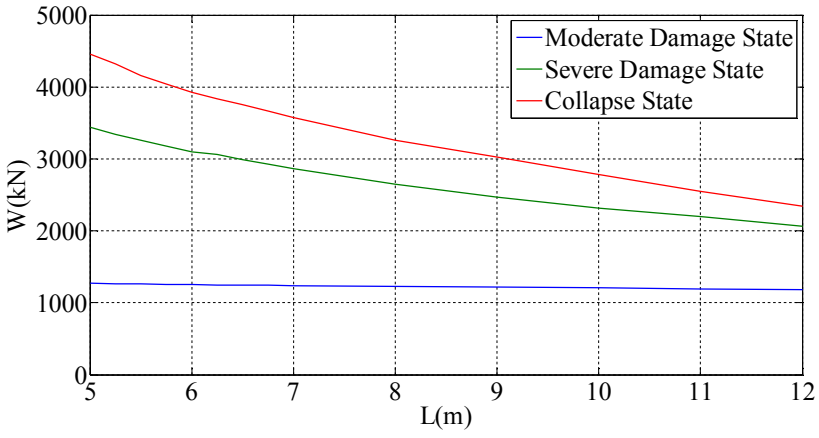

Table B.8. Structural loss estimation curves for the single-storey reinforced concrete industrial buildings which are located at 2nd Earthquake Zone and Z4 Soil Class.

Cross-Section (cm)	Reinforcement Ratio	Structural Loss Estimation Curves
35×35	Minimum	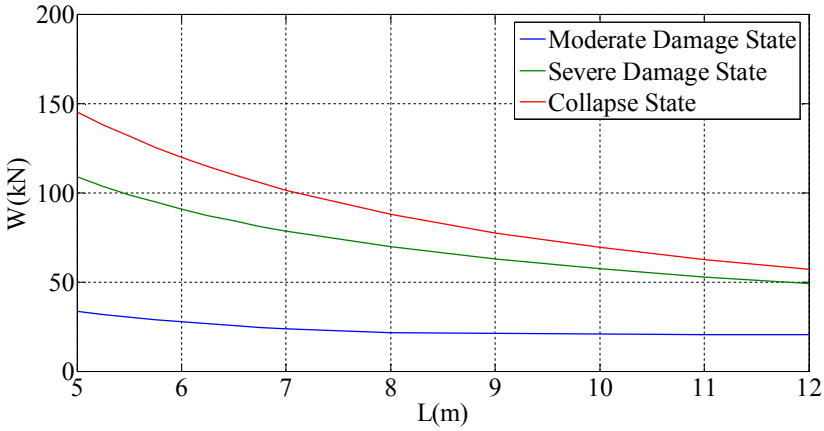
	Moderate	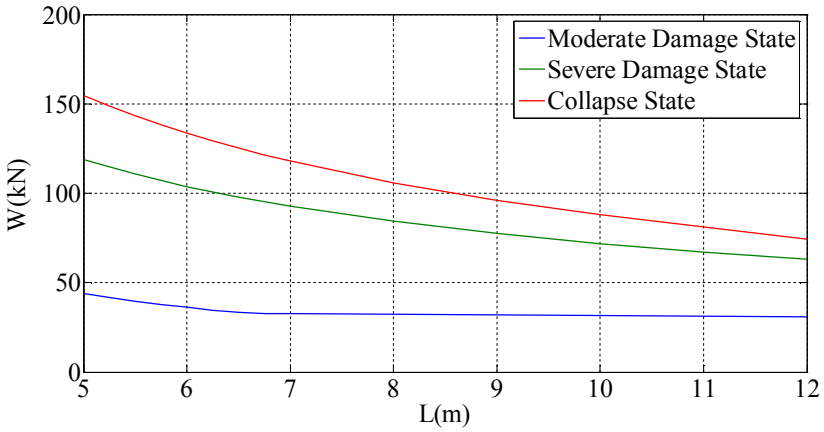
	High	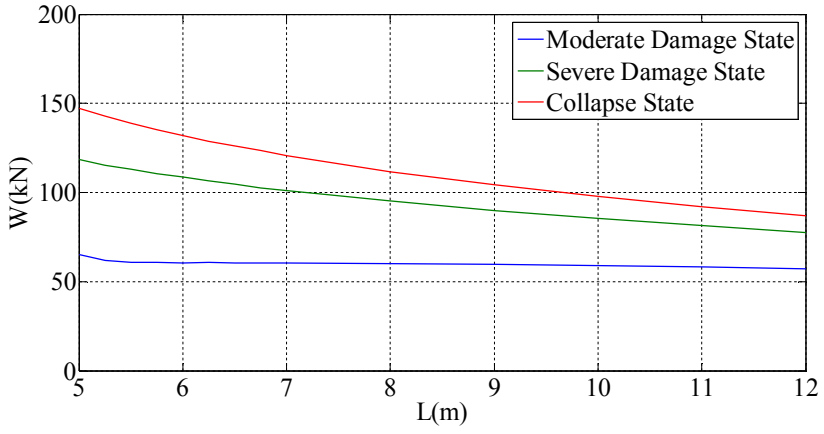

Table B.8. Structural loss estimation curves for the single-storey reinforced concrete industrial buildings which are located at 2nd Earthquake Zone and Z4 Soil Class (cont.).

Cross-Section (cm)	Reinforcement Ratio	Structural Loss Estimation Curves
40×40	Minimum	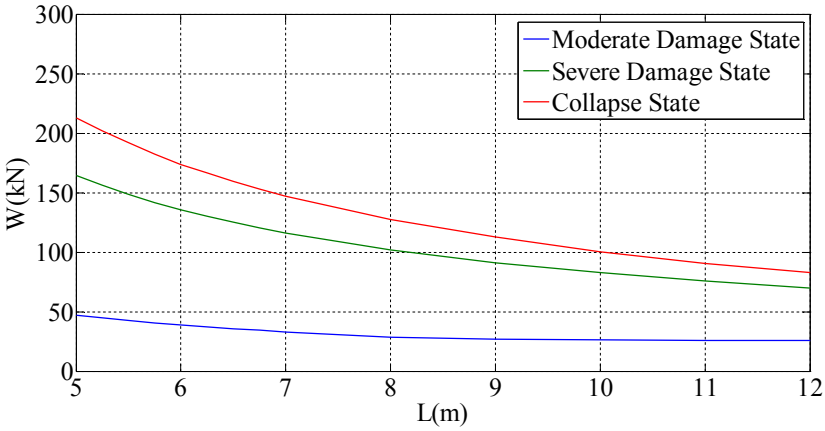
	Moderate	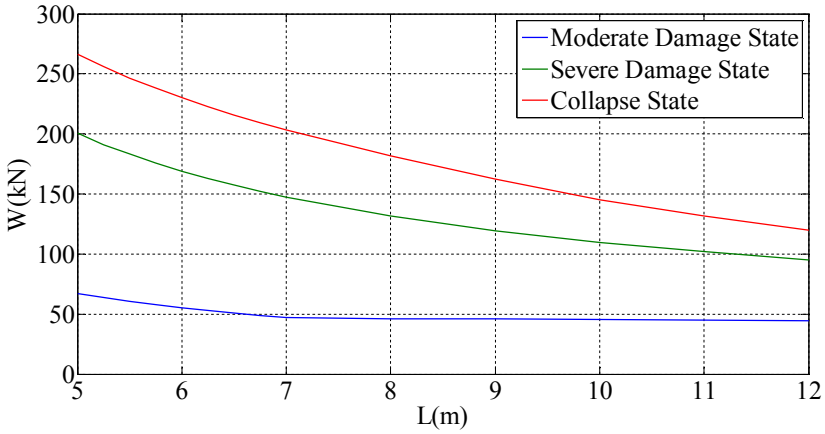
	High	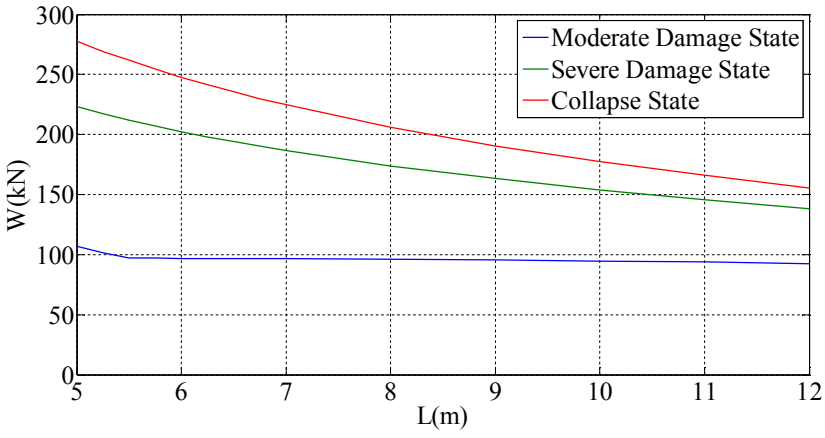

Table B.8. Structural loss estimation curves for the single-storey reinforced concrete industrial buildings which are located at 2nd Earthquake Zone and Z4 Soil Class (cont.).

Cross-Section (cm)	Reinforcement Ratio	Structural Loss Estimation Curves
45×45	Minimum	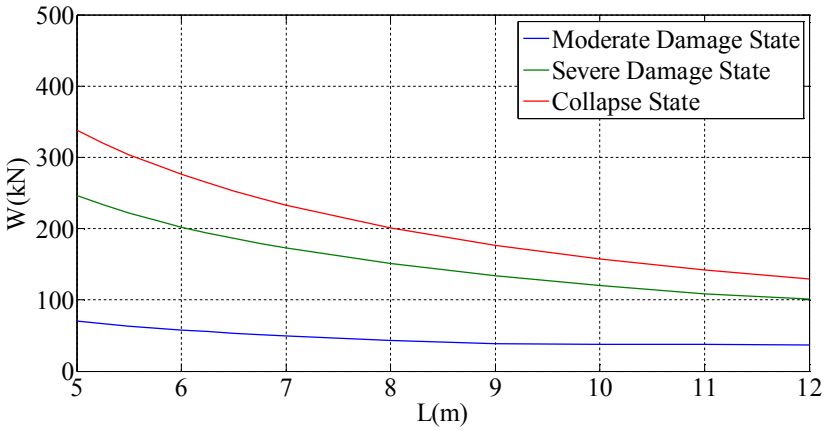
	Moderate	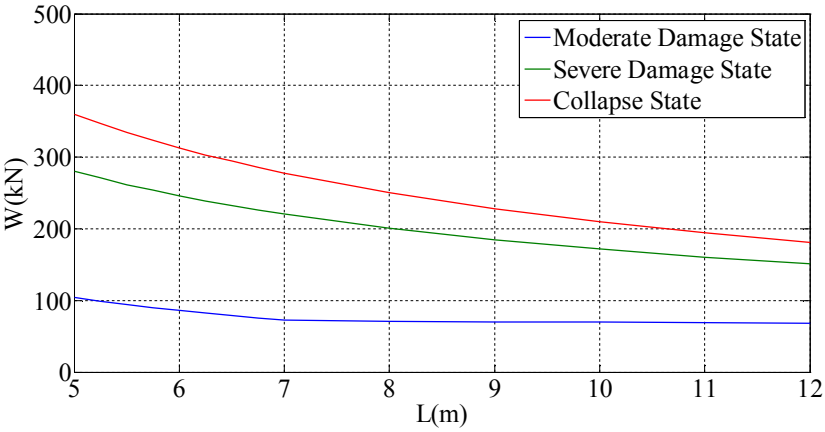
	High	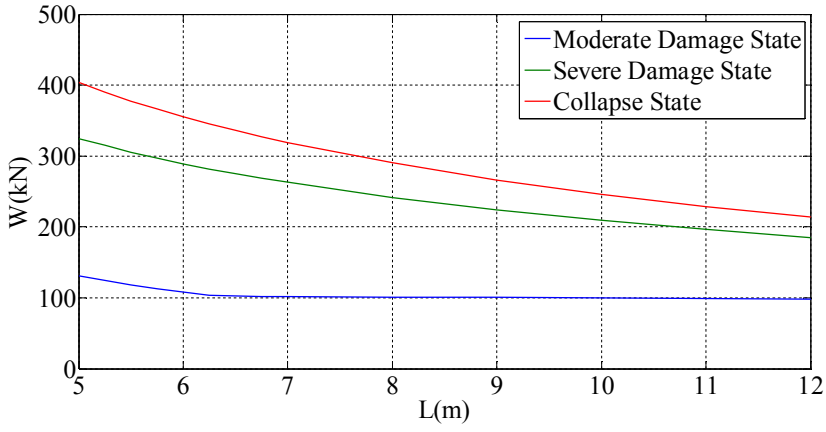

Table B.8. Structural loss estimation curves for the single-storey reinforced concrete industrial buildings which are located at 2nd Earthquake Zone and Z4 Soil Class (cont.).

Cross-Section (cm)	Reinforcement Ratio	Structural Loss Estimation Curves
50×50	Minimum	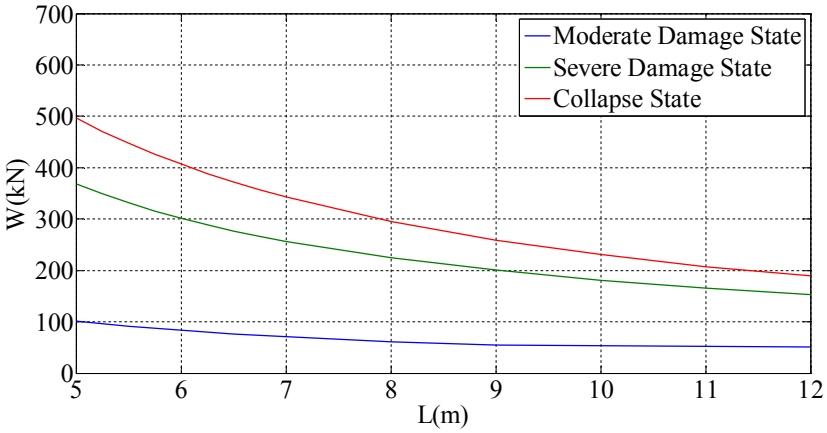
	Moderate	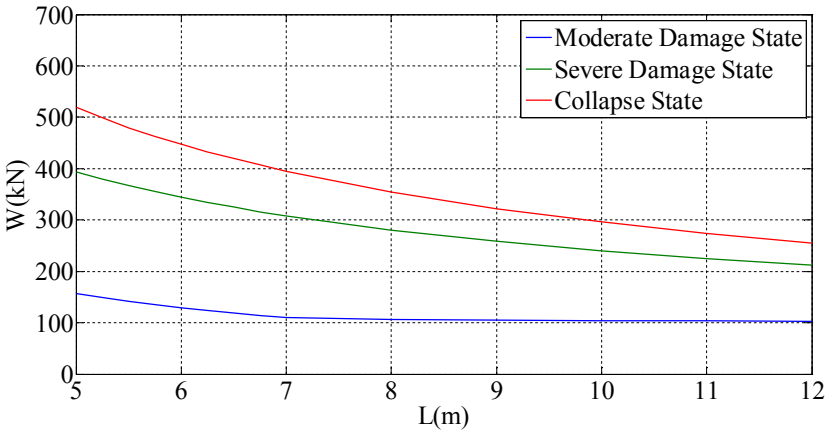
	High	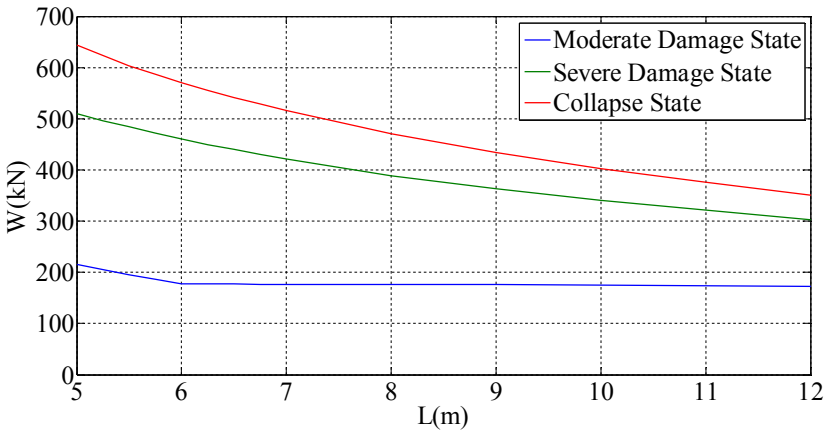

Table B.8. Structural loss estimation curves for the single-storey reinforced concrete industrial buildings which are located at 2nd Earthquake Zone and Z4 Soil Class (cont.).

Cross-Section (cm)	Reinforcement Ratio	Structural Loss Estimation Curves
55×55	Minimum	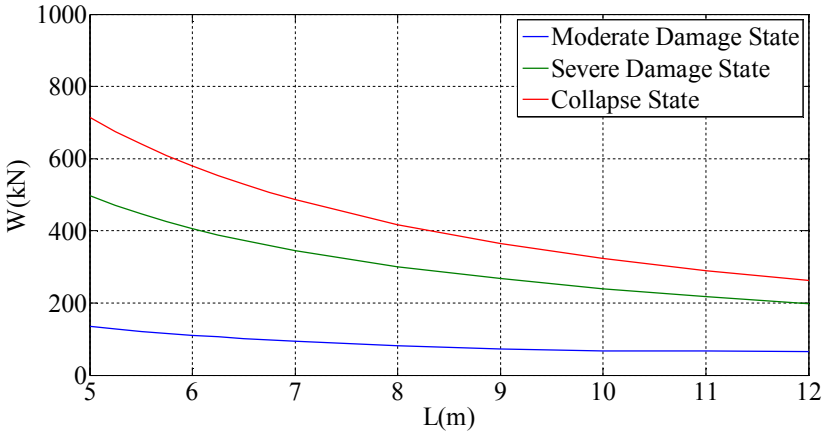
	Moderate	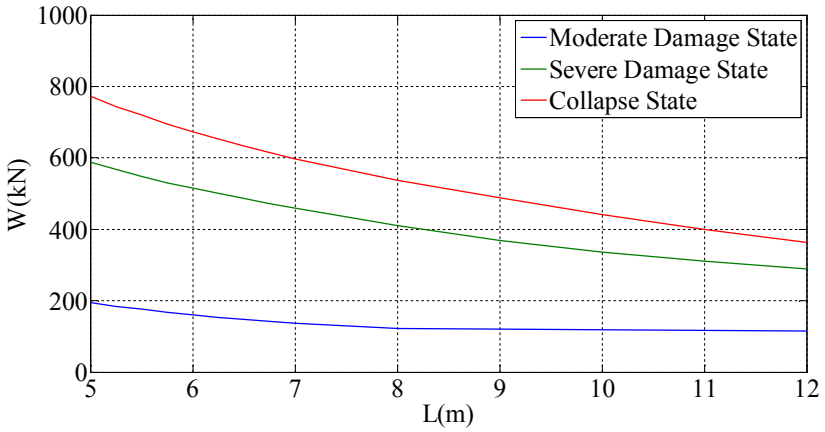
	High	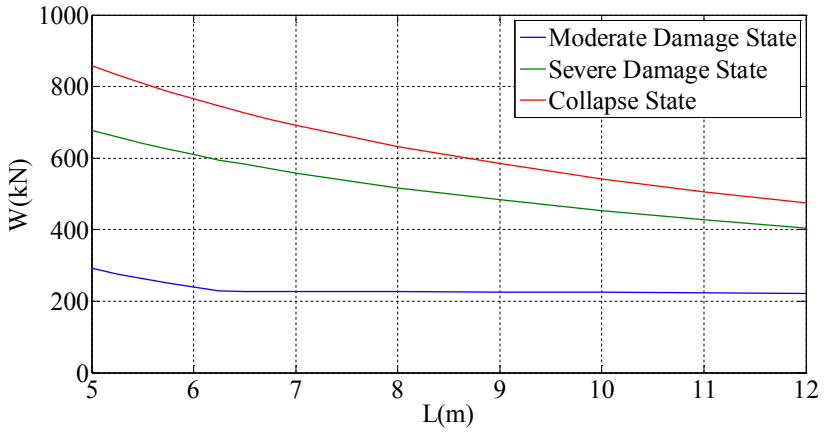

Table B.8. Structural loss estimation curves for the single-storey reinforced concrete industrial buildings which are located at 2nd Earthquake Zone and Z4 Soil Class (cont.).

Cross-Section (cm)	Reinforcement Ratio	Structural Loss Estimation Curves
60×60	Minimum	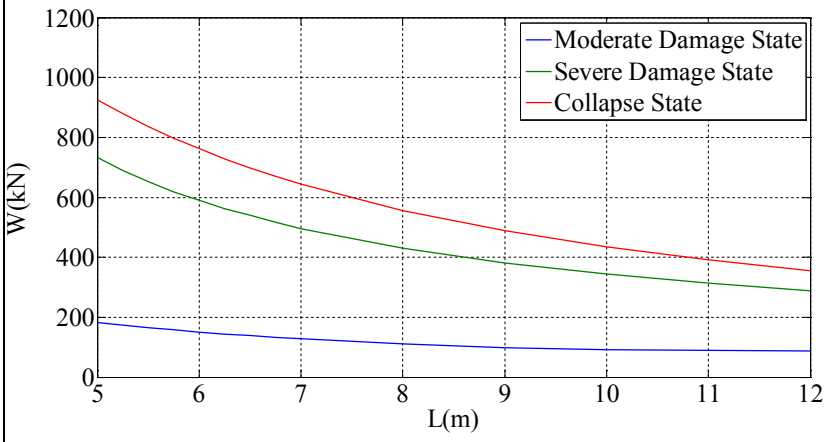
	Moderate	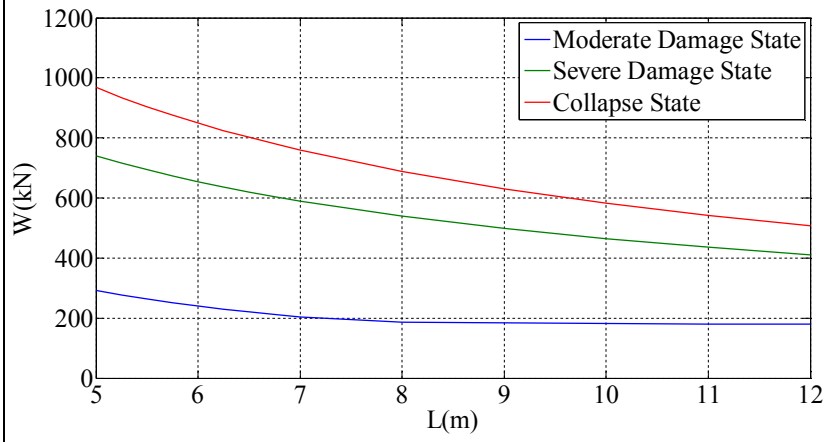
	High	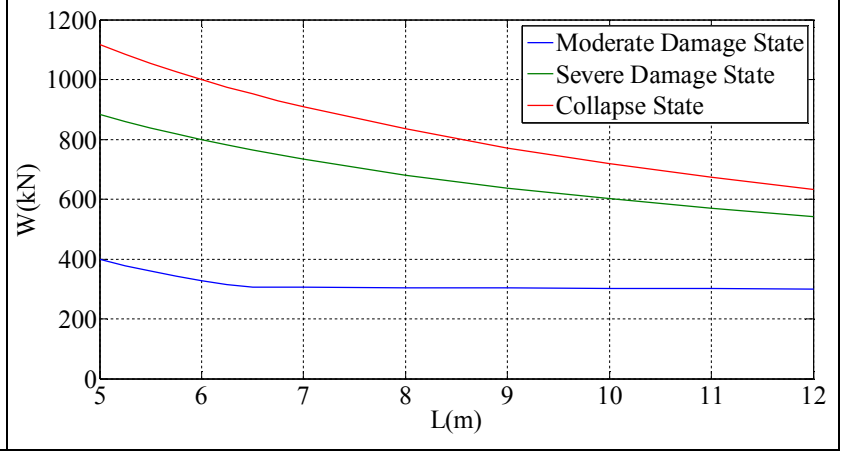

Table B.8. Structural loss estimation curves for the single-storey reinforced concrete industrial buildings which are located at 2nd Earthquake Zone and Z4 Soil Class (cont.).

Cross-Section (cm)	Reinforcement Ratio	Structural Loss Estimation Curves
70×70	Minimum	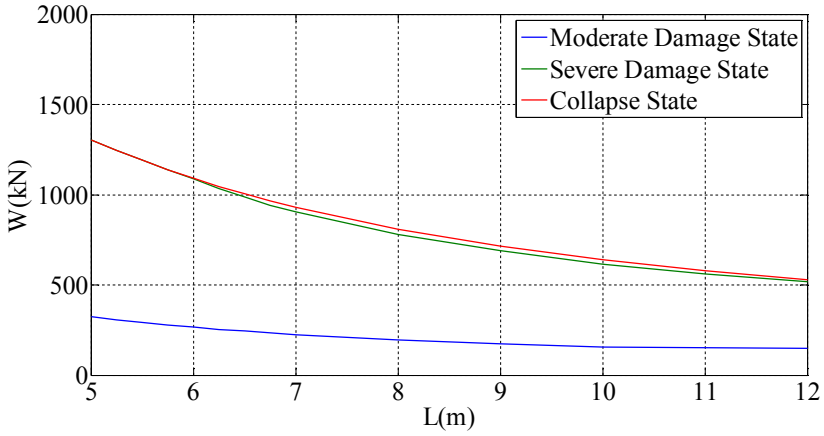
	Moderate	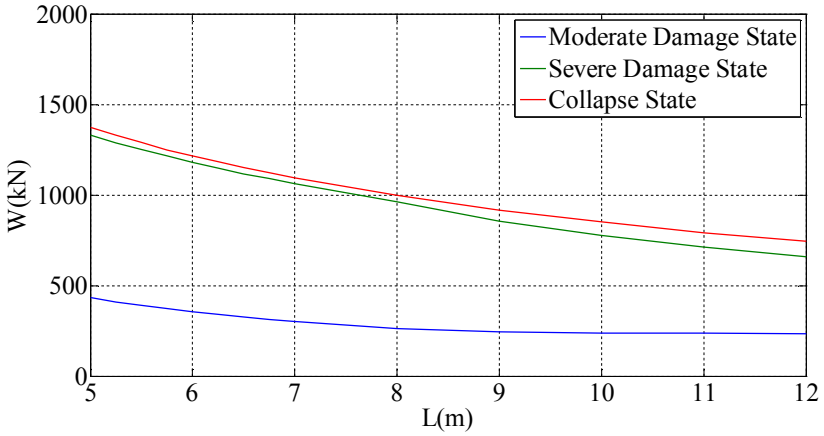
	High	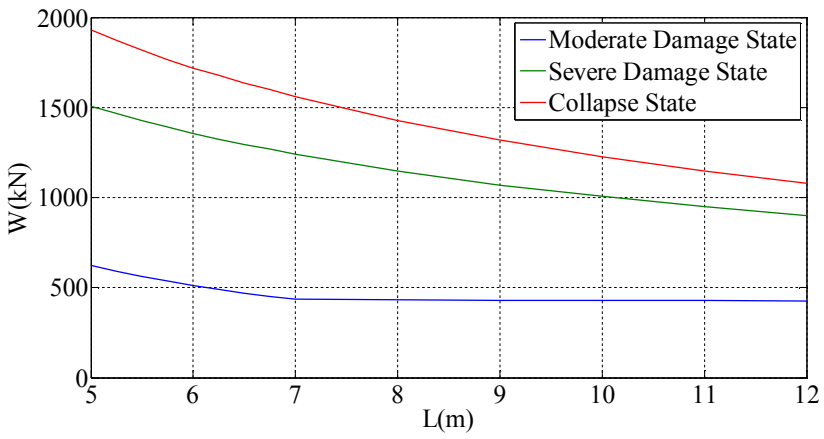

Table B.8. Structural loss estimation curves for the single-storey reinforced concrete industrial buildings which are located at 2nd Earthquake Zone and Z4 Soil Class (cont.).

Cross-Section (cm)	Reinforcement Ratio	Structural Loss Estimation Curves
80×80	Minimum	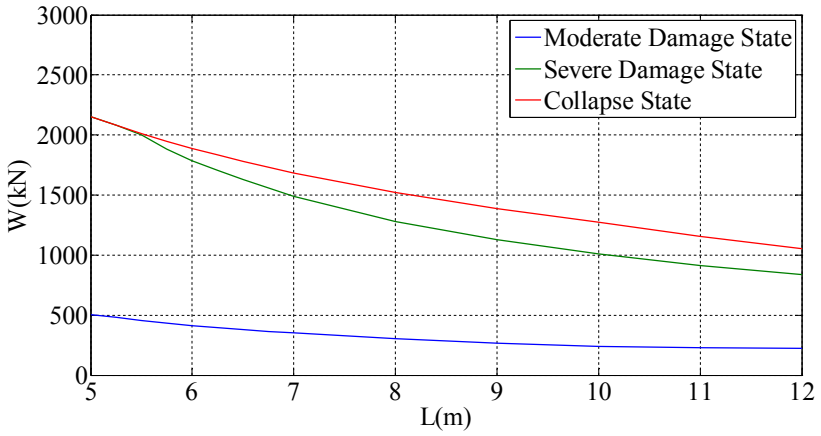
	Moderate	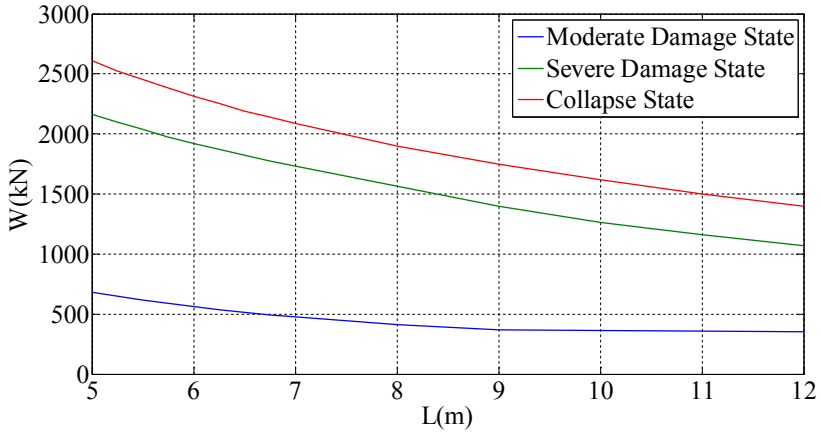
	High	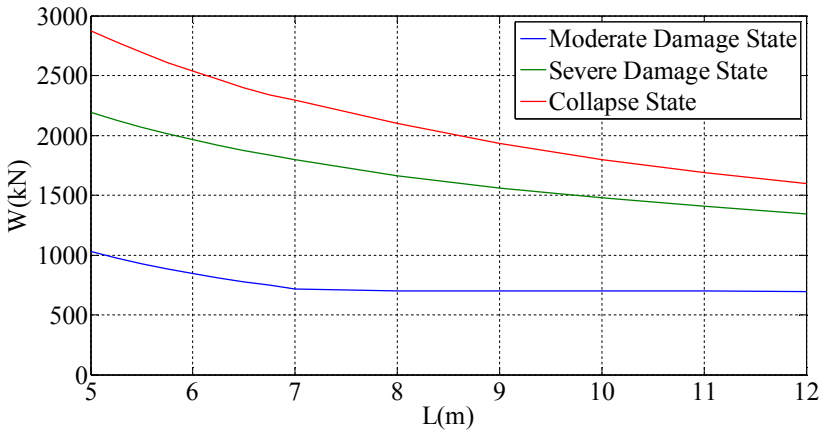

Table B.9. Structural loss estimation curves for the single-storey reinforced concrete industrial buildings which are located at 3rd Earthquake Zone and Z1 Soil Class.

Cross-Section (cm)	Reinforcement Ratio	Structural Loss Estimation Curves
35×35	Minimum	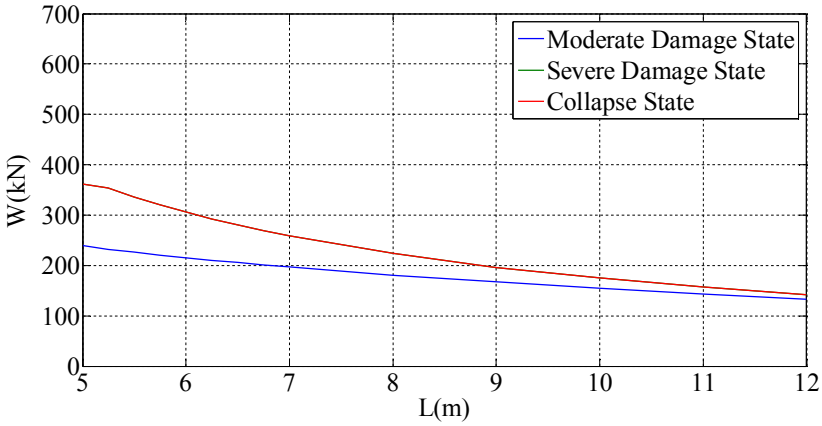
	Moderate	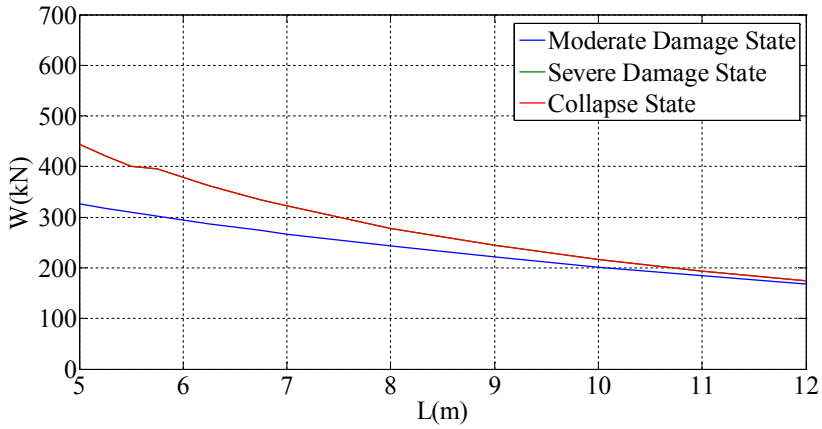
	High	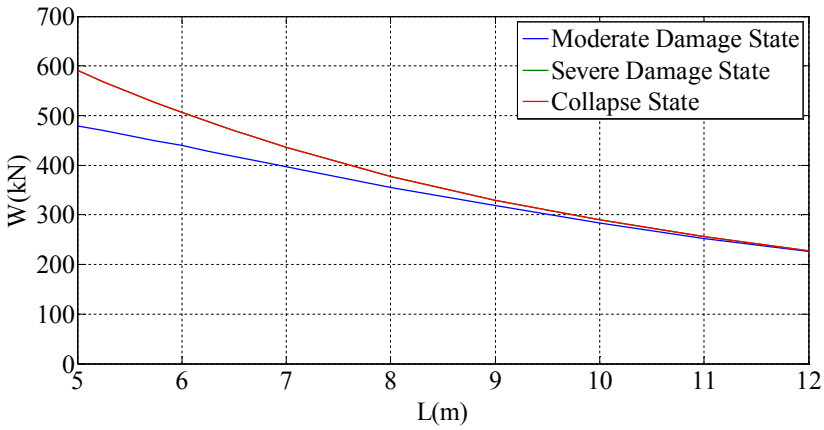

Table B.9. Structural loss estimation curves for the single-storey reinforced concrete industrial buildings which are located at 3rd Earthquake Zone and Z1 Soil Class (cont.).

Cross-Section (cm)	Reinforcement Ratio	Structural Loss Estimation Curves
40×40	Minimum	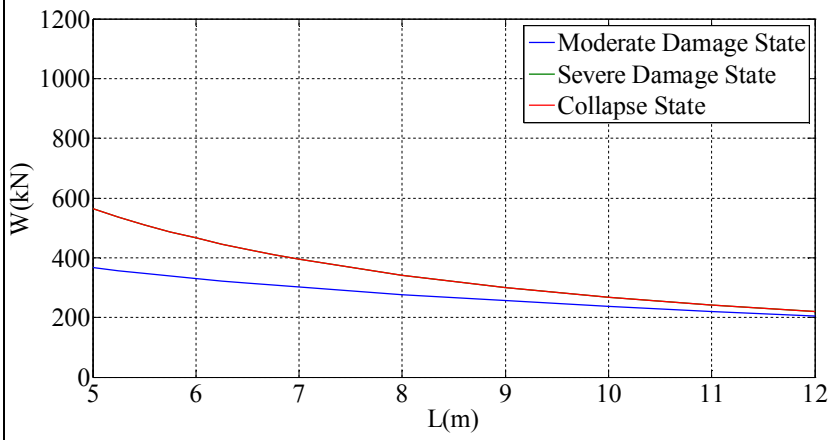
	Moderate	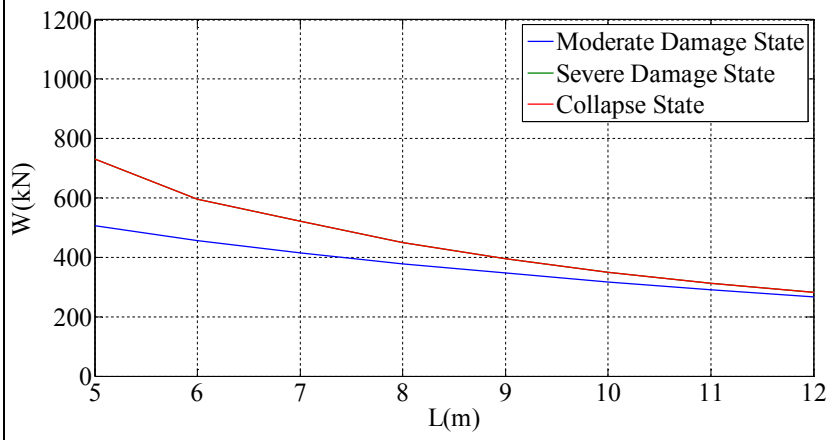
	High	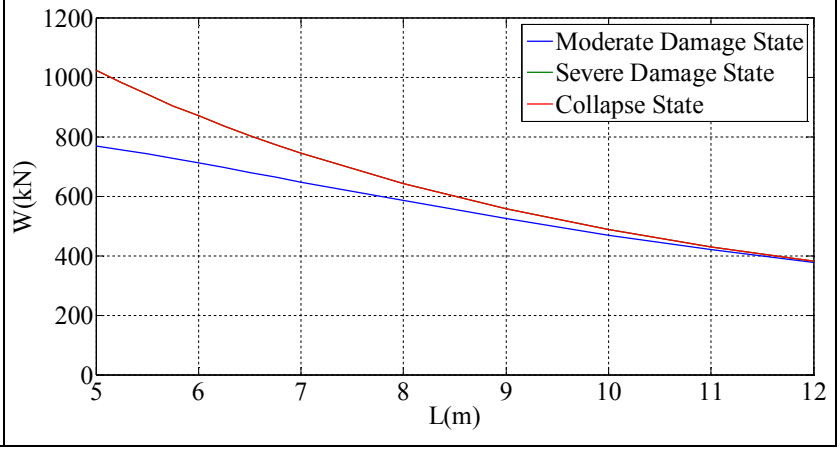

Table B.9. Structural loss estimation curves for the single-storey reinforced concrete industrial buildings which are located at 3rd Earthquake Zone and Z1 Soil Class (cont.).

Cross-Section (cm)	Reinforcement Ratio	Structural Loss Estimation Curves
45×45	Minimum	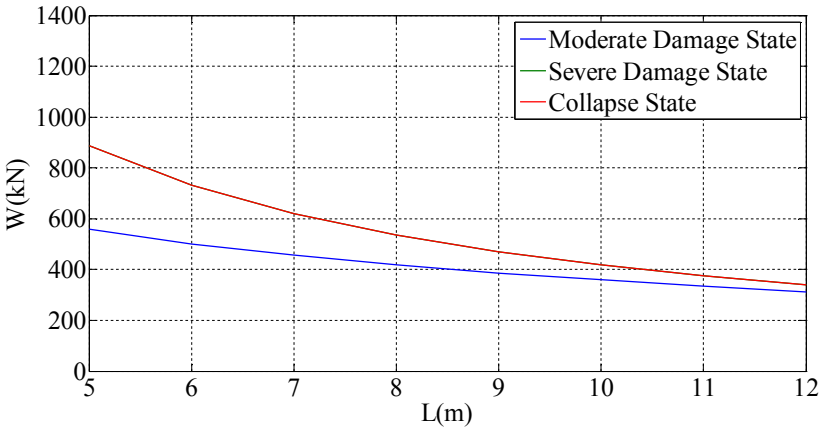
	Moderate	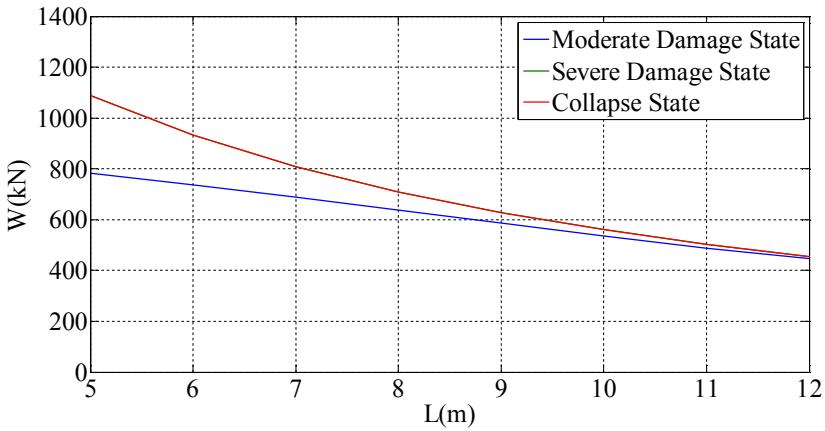
	High	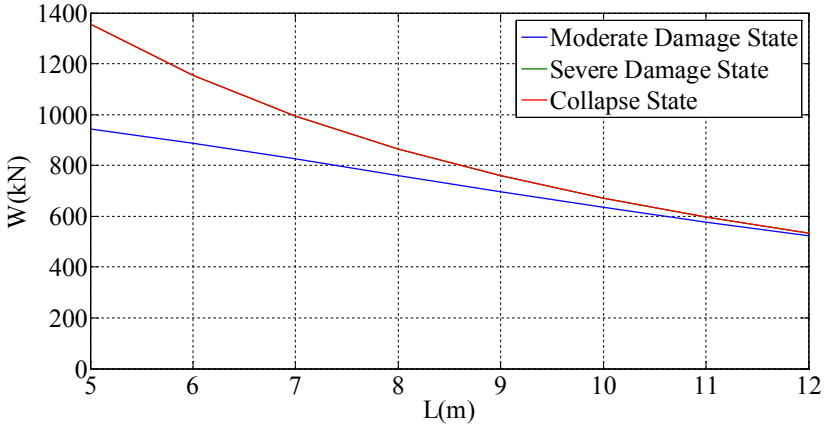

Table B.9. Structural loss estimation curves for the single-storey reinforced concrete industrial buildings which are located at 3rd Earthquake Zone and Z1 Soil Class (cont.).

Cross-Section (cm)	Reinforcement Ratio	Structural Loss Estimation Curves
50×50	Minimum	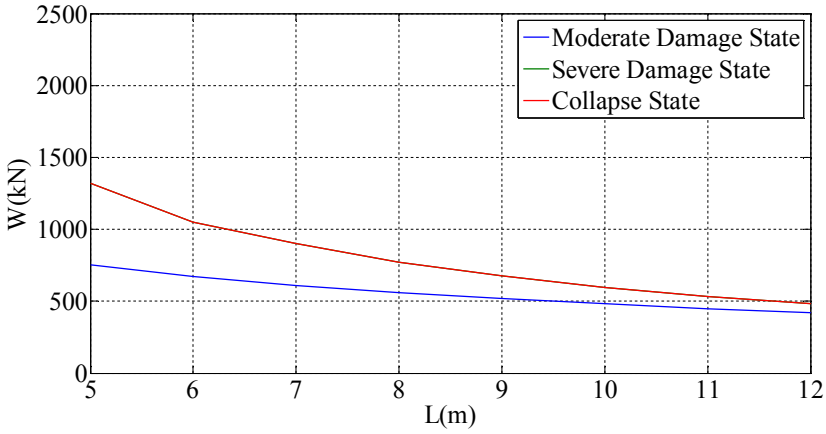
	Moderate	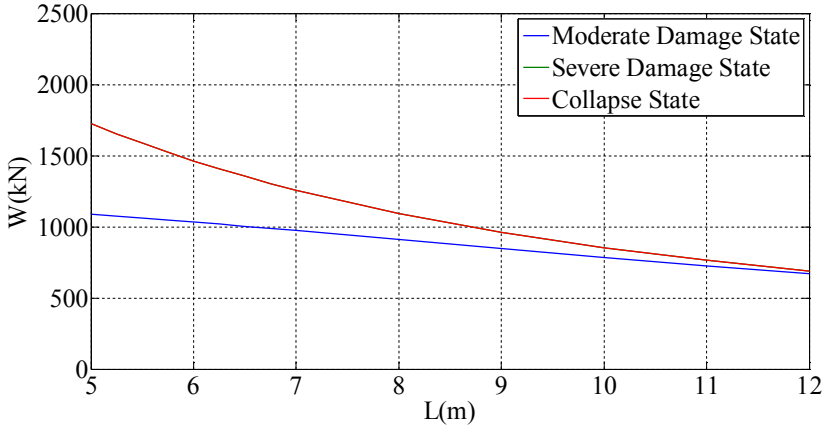
	High	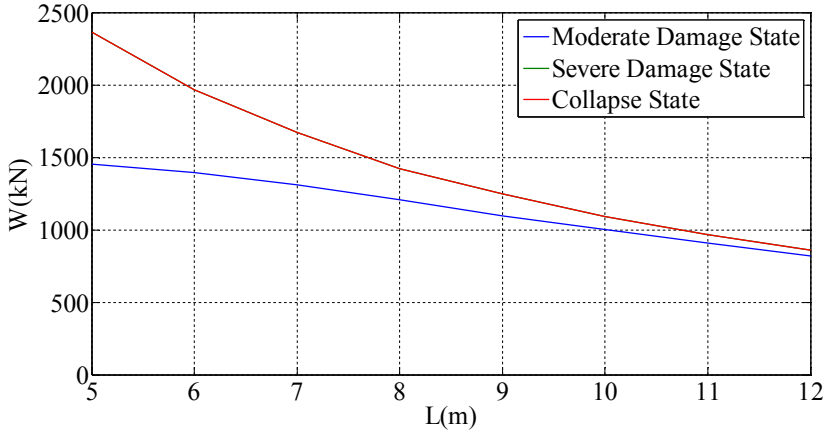

Table B.9. Structural loss estimation curves for the single-storey reinforced concrete industrial buildings which are located at 3rd Earthquake Zone and Z1 Soil Class (cont.).

Cross-Section (cm)	Reinforcement Ratio	Structural Loss Estimation Curves
55×55	Minimum	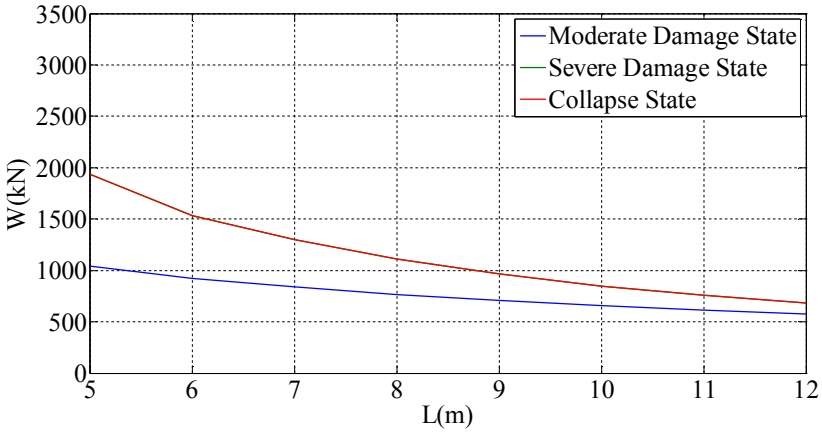
	Moderate	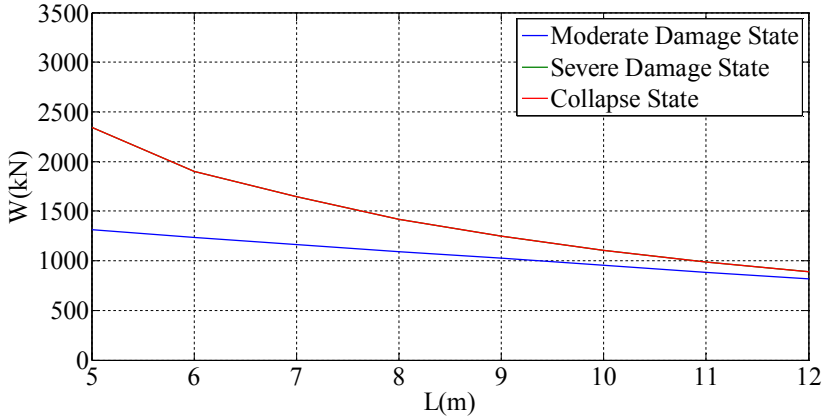
	High	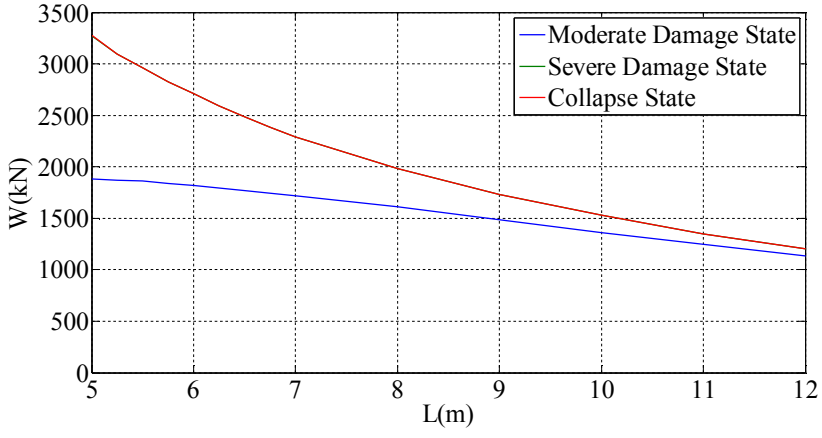

Table B.9. Structural loss estimation curves for the single-storey reinforced concrete industrial buildings which are located at 3rd Earthquake Zone and Z1 Soil Class (cont.).

Cross-Section (cm)	Reinforcement Ratio	Structural Loss Estimation Curves
60×60	Minimum	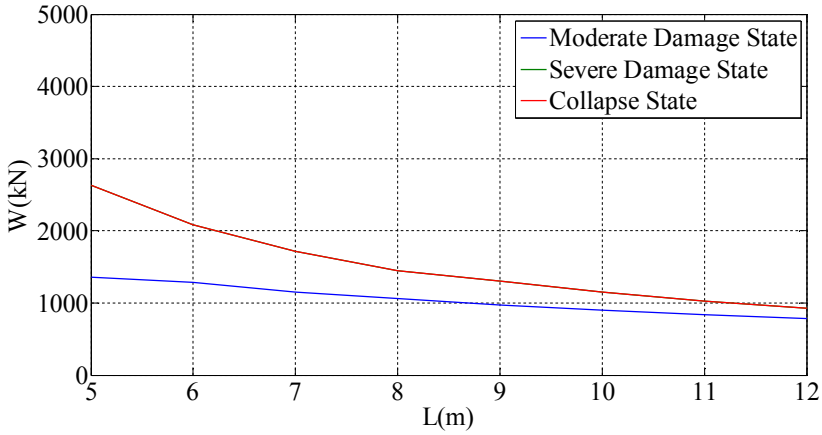
	Moderate	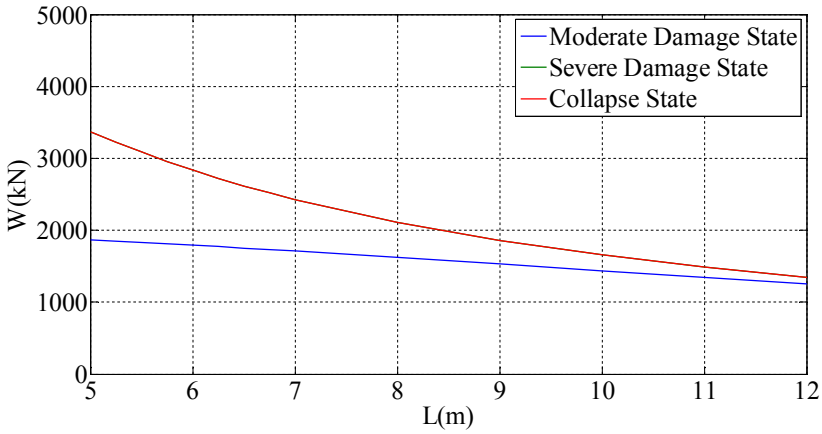
	High	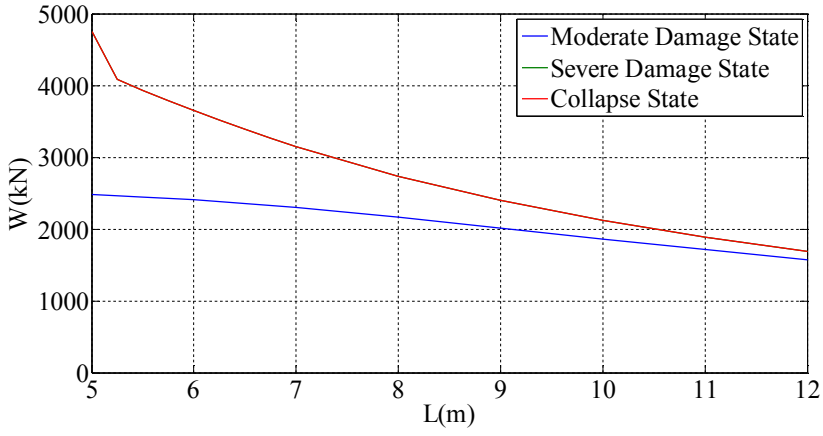

Table B.9. Structural loss estimation curves for the single-storey reinforced concrete industrial buildings which are located at 3rd Earthquake Zone and Z1 Soil Class (cont.).

Cross-Section (cm)	Reinforcement Ratio	Structural Loss Estimation Curves
70×70	Minimum	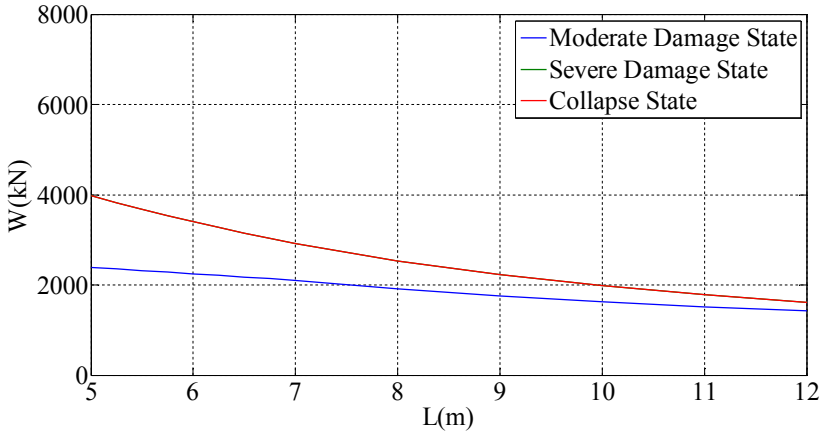
	Moderate	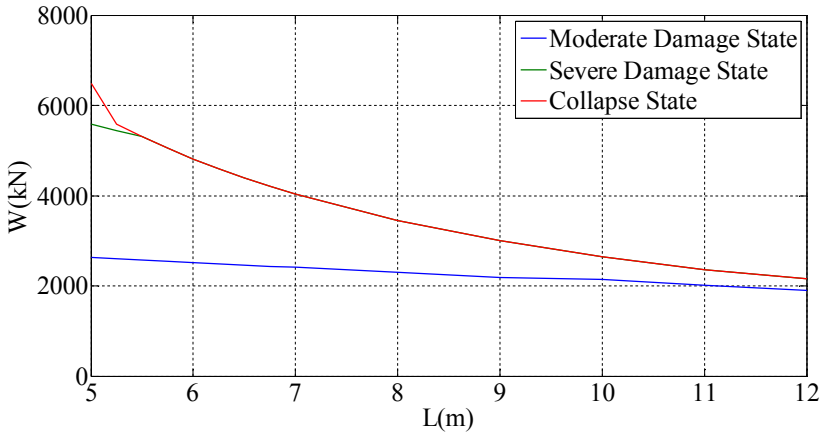
	High	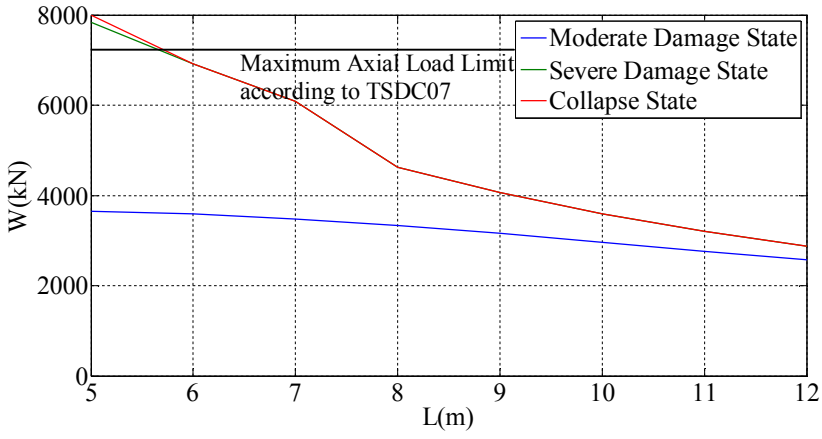

Table B.9. Structural loss estimation curves for the single-storey reinforced concrete industrial buildings which are located at 3rd Earthquake Zone and Z1 Soil Class (cont.).

Cross-Section (cm)	Reinforcement Ratio	Structural Loss Estimation Curves
80×80	Minimum	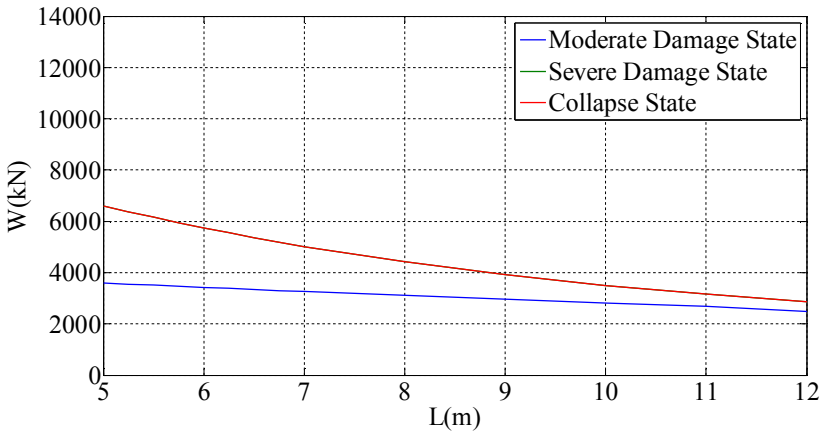
	Moderate	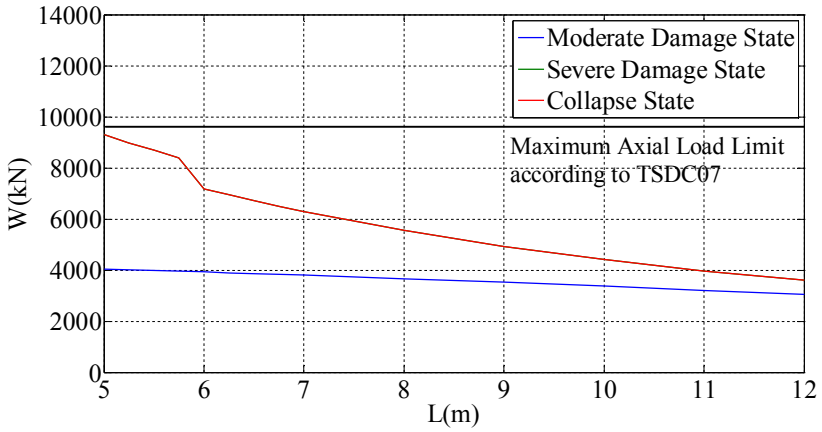
	High	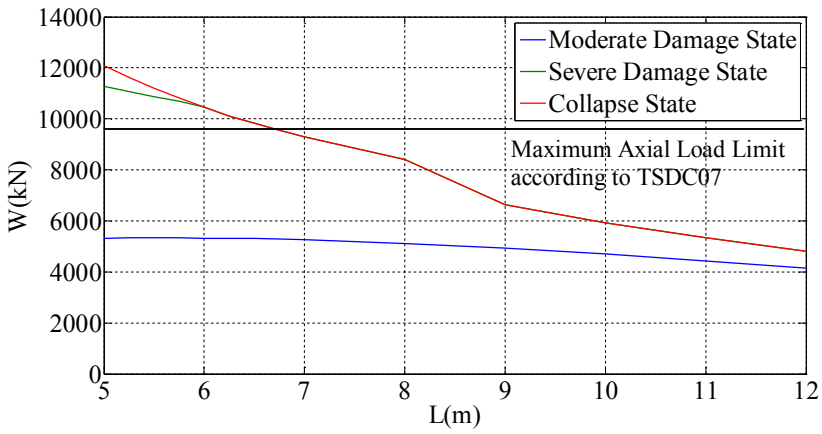

Table B.10. Structural loss estimation curves for the single-storey reinforced concrete industrial buildings which are located at 3rd Earthquake Zone and Z2 Soil Class.

Cross-Section (cm)	Reinforcement Ratio	Structural Loss Estimation Curves
35×35	Minimum	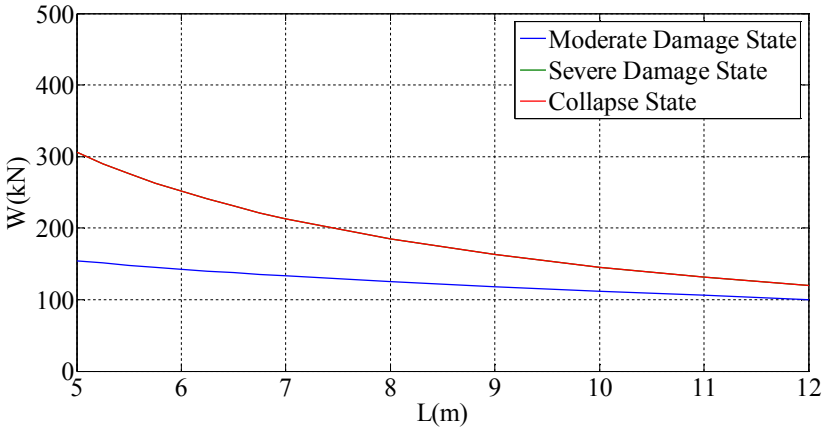
	Moderate	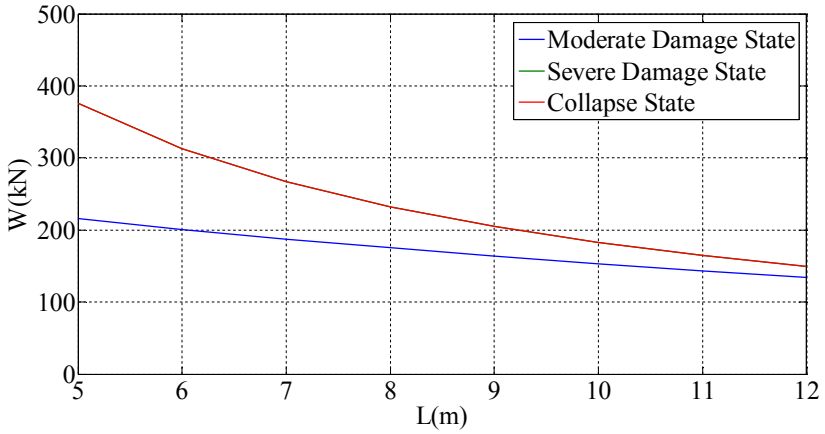
	High	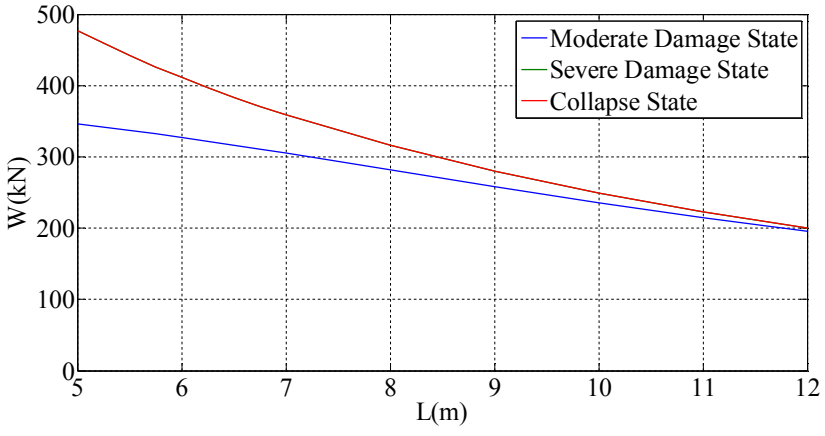

Table B.10. Structural loss estimation curves for the single-storey reinforced concrete industrial buildings which are located at 3rd Earthquake Zone and Z2 Soil Class (cont.).

Cross-Section (cm)	Reinforcement Ratio	Structural Loss Estimation Curves
40×40	Minimum	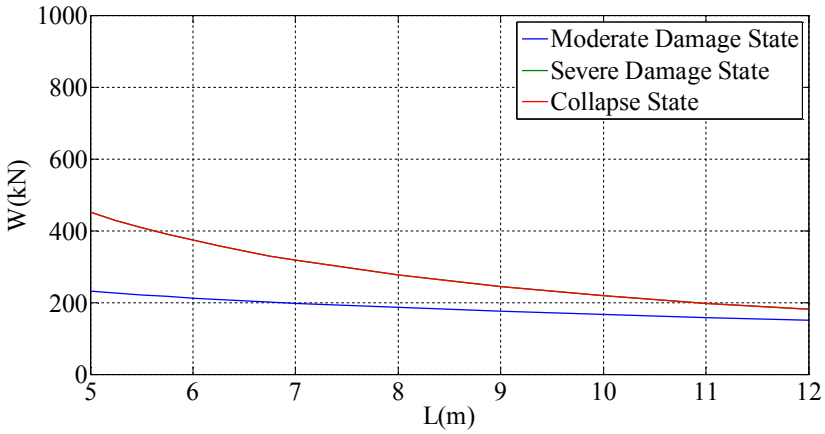
	Moderate	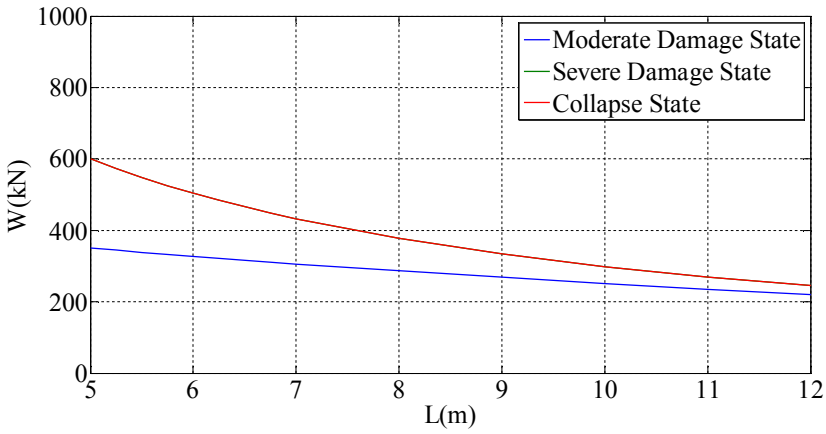
	High	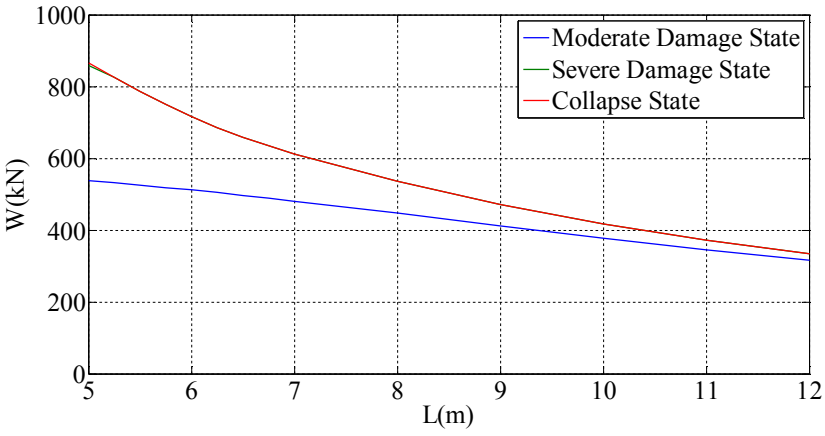

Table B.10. Structural loss estimation curves for the single-storey reinforced concrete industrial buildings which are located at 3rd Earthquake Zone and Z2 Soil Class (cont.).

Cross-Section (cm)	Reinforcement Ratio	Structural Loss Estimation Curves
45×45	Minimum	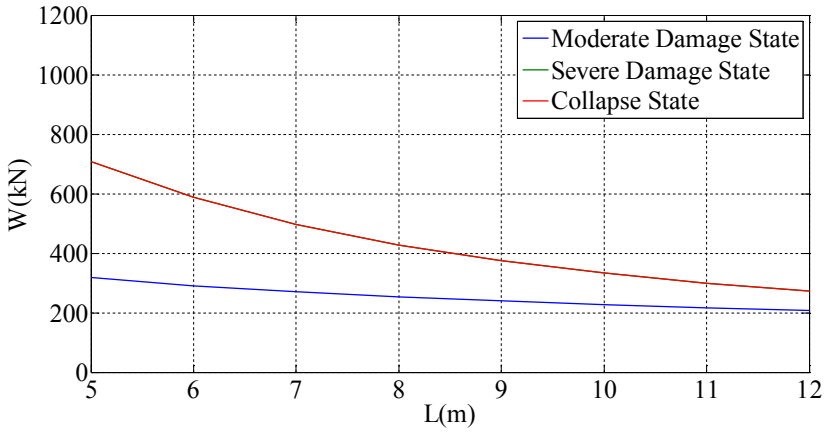
	Moderate	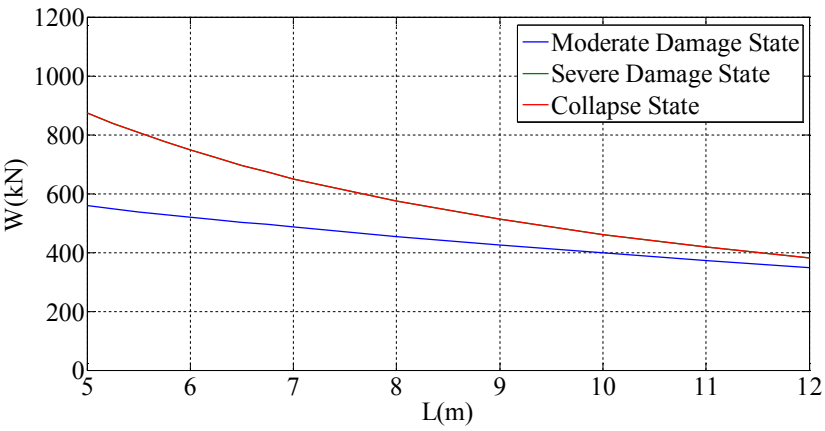
	High	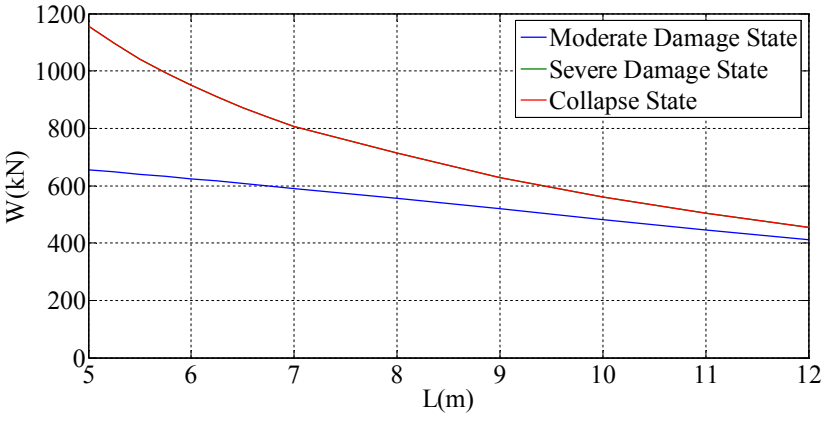

Table B.10. Structural loss estimation curves for the single-storey reinforced concrete industrial buildings which are located at 3rd Earthquake Zone and Z2 Soil Class (cont.).

Cross-Section (cm)	Reinforcement Ratio	Structural Loss Estimation Curves
50×50	Minimum	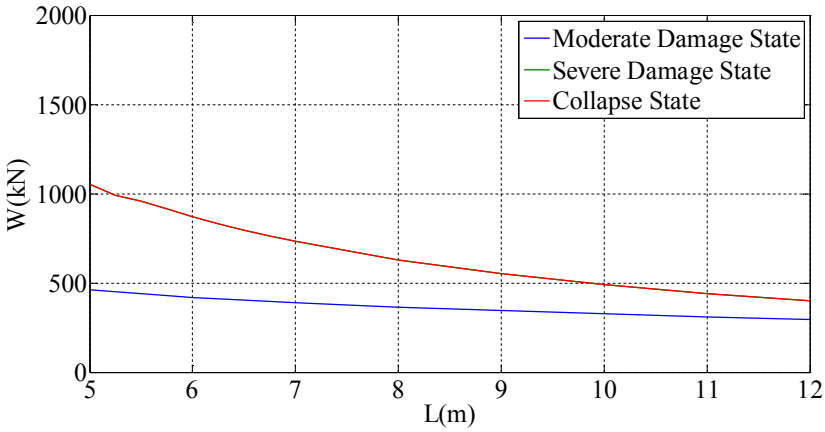
	Moderate	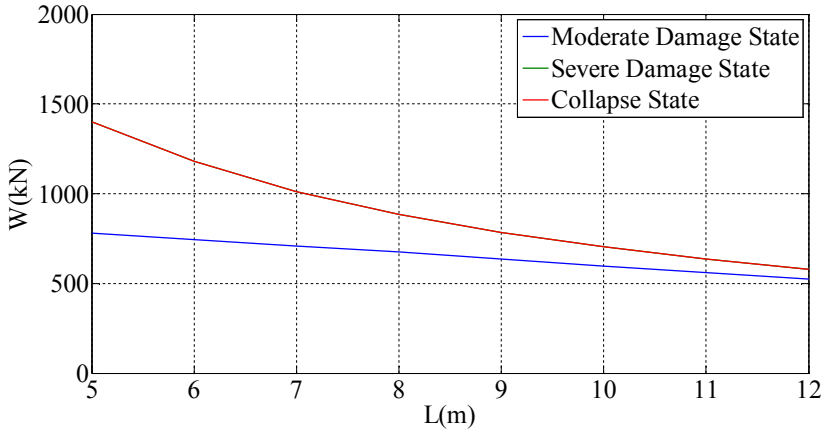
	High	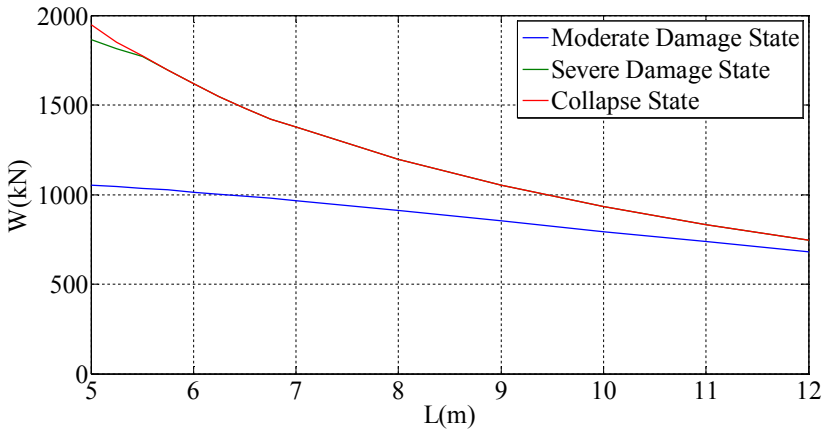

Table B.10. Structural loss estimation curves for the single-storey reinforced concrete industrial buildings which are located at 3rd Earthquake Zone and Z2 Soil Class (cont.).

Cross-Section (cm)	Reinforcement Ratio	Structural Loss Estimation Curves
55×55	Minimum	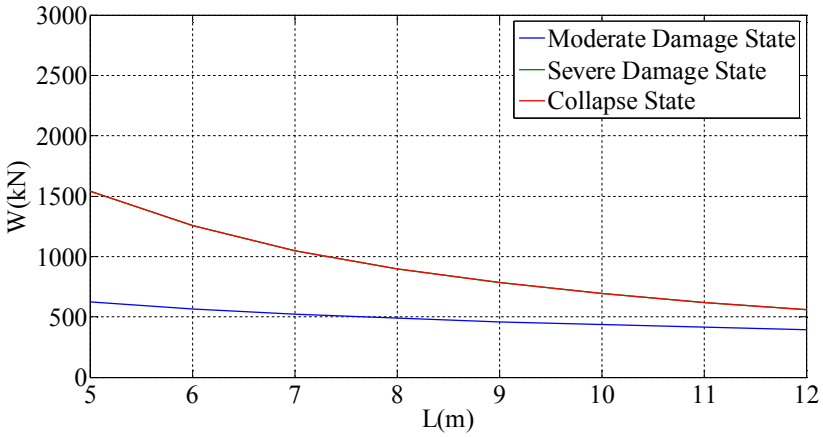
	Moderate	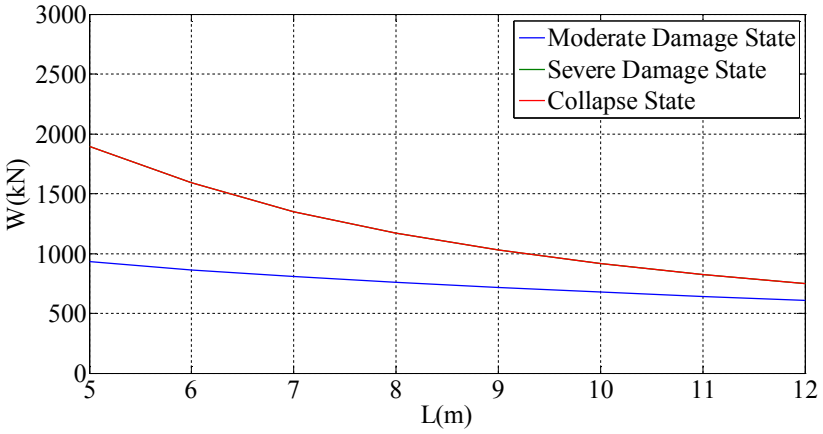
	High	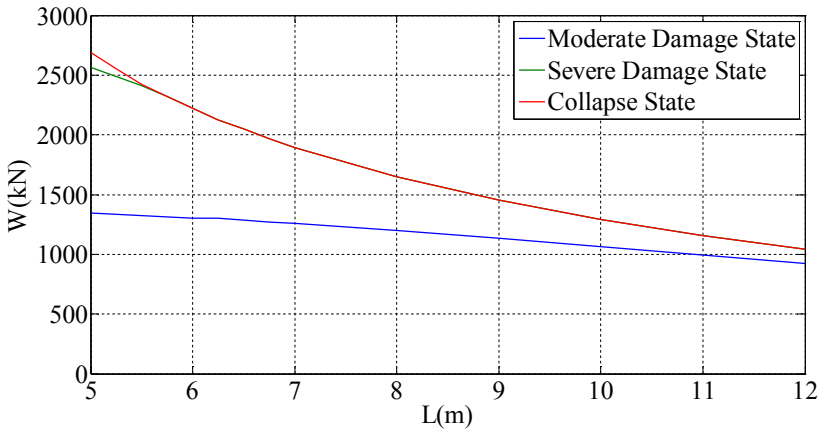

Table B.10. Structural loss estimation curves for the single-storey reinforced concrete industrial buildings which are located at 3rd Earthquake Zone and Z2 Soil Class (cont.).

Cross-Section (cm)	Reinforcement Ratio	Structural Loss Estimation Curves
60×60	Minimum	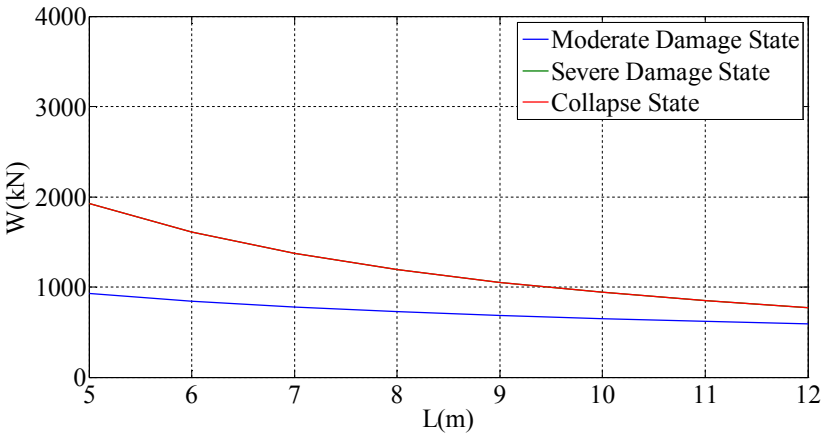
	Moderate	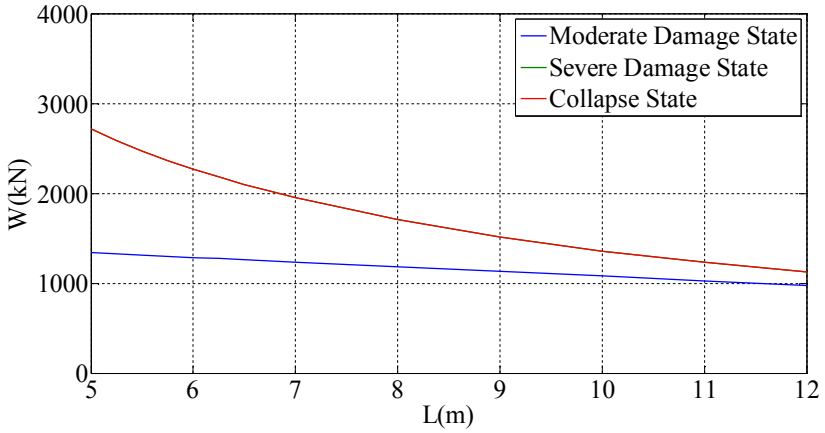
	High	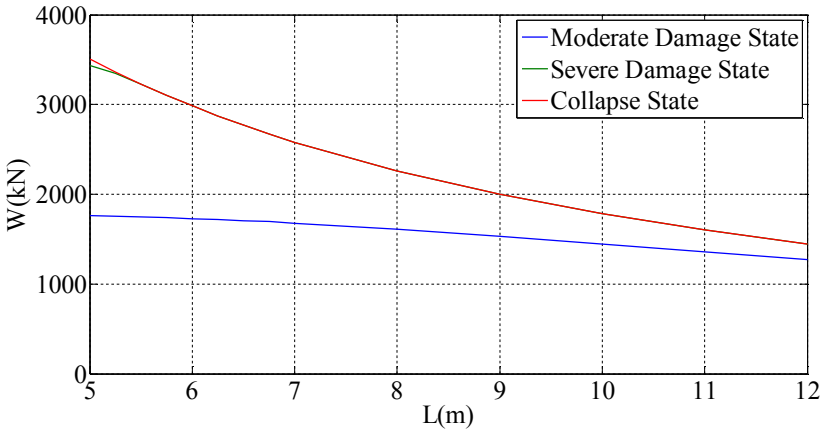

Table B.10. Structural loss estimation curves for the single-storey reinforced concrete industrial buildings which are located at 3rd Earthquake Zone and Z2 Soil Class (cont.).

Cross-Section (cm)	Reinforcement Ratio	Structural Loss Estimation Curves
70×70	Minimum	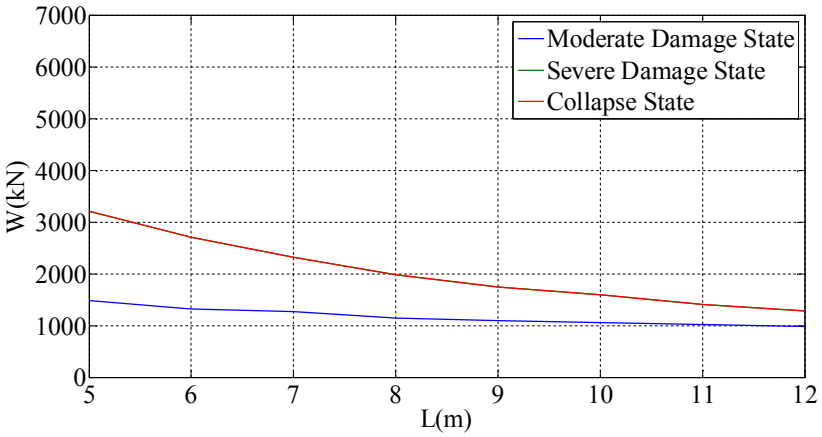
	Moderate	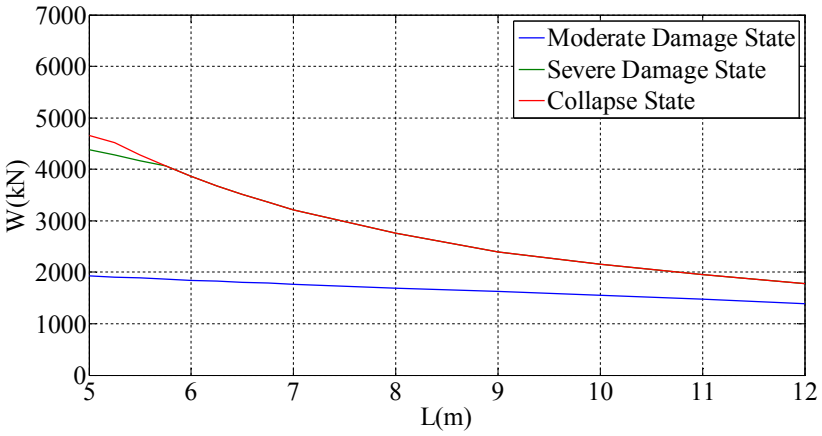
	High	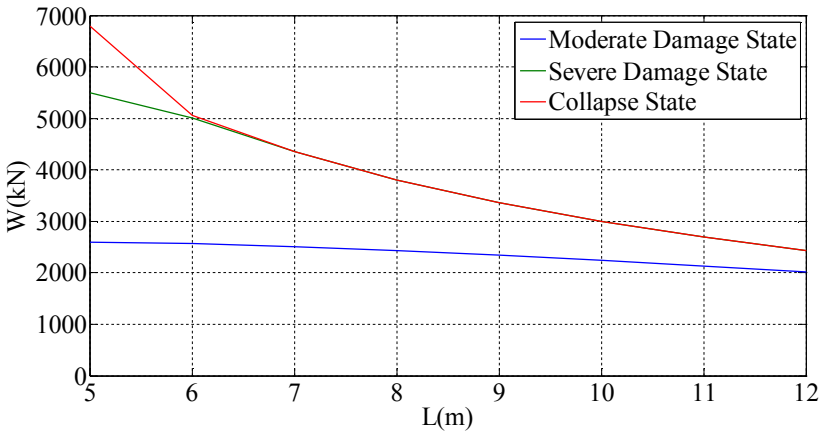

Table B.10. Structural loss estimation curves for the single-storey reinforced concrete industrial buildings which are located at 3rd Earthquake Zone and Z2 Soil Class (cont.).

Cross-Section (cm)	Reinforcement Ratio	Structural Loss Estimation Curves
80×80	Minimum	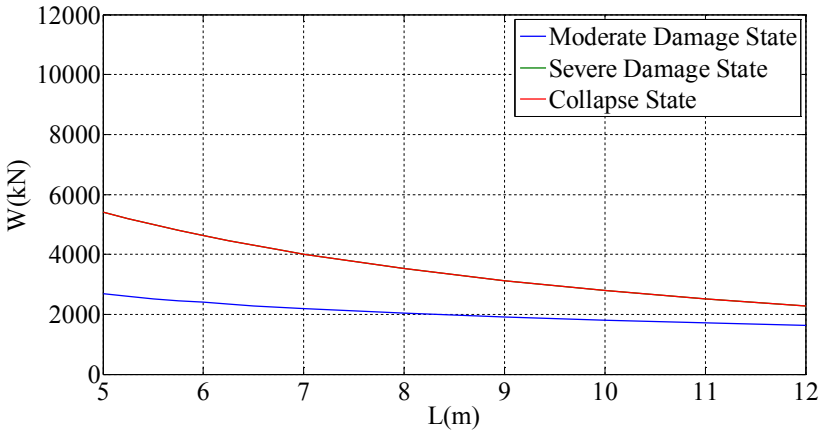
	Moderate	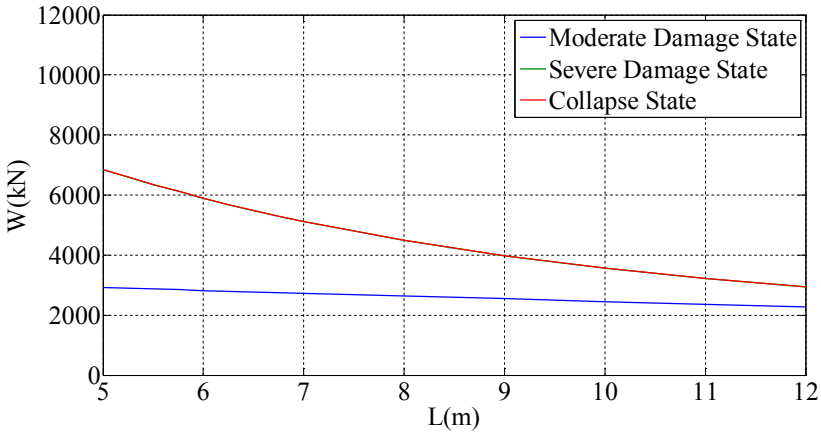
	High	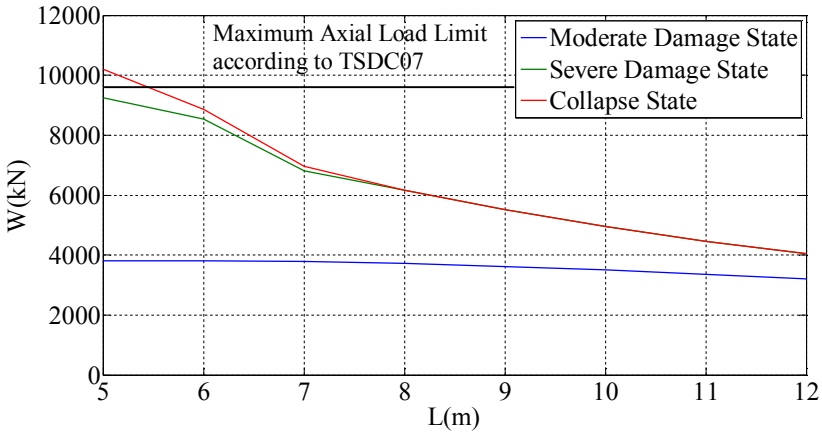

Table B.11. Structural loss estimation curves for the single-storey reinforced concrete industrial buildings which are located at 3rd Earthquake Zone and Z3 Soil Class.

Cross-Section (cm)	Reinforcement Ratio	Structural Loss Estimation Curves
35×35	Minimum	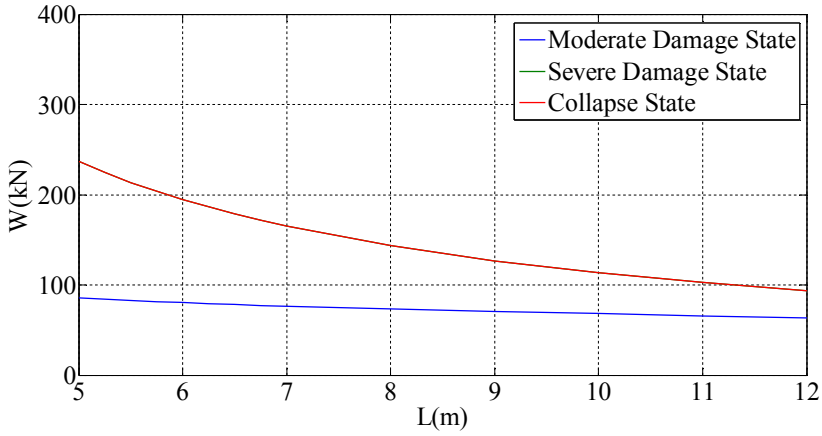
	Moderate	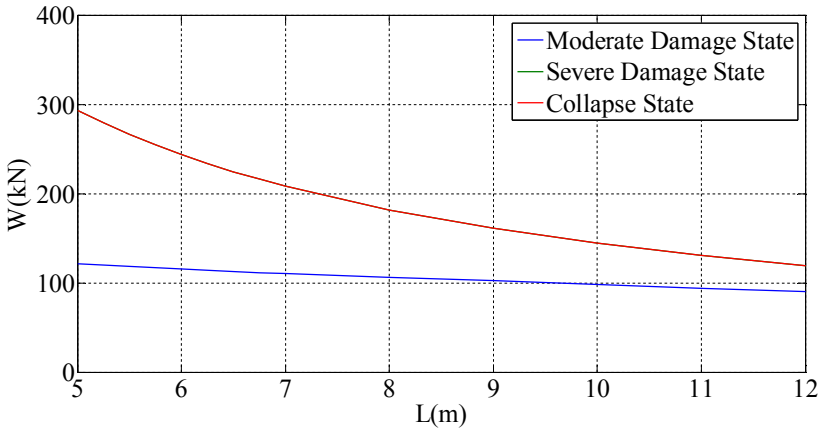
	High	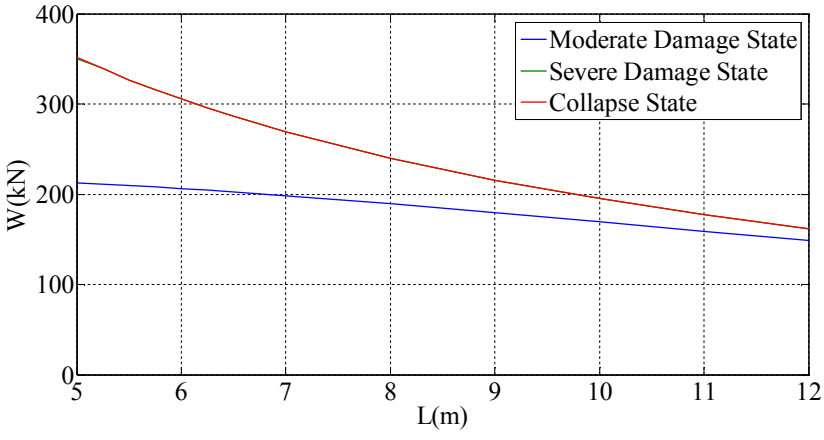

Table B.11. Structural loss estimation curves for the single-storey reinforced concrete industrial buildings which are located at 3rd Earthquake Zone and Z3 Soil Class (cont.).

Cross-Section (cm)	Reinforcement Ratio	Structural Loss Estimation Curves
40×40	Minimum	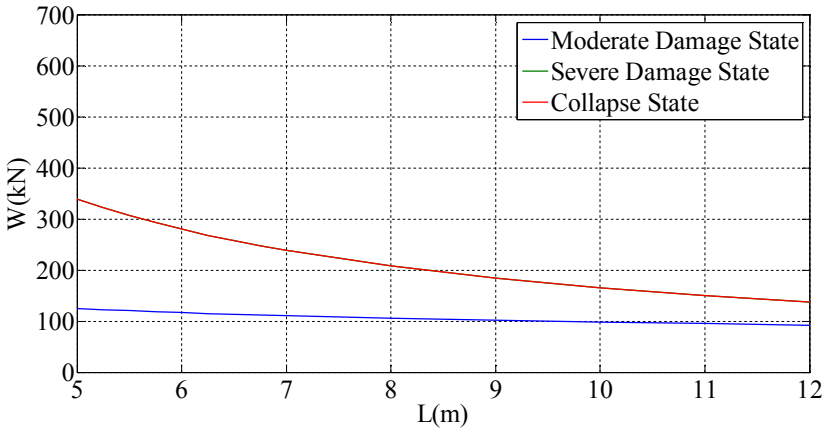
	Moderate	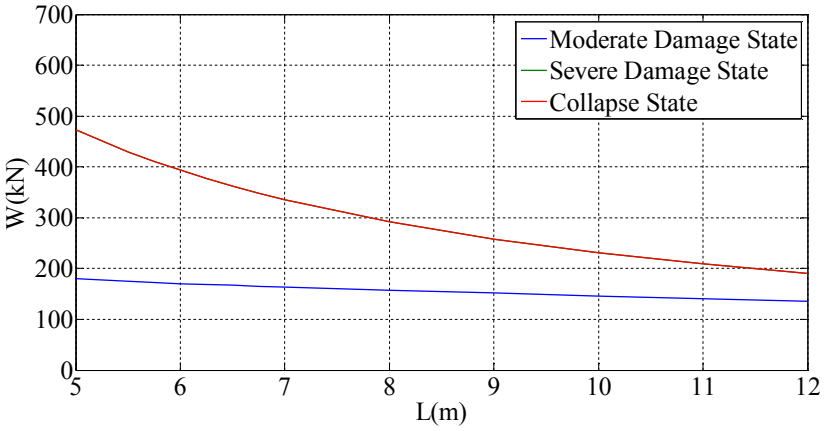
	High	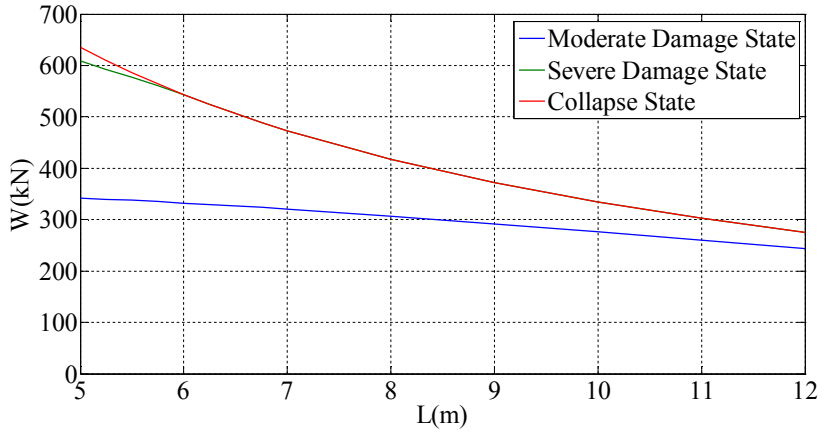

Table B.11. Structural loss estimation curves for the single-storey reinforced concrete industrial buildings which are located at 3rd Earthquake Zone and Z3 Soil Class (cont.).

Cross-Section (cm)	Reinforcement Ratio	Structural Loss Estimation Curves
45×45	Minimum	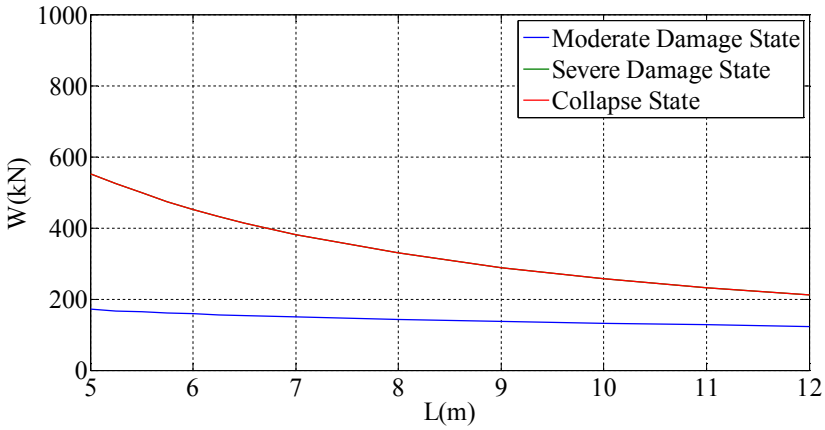
	Moderate	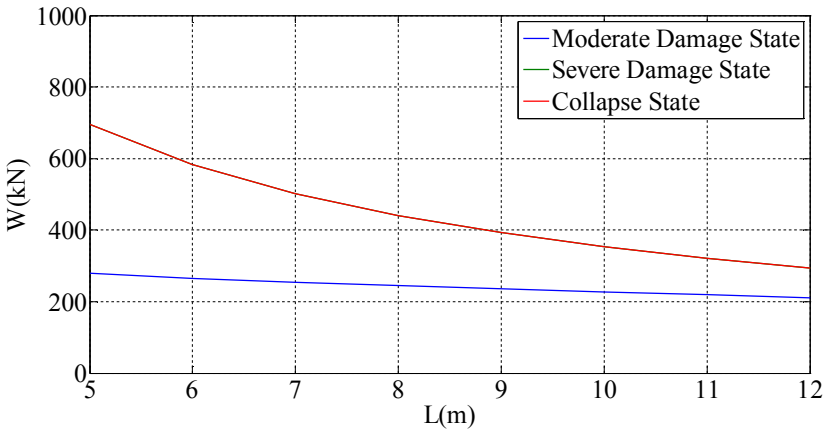
	High	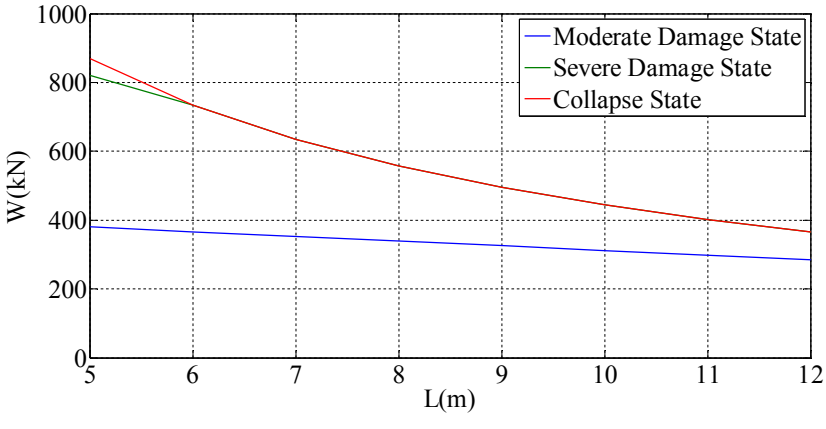

Table B.11. Structural loss estimation curves for the single-storey reinforced concrete industrial buildings which are located at 3rd Earthquake Zone and Z3 Soil Class (cont.).

Cross-Section (cm)	Reinforcement Ratio	Structural Loss Estimation Curves
50×50	Minimum	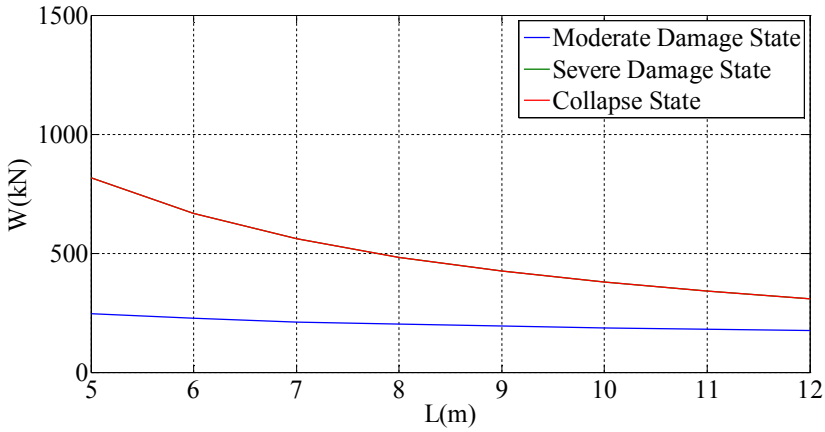
	Moderate	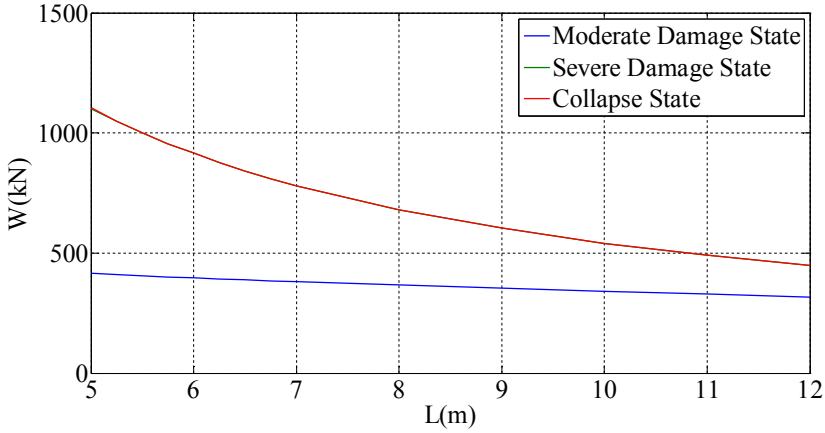
	High	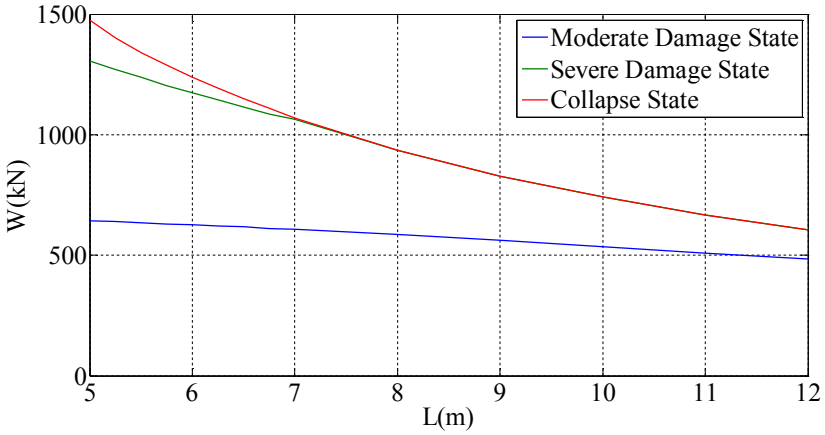

Table B.11. Structural loss estimation curves for the single-storey reinforced concrete industrial buildings which are located at 3rd Earthquake Zone and Z3 Soil Class (cont.).

Cross-Section (cm)	Reinforcement Ratio	Structural Loss Estimation Curves
55×55	Minimum	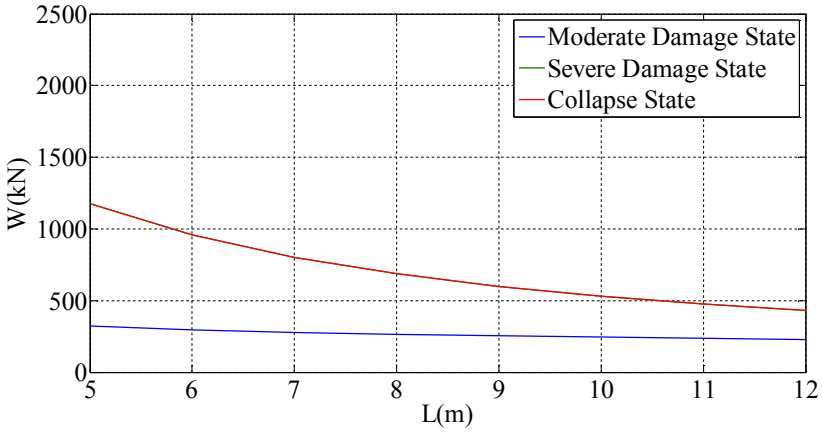
	Moderate	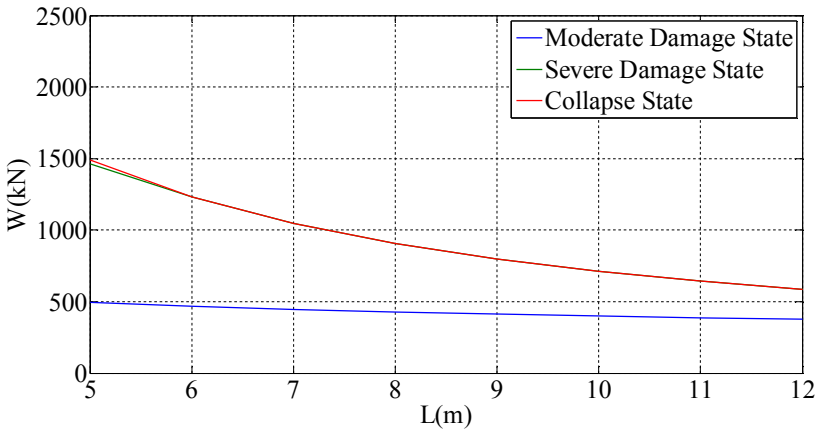
	High	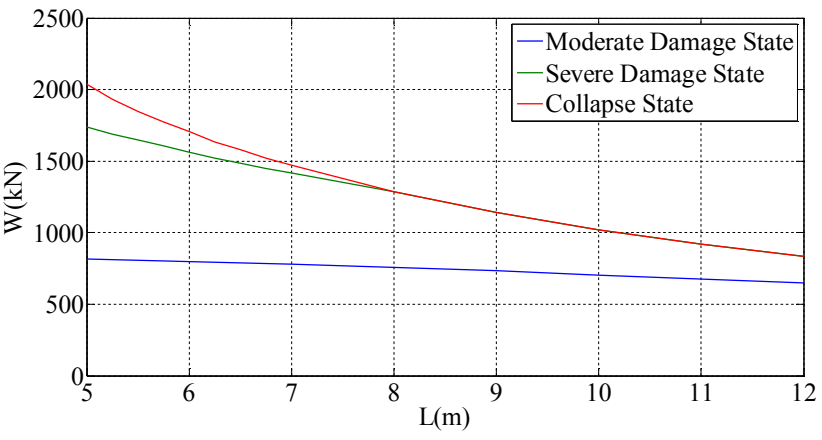

Table B.11. Structural loss estimation curves for the single-storey reinforced concrete industrial buildings which are located at 3rd Earthquake Zone and Z3 Soil Class (cont.).

Cross-Section (cm)	Reinforcement Ratio	Structural Loss Estimation Curves
60×60	Minimum	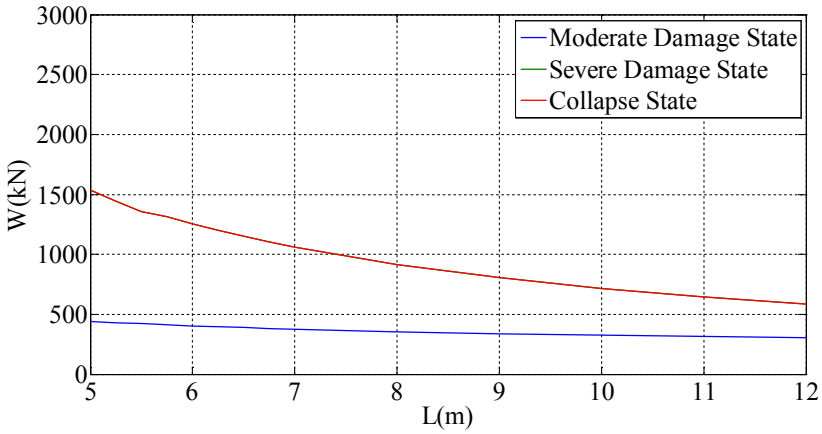
	Moderate	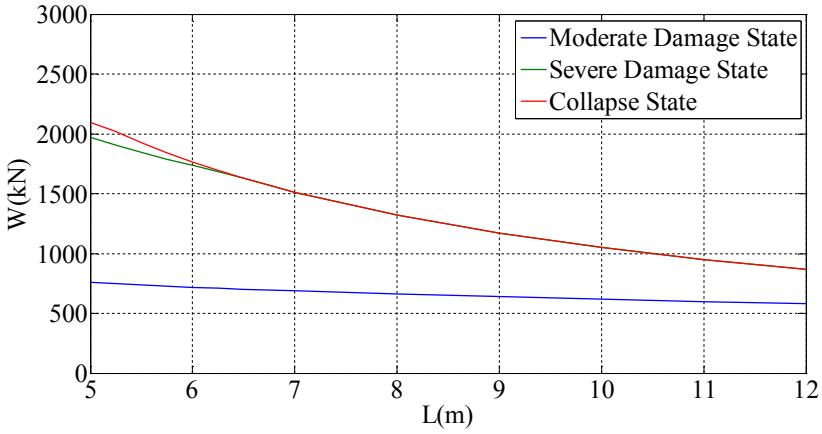
	High	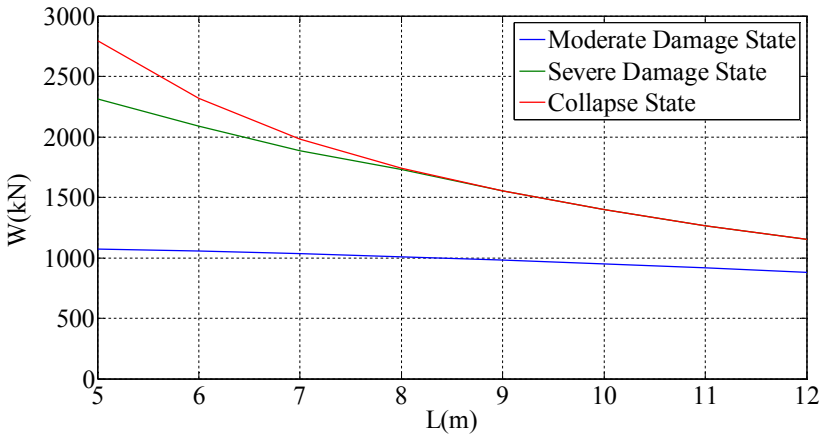

Table B.11. Structural loss estimation curves for the single-storey reinforced concrete industrial buildings which are located at 3rd Earthquake Zone and Z3 Soil Class (cont.).

Cross-Section (cm)	Reinforcement Ratio	Structural Loss Estimation Curves
70×70	Minimum	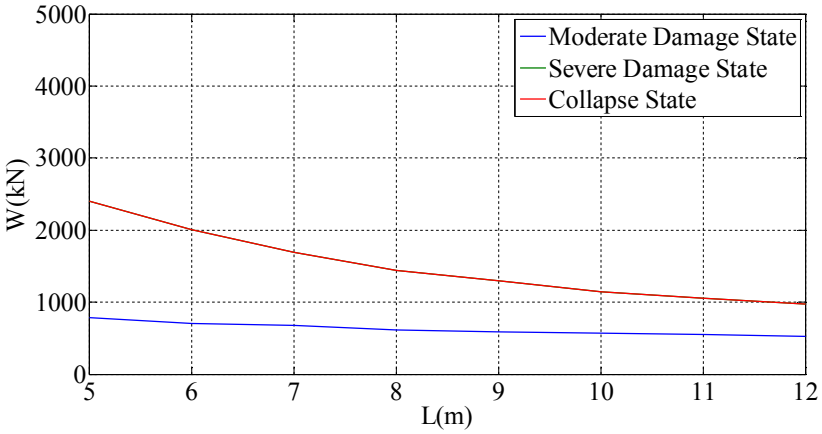
	Moderate	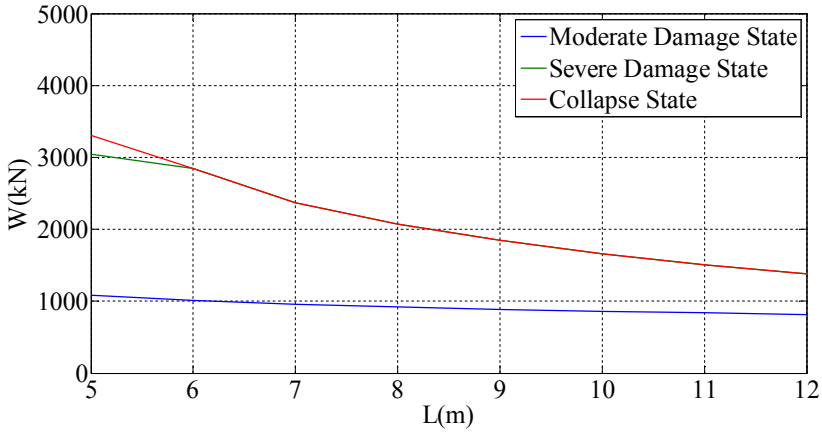
	High	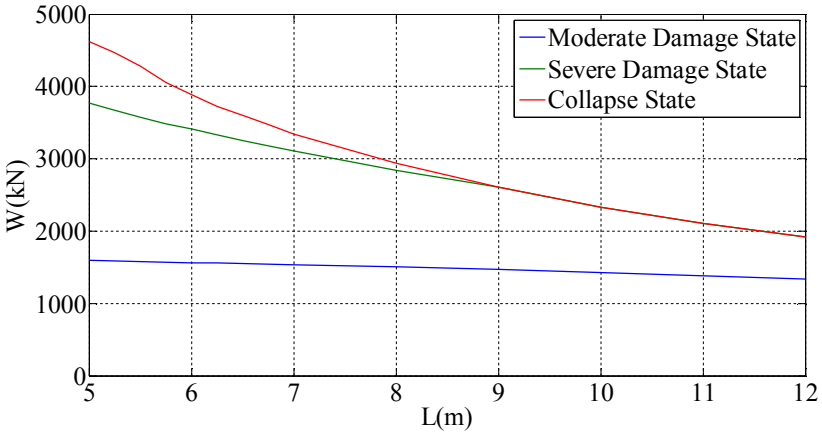

Table B.11. Structural loss estimation curves for the single-storey reinforced concrete industrial buildings which are located at 3rd Earthquake Zone and Z3 Soil Class (cont.).

Cross-Section (cm)	Reinforcement Ratio	Structural Loss Estimation Curves
80×80	Minimum	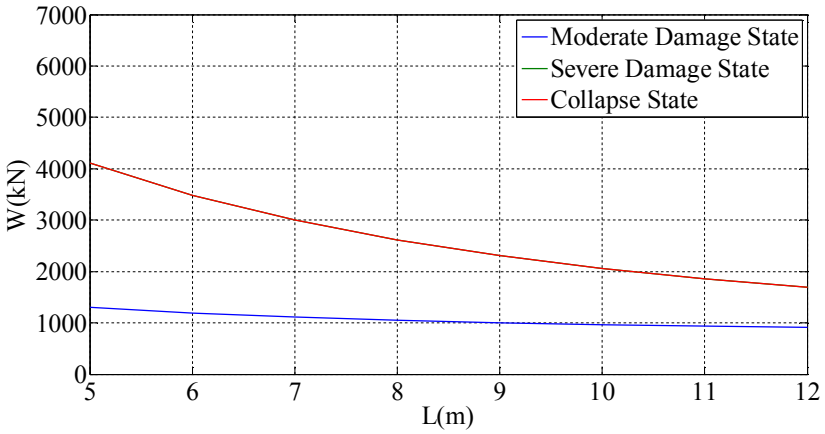
	Moderate	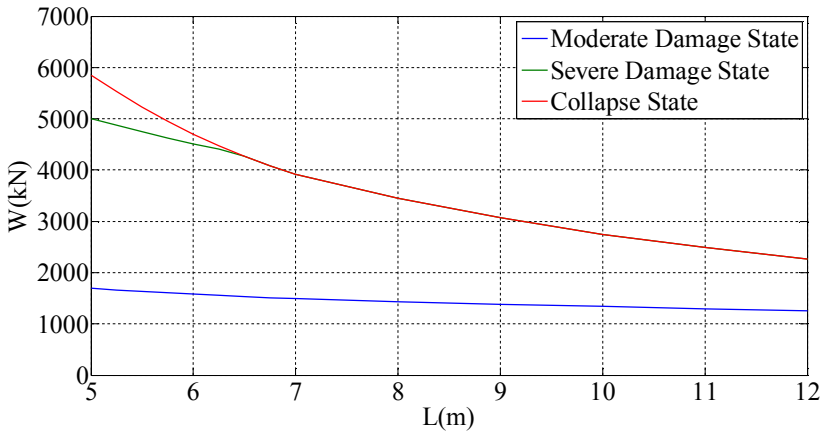
	High	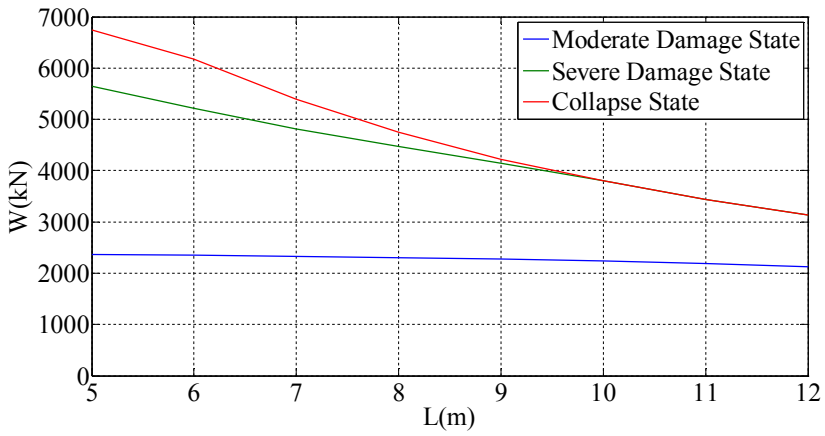

Table B.12. Structural loss estimation curves for the single-storey reinforced concrete industrial buildings which are located at 3rd Earthquake Zone and Z4 Soil Class.

Cross-Section (cm)	Reinforcement Ratio	Structural Loss Estimation Curves
35×35	Minimum	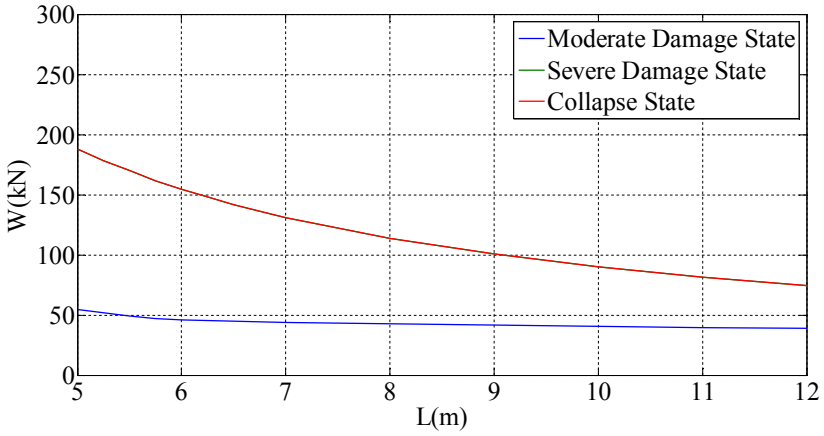
	Moderate	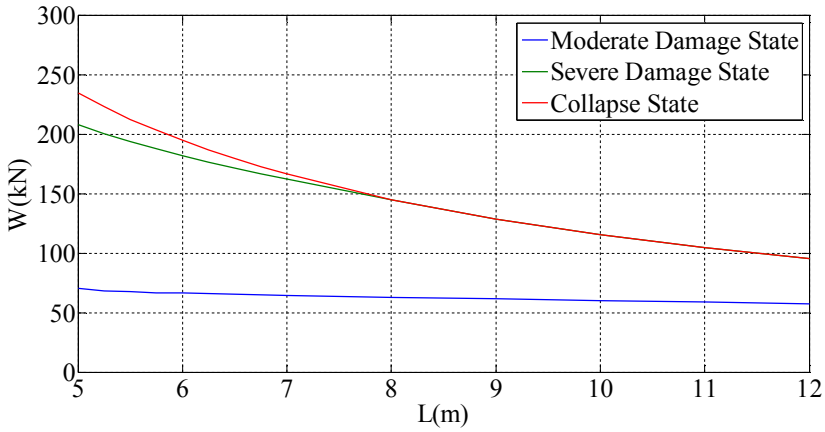
	High	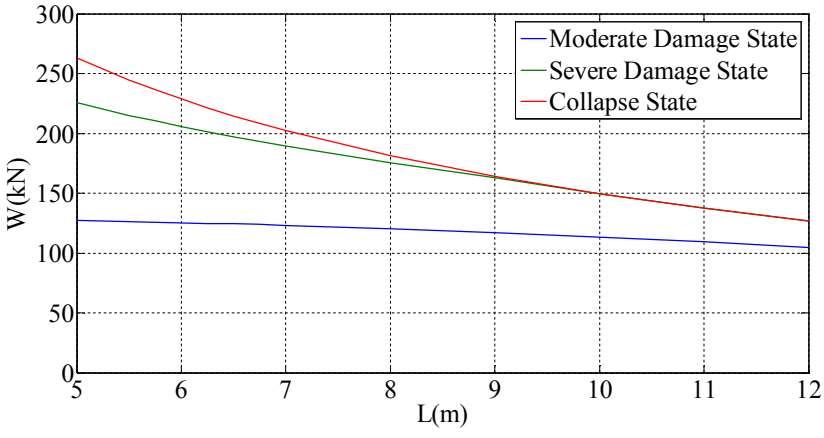

Table B.12. Structural loss estimation curves for the single-storey reinforced concrete industrial buildings which are located at 3rd Earthquake Zone and Z4 Soil Class (cont.).

Cross-Section (cm)	Reinforcement Ratio	Structural Loss Estimation Curves
40×40	Minimum	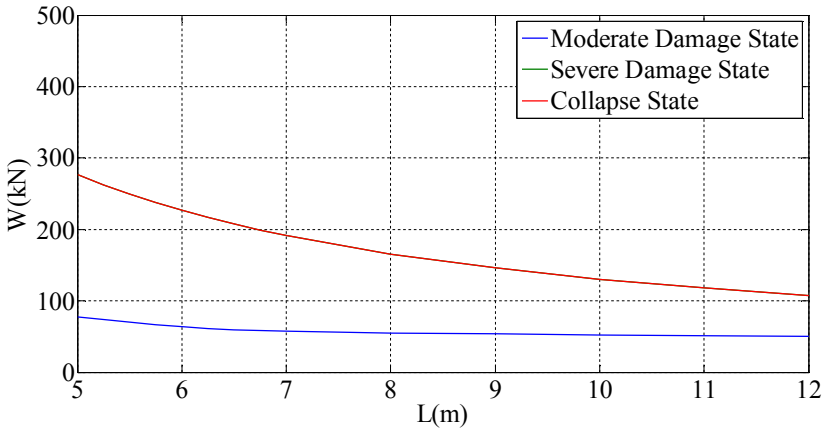
	Moderate	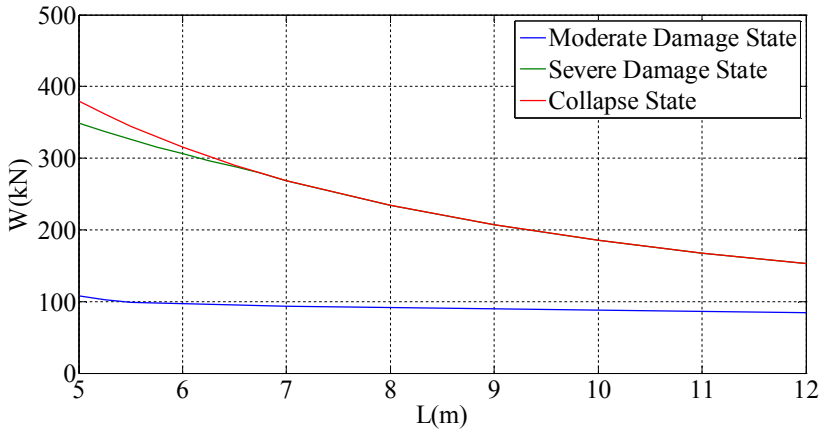
	High	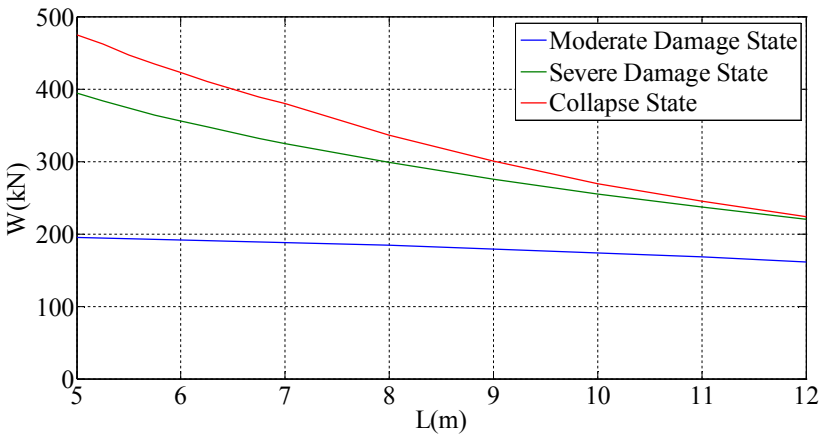

Table B.12. Structural loss estimation curves for the single-storey reinforced concrete industrial buildings which are located at 3rd Earthquake Zone and Z4 Soil Class (cont.).

Cross-Section (cm)	Reinforcement Ratio	Structural Loss Estimation Curves
45×45	Minimum	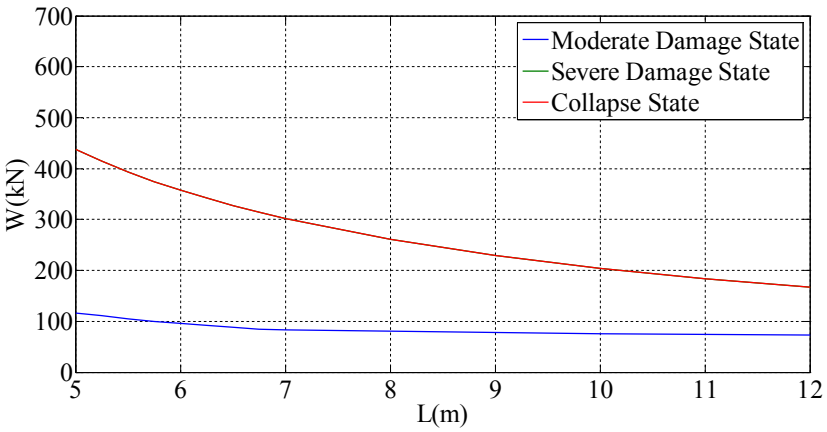
	Moderate	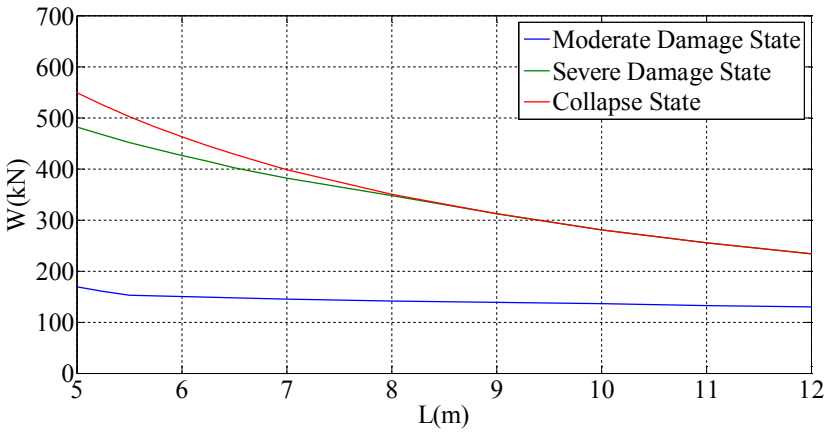
	High	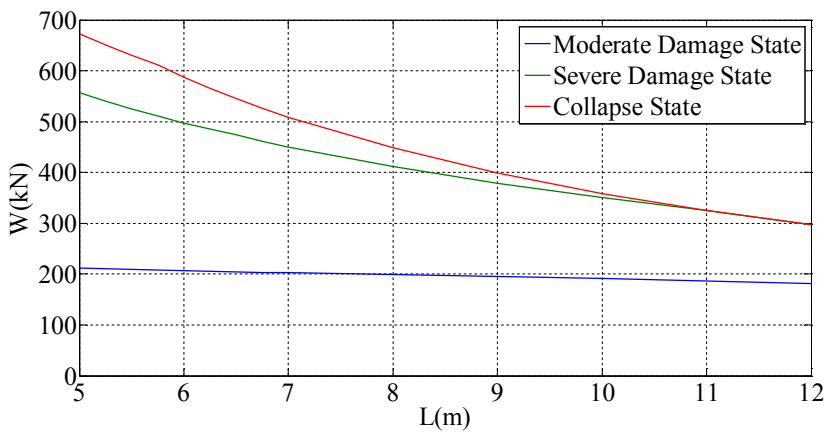

Table B.12. Structural loss estimation curves for the single-storey reinforced concrete industrial buildings which are located at 3rd Earthquake Zone and Z4 Soil Class (cont.).

Cross-Section (cm)	Reinforcement Ratio	Structural Loss Estimation Curves
50×50	Minimum	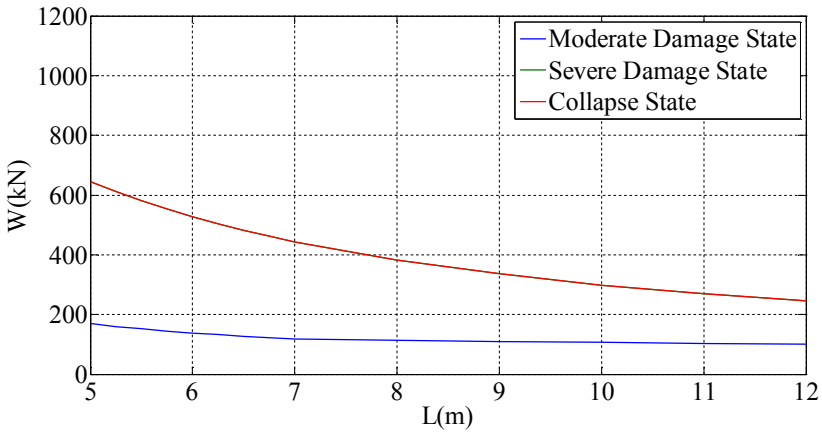
	Moderate	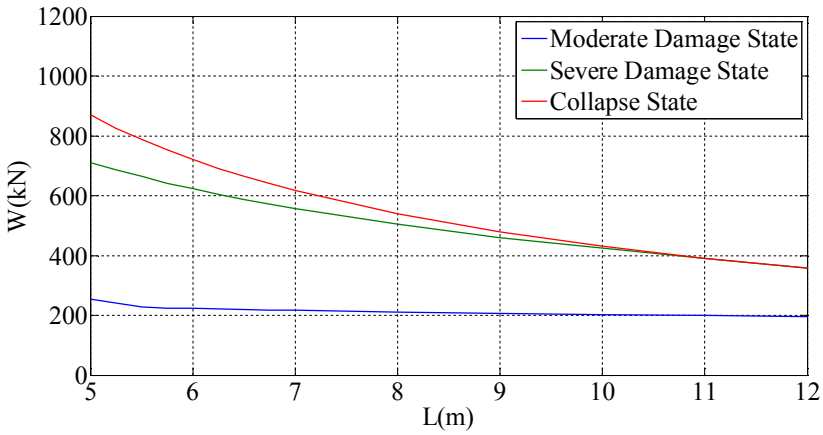
	High	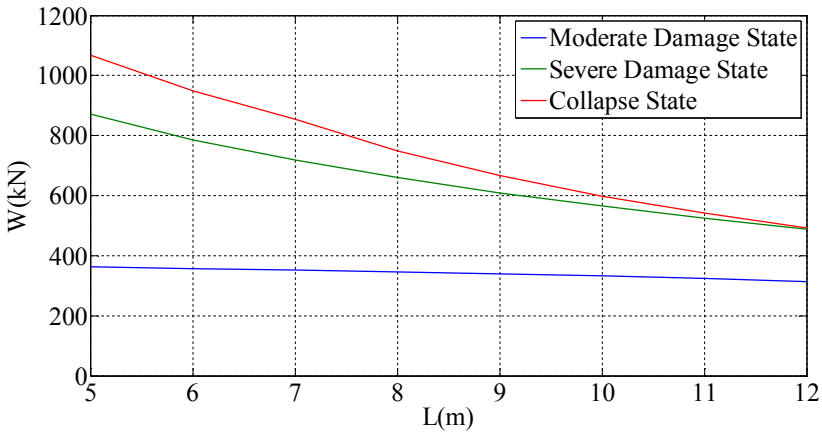

Table B.12. Structural loss estimation curves for the single-storey reinforced concrete industrial buildings which are located at 3rd Earthquake Zone and Z4 Soil Class (cont.).

Cross-Section (cm)	Reinforcement Ratio	Structural Loss Estimation Curves
55×55	Minimum	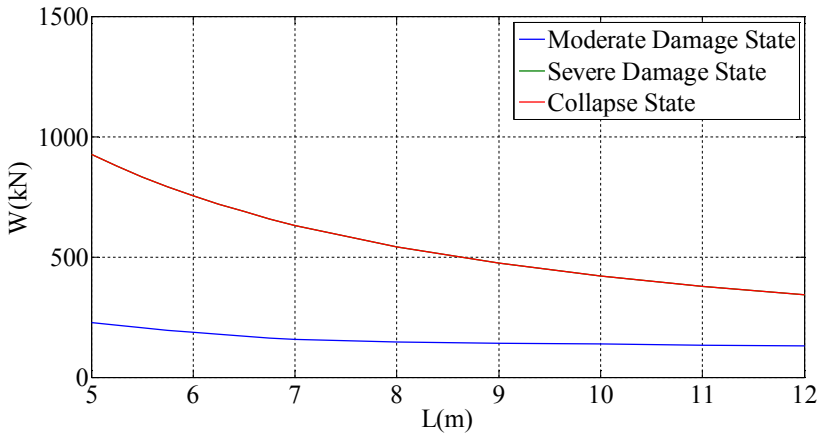
	Moderate	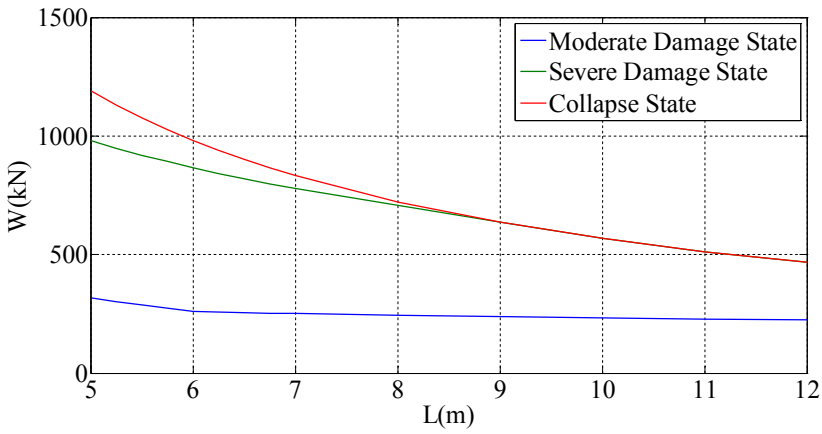
	High	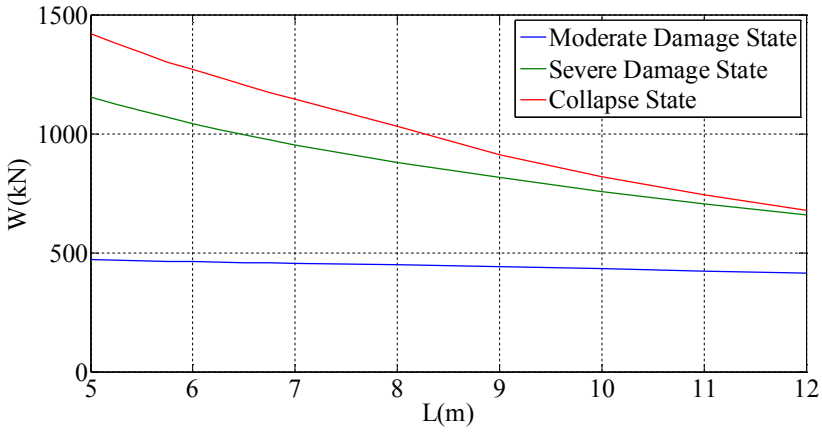

Table B.12. Structural loss estimation curves for the single-storey reinforced concrete industrial buildings which are located at 3rd Earthquake Zone and Z4 Soil Class (cont.).

Cross-Section (cm)	Reinforcement Ratio	Structural Loss Estimation Curves
60×60	Minimum	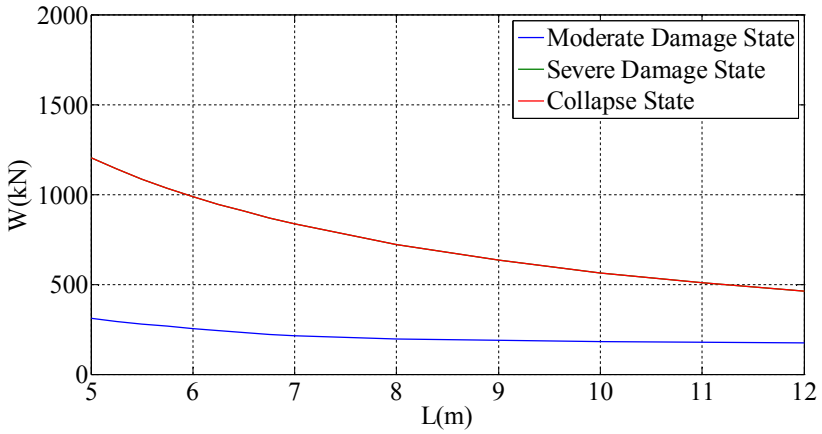
	Moderate	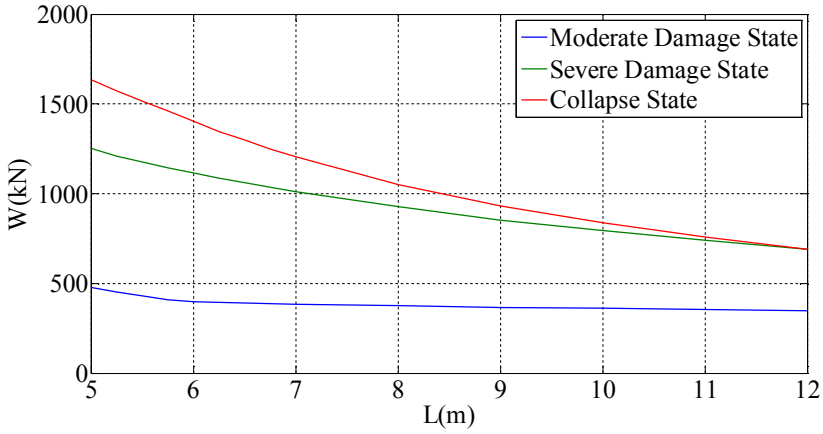
	High	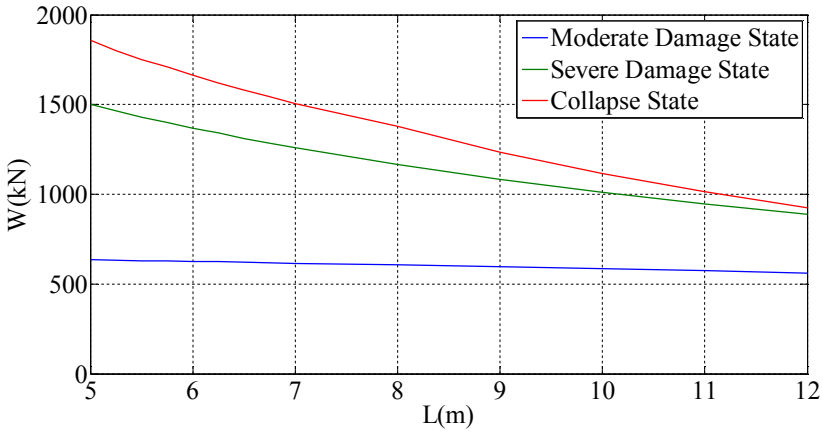

Table B.12. Structural loss estimation curves for the single-storey reinforced concrete industrial buildings which are located at 3rd Earthquake Zone and Z4 Soil Class (cont.).

Cross-Section (cm)	Reinforcement Ratio	Structural Loss Estimation Curves
70×70	Minimum	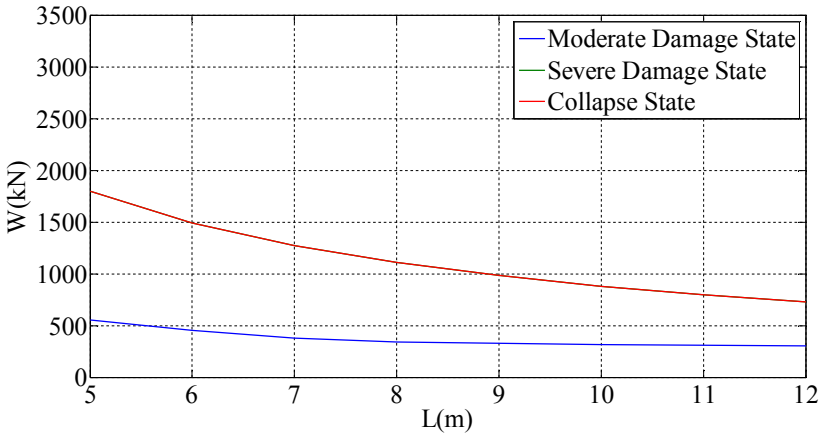
	Moderate	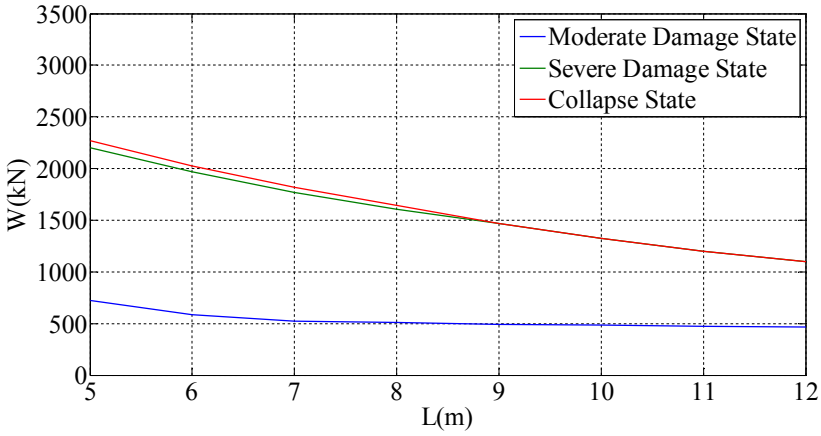
	High	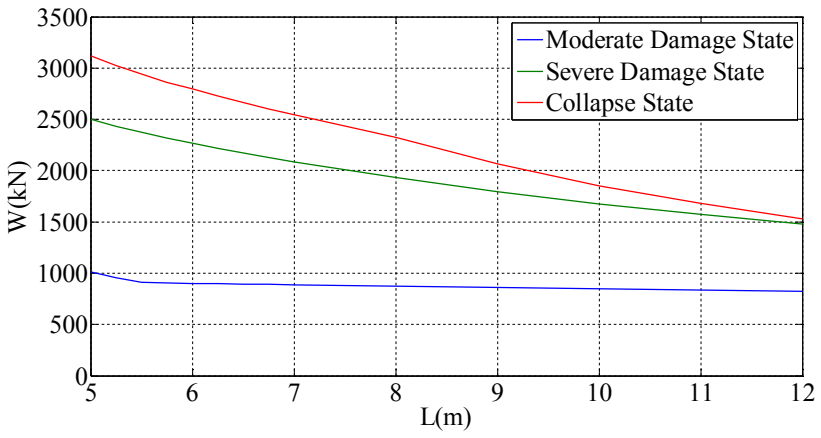

Table B.12. Structural loss estimation curves for the single-storey reinforced concrete industrial buildings which are located at 3rd Earthquake Zone and Z4 Soil Class (cont.).

Cross-Section (cm)	Reinforcement Ratio	Structural Loss Estimation Curves
80×80	Minimum	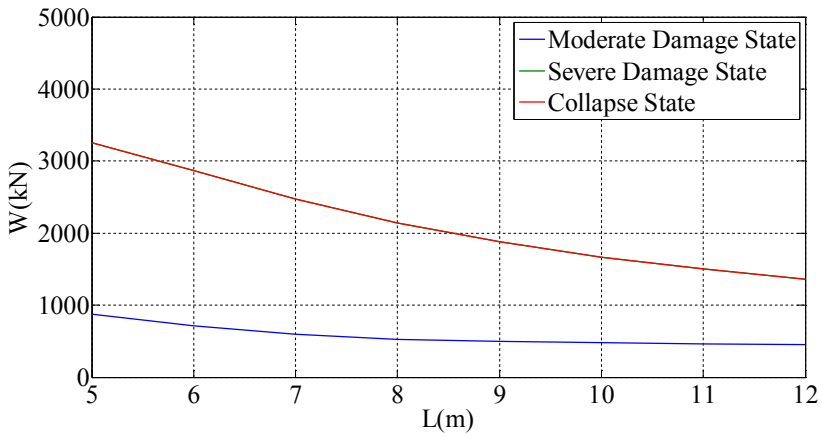
	Moderate	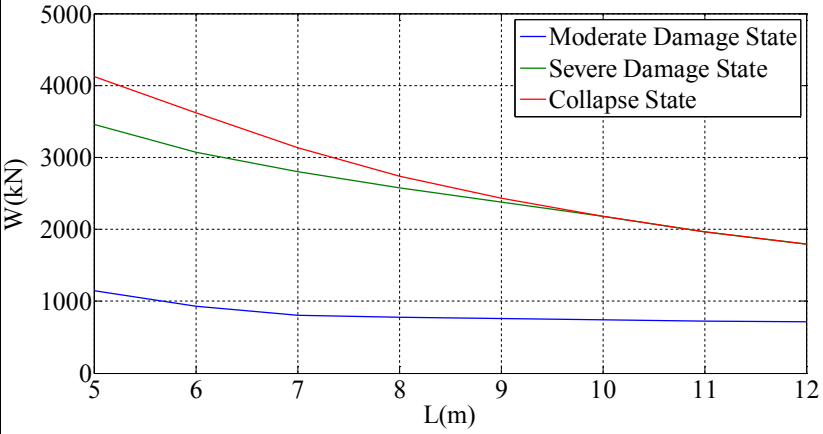
	High	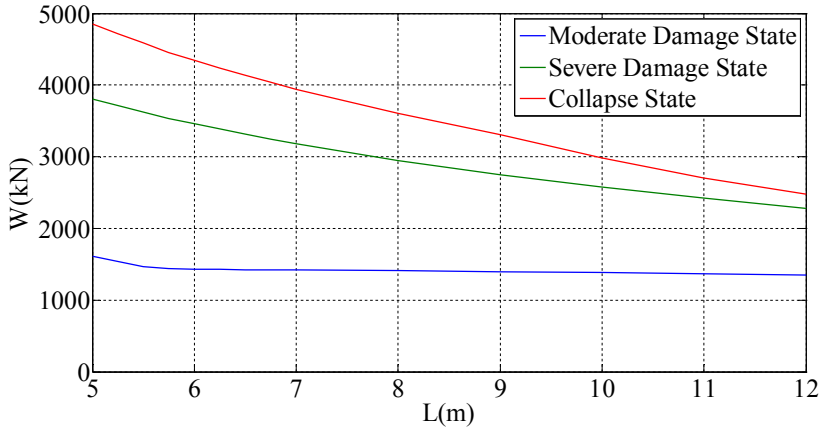

Table B.13. Structural loss estimation curves for the single-storey reinforced concrete industrial buildings which are located at 4th Earthquake Zone and Z1 Soil Class.

Cross-Section (cm)	Reinforcement Ratio	Structural Loss Estimation Curves
35×35	Minimum	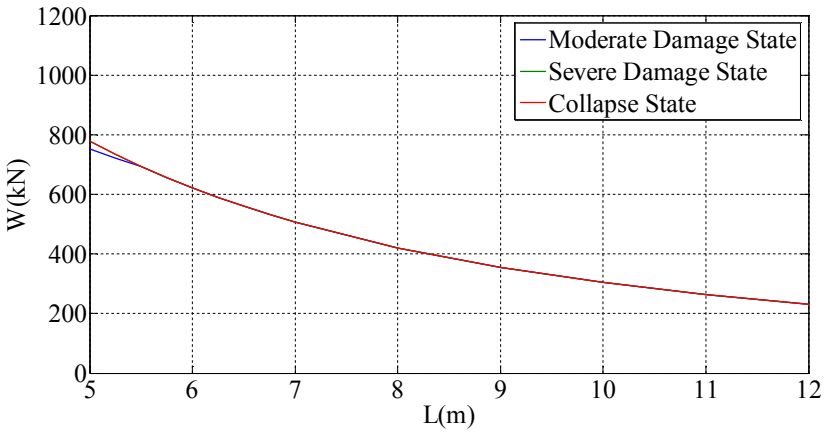
	Moderate	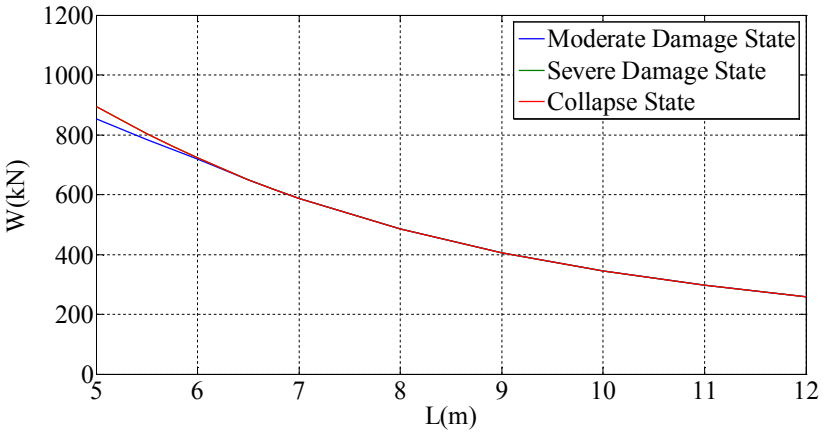
	High	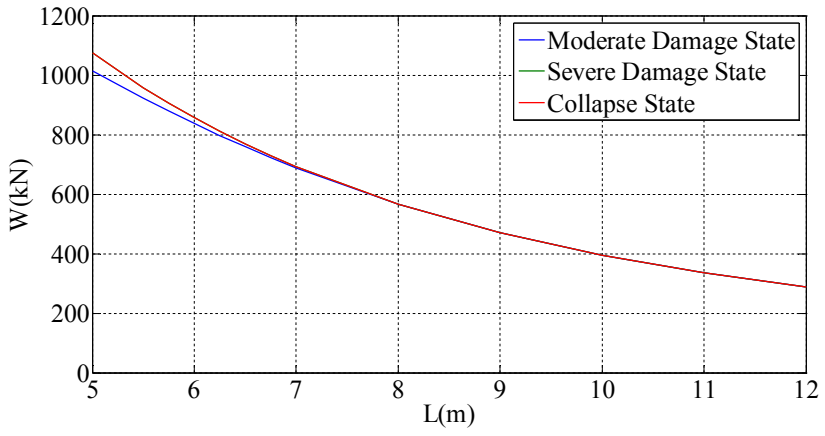

Table B.13. Structural loss estimation curves for the single-storey reinforced concrete industrial buildings which are located at 4th Earthquake Zone and Z1 Soil Class (cont.).

Cross-Section (cm)	Reinforcement Ratio	Structural Loss Estimation Curves
40×40	Minimum	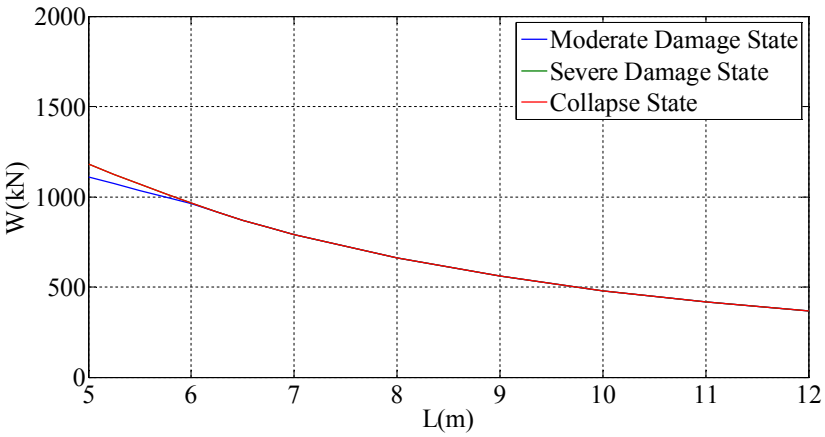
	Moderate	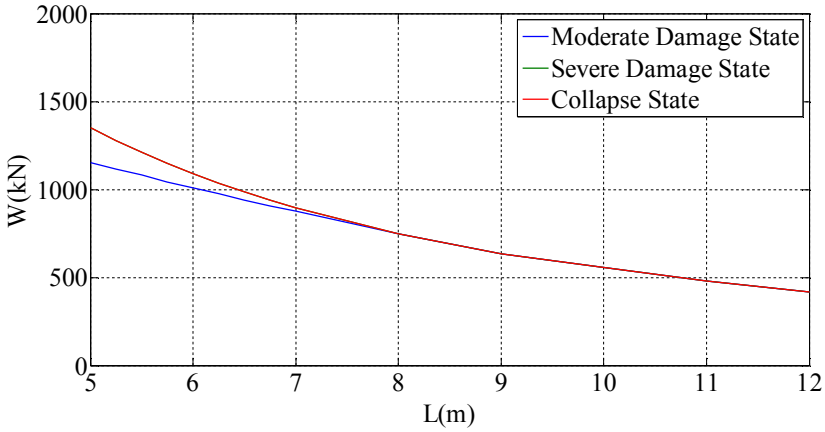
	High	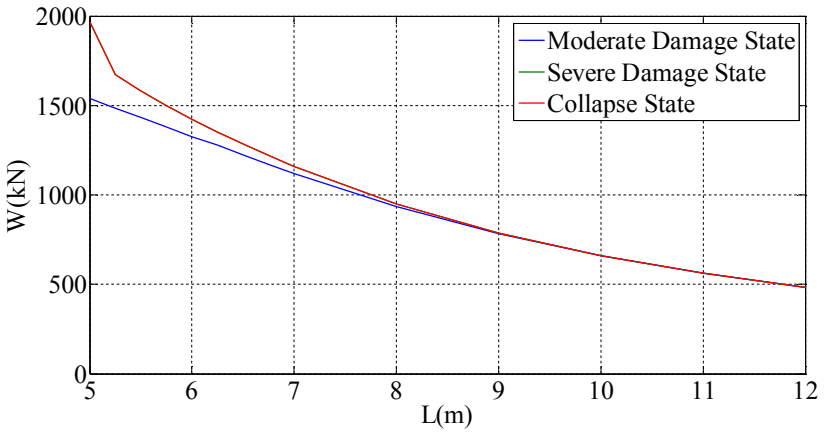

Table B.13. Structural loss estimation curves for the single-storey reinforced concrete industrial buildings which are located at 4th Earthquake Zone and Z1 Soil Class (cont.).

Cross-Section (cm)	Reinforcement Ratio	Structural Loss Estimation Curves
45×45	Minimum	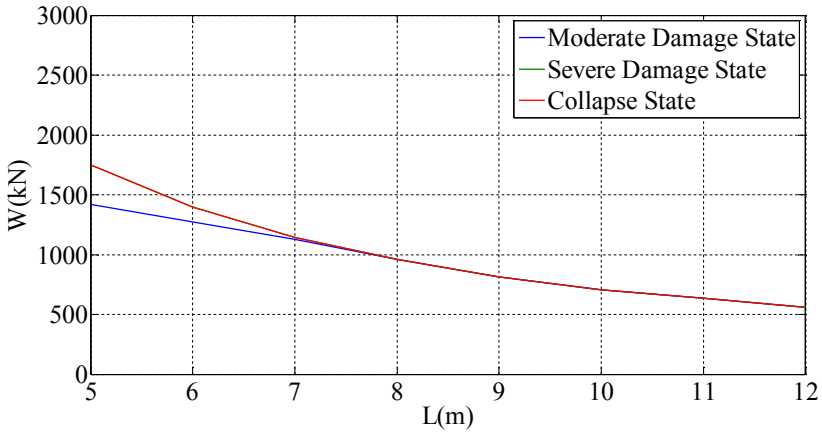
	Moderate	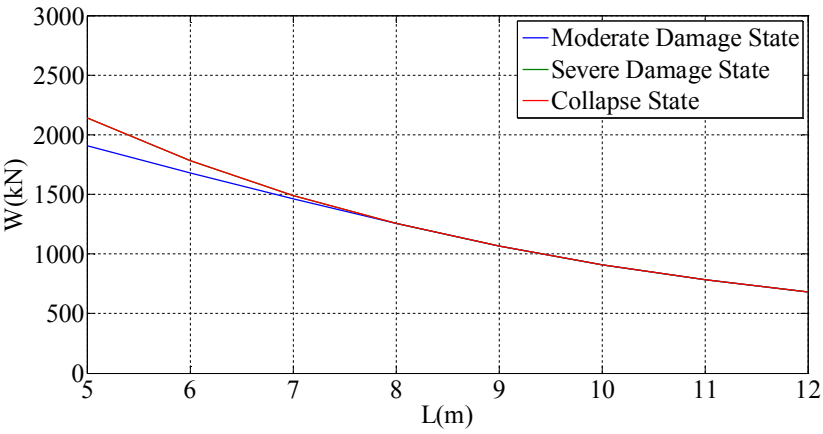
	High	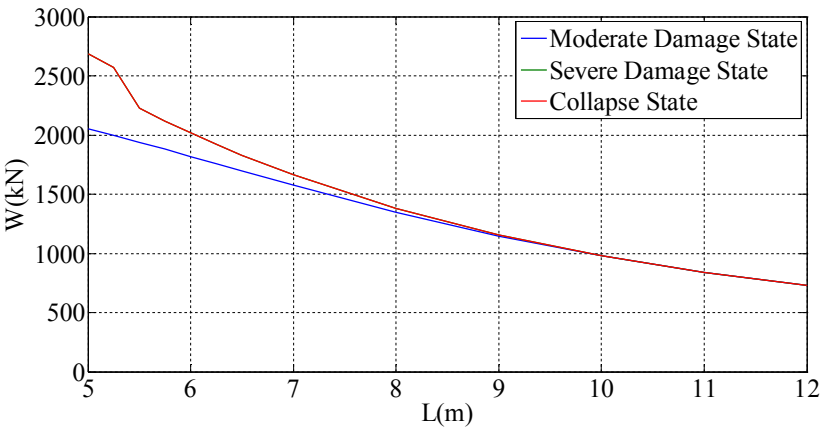

Table B.13. Structural loss estimation curves for the single-storey reinforced concrete industrial buildings which are located at 4th Earthquake Zone and Z1 Soil Class (cont.).

Cross-Section (cm)	Reinforcement Ratio	Structural Loss Estimation Curves
50×50	Minimum	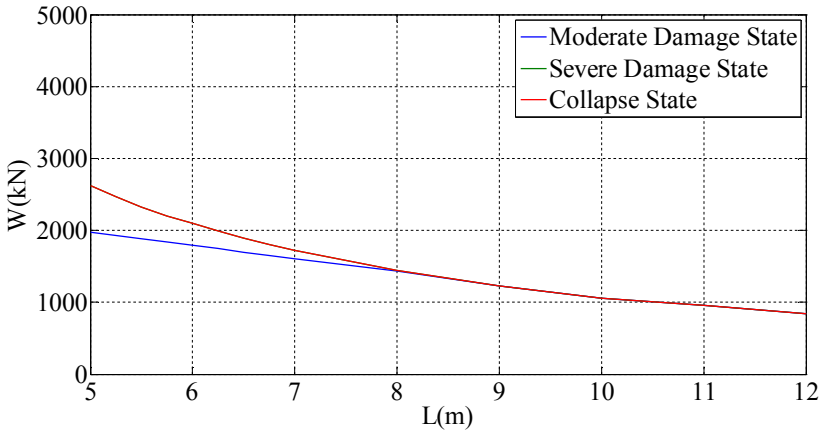
	Moderate	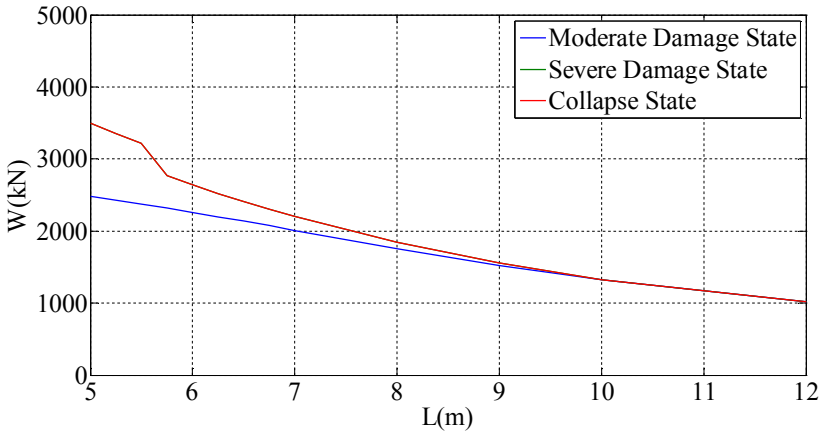
	High	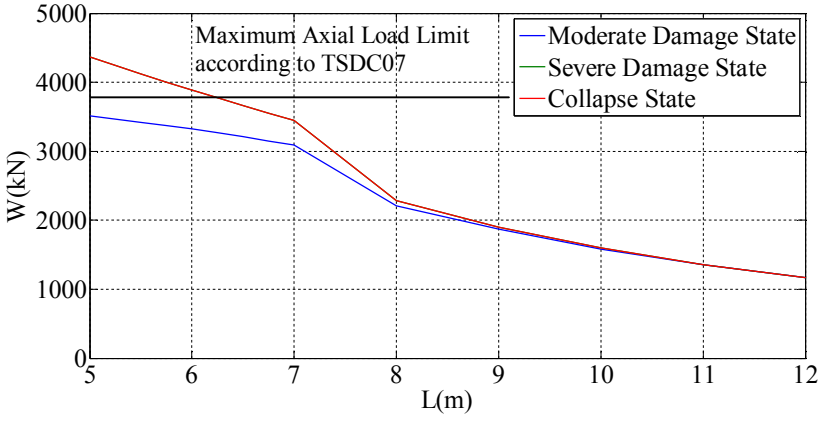

Table B.13. Structural loss estimation curves for the single-storey reinforced concrete industrial buildings which are located at 4th Earthquake Zone and Z1 Soil Class (cont.).

Cross-Section (cm)	Reinforcement Ratio	Structural Loss Estimation Curves
55×55	Minimum	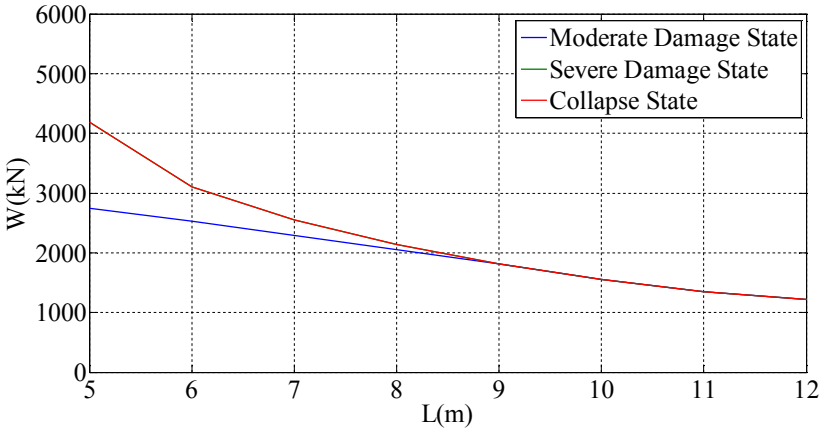
	Moderate	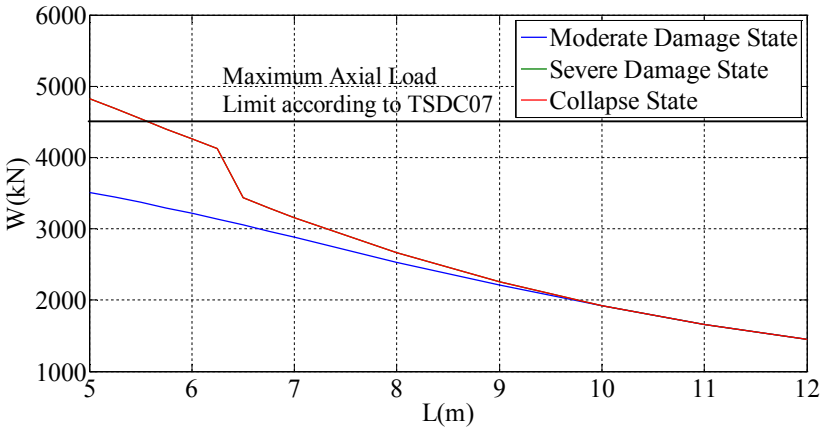
	High	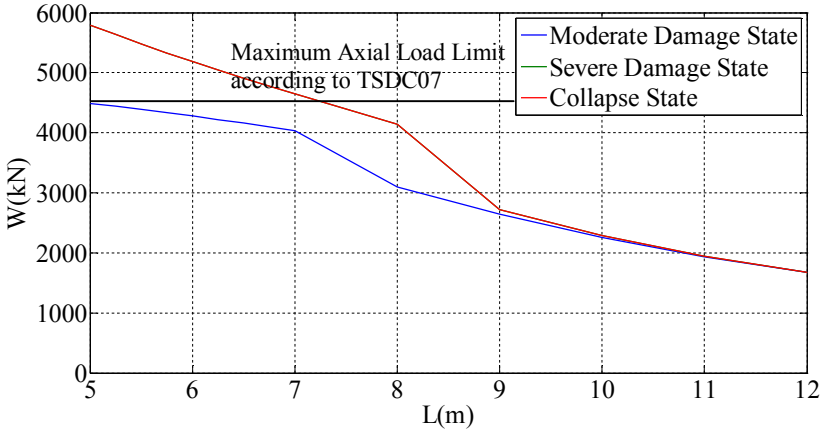

Table B.13. Structural loss estimation curves for the single-storey reinforced concrete industrial buildings which are located at 4th Earthquake Zone and Z1 Soil Class (cont.).

Cross-Section (cm)	Reinforcement Ratio	Structural Loss Estimation Curves
60×60	Minimum	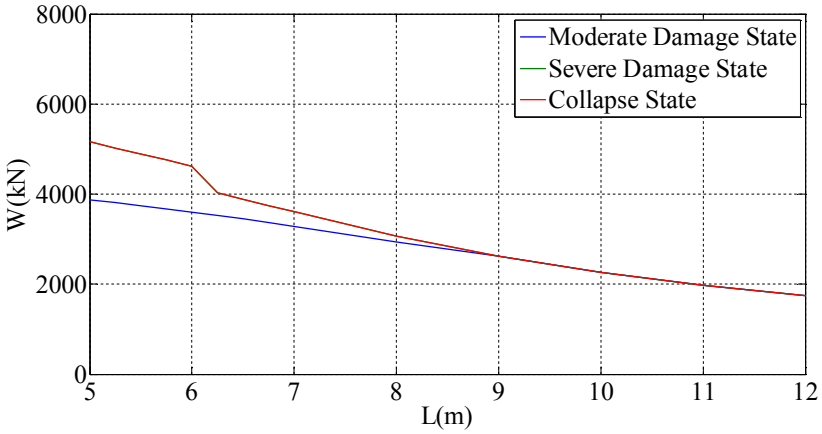
	Moderate	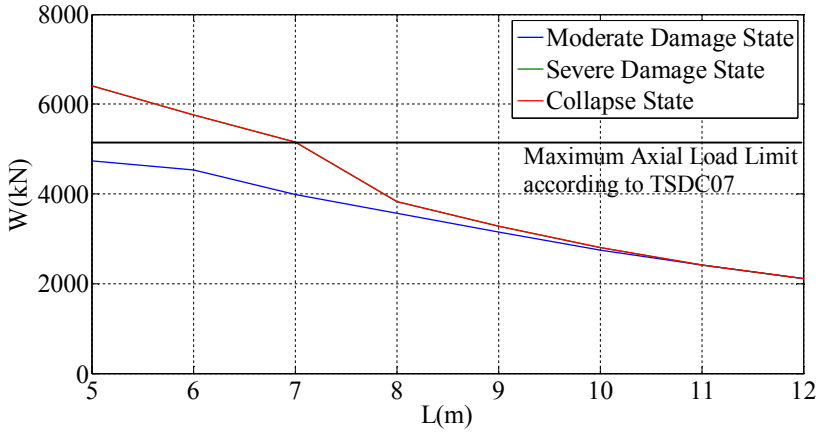
	High	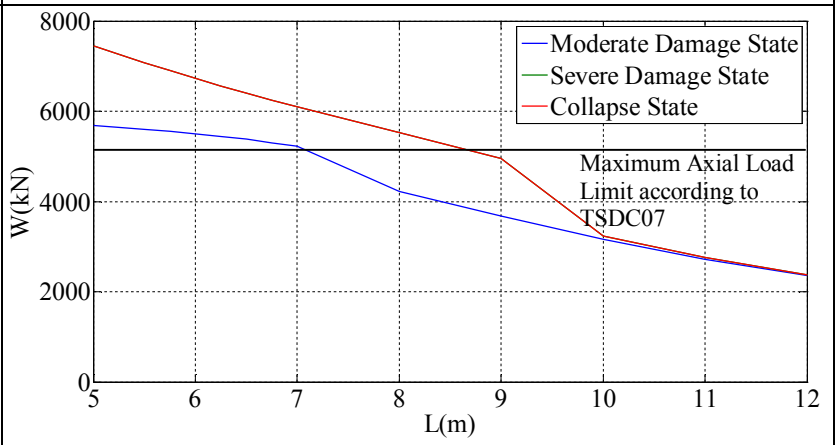

Table B.13. Structural loss estimation curves for the single-storey reinforced concrete industrial buildings which are located at 4th Earthquake Zone and Z1 Soil Class (cont.).

Cross-Section (cm)	Reinforcement Ratio	Structural Loss Estimation Curves
70×70	Minimum	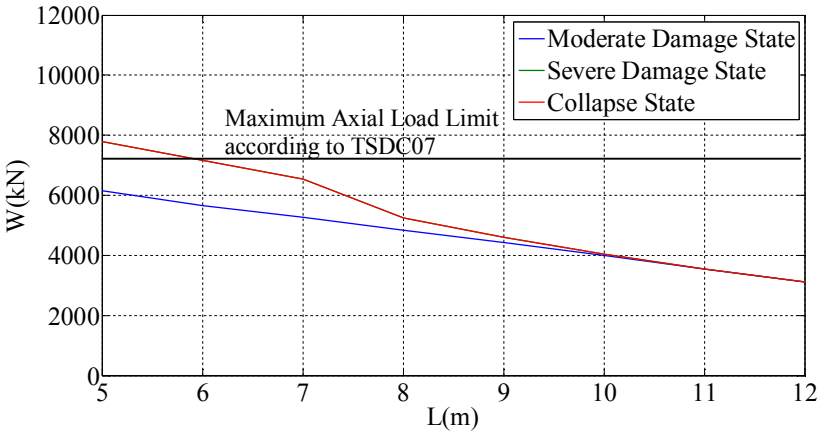
	Moderate	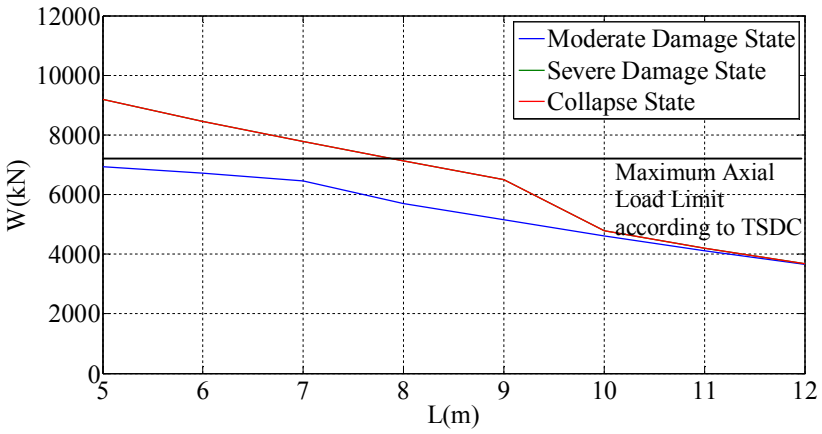
	High	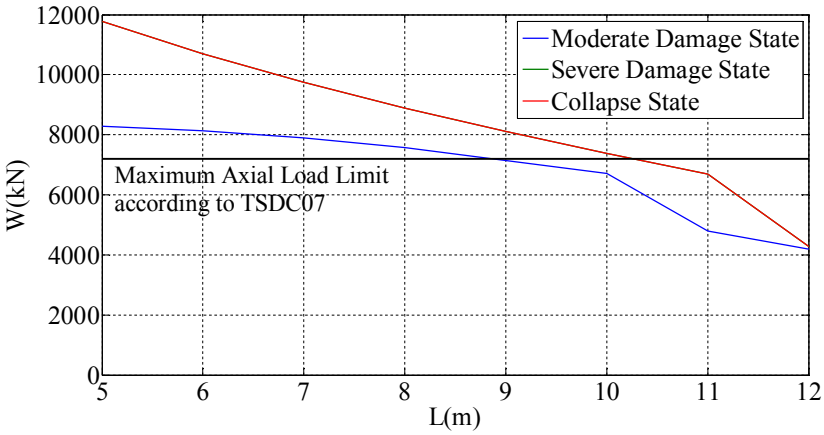

Table B.13. Structural loss estimation curves for the single-storey reinforced concrete industrial buildings which are located at 4th Earthquake Zone and Z1 Soil Class (cont.).

Cross-Section (cm)	Reinforcement Ratio	Structural Loss Estimation Curves
80×80	Minimum	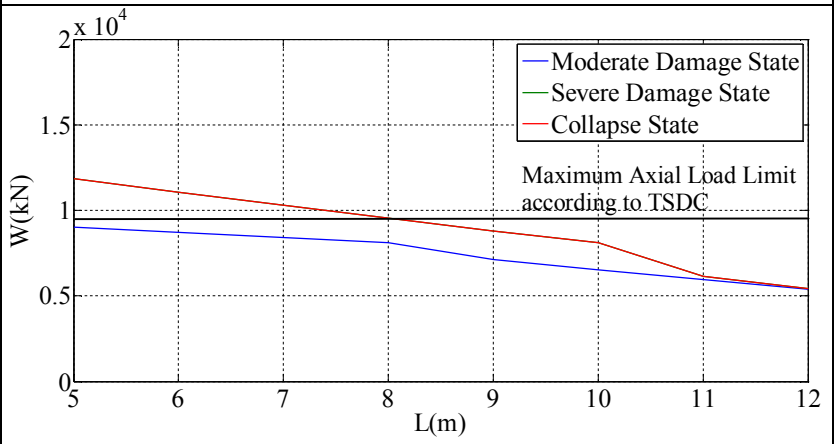
	Moderate	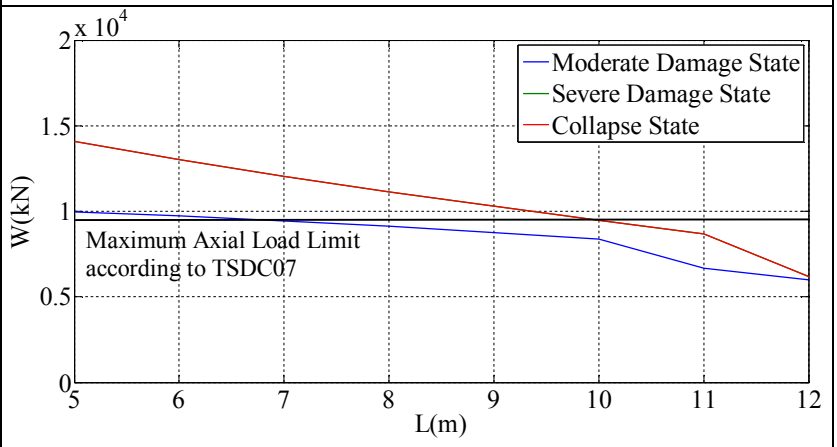
	High	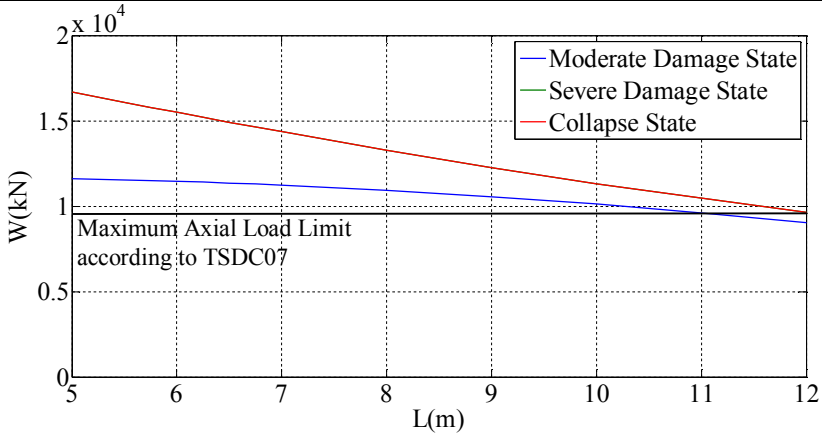

Table B.14. Structural loss estimation curves for the single-storey reinforced concrete industrial buildings which are located at 4th Earthquake Zone and Z2 Soil Class.

Cross-Section (cm)	Reinforcement Ratio	Structural Loss Estimation Curves
35×35	Minimum	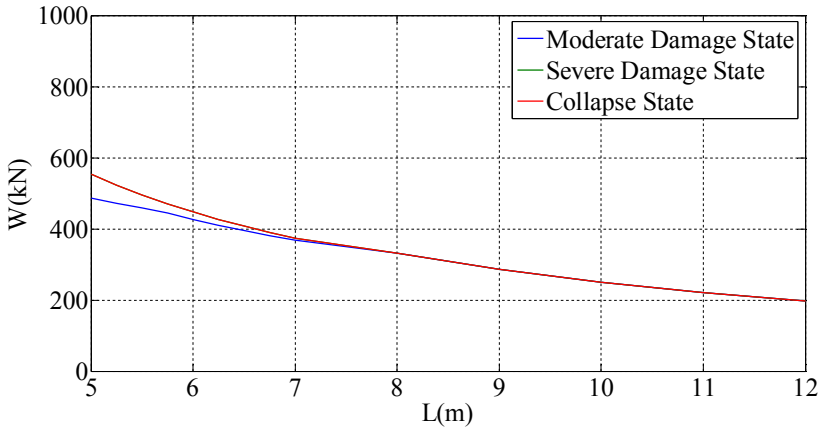
	Moderate	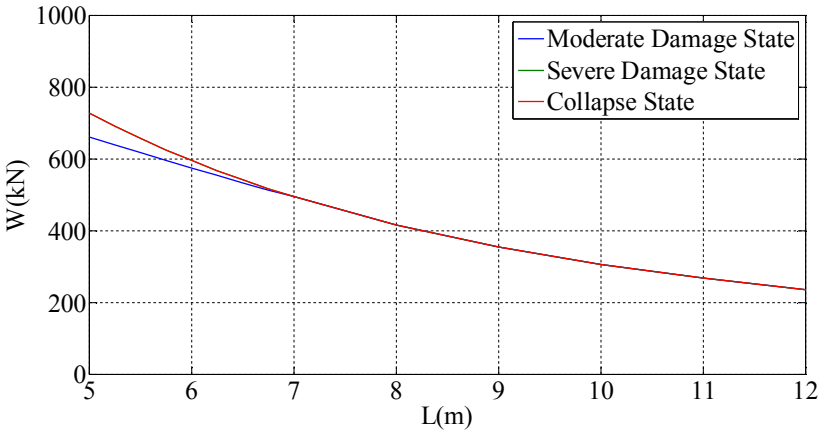
	High	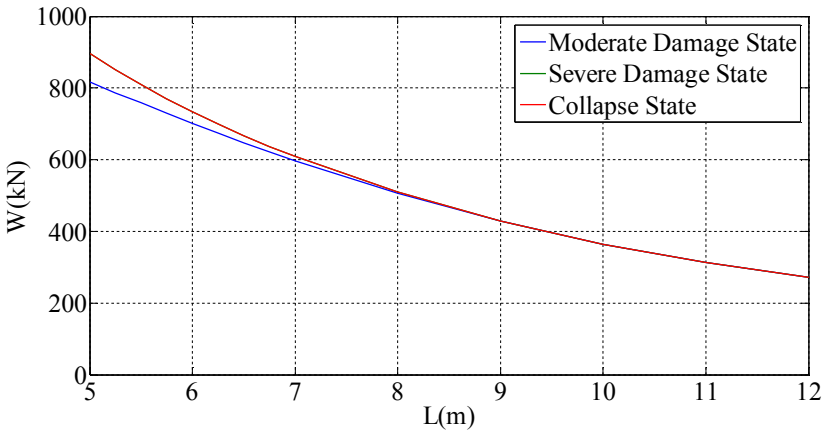

Table B.14. Structural loss estimation curves for the single-storey reinforced concrete industrial buildings which are located at 4th Earthquake Zone and Z2 Soil Class (cont.).

Cross-Section (cm)	Reinforcement Ratio	Structural Loss Estimation Curves
40×40	Minimum	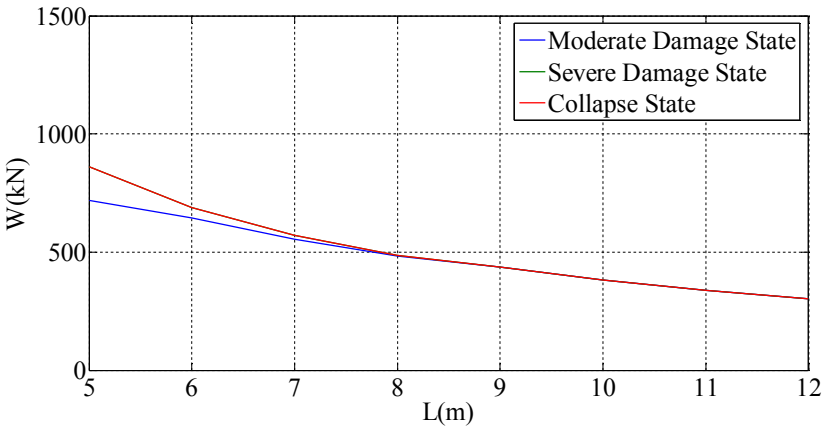
	Moderate	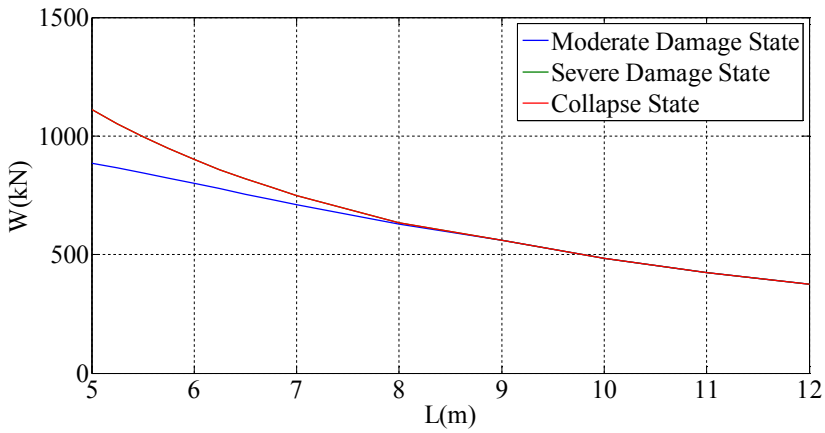
	High	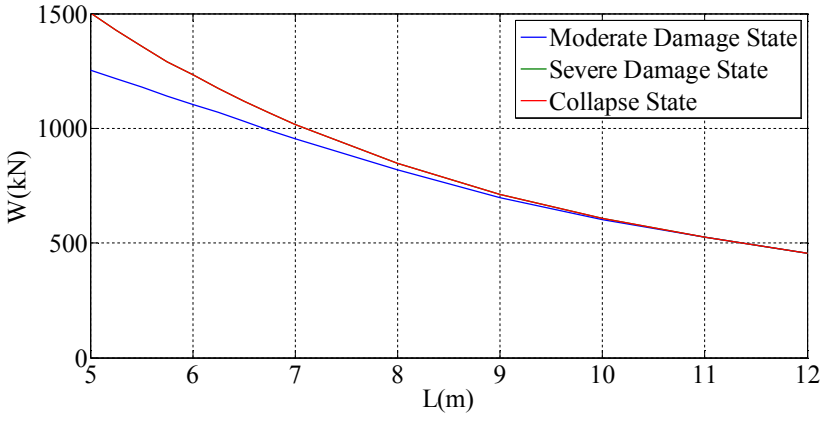

Table B.14. Structural loss estimation curves for the single-storey reinforced concrete industrial buildings which are located at 4th Earthquake Zone and Z2 Soil Class (cont.).

Cross-Section (cm)	Reinforcement Ratio	Structural Loss Estimation Curves
45×45	Minimum	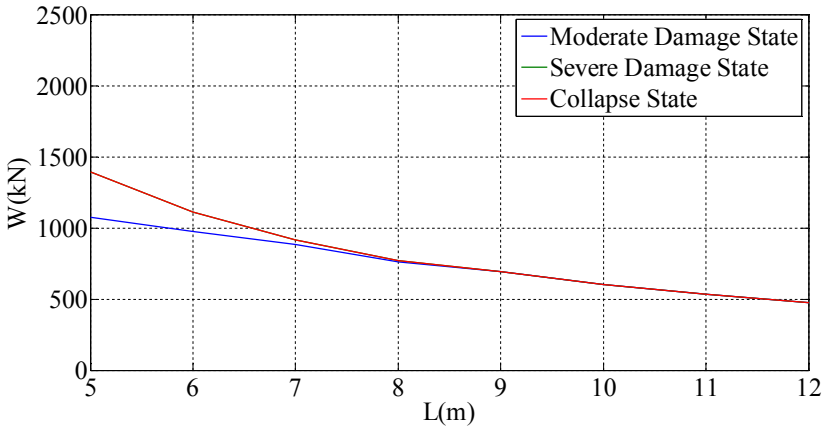
	Moderate	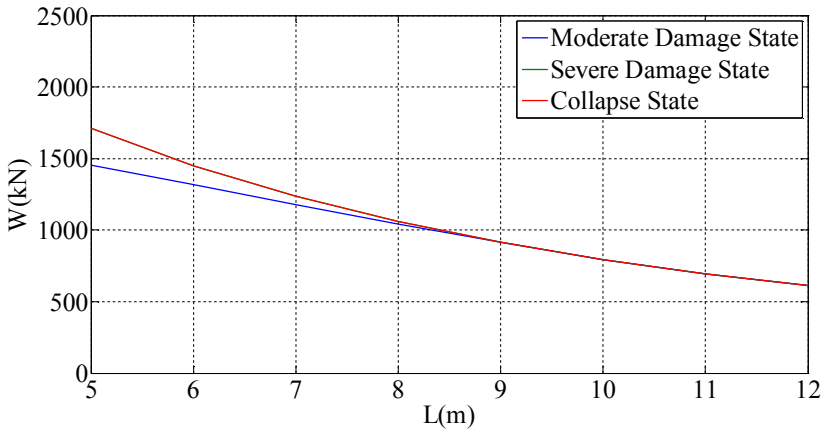
	High	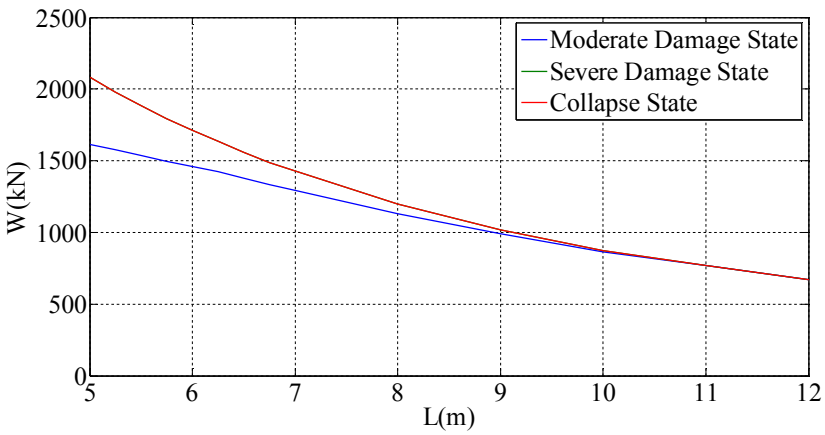

Table B.14. Structural loss estimation curves for the single-storey reinforced concrete industrial buildings which are located at 4th Earthquake Zone and Z2 Soil Class (cont.).

Cross-Section (cm)	Reinforcement Ratio	Structural Loss Estimation Curves
50×50	Minimum	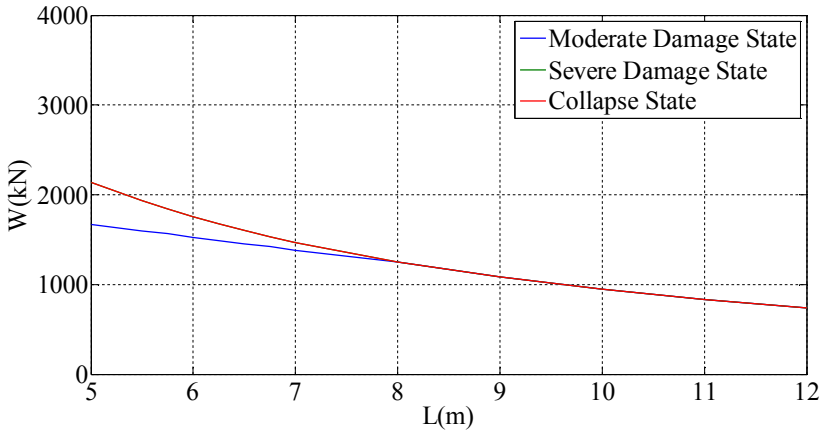
	Moderate	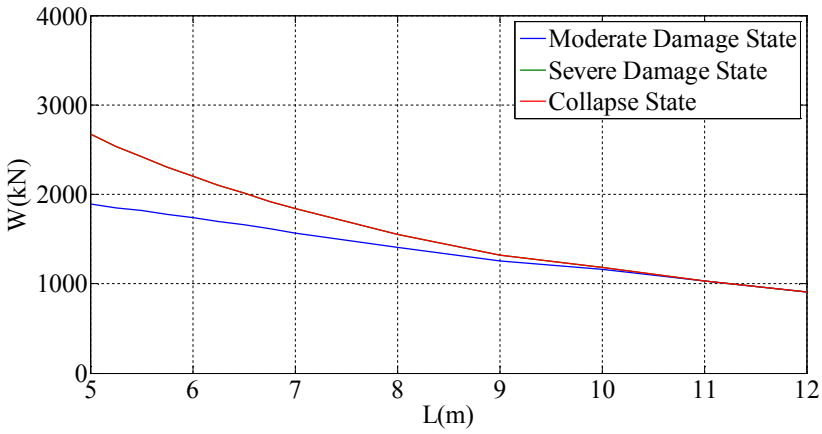
	High	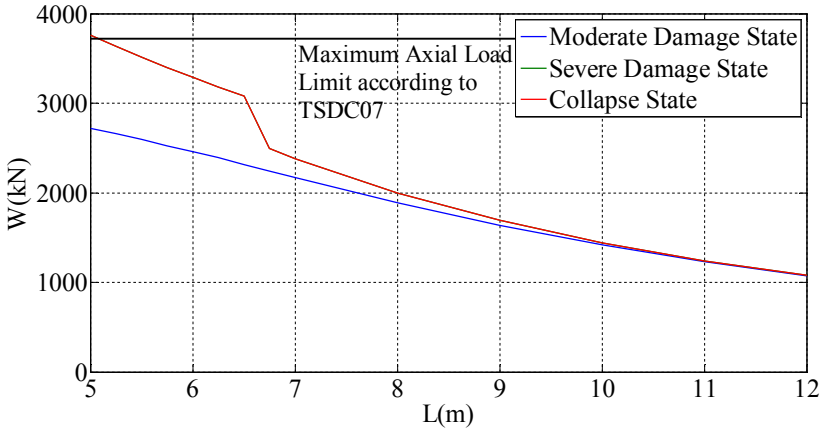

Table B.14. Structural loss estimation curves for the single-storey reinforced concrete industrial buildings which are located at 4th Earthquake Zone and Z2 Soil Class (cont.).

Cross-Section (cm)	Reinforcement Ratio	Structural Loss Estimation Curves
55×55	Minimum	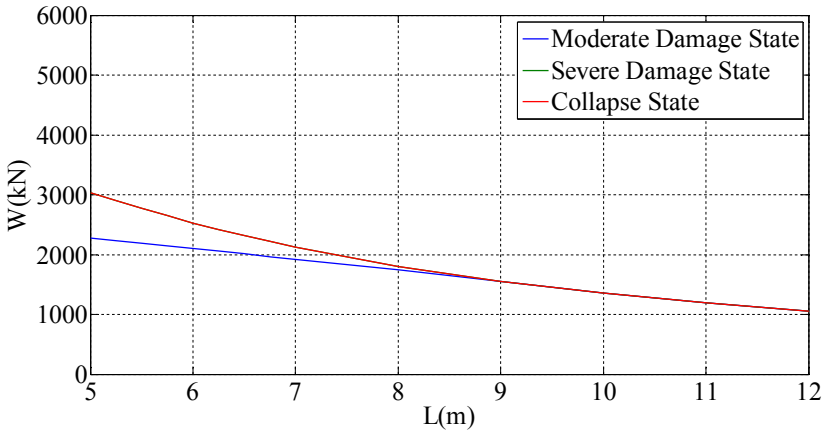
	Moderate	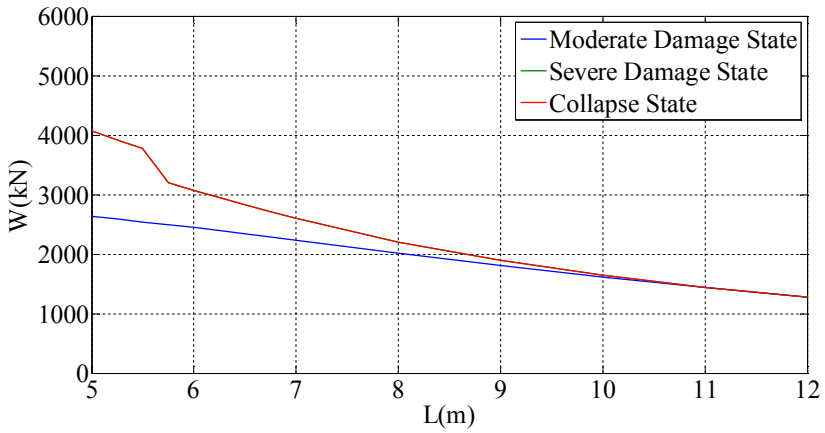
	High	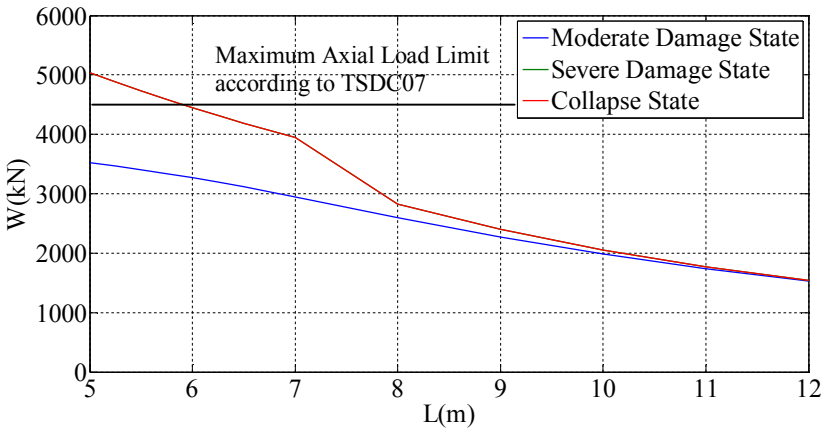

Table B.14. Structural loss estimation curves for the single-storey reinforced concrete industrial buildings which are located at 4th Earthquake Zone and Z2 Soil Class (cont.).

Cross-Section (cm)	Reinforcement Ratio	Structural Loss Estimation Curves
60×60	Minimum	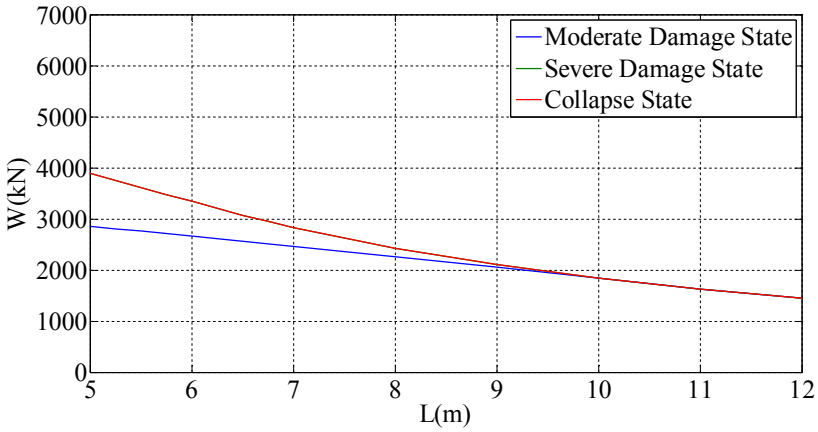
	Moderate	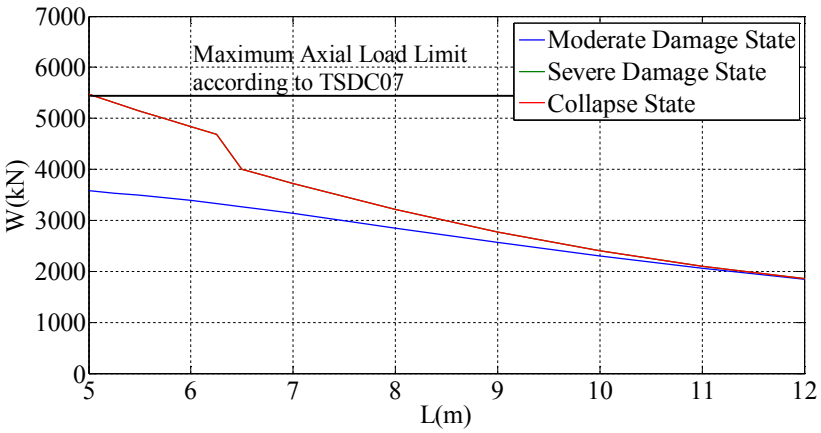
	High	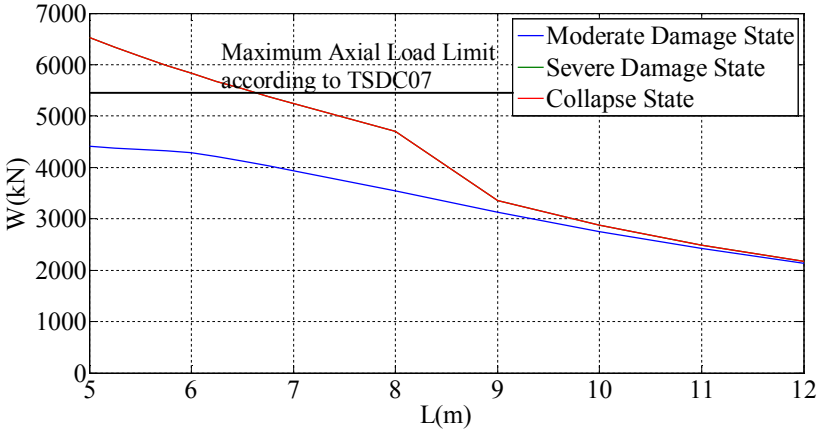

Table B.14. Structural loss estimation curves for the single-storey reinforced concrete industrial buildings which are located at 4th Earthquake Zone and Z2 Soil Class (cont.).

Cross-Section (cm)	Reinforcement Ratio	Structural Loss Estimation Curves
70×70	Minimum	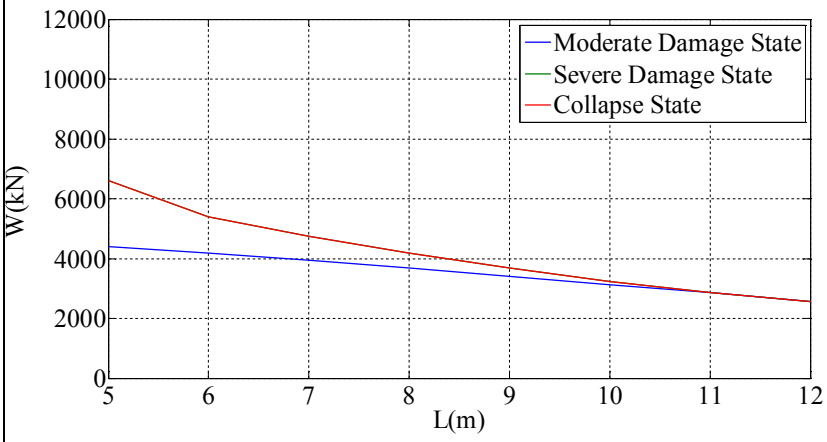
	Moderate	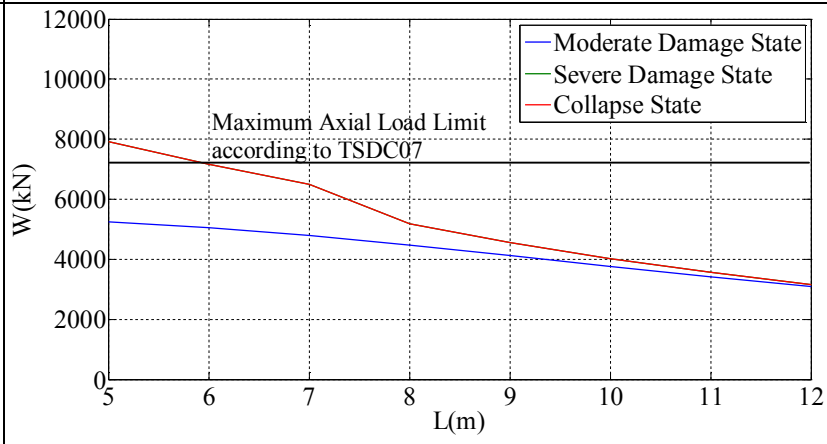
	High	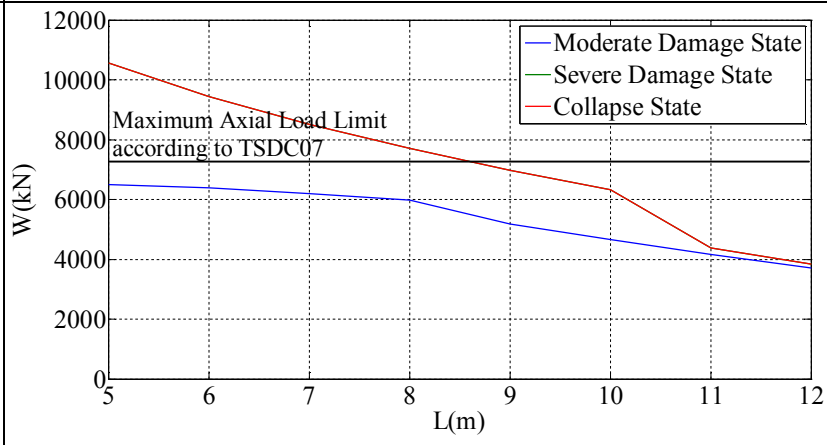

Table B.14. Structural loss estimation curves for the single-storey reinforced concrete industrial buildings which are located at 4th Earthquake Zone and Z2 Soil Class (cont.).

Cross-Section (cm)	Reinforcement Ratio	Structural Loss Estimation Curves
80×80	Minimum	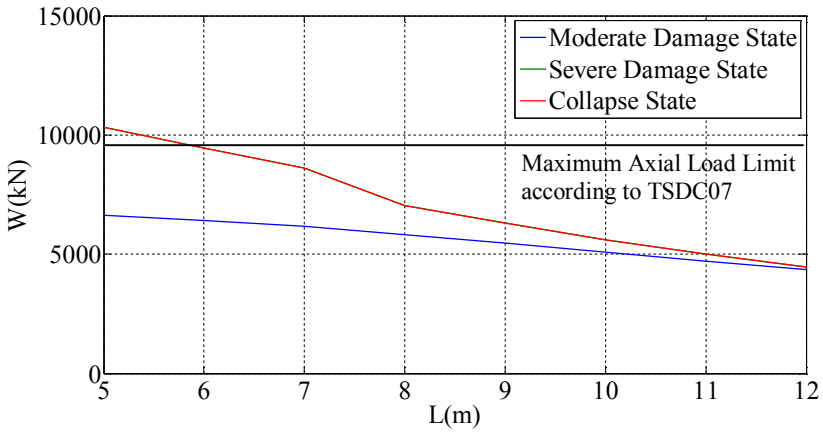
	Moderate	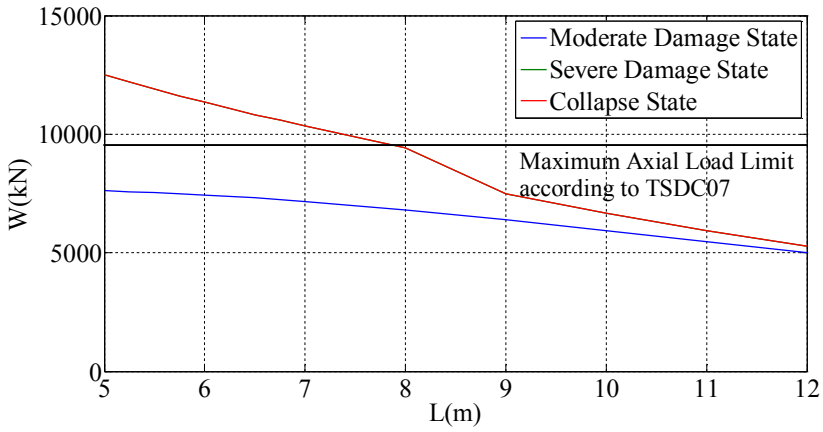
	High	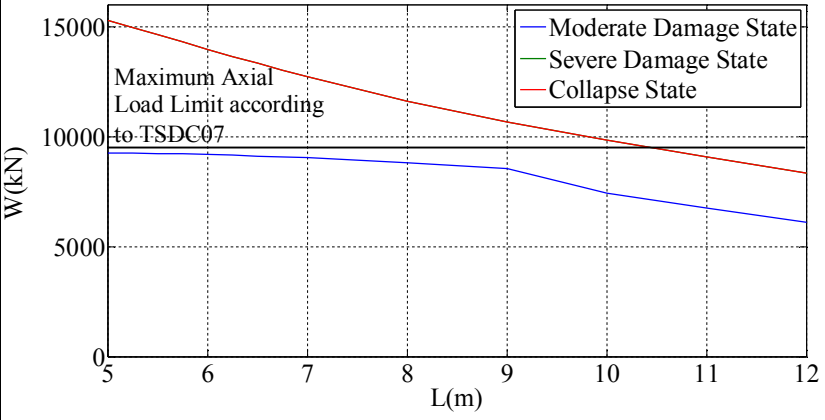

Table B.15. Structural loss estimation curves for the single-storey reinforced concrete industrial buildings which are located at 4th Earthquake Zone and Z3 Soil Class.

Cross-Section (cm)	Reinforcement Ratio	Structural Loss Estimation Curves
35×35	Minimum	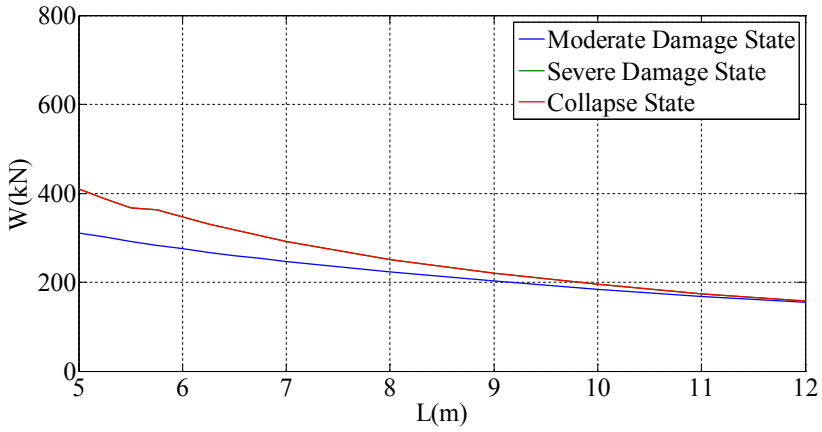
	Moderate	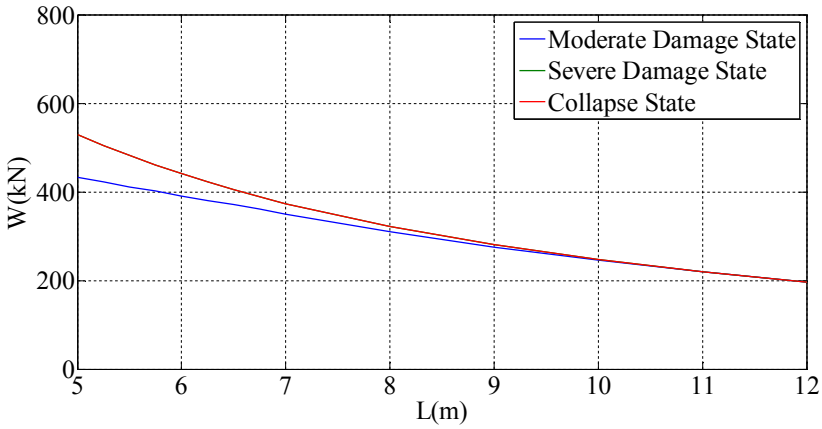
	High	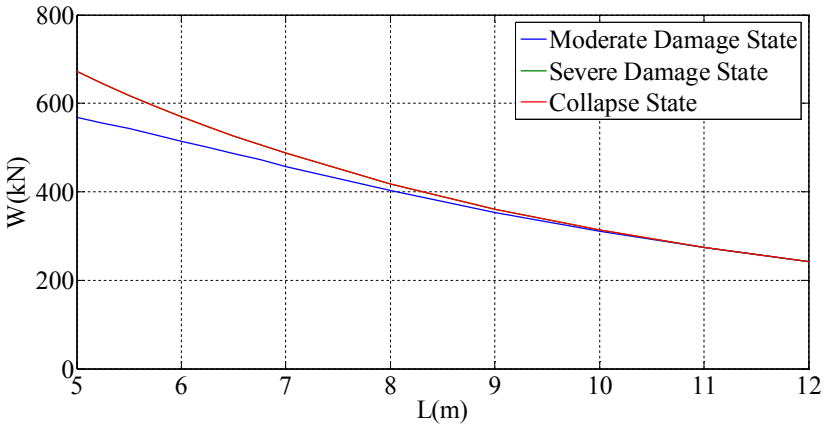

Table B.15. Structural loss estimation curves for the single-storey reinforced concrete industrial buildings which are located at 4th Earthquake Zone and Z3 Soil Class (cont.).

Cross-Section (cm)	Reinforcement Ratio	Structural Loss Estimation Curves
40×40	Minimum	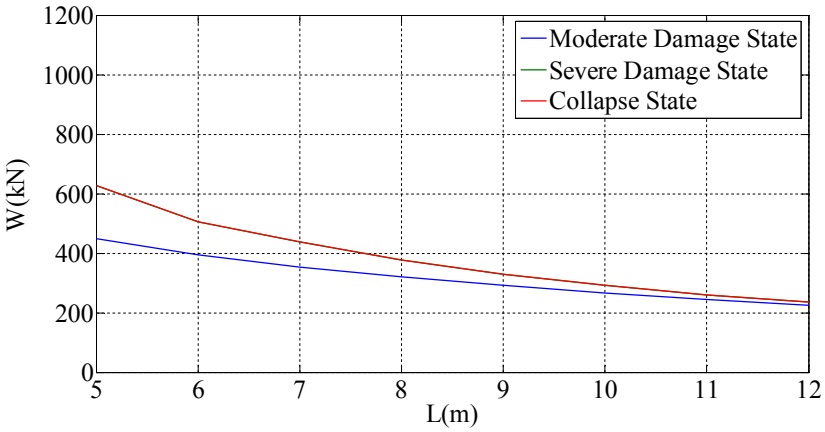
	Moderate	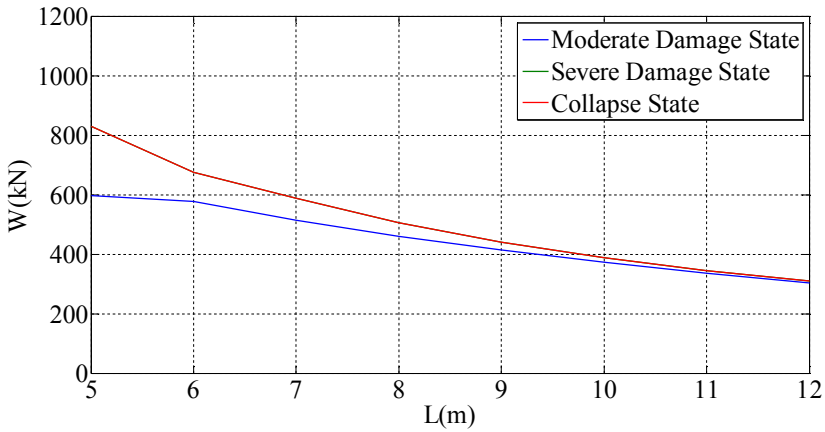
	High	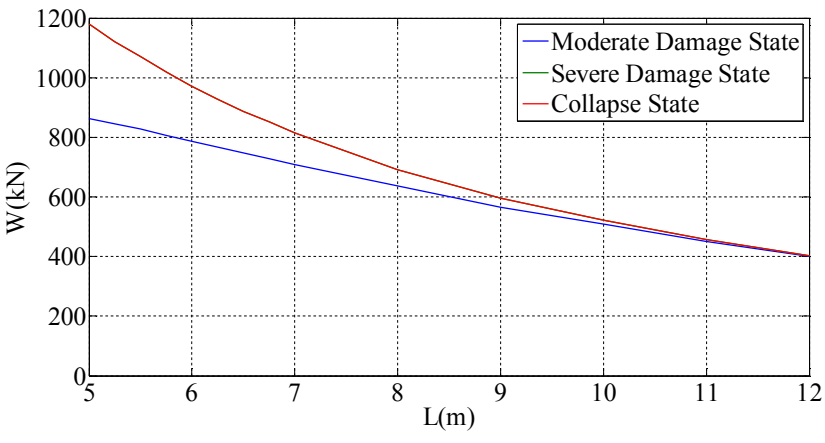

Table B.15. Structural loss estimation curves for the single-storey reinforced concrete industrial buildings which are located at 4th Earthquake Zone and Z3 Soil Class (cont.).

Cross-Section (cm)	Reinforcement Ratio	Structural Loss Estimation Curves
45×45	Minimum	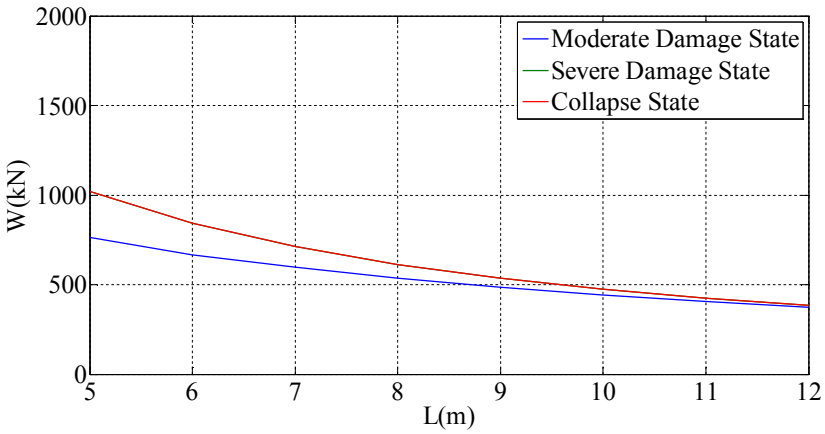
	Moderate	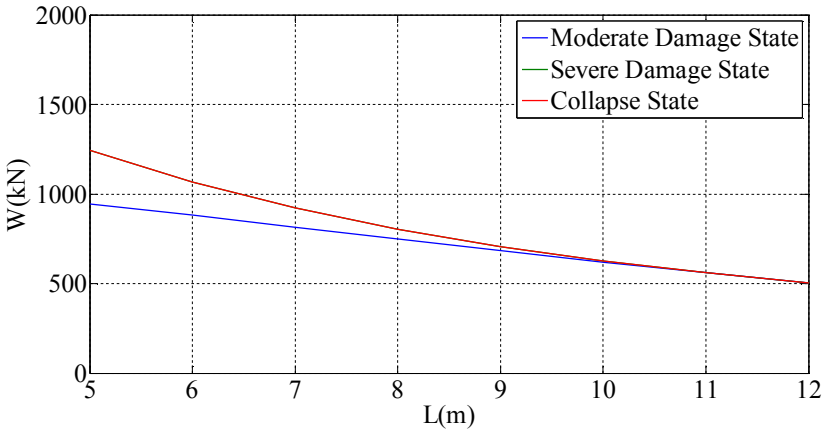
	High	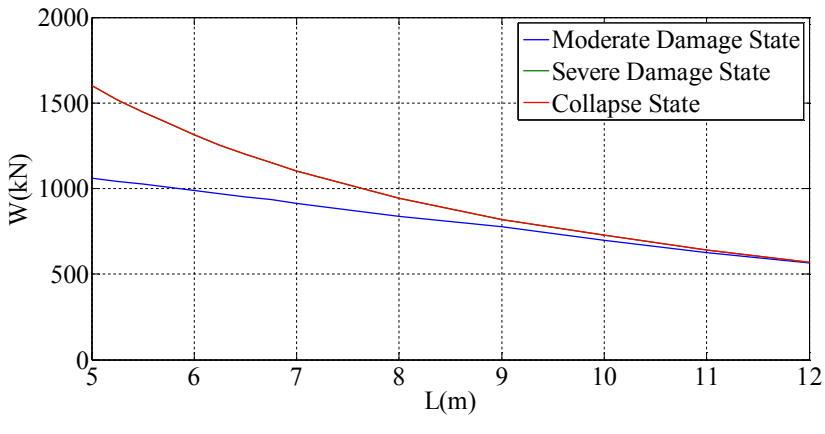

Table B.15. Structural loss estimation curves for the single-storey reinforced concrete industrial buildings which are located at 4th Earthquake Zone and Z3 Soil Class (cont.).

Cross-Section (cm)	Reinforcement Ratio	Structural Loss Estimation Curves
50×50	Minimum	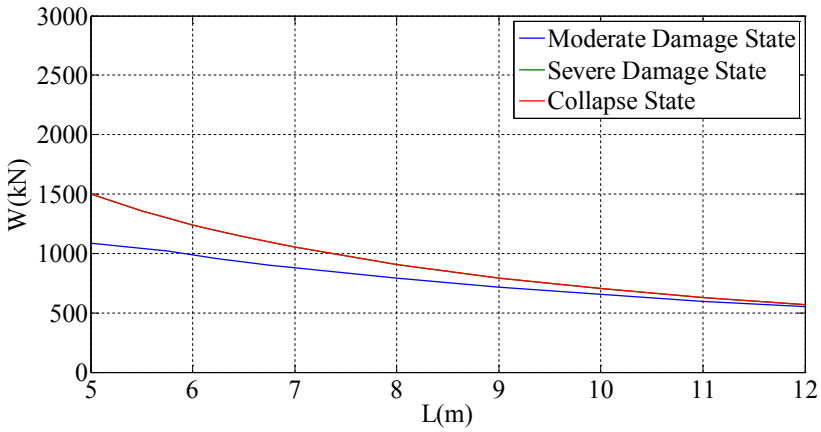
	Moderate	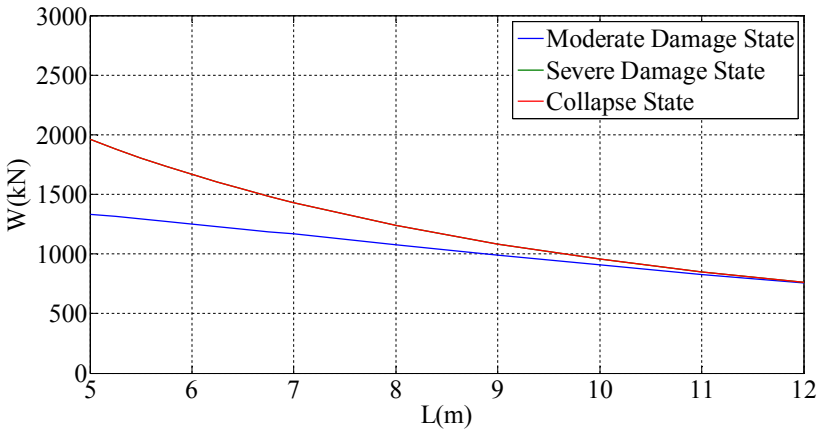
	High	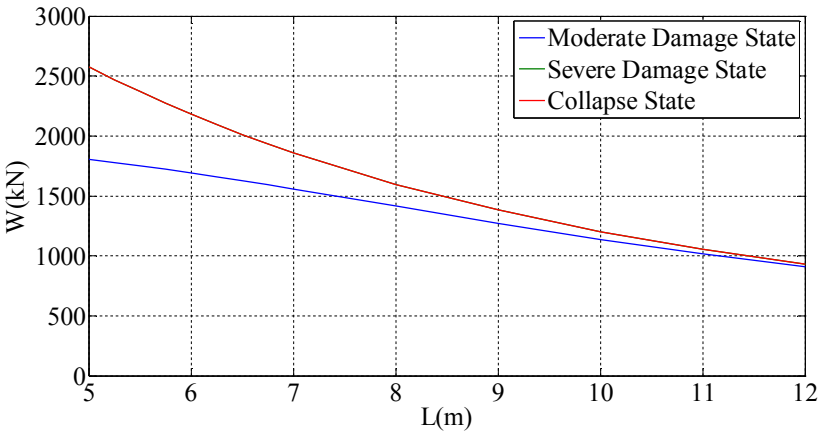

Table B.15. Structural loss estimation curves for the single-storey reinforced concrete industrial buildings which are located at 4th Earthquake Zone and Z3 Soil Class (cont.).

Cross-Section (cm)	Reinforcement Ratio	Structural Loss Estimation Curves
55×55	Minimum	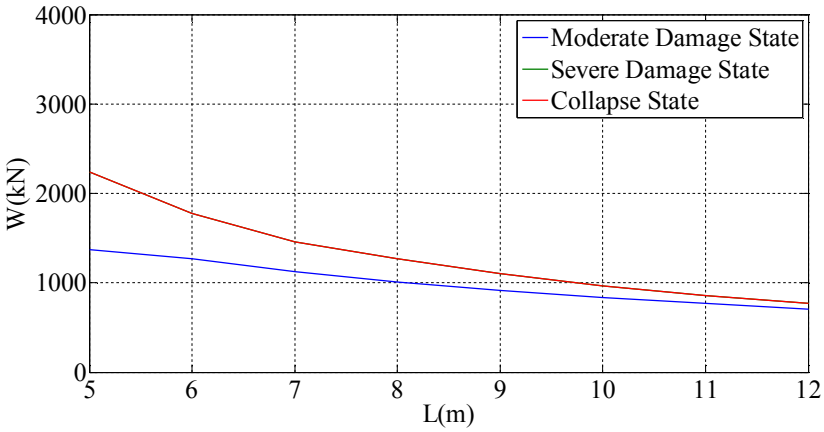
	Moderate	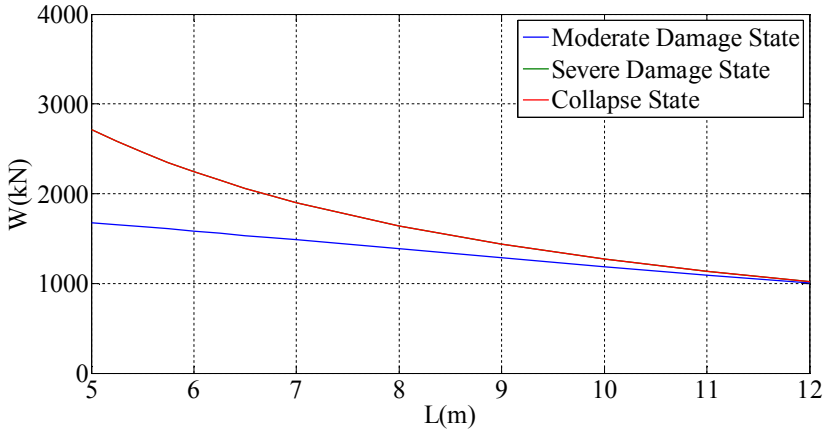
	High	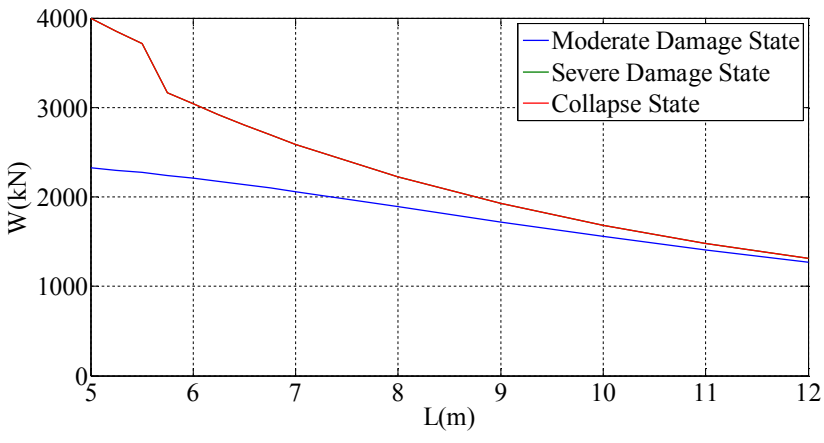

Table B.15. Structural loss estimation curves for the single-storey reinforced concrete industrial buildings which are located at 4th Earthquake Zone and Z3 Soil Class (cont.).

Cross-Section (cm)	Reinforcement Ratio	Structural Loss Estimation Curves
60×60	Minimum	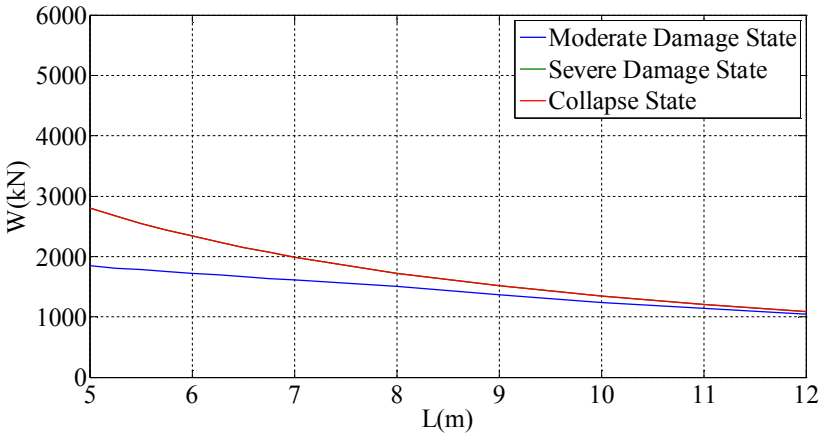
	Moderate	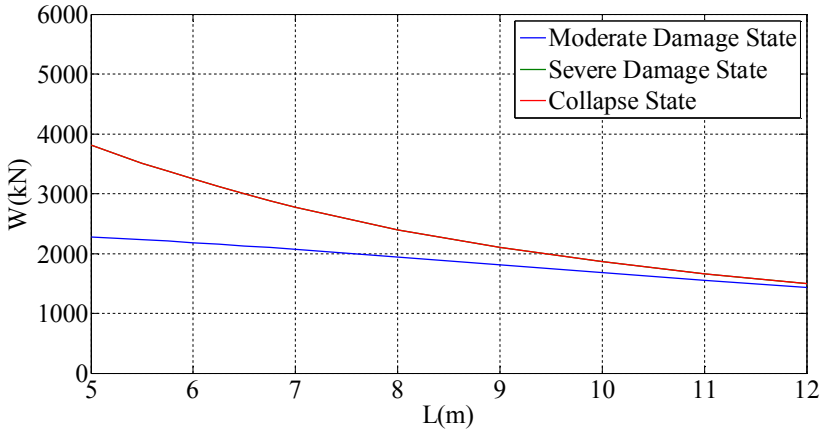
	High	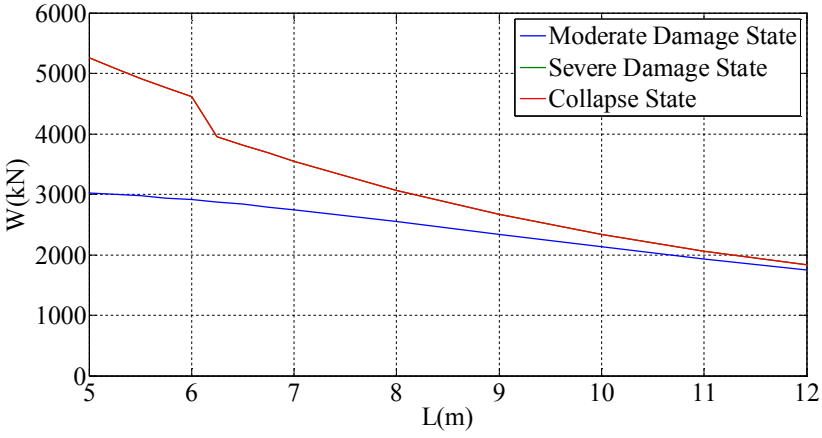

Table B.15. Structural loss estimation curves for the single-storey reinforced concrete industrial buildings which are located at 4th Earthquake Zone and Z3 Soil Class (cont.).

Cross-Section (cm)	Reinforcement Ratio	Structural Loss Estimation Curves
70×70	Minimum	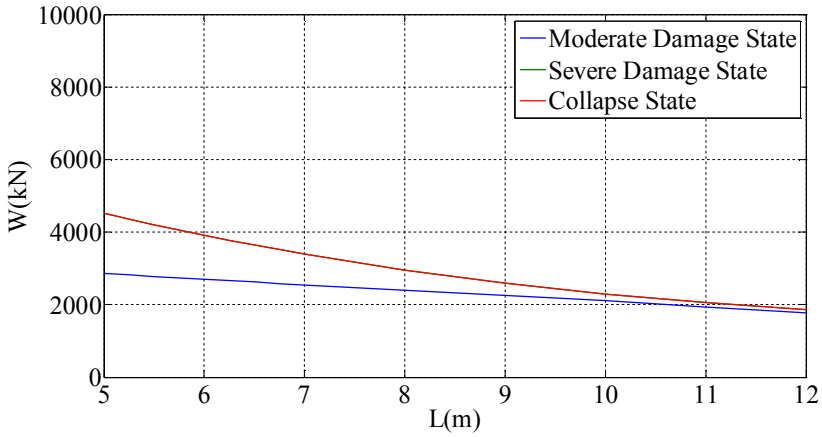
	Moderate	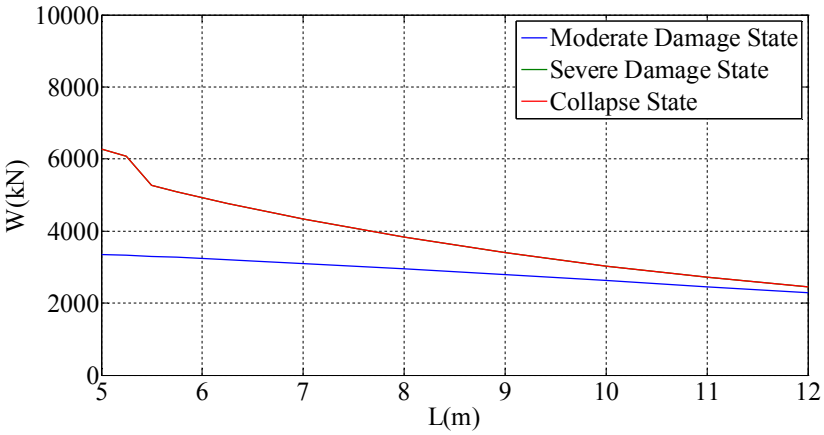
	High	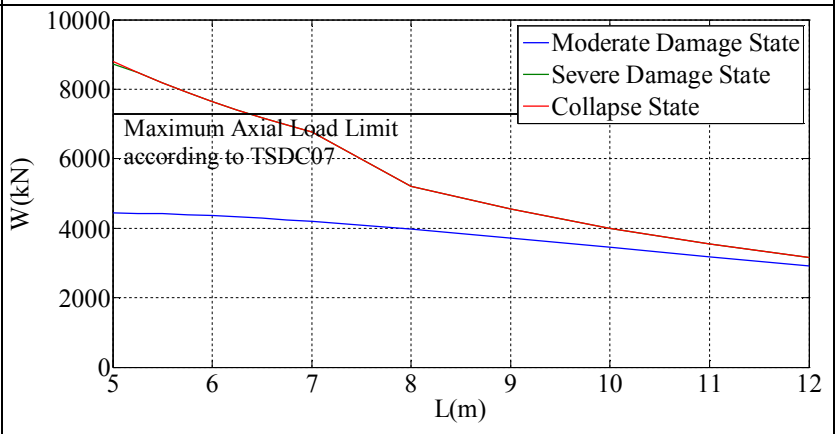

Table B.15. Structural loss estimation curves for the single-storey reinforced concrete industrial buildings which are located at 4th Earthquake Zone and Z3 Soil Class (cont.).

Cross-Section (cm)	Reinforcement Ratio	Structural Loss Estimation Curves
80×80	Minimum	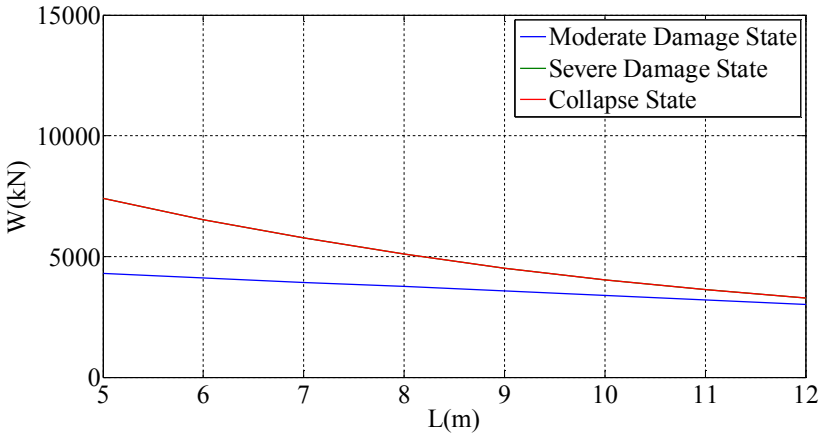
	Moderate	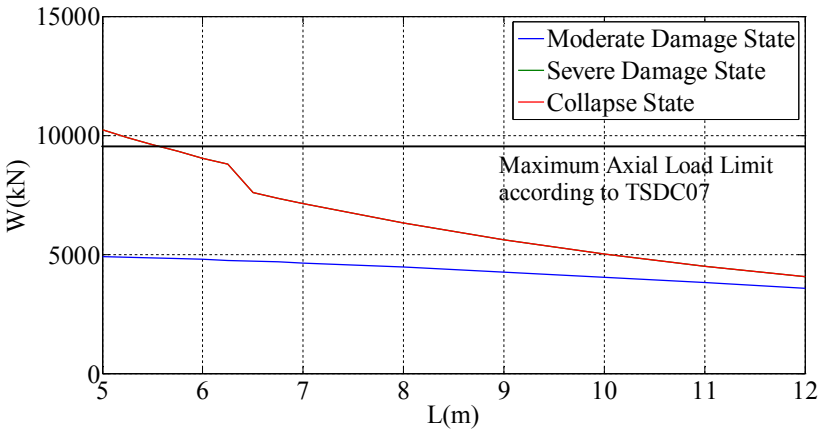
	High	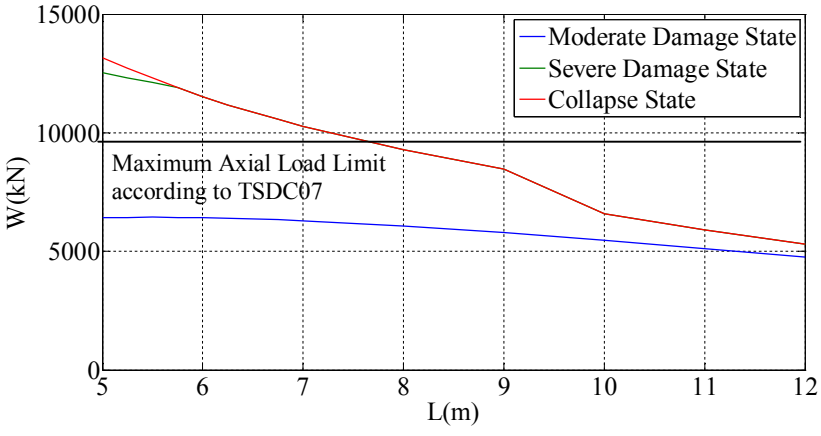

Table B.16. Structural loss estimation curves for the single-storey reinforced concrete industrial buildings which are located at 4th Earthquake Zone and Z4 Soil Class.

Cross-Section (cm)	Reinforcement Ratio	Structural Loss Estimation Curves
35×35	Minimum	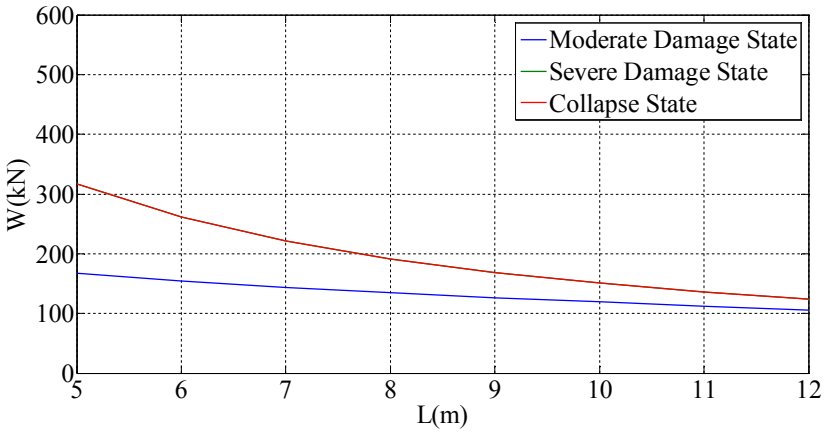
	Moderate	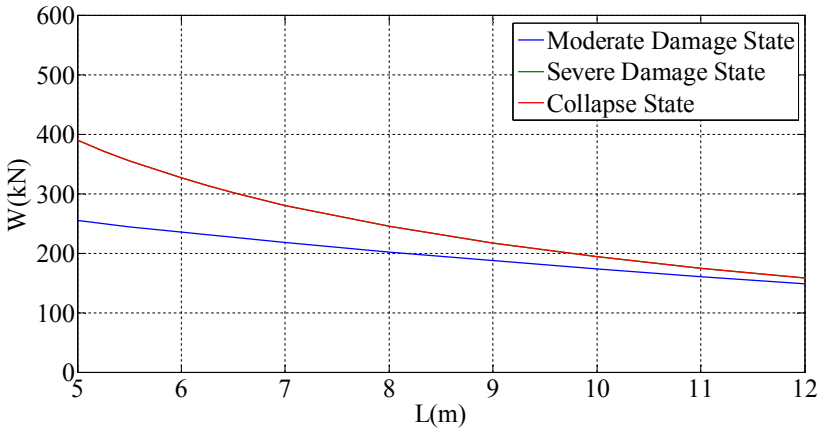
	High	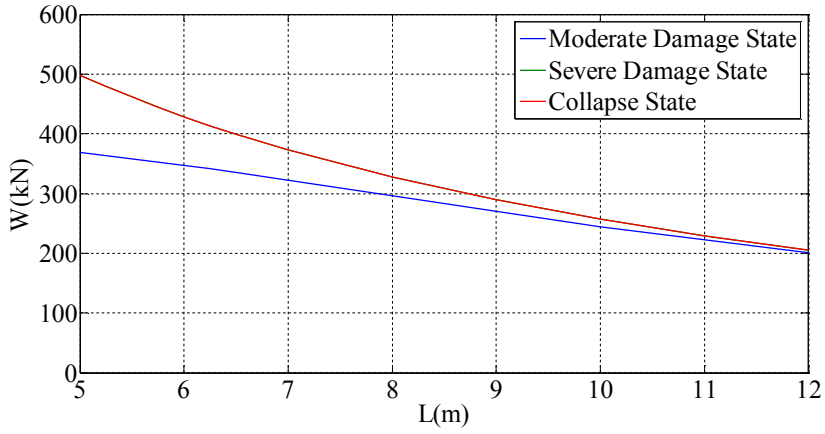

Table B.16. Structural loss estimation curves for the single-storey reinforced concrete industrial buildings which are located at 4th Earthquake Zone and Z4 Soil Class (cont.).

Cross-Section (cm)	Reinforcement Ratio	Structural Loss Estimation Curves
40×40	Minimum	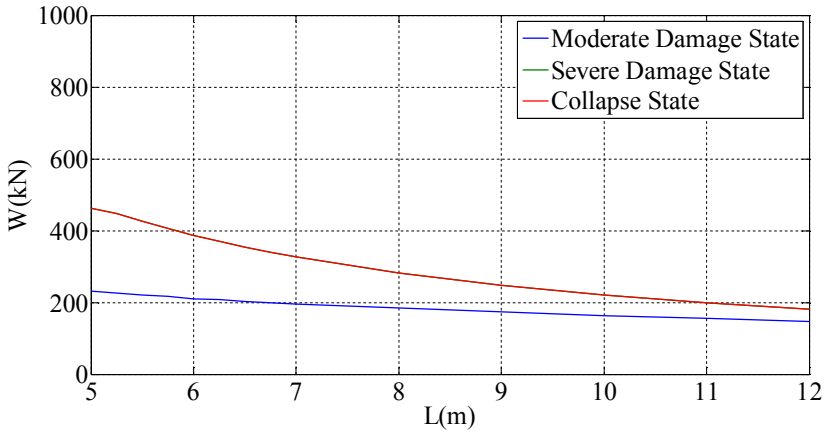
	Moderate	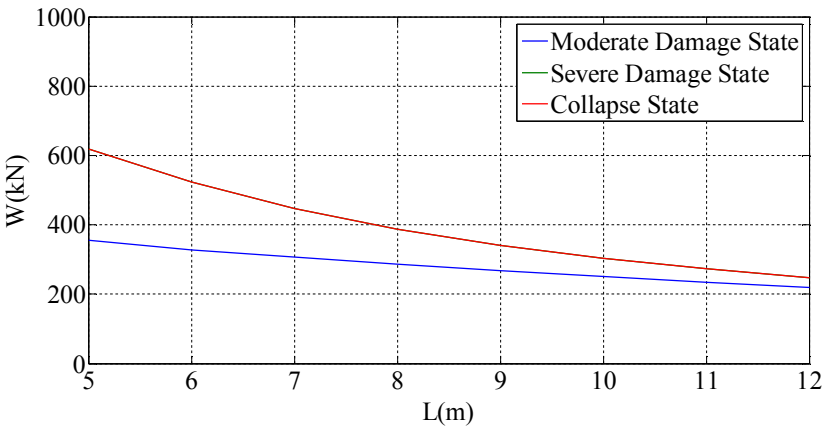
	High	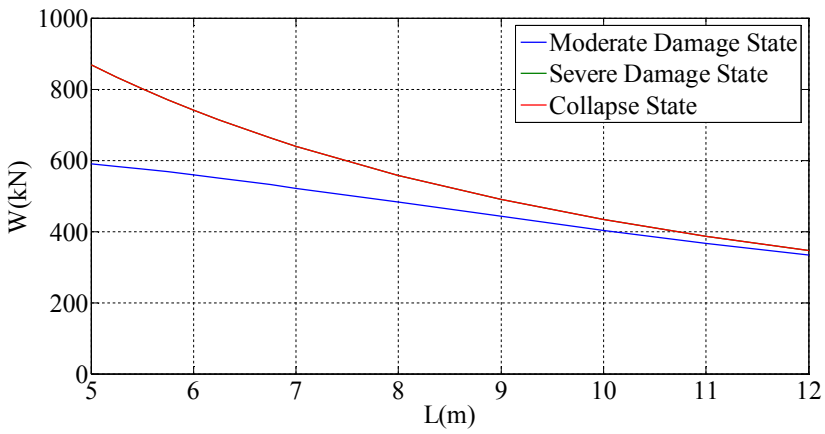

Table B.16. Structural loss estimation curves for the single-storey reinforced concrete industrial buildings which are located at 4th Earthquake Zone and Z4 Soil Class (cont.).

Cross-Section (cm)	Reinforcement Ratio	Structural Loss Estimation Curves
45×45	Minimum	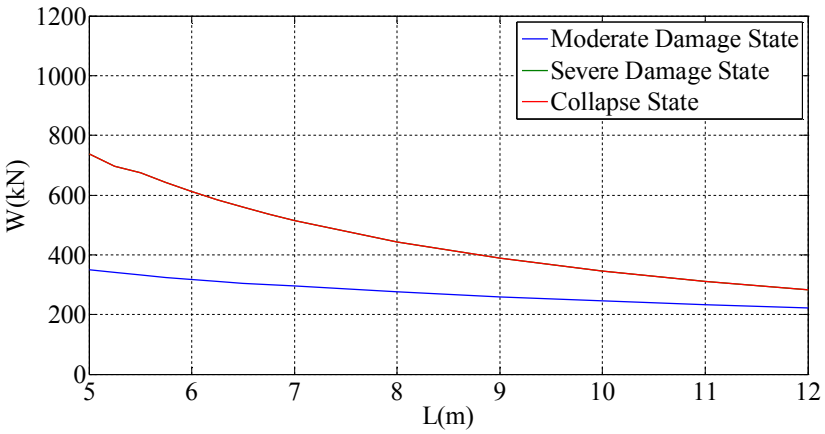
	Moderate	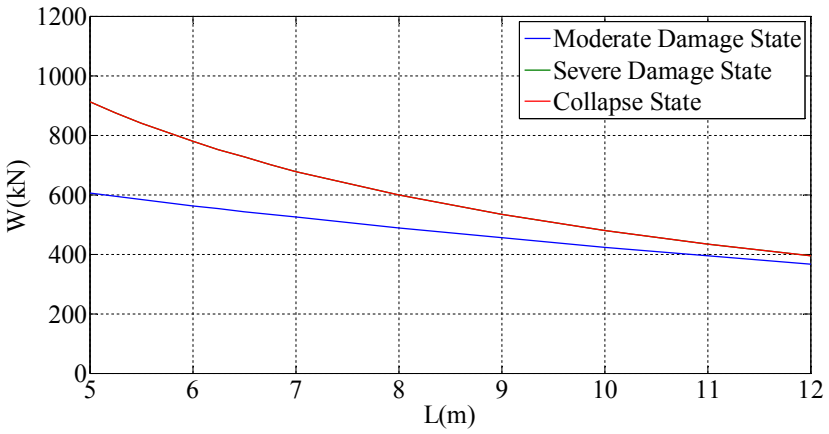
	High	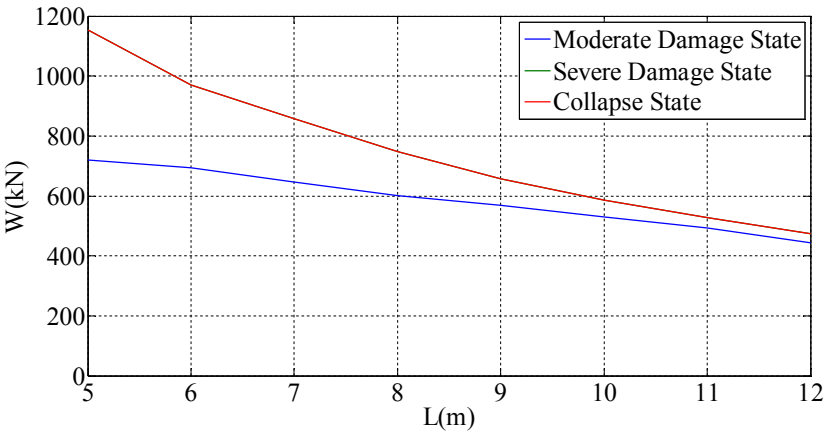

Table B.16. Structural loss estimation curves for the single-storey reinforced concrete industrial buildings which are located at 4th Earthquake Zone and Z4 Soil Class (cont.).

Cross-Section (cm)	Reinforcement Ratio	Structural Loss Estimation Curves
50×50	Minimum	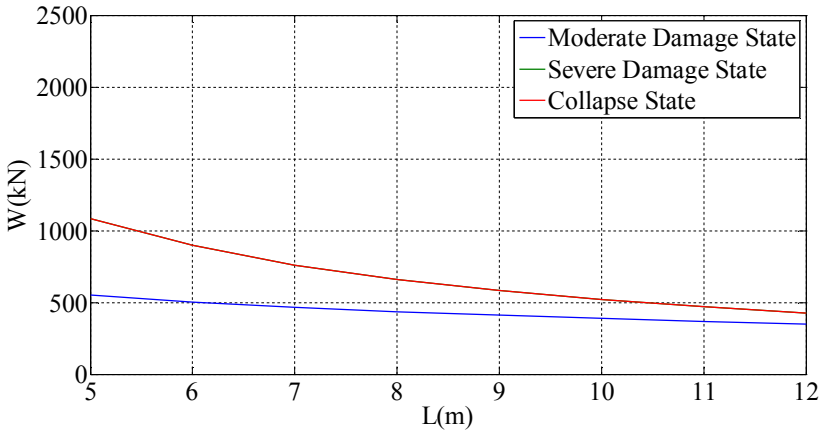
	Moderate	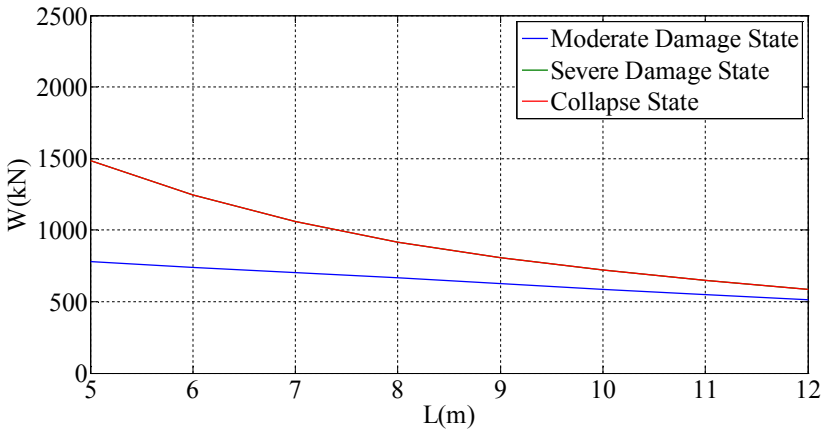
	High	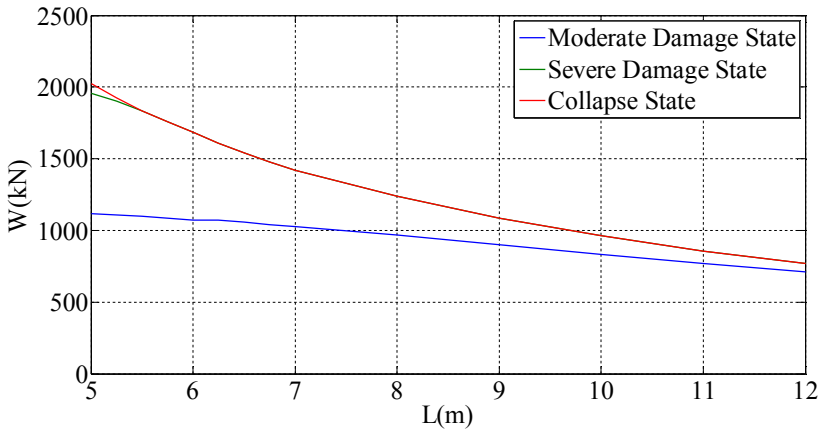

Table B.16. Structural loss estimation curves for the single-storey reinforced concrete industrial buildings which are located at 4th Earthquake Zone and Z4 Soil Class (cont.).

Cross-Section (cm)	Reinforcement Ratio	Structural Loss Estimation Curves
55×55	Minimum	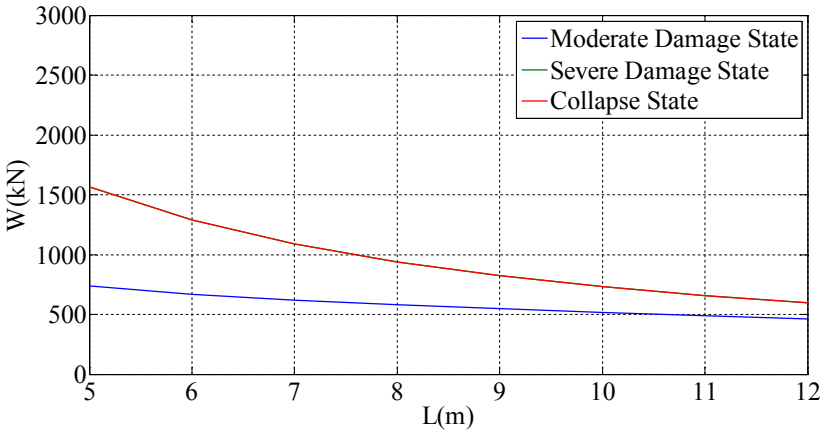
	Moderate	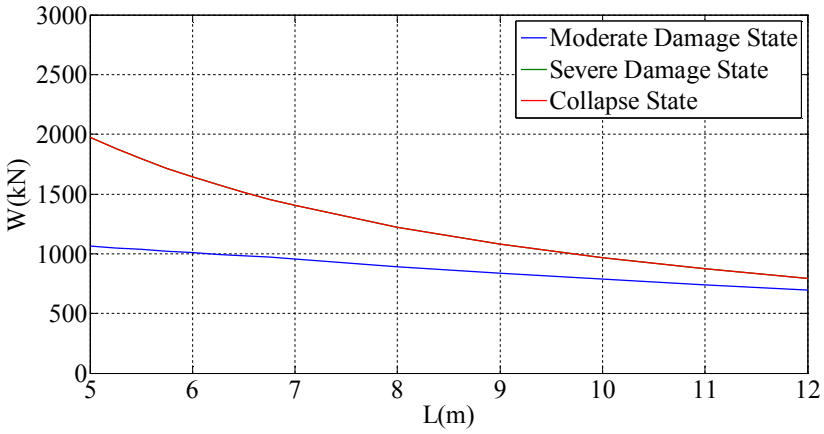
	High	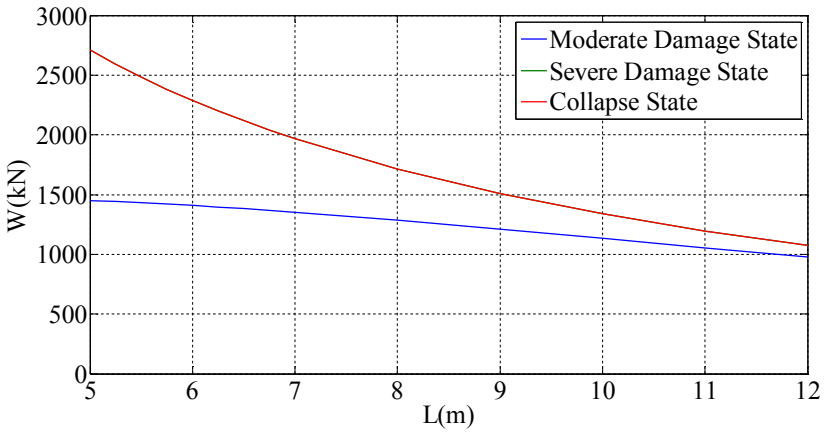

Table B.16. Structural loss estimation curves for the single-storey reinforced concrete industrial buildings which are located at 4th Earthquake Zone and Z4 Soil Class (cont.).

Cross-Section (cm)	Reinforcement Ratio	Structural Loss Estimation Curves
60×60	Minimum	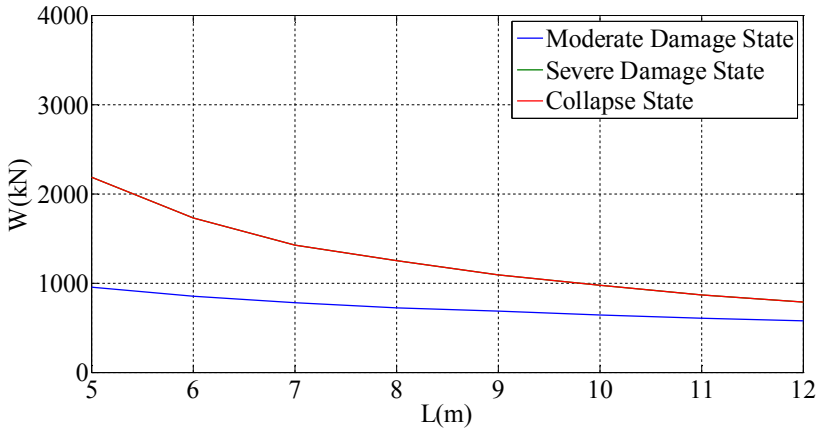
	Moderate	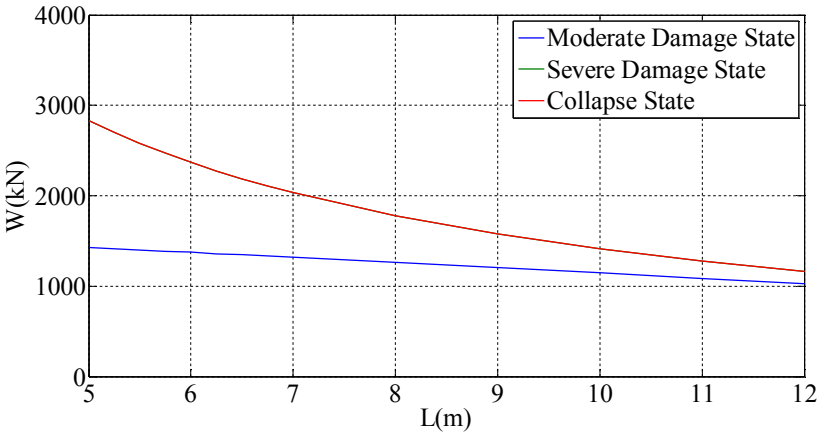
	High	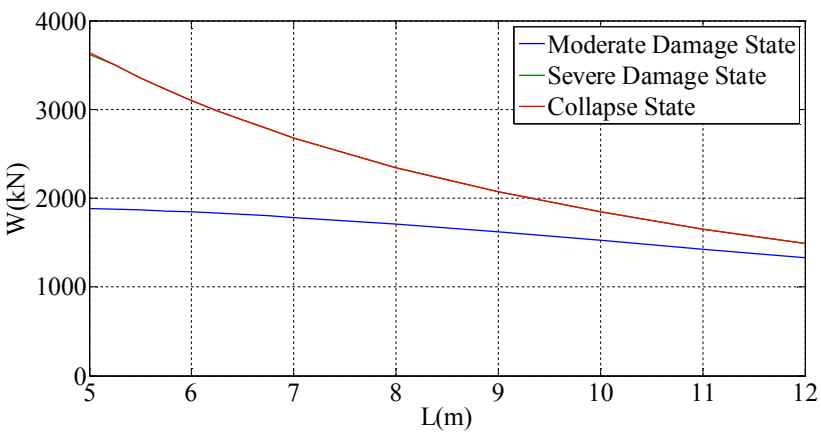

Table B.16. Structural loss estimation curves for the single-storey reinforced concrete industrial buildings which are located at 4th Earthquake Zone and Z4 Soil Class (cont.).

Cross-Section (cm)	Reinforcement Ratio	Structural Loss Estimation Curves
70×70	Minimum	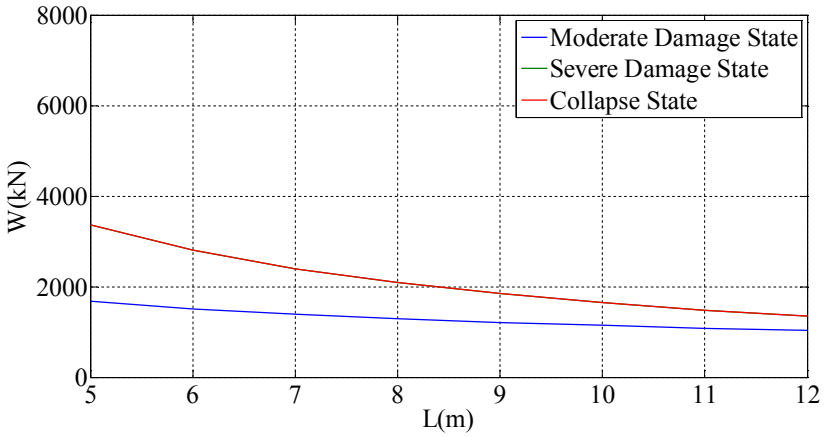
	Moderate	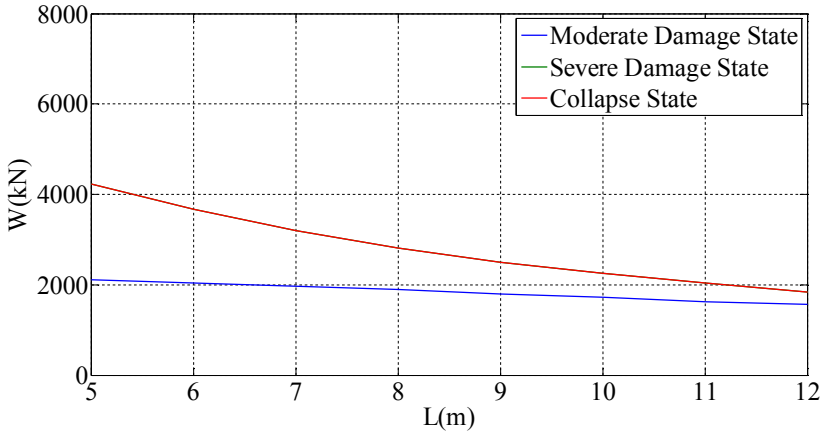
	High	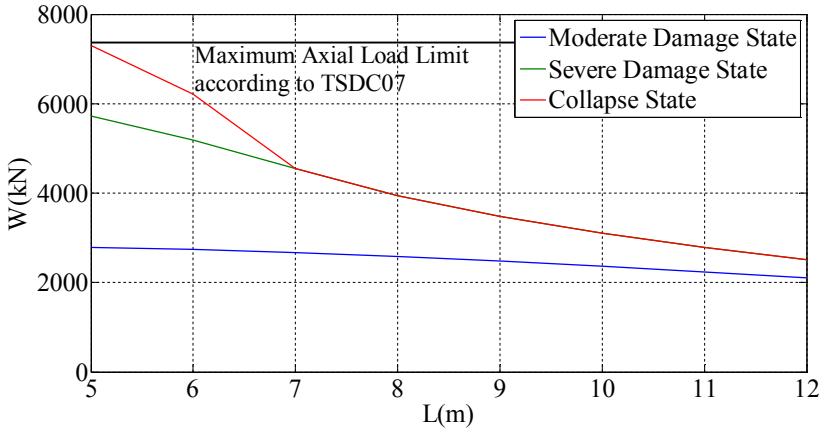

Table B.16. Structural loss estimation curves for the single-storey reinforced concrete industrial buildings which are located at 4th Earthquake Zone and Z4 Soil Class (cont.).

Cross-Section (cm)	Reinforcement Ratio	Structural Loss Estimation Curves
80×80	Minimum	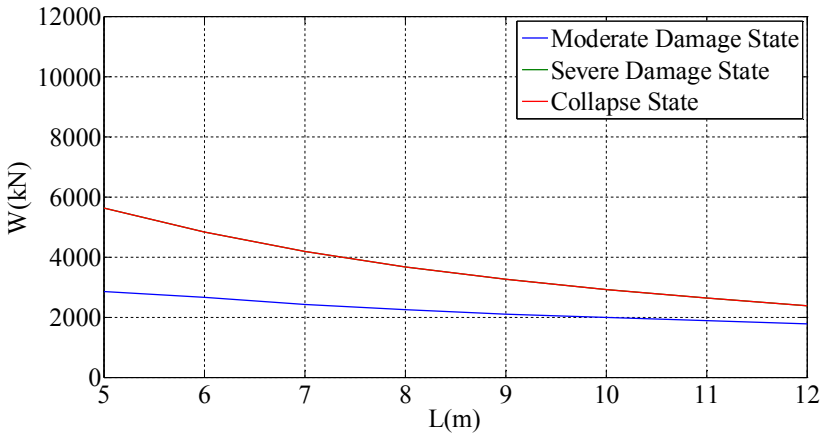
	Moderate	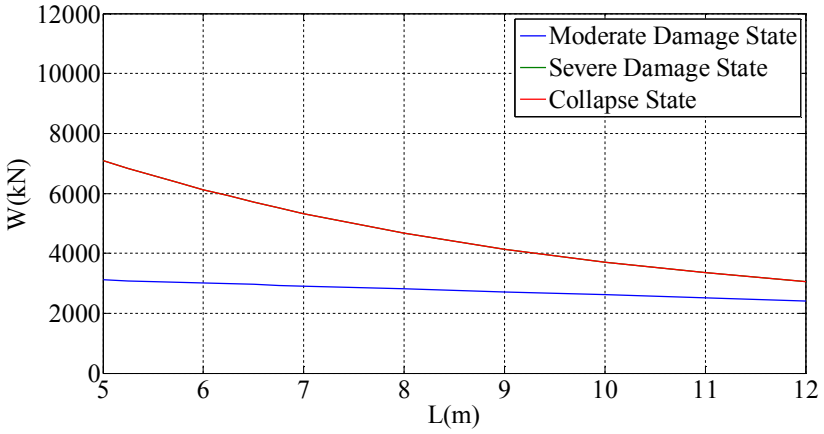
	High	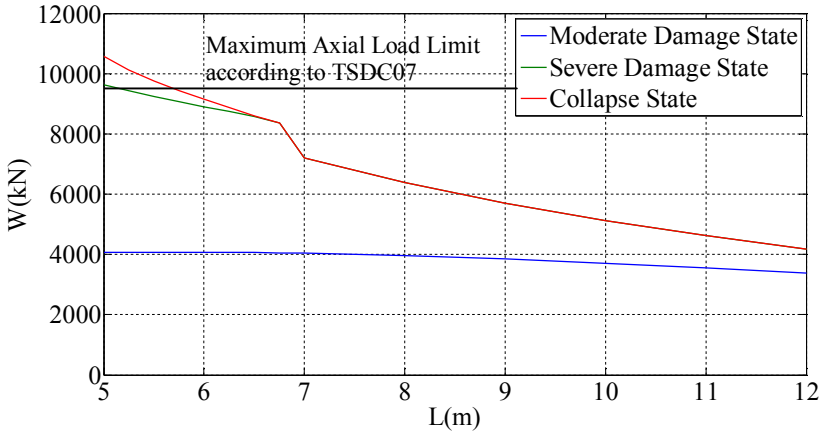

APPENDIX C: STRUCTURAL INFORMATION DATA CHARTS FOR THE BUILDING INVENTORY

In the following Data Charts, structural properties and also the axial loads calculated for the each industrial building within the inventory, were summarized.

Table C.1. Axial load calculation data chart for different reinforced concrete industrial buildings of which the structural properties were estimated during the site surveys.

Str.	Column Cross-Section	Span Length (m)	Axis Distance (m)	Height (m)	Roof Type			Axial Load (kN)
1	60 × 60 cm (ρ=1%) Reinforced Concrete Column	14 (>2)	11	6	Steel Beam (-I-) IPE 550	Steel Purlin	Sandwich Panel (Rock-wool insulation)	89
2	60 × 60 cm (ρ= unknown) Precast Column	18 (>2)	10	9	Pre-cast Beam	Pre-cast Purlin	Sandwich Panel (Rock-wool insulation)	286
3	80 × 80 cm (ρ= unknown) Reinforced Concrete Column	24 (>2)	18	7.5	Steel Space Truss System		Sandwich Panel (Rock-wool insulation)	214
4	60 × 60 cm (ρ= unknown) Reinforced Concrete Column	20 (>2)	10	9	Pre-cast Beam	Pre-cast Purlin	Sandwich Panel (Poly-urethane Isolation)	309
5	60 × 60 cm (ρ= unknown) Reinforced Concrete Column	24 (>2)	24	7.5	Steel Space Truss System		Metal Sheet (No Insulation)	168

Table C.1. Axial load calculation data chart for different reinforced concrete industrial buildings of which the structural properties were estimated during the site surveys (cont.).

Str.	Column Cross-Section	Span Length (m)	Axis Distance (m)	Height (m)	Roof Type			Axial Load (kN)
6	60 × 60 cm (ρ= unknown) Reinforced Concrete Column	24 (>2)	24	9	Steel Space Truss System		Metal Sheet (No Insulation)	175
7	70 × 70 cm (ρ= unknown) Reinforced Concrete Column	21 (>2)	21	7	Steel Space Truss System		Metal Sheet (No Insulation)	147
8	60 × 60 cm (ρ= unknown) Reinforced Concrete Column	37.5 (>2)	7.5	9	Steel Space Truss System		Metal Sheet (No Insulation)	107
9	40 × 40 cm (ρ= unknown) Reinforced Concrete Column	10 (>2)	5	6	Steel Space Truss System		Metal Sheet (No Insulation)	24
10	50 × 50 cm (ρ= unknown) Reinforced Concrete Column	12 (>2)	6	5	Steel Space Truss System		Metal Sheet (No Insulation)	33
11	45 × 45 cm (ρ= unknown) Precast Column	22 (>2)	7.5	7.5	Pre-cast Beam	Pre-cast Purlin	Sandwich Panel (Rock wool Isolation)	243
12	60 × 60 cm (ρ= unknown) Precast Column	20 (>2)	7.5	8.5	Pre-cast Beam	Pre-cast Purlin	Sandwich Panel (Rock wool Isolation)	226

Table C.1. Axial load calculation data chart for different reinforced concrete industrial buildings of which the structural properties were estimated during the site surveys (cont.).

Str.	Column Cross-Section	Span Length (m)	Axis Distance (m)	Height (m)	Roof Type			Axial Load (kN)
13	45 × 45 cm (ρ= unknown) Precast Column	17 (>2)	7.5	8.5	Pre-cast Beam	Pre-cast Purlin	Sandwich Panel (Rock wool Isolation)	184
14	45 × 45 cm (ρ= unknown) Precast Column	20 (>2)	8	8	Pre-cast Beam	Pre-cast Purlin	Sandwich Panel (Rock wool Isolation)	216
15	35 × 35 cm (ρ= unknown) Precast Column	20 (>2)	7.5	6	Pre-cast Beam	Pre-cast Purlin	Sandwich Panel (Rock wool Isolation)	196
16	40 × 40 cm (ρ= unknown) Precast Column	17 (>2)	7.5	6	Pre-cast Beam	Pre-cast Purlin	Sandwich Panel (Rock wool Isolation)	174
17	70 × 70 cm (ρ=1%) Reinforced Column	18 (>2)	10	6	Steel Truss	Steel Purlin	Sandwich Panel (Poly-urethane Isolation)	141
18	70 × 70 cm (ρ=1.7%) Reinforced Column	22,5 (>2)	8	9	Steel Beam (-I-) IPE 550	Steel Purlin	Sandwich Panel (Rock wool Isolation)	123
19	70 × 70 cm (ρ=1%) Reinforced Column	9 (>2)	7	6	Steel Beam	Steel Purlin	Trape-zoidal Steel Sheet (Rock wool Isolation)	63

Table C.1. Axial load calculation data chart for different reinforced concrete industrial buildings of which the structural properties were estimated during the site surveys (cont.).

Str.	Column Cross-Section	Span Length (m)	Axis Distance (m)	Height (m)	Roof Type			Axial Load (kN)
20	80 × 80 cm (ρ=1%) Reinforced Column	15 (>2)	7.5	7	Steel Beam (-I-) IPN 360	Steel Purlin	Trape-zoidal Steel Sheet (Rock wool Isolation)	95
21	60 × 60 cm (ρ= unknown) Precast Column	14 (>2)	12	11	Pre-cast Beam	Pre-cast Purlin	Sandwich Panel (Poly-urethane Isolation)	278
22	50 × 50 cm (ρ=1%) Precast Column	15 (>2)	7.5	7.75	Pre-cast Beam	Pre-cast Purlin	Sandwich Panel (Poly-urethane Isolation)	152
23	45 × 45 cm (ρ=1.3%) Precast Column	15 (>2)	7.5	5	Pre-cast Beam	Pre-cast Purlin	Sandwich Panel (Poly-urethane Isolation)	145
24	80 × 80 cm (ρ=1%) Reinforced Column	14.75 (>2)	9.2	10,5	Steel Beam (-I-) IPE 550	Steel Purlin	Metal Sheet (Rock wool Isolation)	140
25	80 × 80 cm (ρ=1.8%) Reinforced Column	27 (<2)	9	8	Steel Truss	Steel Purlin	Sandwich Panel (Rock wool Isolation)	114
26	55 × 55 cm (ρ= unknown) Precast Column	16 (>2)	7.5	6	Pre-cast Beam	Pre-cast Purlin	Sandwich Panel (Poly-urethane Isolation)	158

Table C.1. Axial load calculation data chart for different reinforced concrete industrial buildings of which the structural properties were estimated during the site surveys (cont.).

Str.	Column Cross-Section	Span Length (m)	Axis Distance (m)	Height (m)	Roof Type			Axial Load (kN)
27	60 × 60 cm (ρ= unknown) Reinforced Column	20 (>2)	7.5	6	Steel Beam	Steel Purlin	Trape-zoidal Steel Sheet (Poly-urethane Isolation)	195
28	60 × 60 cm (ρ= unknown) Precast Column	28 (<2)	10	9	Pre-cast Beam	Pre-cast Purlin	Sandwich Panel (Poly-urethane Isolation)	319
29	50 × 50 cm (ρ= unknown) Precast Column	28 (>2)	10	8	Pre-cast Beam	Pre-cast Purlin	Sandwich Panel (Poly-urethane Isolation)	389
30	50 × 50 cm (ρ= unknown) Precast Column	22 (>2)	10	6	Pre-cast Beam	Pre-cast Purlin	Sandwich Panel (Poly-urethane Isolation)	312
31	40 × 40 cm (ρ= unknown) Precast Column	20 (>2)	8	8.5	Pre-cast Beam	Pre-cast Purlin	Sandwich Panel (Glass-wool Isolation)	208
32	50 × 50 cm (ρ= unknown) Precast Column	20 (>2)	14	7.5	Steel Truss	Steel Purlin	Sandwich Panel (Glass-wool Isolation)	147
33	60 × 60 cm (ρ= unknown) Precast Column	25 (>2)	12	8.5	Pre-cast Beam	Pre-cast Purlin	Sandwich Panel (Glass-wool Isolation)	465

Table C.1. Axial load calculation data chart for different reinforced concrete industrial buildings of which the structural properties were estimated during the site surveys (cont.).

Str.	Column Cross-Section	Span Length (m)	Axis Distance (m)	Height (m)	Roof Type			Axial Load (kN)
34	40 × 40 cm (ρ= unknown) Precast Column	15.4 (<2)	5.5	6.5	Pre-cast Beam	Pre-cast Purlin	Sandwich Panel (Glass-wool Isolation)	109
35	40 × 40 cm (ρ= unknown) Precast Column	20 (>2)	6	6	Pre-cast Beam	Pre-cast Purlin	Sandwich Panel (Poly-urethane Isolation)	165
36	60 × 60 cm (ρ= unknown) Precast Column	18 (>2)	7	9	Pre-cast Beam	Pre-cast Purlin	Sandwich Panel (Poly-urethane Isolation)	195
37	50 × 50 cm (ρ= unknown) Precast Column	22 (>2)	7.5	6	Pre-cast Beam	Pre-cast Purlin	Sandwich Panel (Poly-urethane Isolation)	229
38	50 × 50 cm (ρ= unknown) Precast Column	23 (<2)	7.5	7.5	Pre-cast Beam	Pre-cast Purlin	Sandwich Panel (Poly-urethane Isolation)	208
39	60 × 60 cm (ρ= unknown) Reinforced Column	20 (>2)	6	8	Steel Space Truss		Metal Sheet (Rock-wool Isolation)	77
40	60 × 60 cm (ρ= unknown) Reinforced Column	12 (>2)	6	9	Steel Truss	Steel Purlin	Sandwich Panel (Poly-urethane Isolation)	69
41	50 × 50 cm (ρ= unknown) Precast Column	17.5 (>2)	6	7	Steel Truss	Steel Purlin	Metal Sheet (Poly-urethane Isolation)	62

Table C.1. Axial load calculation data chart for different reinforced concrete industrial buildings of which the structural properties were estimated during the site surveys (cont.).

Str.	Column Cross-Section	Span Length (m)	Axis Distance (m)	Height (m)	Roof Type			Axial Load (kN)
42	60 × 60 cm (ρ= unknown) Precast Column	23 (>2)	6	7	Pre-cast Beam	Pre-cast Purlin	Sandwich Panel (Poly-urethane Isolation)	229
43	60 × 60 cm (ρ= unknown) Precast Column	11.5 (>2)	6	7	Pre-cast Beam	Pre-cast Purlin	Sandwich Panel (Poly-urethane Isolation)	121
44	80 × 80 cm (ρ= unknown) Reinforced Column	20 (>2)	14	8	Steel Truss	Steel Purlin	Metal Sheet (Glass-wool Isolation)	185
45	50 × 50 cm (ρ= unknown) Precast Column	20 (<2)	10	7.75	Pre-cast Beam	Pre-cast Purlin	Sandwich Panel (Poly-urethane Isolation)	214
46	50 × 50 cm (ρ= unknown) Precast Column	24 (>2)	10	9.5	Pre-cast Beam	Pre-cast Purlin	Sandwich Panel (Poly-urethane Isolation)	346
47	40 × 40 cm (ρ= unknown) Precast Column	20 (<2)	10	5	Pre-cast Beam	Pre-cast Purlin	Sandwich Panel (Poly-urethane Isolation)	199
48	55 × 55 cm (ρ=1.7%) Precast Column	20 (<2)	10	9	Pre-cast Beam	Pre-cast Purlin	Sandwich Panel (Poly-urethane Isolation)	224
49	60 × 60 cm (ρ=1.1 %) Precast Column	28 (>2)	8	10.5	Steel Truss	Pre-cast Gutter Beam	Sandwich Panel (Poly-urethane Isolation)	153

Table C.1. Axial load calculation data chart for different reinforced concrete industrial buildings of which the structural properties were estimated during the site surveys (cont.).

Str.	Column Cross-Section	Span Length (m)	Axis Distance (m)	Height (m)	Roof Type			Axial Load (kN)
50	60 × 60 cm (ρ= unknown) Precast Column	25 (>2)	8	12	Pre-cast Beam	Pre-cast Purlin	Metal Sheet (Rock-wool Isolation)	313
51	45 × 45 cm (ρ=2.4 %) Precast Column	17 (>2)	8	7	Pre-cast Beam	Pre-cast Purlin	Sandwich Panel (Poly-urethane Isolation)	173
52	55 × 55 cm (ρ=1.8 %) Precast Column	15 (>2)	8	8	Pre-cast Beam	Pre-cast Purlin	Sandwich Panel (Poly-urethane Isolation)	254
53	50 × 50 cm (ρ=3.5 %) Precast Column	24 (>2)	7.8	8.5	Pre-cast Beam	Pre-cast Purlin	Sandwich Panel (Poly-urethane Isolation)	258
54	70 × 70 cm (ρ=2.8 %) Precast Column	24 (>2)	7	9	Pre-cast Beam	Pre-cast Purlin	Sandwich Panel (Rock-wool Isolation)	287
55	70 × 70 cm (ρ=1.8 %) Reinforced Column	22 (>2)	15	7	Steel Truss	Steel Purlin	Metal Sheet (Rock-wool Isolation	193
56	70 × 70 cm (ρ=1.8 %) Reinforced Column	30 (>2)	15	7	Steel Truss	Steel Purlin	Metal Sheet (Poly-urethane Isolation	211
57	70 × 70 cm (ρ=1.8 %) Reinforced Column	30 (>2)	15	5	Steel Truss	Steel Purlin	Metal Sheet (Rock-wool Isolation	234

Table C.1. Axial load calculation data chart for different reinforced concrete industrial buildings of which the structural properties were estimated during the site surveys (cont.).

Str.	Column Cross-Section	Span Length (m)	Axis Distance (m)	Height (m)	Roof Type			Axial Load (kN)
58	70 × 70 cm (ρ=1.8 %) Precast Column	20 (>2)	7.5	8	Pre-cast Beam	Pre-cast Purlin	Metal Sheet (Rock-wool Isolation)	235
59	40 × 40 cm (ρ= unknown) Precast Column	14 (>2)	10	8	Steel Truss	Steel Purlin	Metal Sheet (Rock-wool Isolation	80
60	60 × 60 cm (ρ= unknown) Precast Column	24 (<2)	8	9	Pre-cast Beam	Pre-cast Purlin	Metal Sheet (Rock-wool Isolation	244
61	50 × 50 cm (ρ=2 %) Precast Column	19.5 (<2)	5.5	7.5	Steel Truss	Steel Purlin	Metal Sheet (Poly-urethane Isolation	150
62	60 × 60 cm (ρ= unknown) Precast Column	18.5 (>2)	8	7	Steel Truss	Steel Purlin	Sandwich Panel (Poly-urethane Isolation)	91
63	40 × 40 cm (ρ= unknown) Precast Column	20 (>2)	7	6	Pre-cast Beam	Pre-cast Purlin	Sandwich Panel (Poly-urethane Isolation)	180
64	60 × 60 cm (ρ= unknown) Precast Column	24 (>2)	8	7	Pre-cast Beam	Pre-cast Purlin	Sandwich Panel (Poly-urethane Isolation)	269
65	60 × 60 cm (ρ= unknown) Precast Column	23 (>2)	7.5	12	Pre-cast Beam	Pre-cast Purlin	Sandwich Panel (Poly-urethane Isolation)	240

Table C.1. Axial load calculation data chart for different reinforced concrete industrial buildings of which the structural properties were estimated during the site surveys (cont.).

Str.	Column Cross-Section	Span Length (m)	Axis Distance (m)	Height (m)	Roof Type			Axial Load (kN)
66	50 × 50 cm (ρ= unknown) Precast Column	20 (>2)	8	6.5	Pre-cast Beam	Pre-cast Purlin	Sandwich Panel (Rock-wool Isolation)	216
67	80 × 80 cm (ρ= unknown) Precast Column	25 (>2)	8	10	Pre-cast Beam	Pre-cast Purlin	Sandwich Panel (Rock-wool Isolation)	344
68	60 × 60 cm (ρ= unknown) Precast Column	18 (>2)	7	6	Pre-cast Beam	Pre-cast Purlin	Sandwich Panel (Poly-urethane Isolation)	181
69	40 × 40 cm (ρ= unknown) Precast Column	15 (>2)	7.5	6	Pre-cast Beam	Pre-cast Purlin	Sandwich Panel (Rock-wool Isolation)	148
70	50 × 50 cm (ρ= unknown) Precast Column	20 (>2)	7.5	5.5	Pre-cast Beam	Pre-cast Purlin	Sandwich Panel (Rock-wool Isolation)	204
71	40 × 40 cm (ρ= unknown) Precast Column	17.5 (>2)	7.5	8	Pre-cast Beam	Pre-cast Purlin	Sandwich Panel (Poly-urethane Isolation)	172
72	40 × 40 cm (ρ= unknown) Precast Column	23 (<2)	7.5	10	Pre-cast Beam	Pre-cast Purlin	Sandwich Panel (Poly-urethane Isolation)	204
73	50 × 50 cm (ρ= unknown) Precast Column	23 (<2)	7.5	8	Pre-cast Beam	Pre-cast Purlin	Sandwich Panel (Poly-urethane Isolation)	210

Table C.1. Axial load calculation data chart for different reinforced concrete industrial buildings of which the structural properties were estimated during the site surveys (cont.).

Str.	Column Cross-Section	Span Length (m)	Axis Distance (m)	Height (m)	Roof Type			Axial Load (kN)
74	40 × 40 cm (ρ= unknown) Precast Column	20 (>2)	7.5	6	Pre-cast Beam	Pre-cast Purlin	Sandwich Panel (Poly-urethane Isolation)	187
75	60 × 60 cm (ρ= unknown) Precast Column	22.5 (>2)	7.5	10	Pre-cast Beam	Pre-cast Purlin	Sandwich Panel (Poly-urethane Isolation)	260
76	55 × 55 cm (ρ=2%) Precast Column	25 (>2)	10	6.5	Pre-cast Beam	Pre-cast Purlin	Sandwich Panel (Poly-urethane Isolation)	353
77	50 × 50 cm (ρ= unknown) Precast Column	15 (>2)	6	8	Pre-cast Beam	Pre-cast Purlin	Corru-gated Asbestos Cement	149
78	70 × 70 cm (ρ= unknown) Precast Column	16 (>2)	8	12	Pre-cast Beam	Pre-cast Purlin	Sandwich Panel (Poly-urethane Isolation)	259
79	60 × 60 cm (ρ=1%) Reinforced Column	20 (>2)	20	6	Steel Space Truss		Sandwich Panel (Poly-urethane Isolation)	76
80	60 × 60 cm (ρ=1%) Reinforced Column	20 (>2)	16	8	Steel Space Truss		Metal Sheet (Rock-wool Isolation)	95

APPENDIX D: COMPARING THE PML VALUES AND CORRESPONDING EARTHQUAKE INSURANCE RATES BY USING DIFFERENT LOSS ESTIMATON METHODS

Table D.1. Comparison of the PML values calculated by using different PML estimation methods for each building within the portfolio.

No	John Freeman	Karl V. Steinbrugge	ATC-13	FEMA 154 v:2	HAZUS	Proposed Method	
	PML (%)	PML (%)	PML (%)	PML (%)	PML (%)	Fragility	Risk Based
						PML (%)	PML (%)
1	20	63	22	60	20	17.8	5
2	20	63	22	60	20	54.9	30
3	20	63	22	60	20	17.8	5
4	20	63	7	60	14.7	33.2	30
5	20	63	22	60	20	17.8	30
6	20	63	22	60	20	17.8	30
7	20	63	22	60	20	17.8	5
8	20	63	22	60	20	17.8	30
9	20	63	22	60	20	17.8	5
10	20	63	22	60	20	17.8	5
11	20	57	2	60	4.3	6.6	5
12	20	57	2	60	4.3	6.6	5
13	20	57	2	60	4.3	6.6	5
14	20	57	2	60	4.3	6.6	5
15	20	57	2	60	4.3	6.6	5
16	20	57	2	60	4.3	6.6	5
17	20	57	2	60	4.3	5	5
18	20	63	22	60	15	12.4	5
19	20	63	22	60	14.4	8.3	5
20	20	63	22	60	14.4	8.3	5
21	20	63	7	60	10.2	21.7	30
22	20	63	22	60	14.4	31.3	30
23	20	63	22	60	14.4	31.3	30
24	20	63	22	60	20	17.8	5
25	20	63	22	60	11	5.5	5

Table D.1. Comparison of the PML values calculated by using different PML estimation methods for each building within the portfolio (cont.).

No	John Freeman	Karl V. Steinbrugge	ATC-13	FEMA 154 v:2	HAZUS	Proposed Method	
	PML (%)	PML (%)	PML (%)	PML (%)	PML (%)	Fragility	Risk Based
						PML (%)	PML (%)
26	20	63	22	60	20	54.9	30
27	20	63	7	60	10.2	5.4	5
28	20	72	22	100	29	86	70
29	20	63	22	60	14.4	31.3	100
30	20	63	22	60	14.4	31.3	30
31	20	63	2	60	8.4	19.1	100
32	20	63	2	60	8.4	5.2	5
33	20	63	2	60	8.4	19.1	30
34	20	63	22	60	8.4	19.1	30
35	20	63	22	60	20	54.9	70
36	20	63	22	60	20	54.9	30
37	20	63	22	60	14.4	31.3	30
38	20	63	22	60	14.4	31.3	30
39	20	63	22	60	20	17.8	5
40	20	63	2	60	5.8	5	5
41	20	63	2	60	5.8	5	5
42	20	63	22	60	20	54.9	30
43	20	63	22	60	20	54.9	30
44	20	63	22	60	20	17.8	5
45	20	63	2	60	5.8	10.1	5
46	20	63	2	60	5.8	10.1	30
47	20	63	2	60	5.8	10.1	5
48	20	63	2	60	4	5.9	5
49	20	63	2	60	5.8	19.1	5
50	20	63	22	60	20	54.9	70
51	20	63	22	60	15	24	30
52	20	63	22	60	15	24	30
53	20	63	22	60	11	14.4	5
54	20	63	22	60	15	24	5
55	20	63	22	60	11	5.5	5

Table D.1. Comparison of the PML values calculated by using different PML estimation methods for each building within the portfolio (cont.).

No	John Freeman	Karl V. Steinbrugge	ATC-13	FEMA 154 v:2	HAZUS	Proposed Method	
	PML (%)	PML (%)	PML (%)	PML (%)	PML (%)	Fragility	Risk Based
						PML (%)	PML (%)
56	20	63	22	60	11	5.5	5
57	20	63	22	60	11	14.4	5
58	20	63	22	60	15	24	5
59	20	63	22	60	20	17.8	30
60	20	63	22	60	20	54.9	30
61	20	63	7	60	7.4	5	5
62	20	63	22	60	20	17.8	5
63	20	63	22	60	20	54.9	100
64	20	63	22	60	20	54.9	30
65	20	63	22	60	20	54.9	30
66	20	63	7	60	10.2	21.7	30
67	20	63	7	60	10.2	21.7	5
68	20	63	2	60	5.8	10.1	5
69	20	63	2	60	4.3	6.6	5
70	20	57	2	60	4.3	6.6	5
71	20	57	2	60	4.3	6.6	5
72	20	57	2	60	4.3	6.6	5
73	20	57	2	60	4.3	6.6	5
74	20	57	2	60	4.3	6.6	5
75	20	57	2	60	4.3	6.6	5
76	20	63	7	60	7.4	9.2	5
77	20	63	22	60	14.4	31.3	30
78	20	63	7	60	5.8	10.1	5
79	20	63	22	60	14.4	8.3	5
80	20	63	22	60	14.4	8.3	5
Avg	**20**	**62.1**	**13.9**	**60.5**	**12.6**	**21.05**	**19.1**

Table D.2. Comparison of the earthquake insurance rates calculated by using different PML estimation methods for each building within the portfolio.

No	Earthquake Insurance Rates (‰)						
	John Freeman	Karl V. Steinbrugge	ATC-13	FEMA 154 v:2	HAZUS	Proposed Method	
						Fragility	Risk Based
1	0.77	2.97	0.87	2.81	0.77	0.65	0.13
2	0.77	2.97	0.87	2.81	0.77	2.55	1.28
3	0.77	2.97	0.87	2.81	0.77	0.65	0.13
4	0.77	2.97	0.18	2.81	0.50	1.44	1.28
5	0.77	2.97	0.87	2.81	0.77	0.65	1.28
6	0.77	2.97	0.87	2.81	0.77	0.65	1.28
7	0.77	2.97	0.87	2.81	0.77	0.65	0.13
8	0.77	2.97	0.87	2.81	0.77	0.65	1.28
9	0.77	2.97	0.87	2.81	0.77	0.65	0.13
10	0.77	2.97	0.87	2.81	0.77	0.65	0.13
11	0.77	2.66	0.05	2.81	0.11	0.17	0.13
12	0.77	2.66	0.05	2.81	0.11	0.17	0.13
13	0.77	2.66	0.05	2.81	0.11	0.17	0.13
14	0.77	2.66	0.05	2.81	0.11	0.17	0.13
15	0.77	2.66	0.05	2.81	0.11	0.17	0.13
16	0.77	2.66	0.05	2.81	0.11	0.17	0.13
17	0.77	2.66	0.05	2.81	0.11	0.13	0.13
18	0.77	2.97	0.87	2.81	0.51	0.38	0.13
19	0.77	2.97	0.87	2.81	0.48	0.21	0.13
20	0.77	2.97	0.87	2.81	0.48	0.21	0.13
21	0.77	2.97	0.18	2.81	0.26	0.85	1.28
22	0.77	2.97	0.87	2.81	0.48	1.34	1.28
23	0.77	2.97	0.87	2.81	0.48	1.34	1.28
24	0.77	2.97	0.87	2.81	0.77	0.65	0.13
25	0.77	2.97	0.87	2.81	0.31	0.14	0.13
26	0.77	2.97	0.87	2.81	0.77	2.55	1.28
27	0.77	2.97	0.18	2.81	0.26	0.14	0.13
28	0.77	3.43	0.87	4.86	1.23	4.14	3.33
29	0.77	2.97	0.87	2.81	0.48	1.34	4.86
30	0.77	2.97	0.87	2.81	0.48	1.34	1.28
31	0.77	2.97	0.05	2.81	0.21	0.72	4.86
32	0.77	2.97	0.05	2.81	0.21	0.13	0.13

Table D.2. Comparison of the earthquake insurance rates calculated by using different PML estimation methods for each building within the portfolio (cont.).

No	Earthquake Insurance Rates (‰)						
	John Freeman	Karl V. Steinbrugge	ATC-13	FEMA 154 v:2	HAZUS	Proposed Method	
						Fragility	Risk Based
33	0.77	2.97	0.05	2.81	0.21	0.72	1.28
34	0.77	2.97	0.05	2.81	0.21	0.72	1.28
35	0.77	2.97	0.87	2.81	0.77	2.55	3.33
36	0.77	2.97	0.87	2.81	0.77	2.55	1.28
37	0.77	2.97	0.87	2.81	0.48	1.34	1.28
38	0.77	2.97	0.87	2.81	0.48	1.34	1.28
39	0.77	2.97	0.87	2.81	0.77	0.65	0.13
40	0.77	2.97	0.05	2.81	0.15	0.13	0.13
41	0.77	2.97	0.05	2.81	0.15	0.13	0.13
42	0.77	2.97	0.87	2.81	0.77	2.55	1.28
43	0.77	2.97	0.87	2.81	0.77	2.55	1.28
44	0.77	2.97	0.87	2.81	0.77	0.65	0.13
45	0.77	2.97	0.05	2.81	0.15	0.26	0.13
46	0.77	2.97	0.05	2.81	0.15	0.26	1.28
47	0.77	2.97	0.05	2.81	0.15	0.26	0.13
48	0.77	2.97	0.05	2.81	0.10	0.15	0.13
49	0.77	2.97	0.05	2.81	0.15	0.72	0.13
50	0.77	2.97	0.87	2.81	0.77	2.55	3.33
51	0.77	2.97	0.87	2.81	0.51	0.97	1.28
52	0.77	2.97	0.87	2.81	0.51	0.97	1.28
53	0.77	2.97	0.87	2.81	0.31	0.48	0.13
54	0.77	2.97	0.87	2.81	0.51	0.97	0.13
55	0.77	2.97	0.87	2.81	0.31	0.14	0.13
56	0.77	2.97	0.87	2.81	0.31	0.14	0.13
57	0.77	2.97	0.87	2.81	0.31	0.48	0.13
58	0.77	2.97	0.87	2.81	0.51	0.97	0.13
59	0.77	2.97	0.87	2.81	0.77	0.65	1.28
60	0.77	2.97	0.87	2.81	0.77	2.55	1.28
61	0.77	2.97	0.18	2.81	0.19	0.13	0.13
62	0.77	2.97	0.87	2.81	0.77	0.65	0.13
63	0.77	2.97	0.87	2.81	0.77	2.55	4.86
64	0.77	2.97	0.87	2.81	0.77	2.55	1.28

Table D.2. Comparison of the earthquake insurance rates calculated by using different PML estimation methods for each building within the portfolio (cont.).

No	Earthquake Insurance Rates (‰)						
	John Freeman	Karl V. Steinbrugge	ATC-13	FEMA 154 v:2	HAZUS	Proposed Method	
						Fragility	Risk Based
65	0.77	2.97	0.87	2.81	0.77	2.55	1.28
66	0.77	2.97	0.18	2.81	0.26	0.85	1.28
67	0.77	2.97	0.18	2.81	0.26	0.85	0.13
68	0.77	2.97	0.05	2.81	0.15	0.26	0.13
69	0.77	2.97	0.05	2.81	0.11	0.17	0.13
70	0.77	2.66	0.05	2.81	0.11	0.17	0.13
71	0.77	2.66	0.05	2.81	0.11	0.17	0.13
72	0.77	2.66	0.05	2.81	0.11	0.17	0.13
73	0.77	2.66	0.05	2.81	0.11	0.17	0.13
74	0.77	2.66	0.05	2.81	0.11	0.17	0.13
75	0.77	2.66	0.05	2.81	0.11	0.17	0.13
76	0.77	2.97	0.18	2.81	0.19	0.23	0.13
77	0.77	2.97	0.87	2.81	0.48	1.34	1.28
78	0.77	2.97	0.05	2.81	0.15	0.26	0.13
79	0.77	2.97	0.87	2.81	0.48	0.21	0.13
80	0.77	2.97	0.87	2.81	0.48	0.21	0.13
Avg	**0.77**	**2.92**	**0.53**	**2.84**	**0.43**	**0.85**	**0.80**

REFERENCES

Air Worldwide (AIR), 2011, *Damage Survey Report, Tohoku, Japan Earthquake*, http://www.airworldwide.com/Publications/Presentations/AIR-Surveys-Damage from-the-Tohoku- Earthquake-and-Tsunami-(Summary-and-Slideshow), accessed on June 2012.

Applied Technology Council (ATC), 1985, *Earthquake Damage Evaluation for California, ATC 13*, Redwood City, California.

Applied Technology Council (ATC), 1996, *Seismic Evaluation and Retrofit of Concrete Buildings, ATC 40*, Redwood City, California.

Applied Technology Council (ATC), 2002, *Commentary on the use of ATC-13 Earthquake Damage Evaluation Data for Probable Maximum Loss Studies of California Buildings, ATC 13-1*, Redwood City, California.

Arslan, M., H., Korkmaz H., Gülay F., G., 2006, ‘‘Damage and Failure Pattern of Prefabricated Structures after Major Earthquakes in Turkey and Shortfalls of the Turkish Earthquake Code’’, *Engineering Failure Analysis, Elsevier*, Vol. 13, pp. 537-557.

Aschheim, M., 2001, *Preliminary Observations: The Izmit Earthquake of 17 August 1999*, EERI Reconnaissance Team, Mid-America Earthquake Center, University of Illinois at Urbana-Champaign.

ASTM, 2007, ASTM E2026-07, *Standard Guide for the Estimation of Probable Loss to Buildings from Earthquakes*, American Society for Testing and Materials, West Conshohocken, Pennsylvania.

Bommer J., Spence, R., Erdik, M., Tabuchi, S., Aydinoglu, N., Booth, E., Del, Re, D., Peterken, O., 2002, ‘‘Development of an Earthquake Loss Model for Turkish Catastrophe Insurance’’, *Journal of Seismology*, Vol.6, pp. 431-446.

DEE-KOERI, 2003, *Earthquake Risk Assessment for the Istanbul Metropolitan Area*, Report prepared by Deparment of Earthquake Engineering, Kandilli Observatory and Earthquake Research Institute, Bogazici University Press, Istanbul, Turkey.

Deniz, A., 2006, *Estimation of Earthquake Insurance Premium Rates based on Stochastic Methods*, M.S. Thesis, Middle East Technical University, Ankara, Turkey.

Deniz, A., and Yücemen, M. S., 2009, ‘‘Assessment of Earthquake Rates for the Turkish Catastrophe Insurance Pool’’, *Georisk: Assessment and Management of Risk for Engineered Systems and Geohazards*, Vol. 3:2, pp. 67-74.

Durukal, E., Erdik, M., Sesetyan, K., Fahjan, Y., 2006, ‘‘Building Loss Estimation for Earthquake Insurance Pricing’’, *Proceedings of the 1906 Earthquake Conference*, CD, Paper No: 1311, EERI, Oakland.

Durukal, E., Erdik, M., Uçkan, E., 2008, ‘‘Earthquake Risk to Industry in İstanbul and its Management’’, *Springer, Nat Hazards*, Vol: 44, pp.199-212.

Eren, C., 2014, ‘‘Rapid Loss Estimation Methodology for Single-Storey Reinforced Concrete Industrial Buildings’’, *Technical Journal of Turkish Chamber of Civil Engineers*, Vol. 25, No.2, pp. 6725-6756 (in Turkish).

Ersoy U., C., 1985, *Betonarme Cilt: 1 Temel İlkeler ve Taşıma Gücü Hesabı (Reinforced Concrete Structures Part 1: Main Principles and Ultimate Strength Design)*, Evrim Yayınları, Turkey (in Turkish).

Faber, M. H., 2007, *Lecture Notes: Statistics and Probability Theory, Exercises Tutorial 7*, http://www.ibk.ethz.ch/emeritus/fa/education/ss_statistics/07Statistik/Exercise_ tutorial_7_SS07_web.pdf, Swiss Federal Institute of Technology Zurich, EZTH, accessed on September 2013.

Federal Emergency Management Agency (FEMA), 2001, *HAZUS 99, Earthquake Loss Estimation Methodology, Technical and User's Manual*, Washington, DC.

Federal Emergency Management Agency (FEMA), 2002, *FEMA 154, Rapid Visual Screening of Buildings for Potential Seismic Hazards: A Handbook*, Second Edition, Washington, DC.

Fischinger, M., Kramar, M., Isakovic, T., 2008, ''Cyclic Response of Slender RC Columns Typical of Precast Industrial Buildings'', *Springer Science and Business Media B.V., Earthquake Engineering*, Vol. 6, pp. 519-534.

Freeman, J.,R., 1932, *Earthquake Damage and Earthquake Insurance: Studies of a Rational Basis for Earthquake Insurance, also Studies of Engineering Data for Earthquake-resisting Construction*, New York: McGraw-Hill

Goda, K., Yoshikawa, H., 2012, ''Earthquake Insurance Portfolio Analysis of Wood-frame Houses in South Western British Columbia, Canada'', *Springer Science and Business Media B.V., Earthquake Engineering*, Vol. 10 pp. 615-643.

Gurpinar, A., Abali, M., Yücemen, M. S., Yesilcay. Y., 1978, *Feasibility of Obligatory Earthquake Insurance in Turkey*, METU/ EERI Report No. 78–05, Ankara (in Turkish).

Karaesmen, E., 2001, *Prefabrication in Turkey: Facts and Figures*, Department of Civil Engineering, Middle East Technical University, Ankara, Turkey.

Kayhan, A. H., Senel, S. M., 2005, ''Performance Evaluation of Single-Spanned, Single-Storey Precast Industrial Buildings'', *2005 Kocaeli Earthquake Symposium*, Turkey.

Kayhan, A. H., Senel, S. M., 2010a, ''Fragility Curves for Single Story Precast Industrial Buildings'', *Technical Journal of Turkish Chamber of Civil Engineers*, Vol. 21, No.4, pp. 5161-5184 (in Turkish).

Kayhan, A. H., Senel, S. M., 2010b, ‘‘Fragility Based Damage Assessment in Existing Precast Industrial Buildings: A Case Study for Turkey’’, *Structural Engineering and Mechanics*, Vol.34, No.1.

Kircher, C. A., Reitherman, R. K., Whitman R. V., Arnold, C., 1997a, ‘‘Estimation of Earthquake Losses to Buildings’’, *Earthquake Spectr*a, Vol. 13, No. 4, pp. 703-720, Earthquake Research Institute, Oakland, California.

Kircher, C. A., Nassar, A. A., Kustu, O., Holmes, W. T., 1997b, ‘‘Development of Building Damage Functions for Earthquake Loss Estimation’’, Earthquake Spectra, Vol. 13, No. 4, Earthquake Research Institute, Oakland, California.

Kwak, H., Kim, J., 2007, ‘‘P-Δ Effect of Slender RC Columns under Seismic Load’’, *Elsevier, Engineering Structures*, Vol. 29, pp. 3121–3133.

McCornack, T. C., Rad, F. N., 1997, ‘‘An Earthquake Loss Estimation Methodology for Buildings Based on ATC-13 and ATC-21’’, *Earthquake Spectra*, Vol. 13, No. 4, Earthquake Research Institute, Oakland, California

National Institute of Building Science (NIBS), HAZUS, 1997, *Earthquake Loss Estimation Methodology, HAZUS97: Technical Manual*, Report Prepared for Federal Emergency Management Agency, Washington, DC.

Odabaşı, Y., 2000, *Ahşap ve Çelik Yapı Elemanları (Wood and Steel Structural Members)*, Beta Basım Yayım Dağıtım, Turkey (in Turkish).

Ozden, S., Barka, G., Ataköy, H., Hancioğlu, B., Ozkan, U., 2013, ‘‘Earthquake Experience of Turkish Precast Industry’’, *Proceedings of the 4th ECCOMAS Thematic Conference on Computational Methods in Structural Dynamics and Earthquake Engineering*, Kos Island, Greece.

Park, R., and Pauley, T., 1975, *Reinforced Concrete Structures*, John Wiley & Sons Inc. New York.

Posada, M., Wood, S. L., 2002, ‘‘Seismic Performance of Precast Industrial Buildings in Turkey’’, *7th U.S. National Conference on Earthquake Engineering*, Boston

RMS, 2000, *Event Report, Kocaeli, Turkey Earthquake*, http://www.rms.com/Publications/Turkey_Event.pdf, accessed on August 2011.

Steinbrugge, K. V., 1982, *Earthquake, Volcanoes, and Tsunamis: An Anatomy of Hazards*, New York: Skandia America Group.

Şenel, S. M., Palancı, M., Kalkan, A., Yılmaz, Y., 2013, ‘‘Investigation of Shear and Overturning Safety of Hinged Connections in Existing Precast Buildings’’, *Technical Journal of Turkish Chamber of Civil Engineers*, Vol. 25, No.4, pp. 6505-6528 (in Turkish).

Tezcan, S., Bal, E., Karakoc, C., Gunay, G., Yalcın, C., 2007, *Assessment Report on Comparing Existing Rapid Grading Methods for Estimating Collapse Risk of Buildings During Earthquakes*, Kadıköy Municipality, Environment Safety Management, İstanbul.

TCIP, Turkish Catastrophe Insurance Pool, 2014, *Tariffs and Premium*, http://www.tcip.gov.tr/zorunlu-deprem-sigortasi-tarife-ve-primler.html, accessed on April 2014.

Trifunac, M. D., Brady, A. G., 1975 ‘‘On the Correlation of Seismic Intensity with Peaks of Recorded Strong Ground Motion’’, *Bulletin of Seismological Society of America*, Vol. 65, No.1, pp. 139-162.

Turkish Seismic Code, 1998, *Specifications for Structures to be Built in Seismic Areas*, Ministry of Public Works and Settlement, Ankara (in Turkish).

TSDC07, Turkish Seismic Code, 2007*, Specifications for Structures to be Built in Seismic Areas*, Ministry of Public Works and Settlement, Ankara (in Turkish).

Whitman, R. V., Anagos, T., Kricher, C. A., Lagorio, H. J., Lawson, R. S., Schneider, P., 1997, ‘‘Development of a National Earthquake Loss Estimation Methodology’’, *Earthquake Spectra*, Vol. 13, No. 4, Earthquake Research Institute, Oakland, California.

Yao, T. P. J., 1981, *Probabilistic Methods for the Evaluation of Seismic Damage of Existing Structures*, Purdue University, West Lafayette.

Yücemen, M. S., 2005, ‘‘Probabilistic Assessment of Earthquake Insurance Rates for Turkey’’, *Springer Science, Natural Hazards*, Vol. 35, pp. 291–313.

Yücemen, M. S., Yilmaz, C., Erdik, M., 2008, ‘‘Probabilistic Assessment of Earthquake Insurance Rates for Important Structures: Application to Gumusova-Gerede Motorway’’, *Elsevier Science, Structural Safety*, Vol. 30, pp. 420-435.

Zhao, X., Wu, Y., Leung, A., Lam, H. F., 2011, ‘‘Plastic Hinge Length in Reinforced Concrete Flexural Members’’, *The Twelfth East Asia-Pacific Conference on Structural Engineering and Construction*, Procedia Engineering, Elsevier, Vol. 14, pp. 1266-1274.

Zorbozan, M., Barka, G., Sarıfakıoğlu, F., 1998, Ceyhan ‘‘Damages Occurred in Precast Concrete Buildings during Ceyhan Earthquake, their Causes and Proposed Solutions’’ *Journal of Prefabricated Concrete,* Vol. 48, pp.20-24, Turkish Chamber of Prefabrication, Ankara (in Turkish).